Design and Evaluation of Geometric Nonlinearities using Joined-Wing SensorCraft Flight Test Article

Jeffrey Samuel Garnand-Royo

Thesis submitted to the Faculty of the

Virginia Polytechnic Institute and State University

in partial fulfillment of the requirements for the degree of

Master of Science

in

Aerospace Engineering

Robert A. Canfield, Chair

Craig A. Woolsey

Ned J. Lindsley

May 6, 2013

Blacksburg, Virginia

Keywords:Joined Wing, SensorCraft, Flight Test, Unmanned Aircraft, Unmanned Aerial Vehicle, UAV, UAS, Scaling, Remotely Piloted Vehicle, RPV

Design and Evaluation of Geometric Nonlinearities using Joined-Wing SensorCraft Flight Test Article

Jeffrey Samuel Garnand-Royo

ABSTRACT

The Boeing Joined-Wing SenorCraft is a novel aircraft design that has many potential benefits, especially for surveillance missions. However, computational studies have shown the potential for nonlinear structural responses in the joined-wing configuration due to aerodynamic loading that could result in aft wing buckling. The design, construction, and flight testing of a $1/9^{th}$ scale, aeroelastically tuned model of the Joined-Wing SensorCraft has been the subject of an ongoing international collaboration aimed at experimentally demonstrating the nonlinear aeroelastic response in flight. To accurately measure and capture the configuration's potential for structural nonlinearity, the test article must exhibit equivalent structural flexibility and be designed to meet airworthiness standards. Previous work has demonstrated airworthiness through the successful flight of a Geometrically Scaled Remotely Piloted Vehicle. The work presented in this thesis involves evaluation of an aeroelastically tuned design through ground-based experimentation. The result of these experimental investigations has led to the conclusion that a full redesign of the forward and aft wings must be completed to demonstrate sufficient geometric nonlinearity for the follow-on Aeorelastically Tuned Remotely Piloted Vehicle. This thesis also presents flight test plans for the aeroelastically tuned RPV.

Acknowledgments

I would like to first and foremost thank my primary advisors, Dr. Canfield and Dr. Woolsey for selecting me for such an interesting and wide reaching project. Further thanks is extended for the guidance and patience they both provided me for the past two years as well as my last year of undergraduate work. The support provided by both advisors was an invaluable resource.

I would also like to thank my primary collaborator Jenner Richards. Jenner Richards is one of the most hard working and overall well rounded engineers I have ever had the pleasure to work with. Though we were colleagues on the project, I was constantly learning while working with Jenner, from fabrication work to computational. Jenner was also good enough to put up with me for nearly a year in Victoria, even allowing me to stay with him in his apartment for that time. For that, I can't thank him enough. I would also like to thank Jenner's primary advisor, Dr. Afzal Suleman, for his support in my research efforts while in Victoria.

I would like to thank my predecessor, Tyler Aarons, for his support in the early stages

of my research and also for having confidence in me to carry on the invaluable research and work he began. He was a great mentor for me as I transitioned from undergraduate to graduate studies and for his time and consideration in that regard I would like to thank him.

This project involved the collaboration of many students from both Victoria and Virginia Tech. Out of this group I would first like to thank my primary collaborators at Virginia Tech, Anthony Ricciardi and Charles Eger. I would like to thank all the students I had the pleasure of working with in Canada for being so welcoming and such dedicated researchers (Peter Lu, Ryan Flagg, Willem Brussow, Gord Cooney, Wanjohi Mugo, Shayan, and Casey Keulen). Thanks also goes to the two pilots for the test program effort, Jon Harwood and Kelly Williams. I would also like to thank all of my fellow researchers in the NSL for always being available for help and always keeping me level headed as I performed my research (Ony, Mark, Eddie, Ankit, Kyle, and Artur). I must also thank Waverly Parks for all of her help and constant support throughout my two years of graduate research.

I would also like to acknowledge the two funding sources that supported my research; AFRL and the Virginia Space Grant Consortium Graduate Research Fellowship. Specifically at AFRL, I would like to thank Dr. Ned Lindsley for the support he provided through these research efforts.

Last and certainly not least, I would truly like to thank my parents for providing me with amazing role models. I can not thank my parents enough for all of the support they provided me in not only graduate school but in everything I do. They are always there encouraging me through my successes and my failures. My parents are an inspiration to me and I hope

all of the lego sets they bought, which turned me into an engineer, paid off at least in their eyes.

Contents

List of Figures

NOTE: Unless otherwise indicated, all images courtesy of author.

List of Tables

Chapter 1

Introduction

1.1 Background and Motivation

High altitude, long endurance (HALE) unmanned aerial vehicles (UAVs) are capable of providing revolutionary intelligence, surveillance, and reconnaissance (ISR) capabilities over vast geographic areas when equipped with advanced sensor packages. This capability is an attractive solution for both the military and civil sectors for a variety of missions in which surveillance is a key element.[3] From a military perspective, constant surveillance proves a vital asset in overall mission capability, especially in combat situations. As a result, the Air Force Research Laboratory (AFRL) has called for the development of a SensorCraft concept aircraft designed as an advanced, tactical HALE ISR platform capable of constant battle space awareness over vast geographic areas.[4] To provide constant battle space awareness,

the SensorCraft must exhibit an endurance of 30 plus hours and be capable of a maximum range of 2000 nautical miles.[5] The full scale SensorCraft mission profile is shown in Fig. 1.1.

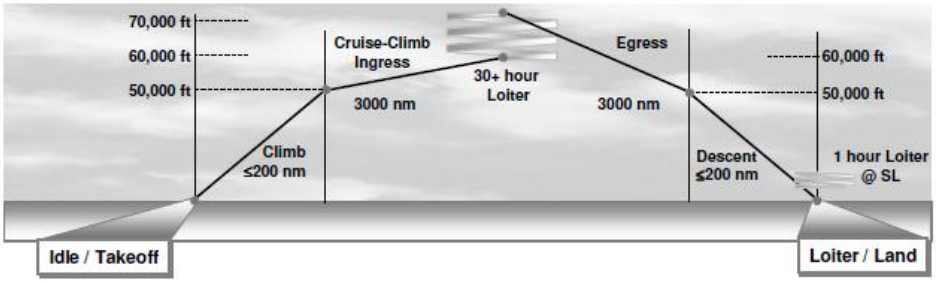

Figure 1.1: Full Scale SensorCraft Mission Profile. Lucia, D., *The SensorCraft Configurations: A Non-Linear AeroServoElastic Challenge for Aviation*, AIAA 2005-1943, 46th AIAA/ASME/ASCE/AHS/ASC Structures, Structural Dynamics and Materials Conference, No. April, Austin, Texas, 2005, pp. 1-7. (Source declared work of the U.S. Government and is not subject to copyright protection in United States)

In response, several companies including Lockheed Martin, Northrop Grumman, and Boeing have developed SensorCraft concepts (Fig. 1.2). Lockheed Martin's original concept utilized a conventional large aspect ratio design while Northrop Grumman approached the task utilizing a flying wing design. Boeing's candidate design was the most unique of the three proposed, and utilized a joined-wing configuration. A joined-wing aircraft is one that employs a forward and aft wing pair. The wing pair is connected such that, in a top profile view, the wing set forms a diamond shape.

Figure 1.2: Lockheed Martin Concept (left); Northrop Grumman concept (middle), Boeing Concept (right) Full Scale SensorCraft Mission Profile. Lucia, D., *The SensorCraft Configurations: A Non-Linear AeroServoElastic Challenge for Aviation*, AIAA 2005-1943, 46th AIAA/ASME/ASCE/AHS/ASC Structures, Structural Dynamics and Materials Conference, No. April, Austin, Texas, 2005, pp. 1-7.(Source declared work of the U.S. Government and is not subject to copyright protection in United States)

The decision to utilize an unconventional joined-wing design presents one primary advantage over competing designs. Due to its configuration, the JWSC provides the ability for persistent 360° penetrating surveillance by embedding sensor packages in both the fore and aft wings (Fig. 1.3).[5]

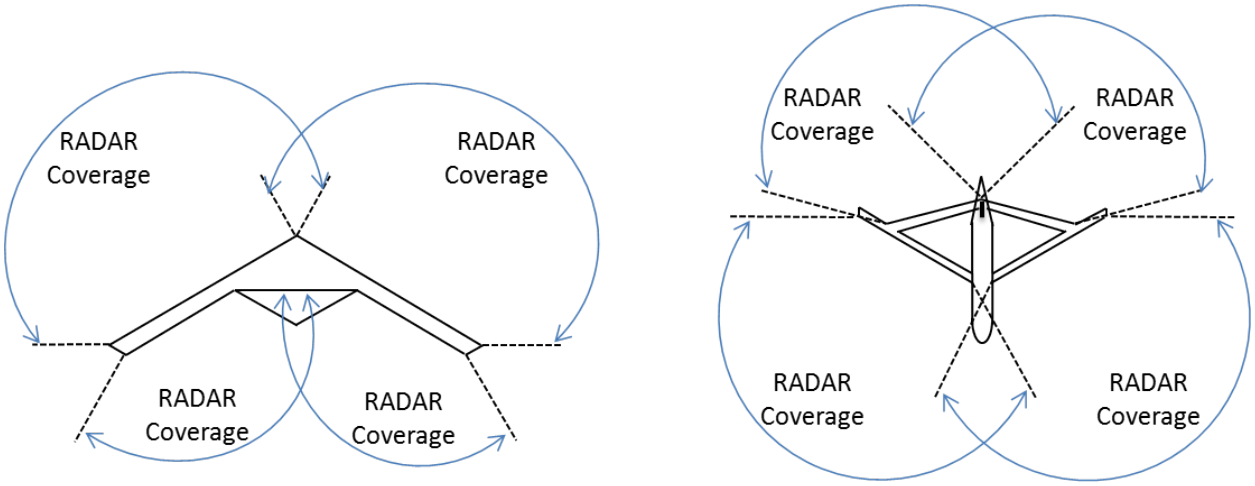

Figure 1.3: Joined-Wing surveillance advantage over conventional wing. Canfield R., *SensorCraft Research at AFIT 2001-2008*, Tech. rep., AF-VT Collaborative Center, September 2009. (Image adapted from source)

The other unique aspect of utilizing a joined wing configuration is the potential for

taking advantage of the Wolkovitch effect.[6] The joined wing configuration forms a truss-like structure that subsequently tilts the bending axis of the aircraft. This tilted axis is normal to the plane defined by the forward and aft wing connection. Due to this shifted bending plane, the optimum internal wing box structure for the configuration differs from that of a traditional cantilever aircraft. The internal wing box benefits from placing the leading edge spar as far forward as possible and the aft spar as aft as possible. Furthermore, material must be concentrated along the upper leading edge of the spar and the lower aft edge of the spar. This focus on beam separation rather than thickness allows for the use of thinner airfoils and thus less weight and favorable transonic performance. Furthermore, the increased wing box depth chord-wise and the use of forward and aft wings provide increased volume for fuel wells. The potential advantages of less weight with increased volume for fuel wells can lead to a configuration suited for long endurance. This nontraditional wing box configuration which leads to these advantages is referred to as the Wolkovitch effect. However, decomposing the lift loads along the bending plane showed a response not typical of traditional aircraft. The in-plane components are reinforced by the truss configuration. The out-of-plane component acts normal to the tilted bending plane bending the wings about this axis. This places the leading upper portion of the wing box in compression while the remaining portion is placed in tension which leads to the potential of leading edge buckling in the wings due to the resulting axial load. The load decomposition is shown in Fig. 1.4(A) along with the resulting compression for the wing box. A traditional wing box is also shown for comparison in Fig. 1.4 (B).

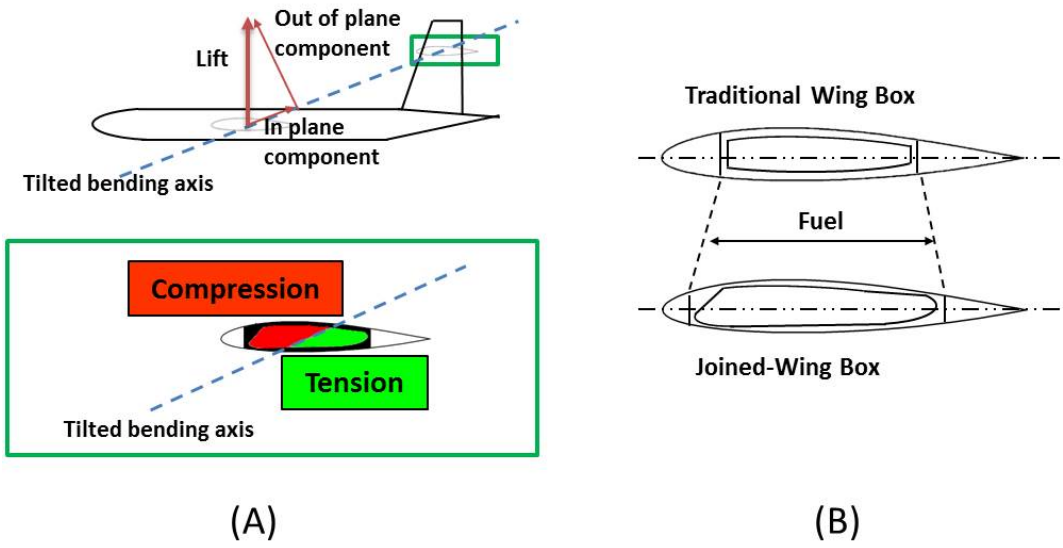

Figure 1.4: (A) Tilted bending axis of joined-wing configuration; (B) Wing Box Comparisons. Wolkovitch, J., *The Joined Wing: An Overview*, Journal of Aircraft, Vol. 23, No. 1, 1986, pp. 161-178. (Image adapted from source)

It has been shown through multiple computational studies, however, that there existed potential for further nonlinear structural responses in the joined wing configuration due to large deflections and follower forces that may lead to buckling of the aft wing.[5,7–9] Any means to counteract this geometric nonlinear response, including strengthening the aft wing, counteracts the joined-wing configuration's weight saving advantage. The nonlinear geometric aeroelastic response of the aft wing is the subject of ongoing investigation and has yet to be quantified in an actual flight test program. This investigation thus requires the design, testing, and evaluation of a reduced scale Boeing JWSC in order to evaluate these geometric nonlinearities.

1.2 Previous Work

There have been many studies relating to the joined-wing concept. This section provides a review of past studies and illustrates their role in relation to the current and ongoing investigation. This section is organized to first present computational studies that have indicated the importance of nonlinearity for the joined-wing configuration, then presents the internal efforts of the particular flight test program this work is associated with, and ends with a description of a few joined-wing HALE surveillance flight articles.

1.2.1 Computational Studies

The joined-wing concept was first introduced by Wolkovtich who published an overview of the concept in 1986.[6] In his overview, Wolkovitch presented several advantages for the joined-wing configuration and explored his conclusions for various design parameters associated with the joined-wing configuration. The most interesting advantages included lower structural weight and lower induced drag as compared to traditional aircraft. Wolkovitch also showed the importance of optimization between structure and aerodynamics in order to achieve the proposed advantages of the configuration.[6]

Kroo, Gallman, and Smith[10] extended Wolkovitch's design exploration by completing a more detailed aerodynamic and structural study. This study explored the use of symmetric and asymmetric material distribution for the internal wing box structure where the thickness of the material was optimized using a fully stressed design. Kroo, Gallman, and Smith

showed that to fully exploit the potential benefits of the joined-wing concept, the use of asymmetric material distribution in the spar is important further confirming the Wolkovitch effect. Furthermore, structural analysis for the study utilized both a nonlinear finite element model and a linear model. Comparison of the two models indicated that a linear and nonlinear analysis were comparable up to the point buckling occurred in the aft wing due to large deflections. This result suggests the need for nonlinear analysis within the design process of a joined-wing configuration and the potential importance of understanding the nonlinearities caused by the unconventional joined-wing configuration.[10]

The previous study by Kroo et al. was continued and presented in two later papers which focused on exploring the joined-wing configurations potential as an alternative to conventional transport designs.[11,12] Gallman, Smith, and Kroo (1993) applied numerical optimization to aircraft design to compare a joined-wing and conventional aircraft configuration for a medium-range transport mission profile. The resulting comparisons were done based on drag, weight, and direct operating cost (DOC). The study showed that initially a joined-wing produced 2% savings in DOC over the conventional aircraft configuration. However, applying an additional buckling constraint increased the DOC of the joined-wing configuration by 5.3% which was 3.2% greater than the conventional transport aircraft for the same mission.[11] The second paper produced by Gallman and Kroo supported these results.[12] Gallman and Kroo (1996) concluded that performing nonlinear structural analysis under given loads using a fully stressed design would produce an optimized joined-wing configuration that was heavier than a traditional configuration. The limiting factor con-

tributing to the inefficiency of the joined-wing in this work was the inclusion of the buckling constraint.[12]

As a result of the work of Gallman and Kroo (1996), interest in the joined-wing concept was deflated as an alternative transport configuration. However, recent development of nonlinear analysis and design tools, and the growing applications of UAVs, especially for HALE missions, have garnered a resurgence of the joined-wing concept. This resurgence is demonstrated in Boeing's decision to utilize a joined-wing configuration for the SensorCraft initiative which placed focus on the design of an aircraft around an optimized collection of sensors (as opposed to the reverse, typical design process).

Livne (2001) conducted a survey of the joined-wing concept, specifically highlighting the concepts relevance to a number of disciplines.[13] The survey presented the importance of structural and aerodynamic analysis and design for such a configuration as well as emphasized the need to perform analysis of an optimized joined-wing design. Performing analysis of an optimized design was necessary in order to obtain meaningful results when investigating the interaction of geometric nonlinearities and aeroelastic behavior. Livne further wrote that geometric structural nonlinearities should be included when performing structural, aeroelastic, and aeroservoelastic analysis. The geometric structural nonlinearities are also a necessary consideration due to the considerable in-plane compression on the aft wing as a result of the joined-wing configuration.[13]

In 2002, Blair and Canfield presented preliminary work on an integrated design process for generating high fidelity analytical weight estimations for a joined-wing configuration.[7] This

weight modeling study incorporated elements of configuration, structural, and aerodynamic analysis. The overlying contribution of this work, however, was the further incorporation of aeroelastic analysis in the design process. Blair and Canfield identified that a correct joined-wing aeroelastic model could potentially offer a successful design that leverages the nonlinear effects (large deformations and geometric nonlinearities) to the advantage of the joined-wing configuration. The results of the study showed that in both a linear buckling analysis and a fully geometrically nonlinear analysis, the critical load for stability was exceeded, thereby further emphasizing the importance of including geometric nonlinearities in the design process to accurately capture the aeroelastic response of the joined-wing configuration.[7] Subsequent studies have also looked at understanding the nonlinear structural and aeroelastic behavior of the joined-wing. Patil (2003) developed a nonlinear aeroelastic analysis methodology that accounted for the large deformations of the wing and fuselage.[14] The methodology was applied to study the nonlinear static and aeroelastic behavior of a joined-wing model. The results in this case showed that the linear and nonlinear analyses were very similar.[14]

Ricciardi et al. modified a nonlinear transient aeroelastic code developed by Patil[14] to calculate gust forcing while considering large structural deviations from steady state trim and to allow spatial gust field definition.[15] The modified code was used to evaluate quasi-static certification methods for a flexible joined-wing and flying wing aircraft. Results showed that quasi-static analysis may be useful for preliminary design of a typical joined-wing model, but insufficiently robust for preliminary design of the flexible flying wing case. Transient analysis

was recommended for detailed design or certification analysis of either configuration.[15]

Roberts, Canfield, and Blair presented work focused on achieving a structural model that was nonlinearly optimized and aerodynamically trimmed through utilization of their developed software and model configuration.[7,16] Their efforts included a buckling analysis on the resulting optimized model, which indicated that a critical load condition throughout the design process was the maneuver speed gust load. Further results showed large geometric nonlinearity near the critical buckling eigenvalue in the form of aft wing buckling. It was concluded that nonlinear analysis is critical to correctly capture the aero-structural responses of the joined-wing configuration. The authors were also able to publish a *Journal of Aircraft* article within the same year highlighting the ability to converge onto a structurally optimized and aerodynamically trimmed conceptual joined-wing design while including these geometric nonlinearities.[8] An interesting result from these studies also showed the potential for the forward wing to buckle.

These previous computational studies have shown the importance of geometric nonlinearities and the use of nonlinear analysis for the atypical joined-wing configuration. However, Blair, Canfield, and Roberts indicated the need for experimental validation of the nonlinear structural mechanisms with the joined-wing configuration.[8] One of the first to experimentally do so was Bond (2008).

The goal of Bond's research presented in her dissertation was to experimentally validate the feasibility of including aft wing twist in the joined-wing configuration for pitch control.[9] An important aspect of this research was the consideration of nonlinear response for the con-

figuration. To meet this goal, Bond's first objective was to demonstrate nonlinear response on an aeroelastically scaled model. Her second objective was to perform a wind tunnel study of a 1:38 scale, half-span, wind tunnel model in order to determine aerodynamic forces to show that pitch control was realizable. Her final task was to validate the nonlinear response of the configuration using a 1:15 scale aluminum, half-span model in a ground based static loading test. Bond's wind tunnel study showed that pitch control was realizable through the use of aft wing twist in a joined-wing configuration. This was demonstrated by using an actuated twist mechanism in the aft wing of the model for controlled wing twist angles between $-15^\circ < \alpha < 15^\circ$. This conclusion alternatively implies, however, that if controlled aft wing twist can control pitch of the aircraft, then uncontrolled aft wing twist could have serious implications of the longitudinal stability of the aircraft. This conclusion further highlights the importance of geometric nonlinearities in the joined-wing configuration. Bond's second experiment attempted to verify the nonlinear response of the sub scale model by comparing the load-deflection curves to the full-scale model. The conclusion of this static loading experiment was that inclusion of follower-forces is important since they have significant impact on the response of this configuration. Bond summarizes one of the most important conclusions from this work: "In analyzing the results of these three tasks, one can conclude that physical experimentation is a necessary practice to undertake, especially to understand the response of geometric nonlinearities."[9] This statement emphasizes the importance for experimental research when considering geometric nonlinearities for a joined-wing configuration. As a result, the statement lends itself to the motivation of the research presented within this

thesis.

1.2.2 Experimental Efforts within CCMS

These previous computational studies and experimental efforts have greatly contributed to the understanding of the joined-wing configuration and the importance of considering geometric nonlinearities for the configuration. However, these geometric nonlinearities and aeroelastic responses have never been demonstrated in flight. In response, the AFRL requested a 1/9th scale RPV of the Boeing joined-wing SensorCraft to be constructed and flown. A 1/9th scale RPV provides a low cost and effective way to investigate these nonlinear aeroelastic responses and serves as a means to validate existing computational models with flight data.

The task of creating a 1/9th scale model of the Boeing JWSC was first investigated in a study performed by Richards.[17] He explored the feasibility of building a $1/9^{th}$ scaled RPV using common building methods, materials, and integrated supporting systems that would satisfy the scaled target mass and test point. Richards also presented a preliminary design for an initial RPV meant to demonstrate the airworthiness of the configuration. A follow-on study recognized and addressed the need to approach the flight task through a multidisciplinary methodology.[18] Along with a proposed multisciplinary framework, the paper also presented an incremental approach to flight testing, beginning with further reduced scaled models and continuing to models with increasing complexity. The knowledge gained from

these reduced scale flights would lead to the flight of a 1/9th scaled rigid model, later deemed the Geometrically Scaled RPV (GSRPV), and the design efforts of a 1/9th Scaled Aeroelastically Scaled RPV, deemed the Aeroelastically Tuned RPV (ATRPV). The GSRPV was proposed as a design meant to exhibit equivalent rigid body dynamics which provided a direct preservation of aerodynamics to that of the full scale article. Richards *et al.* (2011) presented work leading to the flight of the GSRPV, which included an outline of the design and fabrication for the GSRPV, development of the flight test plan for the vehicle, and flight results of reduced complexity models including those for mini-SensorCraft platforms that have the same outer mold line as the GSPRV.[19] Following this progression in the flight test program development, Aarons authored a thesis in which he outlined a detailed flight test plan for the GSPRV.[20] This flight test plan is the foundation of all subsequent flight test plans for the overall program and was a necessary guide in producing the two flight test plans within this thesis.[20] The first flight of the GSRPV (Fig. 1.5) took place in Foremost, Alberta on Saturday October 15, 2011 and consisted of a 7 minute 58 second flight.[21] This flight served as a proof of concept and demonstrated the ability to successfully operate the marginally unstable aircraft. From subsequent post flight analysis, several areas for improvement were identified, such as radio frequency interference, usable fuel, flight duration, and roll control gains. These concerns are considered in the subsequent flight test plans presented in this thesis.[21]

Figure 1.5: GSRPV in flight (left); After flight (right)

1.2.3 Other Experimental Efforts

Besides the internal efforts that led to the flight of a 1/9th Geometrically Scaled RPV of the Boeing joined-wing design, there exist other flight tests of joined-wing aircraft with HALE surveillance applications.

Previous to the GSRPV efforts, a flight test program was developed and implemented at AFRL for a joined-wing design model known as VA-1(Fig. 1.6).[22] The results of this work were limited to investigating the flight characteristics of a rigid model. However, the overall conclusion of its one successful flight was shown the usefulness of a low-cost flight test article when investigating concepts like the joined-wing. The overall benefit of this program prior to the flight test efforts of the Boeing JWSC RPV was the demonstration of ground based experimental techniques. These techniques, including a bifilar pendulum test were adopted and implemented successfully by Aarons[20,21] in the ground test efforts for the GSRPV. As a result, these tests are also extended into the testing efforts for the ATRPV flight test plan.

Figure 1.6: VA-1 top profile view (left); VA-1 remote-controlled joined-wing aircraft (right). McClelland, W.A., *Inetertia Measurement and Dynamic Stability Analysis of a Radio Controlled Joined-Wing Aircraft*, Master's thesis, Graduate School of Engineering and Management, Air Force Institute of Technology, 2006.(Source approved for public release by U.S. Government)

The Navy's RAVEN project also saw the development of a reduced scale joined-wing concept for surveillance missions. To the author's knowledge, the flight article completed a successful flight. The work and results, however, have yet to be published into public domain.

The joined-wing HALE concept has also been applied at a full scale. The Xianlong UAV originally debuted at the Chinese Air Show in 2006 as a joint venture of the Guizhou Aviation Group and the Chengdu Aircraft Design Institute. The original concept exhibited a similar design to the RQ-4 Global Hawk with a similar mission profile. This aircraft completed successful flight in 2009.[23] Recent update to the Xianlong has produced a joined-wing variant. This is the largest known joined-wing aircraft to have been built to date, with an estimated 25 m (82 ft) wing span. To the author's knowledge, the aircraft has yet to see flight.[24]

1.3 Organization

Due to the success of the initial flight operations for the GSRPV, it was decided to proceed to the next phase of the flight test program which involves designing a new set of aeroelastically tuned lifting surfaces and re-winging the aircraft. The research in this thesis reflects the efforts and progress towards an ATRPV to display geometric nonlinearities in flight.

This thesis will begin with an overview of the program (Chapter 2) including the overall collaboration involved. The primary body of this thesis includes experimental investigation and validation of design considerations for the next phase ATRPV (Chapter 3). The experiments performed were ground based static loading tests on the as-built GSRPV, for which the results provided a direct path to realizing the next phase ATRPV. Following the ground-based static loading tests is a description and walk through of the next phase flight test plans which includes plans for a Mini SensorCraft flight program and the next phase 5-meter RPV (Chapters 4). It was decided to implement a Mini SensorCraft flight program prior to the ATRPV efforts in order to incrementally investigate dynamic implications of introducing flexibility into the RPV structure. Furthermore, the Mini SensorCraft flight program provides the ability to investigate flight maneuvers to achieve appropriate loading of the RPV but on a reduced risk platform.

This thesis contains two proposed flight test plans (Appendix C and Appendix D) following the conclusions and recommendations (Chapter 5) of the work presented in the thesis.

Chapter 2

Flight Test Program Overview

2.1 Program Methodology

Due to the unique JWSC geometry, the relative large scale of the RPV, and the challenge of fabricating aeroelastically scaled, flight worthy components, the JWSC Flight Test Program was divided into two distinct phases: a flight demonstration program, and an aeroelastic response program. The flight demonstration program involved the conceptual design of a Geometrically Scaled RPV (GSRPV) with equivalent rigid body dynamics (i.e. preserved aerodynamics, overall mass, and moments of inertia, but no aeroelastic scaling).[21] The design efforts included: defining construction methods; flight test instrumentation selection and integration; control system tuning; and, flight test program development. The flight demonstration program further involved the construction and flight testing of several

preliminary models to determine flying qualities and trim requirements.

The flight test program will conclude with the completion of the aeroelastic response program which is currently being undertaken. The aeroelastic response program involves the construction and development of an Aeroelastically scaled RPV, and a second flight test program. The goal of this work is to design a second wing set that could be swapped onto the geometrically scaled aircraft. Once the design is completed, the aeroelastically scaled aircraft will be flight tested to quantify the nonlinear response of the aircraft experimentally in flight.

Modeling efforts towards aeroelastically scaling the configuration supplied by Boeing has determined that the resulting RPV would be overly stiff. There is a concern that this stiffness would cause the geometric nonlinearities to be of a magnitude that is too difficult to measure in flight. Determining deflections in flight using strain gages, accelerometers, or photographic measurements will likely be noisy due to effects such as turbulence and aircraft dynamics.

2.2 Collaboration

The major organizations involved in this project are Virginia Tech, The University of Victoria (UVic), Quaternion Engineering Inc., the Canadian Centre for Unmanned Vehicle Systems (CCUVS), and the AFRL/ Virginia Tech/ Wright State Collaborative Center for Multidisciplinary Sciences (CCMS) at Virginia Tech. A project organizational chart is presented below (Fig. 2.1). The conceptual JWSC design being investigated is a Boeing design.

Boeing, however, is not directly involved with the overall project.

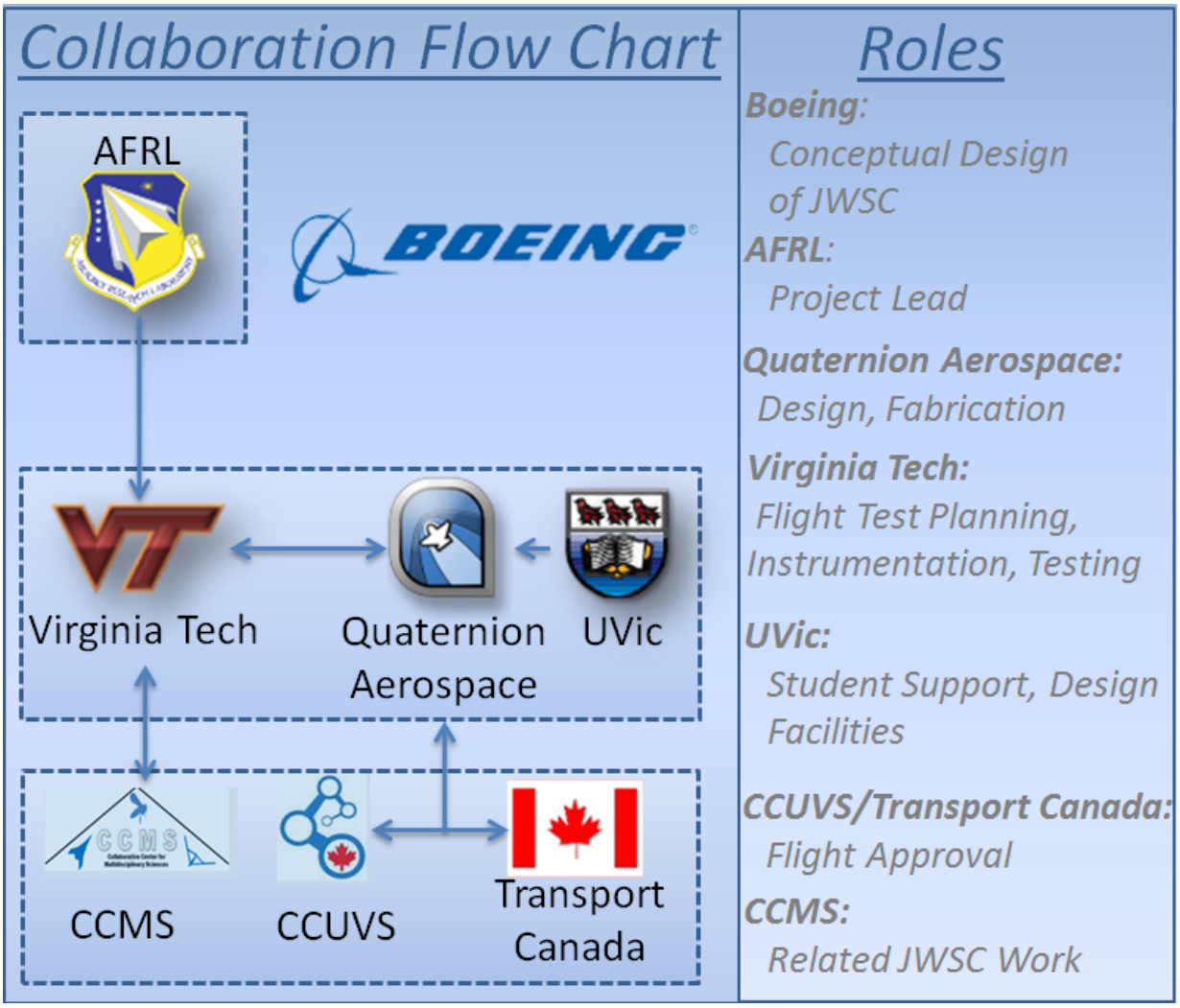

Figure 2.1: Full Scale SensorCraft Mission Profile

The AFRL is the lead test organization (LTO) interested in investigating the geometric nonlinearites of the Boeing JWSC. As the LTO, the AFRL provides funding and guidance for the project. AFRL contracted Virginia Tech as a primary contractor to perform this investigation. As the primary contractor, Virginia Tech subcontracted to Quaternion Aerospace. This partnership allowed Virginia Tech to focus on overall flight test development while

Quaternion Aerospace focused on the design, fabrication, and manufacturing of the RPV. Quaternion Aerospace are subsequently the owners of the test articles. UVic employs the founders and employees of Quaternion Aerospace. Furthermore, UVic provided student co-operative program student employee support and design facilities. CCUVS is a participating test organization, and provided support for the execution of all planned tests. Quaternion Aerospace worked with the CCUVS to obtain flight approval from Transport Canada in order to fly in Canada. Lastly, CCMS is a collaborative center with research groups at Virginia Tech, Wright State, and the University of Maryland. The work within the CCMS consists in part of developing tools for multidisciplinary analysis and design optimization for advanced flight vehicles. This includes HALE aircraft, supersonic vehicles with long range capability, and, prior to 2013, flapping wing micro air vehicles. A large component of the CCMS research taking place at Virginia Tech is focused on the JWSC concept spanning from computational research concerning the aeroelastic response of the JWSC to the JWSC FTP.

Chapter 3

Aeroelastically Tuned RPV Design Investigation

3.1 Methodology

The successful flight of the GSRPV marked the completion of the flight demonstration program and the beginning of the aeroelastic response program. The primary goal of the aeroelastic response program is to experimentally demonstrate and evaluate the nonlinear aeroelastic response of the Boeing JWSC configuration in flight utilizing a 5-meter scaled, aeroelastically tuned model. To begin working towards the overall flight test goals, an aeroelastically tuned RPV design must be decided upon. Focus had been placed on determining the most evident measurable nonlinearity in the joined-wing configuration and tailoring the

structure to accentuate this aeroelastic response. Previous static loading results of the existing GSRPV indicated to the possibility of nonlinear structural response under high loads.[20,21] Specifically, results showed the slope of the boom deflection curve decreased as the loading was increased. Thus, it was prudent to investigate the possible structural nonlinearities of the already manufactured GSRPV. To do this, a comparison between developed finite element (FE) models of the GSRPV and more in-depth experimental static load testing were completed to validate potential nonlinear behavior. Fig. 3.1 below presents a three-phase framework employed to investigate the potential nonlinear behavior and the subsequent course of action to be taken for designing the ATRPV.

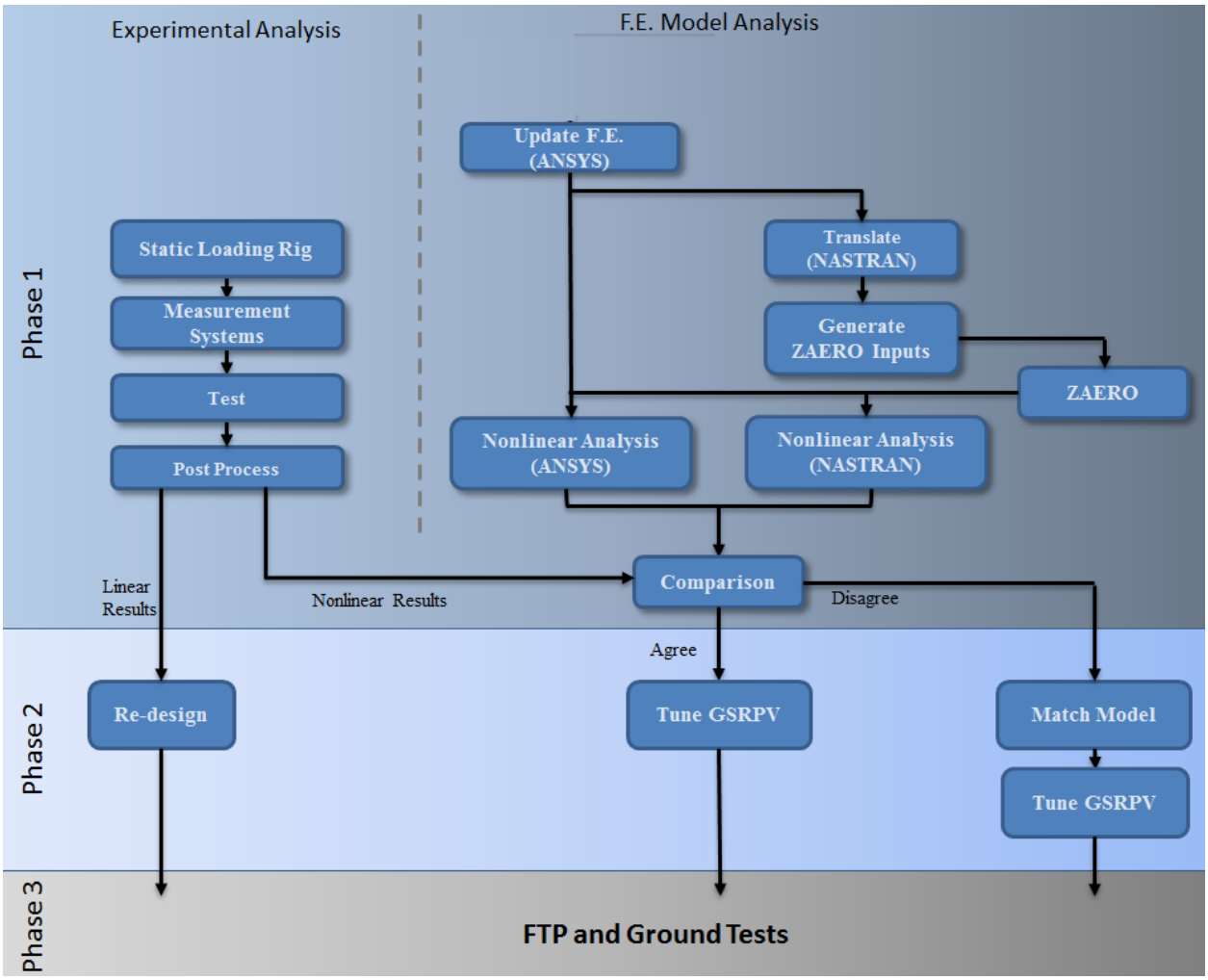

Figure 3.1: Aeroelastic response program design path flowchart

Pertinent to the success of this strategy was the ability to calibrate or match the high fidelity FE models, both in ANSYS and NASTRAN, to reduce the error between the actual GSRPV and FE models during comparison. The first step for the presented response program flowchart was to compare the high fidelity FE models with experimental deflections of the GSRPV under prescribed loads and then calibrate these models to better match the experimental results. This process is shown in phase 1 of Fig. 3.1. The calibrated high

fidelity FE models would produce input modes for a ZAERO model, which would be used to determine aeroelastic response, trim conditions and flight loads.

Using the calculated trim conditions and resulting flight loads from the ZAERO model, nonlinear analysis for both high fidelity models could be performed. In parallel, the calculated flight loads would be used in an experimental static loading case which could provide results to further validate the computational models and ensure that the article could safely handle desired flight loads. Comparing the results from ANSYS, NASTRAN and the static loading of the GSRPV has guided the project into phase 2 and the subsequent design path for the follow-on ATRPV.

The insights gained from these computational models and experimental results guided the project in the appropriate design path required to demonstrate nonlinearities in flight. There were three possible design options presented in phase 2:

1. If static loading resulted in linear deflections, a re-design of components would commence;

2. If experimental loading tests and FE models agreed in nonlinear deflection results, the GSRPV platform would be used for follow-on flight test efforts; and,

3. If the experimental loading tests showed nonlinearity but FE models did not, the models would be further calibrated to match experimental results and the GSRPV would be used for follow-on flight test efforts.

The first design option suggested that the GSRPV platform would be overly stiff to be used as the follow-on ATRPV platform. This design path therefore provided that comparison to the FE models was not needed. The proceeding design option provided that the experimental loading results and the FE models compared well with nonlinear deflections. This would result in a further tuning of the GSRPV platform to further accentuate the existing geometric nonlinearities. The tuned GSRPV platform would then be used as the follow-on ATRPV. The final option was that the static loading showed sufficient nonlinearity but the FE models did not agree. This would require that the FE models be further calibrated to match experimental results and then a possible further tuning of the GSRPV could be performed to accentuate nonlinearities in flight.

3.2 GSRPV Static Loading Test

Having produced a logical framework, an experiment was developed to investigate the GSRPV. The static loading of the as-built GSRPV had three primary goals:

1. Provide experimental data for FE model validation;

2. Verify if nonlinearities exist in the GSRPV test platform; and,

3. Demonstrate that the structure was capable of worst case flight loads.

In order to achieve the prescribed goals, a number of objectives were developed. The first objective was to design and build a test apparatus to perform the static loading on the

GSRPV. The second objective was to determine suitable loading cases for the test. The last objective was to measure displacement at key locations along each lifting surface. It was important to obtain 3D displacement measurements of the key locations to facilitate the FE tuning to the experimental results.

3.2.1 Test Apparatus

The test apparatus in support of the static loading test was designed and manufactured in three pieces which included outer rib casings, a fuselage cage, and a loading pulley system. The first component, the outer rib casings, was designed and placed onto the forward wing, aft wing, and boom. Each rib was designed to act as the load application point; they were composed of two extruded aluminum pieces, each a quarter inch in thickness. Ten outer rib casings were placed on the forward wings in line with every other internal rib. Eight outer ribs were placed on the aft wings, again, in line with every other internal rib. Finally, two outer rib casings were placed onto the boom. Holes were placed along the forward wing outer ribs from 0-70% chord at 5% increments on top and bottom of the ribs. The aft wing outer ribs had designed holes to span 0-50% chord spaced every 10% chord on top and bottom. The holes for the external ribs applied to the boom were placed along the chord line. Furthermore, two holes were placed at 0% and 100% of the chord on each casing in case moment load corrections were needed. One primary advantage of the designed outer rib casings was the ability to apply negative loads if needed. Fig. 3.2 shows a model of the design.

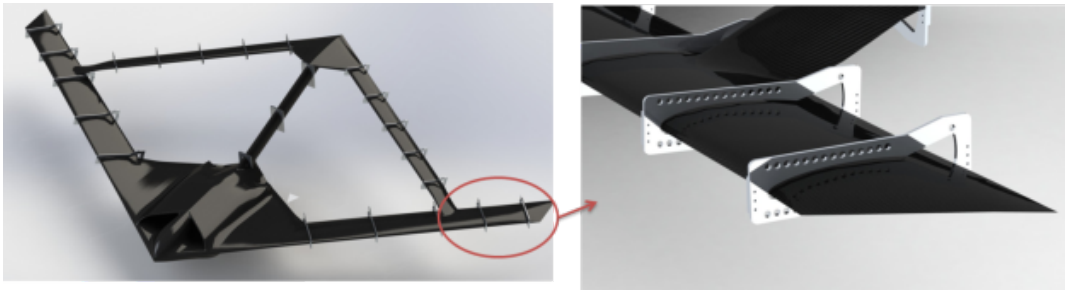

Figure 3.2: Outer rib casings distributed across platform (left); Zoomed in view at wing tip (right)

The outer rib casings were bonded to the wings to avoid shifting of the loads due to movement of the rib casings. Bonding the casings further assured that the load would be distributed evenly chordwise across the rigid internal rib and not the flexible skin. It was necessary to avoid introducing load to the skin to prevent unexpected deflection response of the wing. To bond the outer rib casings without damaging the existing wings, a bonding procedure was developed. The procedure required several bonding layers which included the following in sequential order from the wing skin out: masking tape; tuck tape; three layer fiberglass; thickened epoxy; and, finally the outer rib casing. A result of this procedure is shown in Fig. 3.3.

Figure 3.3: Aft wing outer rib attachment

The second component of the test apparatus was the fuselage cage. With a similar concept to the outer rib casings, it was composed of two half-inch thick extruded aluminum pieces. These pieces sandwiched the fuselage and provide a hard point used to bolt the fuselage to the ground. This cage prevented possible fuselage rotation during load application, which could have skewed results. The cage pieces were applied by the same bonding procedure as the outer rib casings. The fuselage cage was also designed to serve as the bifilar pendulum test apparatus. Fig. 3.4 shows a model of the fuselage cage design.

Figure 3.4: Fuselage cage with steel bracket

The final component of the test apparatus was the load transfer pulley system (Fig. 3.5). Two pulleys transferred the load from a weighted bucket to a specific rib location. The weight was incremented using measured buckets of water. This provided versatility in weight increments without additional costs. Finally, a custom built wooden frame was placed over the GSRPV which provided an overhanging structure to support and transfer the load.

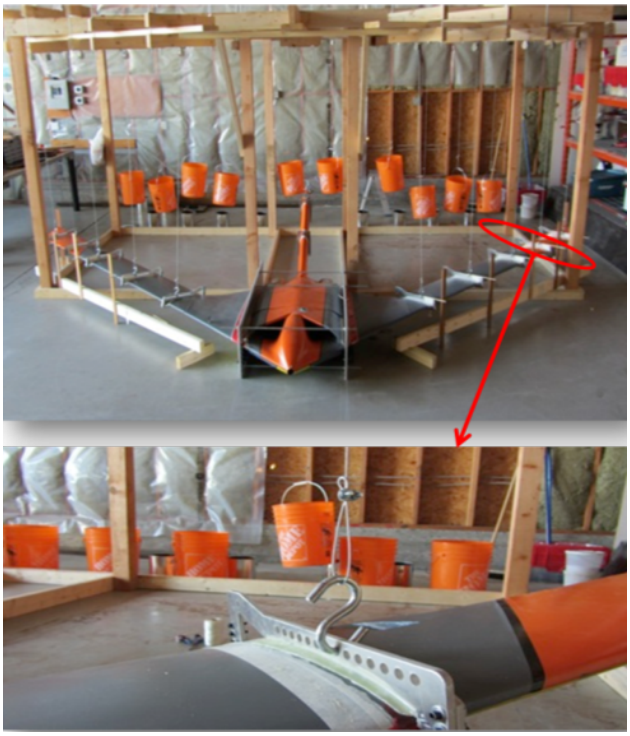

Figure 3.5: Pulley system (top); Zoomed in view of attachment to outer ribs (bottom)

3.2.2 Vehicle Test Configuration and Load Profile

The vehicle used for the static loading test was the GSRPV with and without the aft wings attached. The outer rib locations corresponding to the load locations, and subsequently the deflection measurement locations, are defined in Fig. 3.6. The rib locations are symmetric on both the left and right sides of the aircraft with the same marker indication.

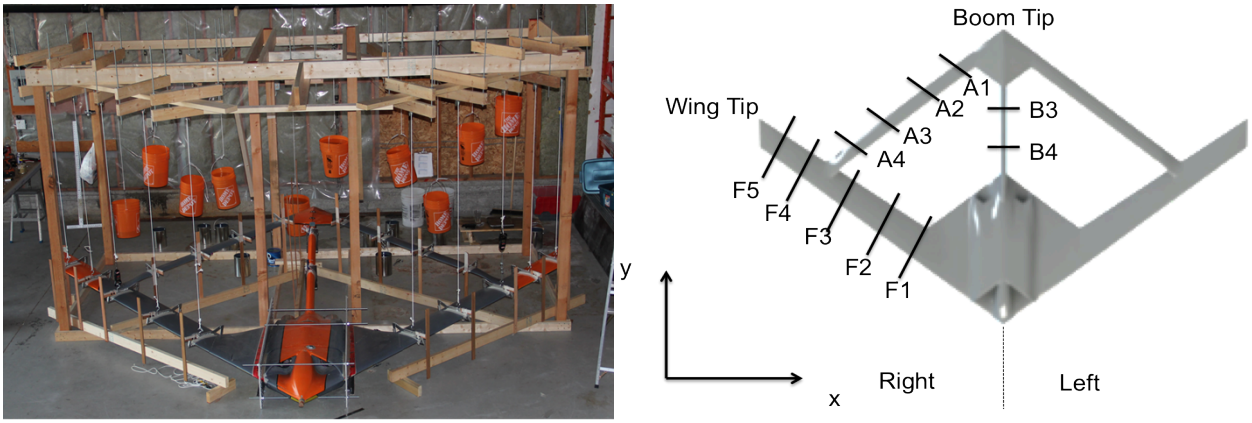

Figure 3.6: Load and measurement locations

Three types of loading tests were completed to investigate the vehicle. The first loading test placed positive point loads symmetrically at the F5 outer rib casing at 30% of the chord while the aft wings were not attached. The first loading test focused on obtaining deflection data of the forward wing using a symmetric point load application on each side of the RPV. The objective was to decouple the influence of the aft wing as a means for component independent tuning of the FE model. The test was repeated using the F3 location as well. Measurements were taken along the forward wing at each outer rib case location and each wing tip. The second loading test focused on applying positive loads to the boom (B3) and measuring the response at each rib location along the boom as well as the boom tip. The GSRPV was again configured without the aft wings attached in order to achieve component independent tuning of the FE model. The last test focused on applying a span-wise loading distribution based on a 3g push-over pull-up maneuver. The load distribution was calculated using a vortex lattice code.[17] The distribution was then discretized and mapped as point loads to each outer rib case location which provided an experimental loading

case representative of the computed span-wise loading. The loading was incremented by 20% of the 3g load for a total of 5 load increments. This final load case was calculated based on the as-flown configuration of the GSRPV (67 kg, 41% static margin).[21] A summary of the test configurations as well as the loading profiles are shown in Tables 3.1 and 3.2 .

Table 3.1: Point Load Increments for GSRPV Static Loading Tests

Load Step	F5 Load,(kg)	F3 Load, (kg)	B3 Load, (kg)
0	0	0	0
1	2	2	3
2	4	4	6
3	6	6	9
4	7	8	12
5	8	10	15

Table 3.2: 3g Maneuver Load Case Profile

		Load Step, (% of 3g load)				
		0.2	0.4	0.6	0.8	1
Load Locations	F1	4.18	8.36	12.54	16.72	20.9
	F2	3.79	7.58	11.37	15.16	18.94
	F3	3.08	6.17	9.25	12.34	15.42
	F4	1.57	3.14	4.72	6.29	7.86
	F5	0.96	1.92	2.88	3.84	4.81
	A1	-0.07	-0.14	-0.21	-0.28	-0.35
	A2	-0.73	-1.47	-2.2	-2.93	-3.66
	A3	0.05	0.11	0.16	0.22	0.27
	A4	0.12	0.24	0.36	0.47	0.59

3.2.3 Test Instrumentation and Test Procedure

For the static loading tests, it was important to obtain movement of a point in 3D space for better comparison to FE analysis. To obtain the 3D travel of a single point, precision calipers and laser pointers were used at each outer rib location. Each rib casing had a laser pointer placed onto it, where the laser projected onto a cedar lath located ahead of the leading edge of the outer casing. For each load increment, the travel of the laser was marked on the vertical lathing, and thus provided the x and z motion. The y coordinate travel was obtained by measuring the distance between the vertical cedar lath marker and the outer rib casings for each loading test. Deflection could be calculated by taking the difference between an undeflected reference point and each measured 3D change for each load step. A mock-up of the measuring technique is shown in Fig. 3.7.

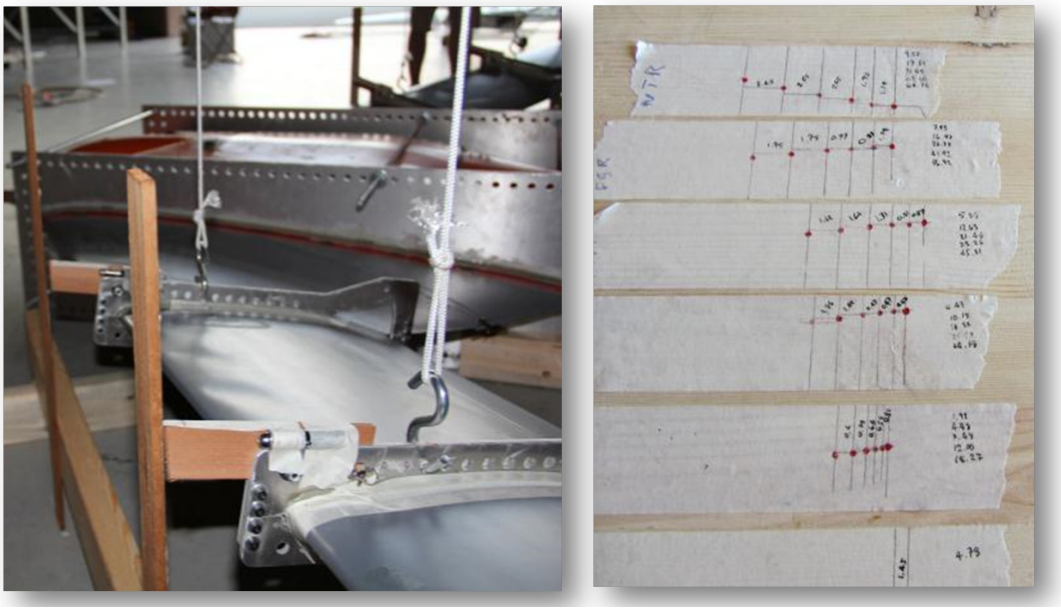

Figure 3.7: Mock setup of measuring technique (left); Captured x and z travel of single point at various measuring locations

3.2.4 Results

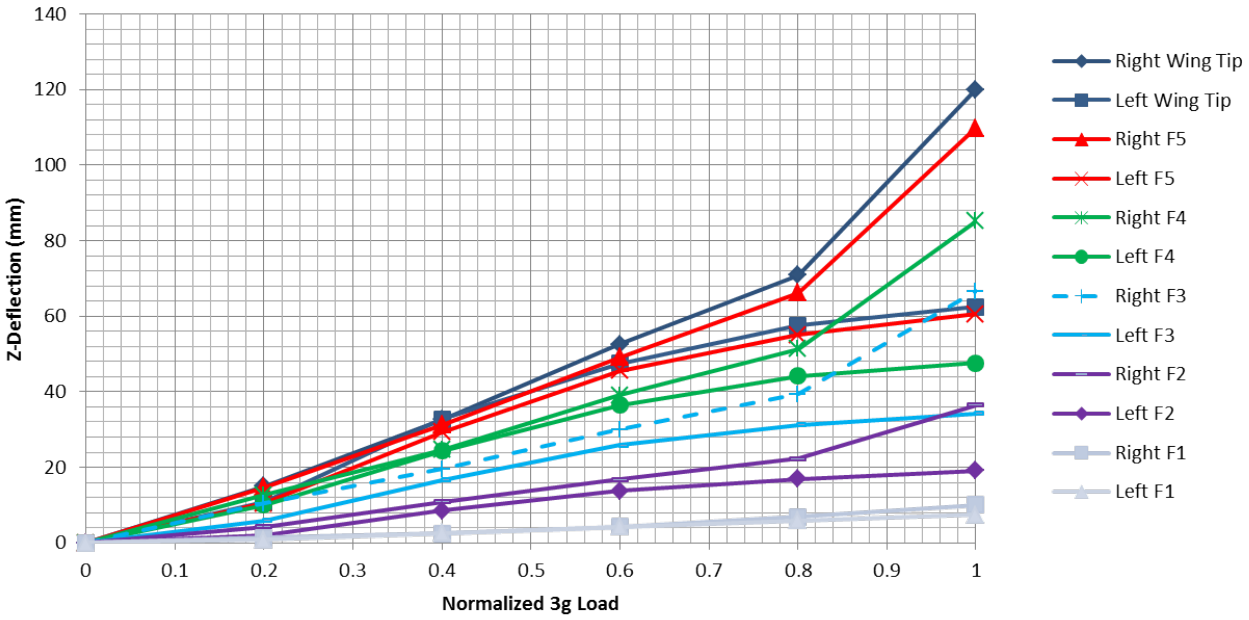

Figure 3.8: Z-deflection results along forward wings for 3g load case

The first results presented (Fig. 3.8) are the right and left forward wing deflections for the 3g distributed load test. Results indicated an asymmetric trend in the structure as the loading increased. Specifically, as the loading increased, the right wing deflection was typically larger than the left wing. It was suspected, based on Fig. 3.8, that the load case was asymmetric due to unaccounted friction in the pulley system. The results suggested that the right half of the RPV experienced a higher loading, resulting in a large positive z-deflection. Furthermore, due to the joined-wing configuration, the asymmetric load was transfered through the aft wings causing the left forward wing to experience a decreased rate of positive z-deflection. This load transferring was most apparent from the 0.8 to 1 load step for the wing tip deflection measurements. These measurements indicated the right wing experienced a large increase in deflection while the left wing experienced a decrease in deflection slope. Taking the uneven loading into account, the trends indicated a rather linear response, meaning the existing GSRPV would be too stiff to produce a nonlinear aeroelastic response in flight. The resulting asymmetric loading behavior of the vehicle was also captured in the aft wing measurements for the 3g distributed load case and during the point load tests of the forward wing without the aft wings. While loads were verified throughout each experiment with the inclusion of scales in-line with each pulley line, and the fuselage was monitored for any sign of rotation during each load increment, the discrepancies remained. The results of the aft wing and forward wing point load tests are presented in Appendix A.

The final test performed was the loading of the boom alone. These results are presented

below in Fig. 3.9 and 3.10. As seen in Fig. 3.9, each measured location along the boom exhibited a linear response in deflection with loading. Each linear regression produced an R^2 of at least 0.99 which further confirms the linearity. Fig. 3.10 presents the loading response at each measurement location. The results indicated that a linear response existed for each load case for the deflection of each measurement location. This result confirmed that all compliance in the boom movement originates directly from the boom/fuselage joint connection and that the boom was stiff along its length.

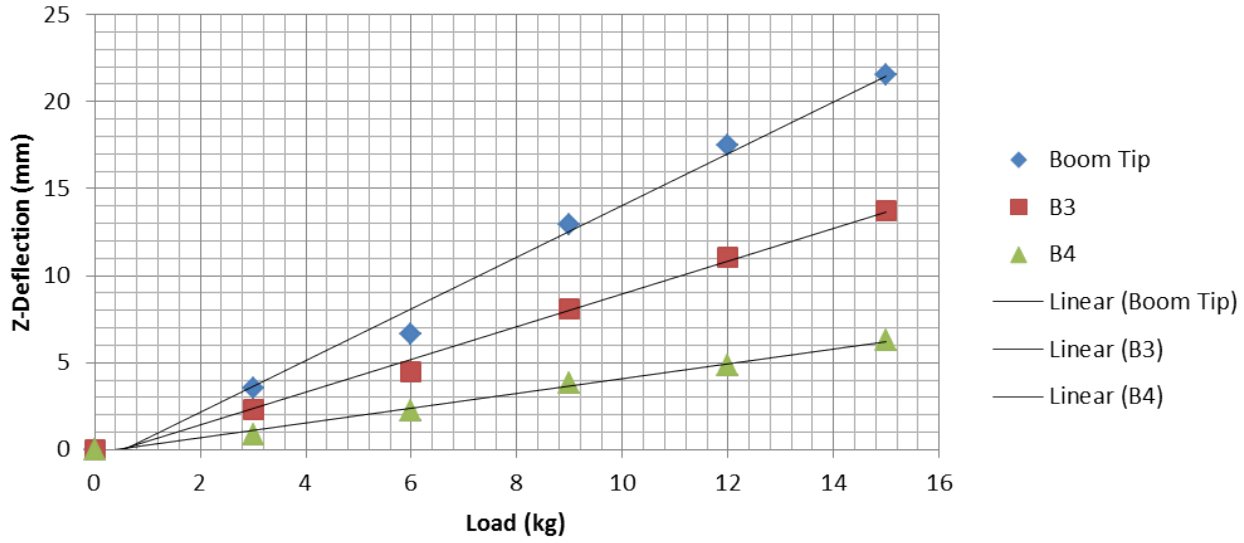

Figure 3.9: Boom z-deflection results for load applied at B3 (no aft wings)

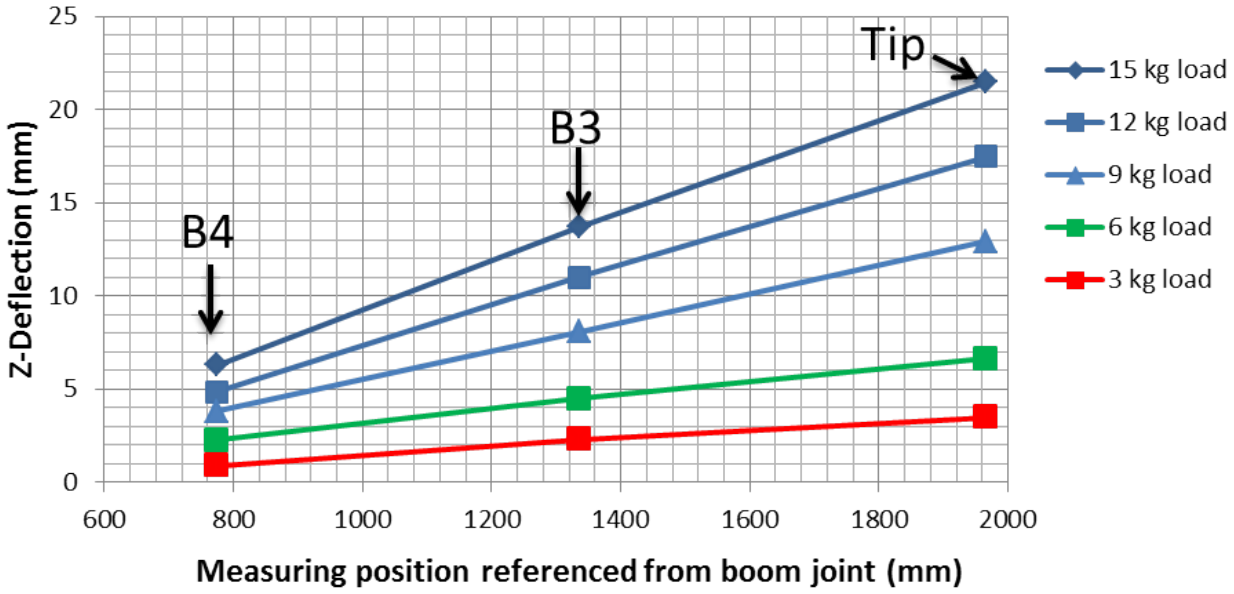

Figure 3.10: Z-deflection results for each measuring location with respect to applied load (no aft wings)

3.2.5 Conclusions

The objective of this experimental investigation was to determine the feasibility of using the existing GSRPV platform to investigate the nonlinear response of the joined-wing configuration in flight. The results of the GSRPV static loading tests showed considerable asymmetric loading of the vehicle, especially at higher loads. This was a result of the loading apparatus and the unaccounted friction in the pulley system. A redesign of the loading apparatus would provide more accurate results. However, despite asymmetric results, it was determined that the trends indicated a rather linear response, meaning the existing GSRPV would be too stiff to produce a nonlinear aeroelastic response in flight. As a result, the findings suggested that the subsequent action to take was a re-design of flight worthy

components for the ATRPV.

Despite discrepancies in the loading tests of the forward and aft wings, the loading test performed on the boom alone indicated a linear response to incremented positive loading. Furthermore, it was shown that all compliance and movement of the boom occurred at the boom/fuselage joint connection. Should the boom remain the same for the follow-on ATRPV design, the movement of the boom due to the compliance of the boom joint is important to consider when tuning the FE models.

3.3 ATRPV Design

Having determined the GSRPV was overly stiff to demonstrate geometric nonlinearities, efforts shifted to the design of flexible components. In order to achieve a response for the ATRPV that demonstrates geometric nonlinearities, initial design efforts were focused on introducing flexibility along the length of the aft wing. This required a complete redesign of the aft wings for the JWSC RPV. The initial proposed design involved an aft wing consisting of a flexible internal ladder structure that would act as the main load bearing entity within the aft wing.[25] A series of aerodynamic shells are used to define the outer mold line of the aft wing, but since they are attached to the internal structure at only one point, they do not carry any of the structural loads (Fig. 3.11).[25]

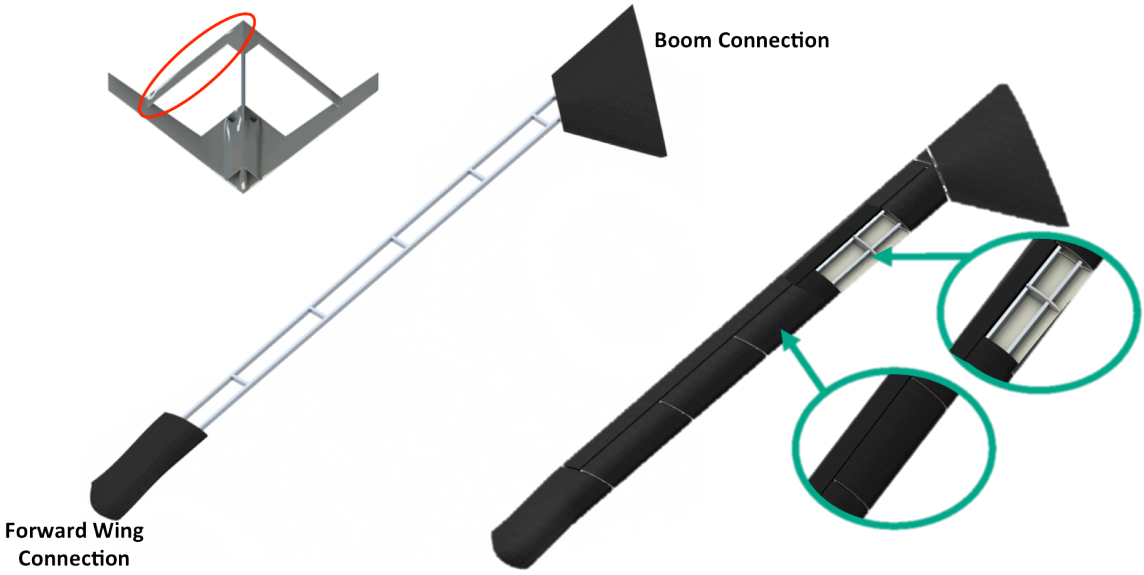

Figure 3.11: Proposed aft wing internal structure (left wing); Proposed aft wing nonstructural aerodynamic shells (right wing)

The shallow cross section of the ladder ensured that large deformations of the aft wing were possible without causing failure in the extreme fibers of the beam. This ladder model was parameterized and subsequently optimized. The model was attached to a tuned beam representing the forward wing such that it matched the structural response of the as-built GSRPV wing. Optimizations show that an aft wing design is possible that will exhibit sufficient nonlinear response.[25]

The redesign of the aft wing has assumed that the forward wing used for the GSRPV would remain the same. The introduction of a more flexible aft wing into the JWSC configuration has implications on the forward wing, however, since the forward wing becomes the true load bearing entity. It was important to know the structural limitations of the forward wing as this value could constrain the design space. It was therefore decided that the forward

wing root bending moment would be used as a measurable failure criterion for the forward wing constraint. Using the ANSYS Mechanical software package, a high fidelity finite element (FE) analysis was completed in order to investigate maximum root bending moment of the forward wing (without aft wing). Aerodynamic loads representing flight maneuvers to be used in flight to investigate the nonlinear aft wing response were used as the basis for the loads of the FE analysis.[25] The FE nonlinear results showed local panel buckling of the spar cap at a location on top of the wing near the root. At this location, failure was predicted in the fifth layer, which was unicarbon, along the interface of the buckled panel and the vertical shear web. The failure mode was normal strain in a direction 90 degrees from the orientation of the unicarbon. The predicted load at which this occurred was 241 N which corresponds to a root bending moment (RBM) of $1.43x10^5$ Nm (equivalent to 37% of the required design limit load). The maximum root bending moment the forward wing can sustain was placed onto the design space as shown in Fig. 5.[25]

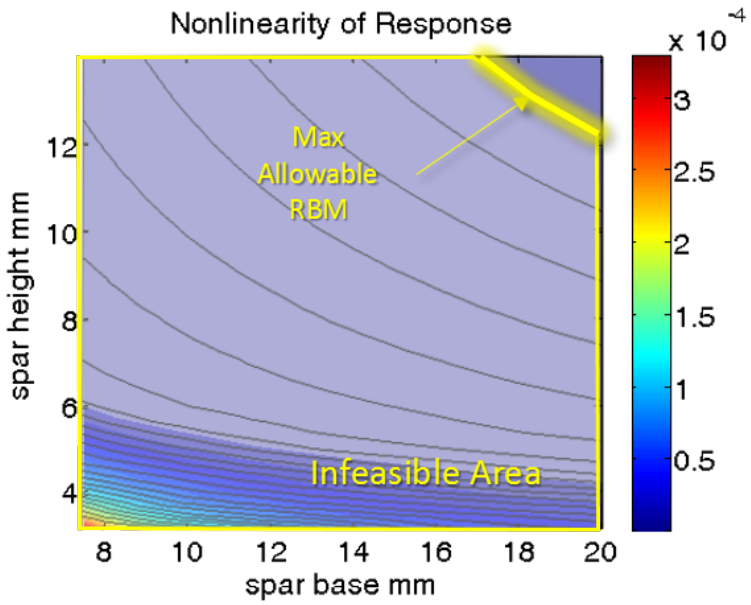

Figure 3.12: Design space showing infeasible region bounded by the forward wing's RBM load limit

The contour plot (Fig. 3.12) represents a quantitative measurement of the degree of nonlinearity of the aft wing response as a function of the aft wing ladder structure geometry. The level curves represent constant values of the RBM required to be carried by the forward wing. The yellow line represents the constraint imposed by the limit load of the current forward wing based on the predictions of the FE analysis.As seen in Fig. 3.12, the optimal region for nonlinearity is within the left most corner for a design spar height of 4 mm and a spar base of 8 mm. However, Fig. 3.12 shows that this area is infeasible due to the inability of the forward wing to support the required loads. In fact, it is likely that any feasible aft wing design will not exhibit sufficient nonlinearity to be effectively measured in flight. While this forward wing was sufficient to carry loads in the GSRPV, which was supported by very rigid aft wings, these FE results predicted that the wings were not capable of supporting

the loads required if a sufficiently compliant aft wing was chosen. In order to validate and potentially update these models, it was required to experimentally validate these results using strain and deflection measurements in an experimental setup.

3.4 Cantilever Tests

Despite the efforts to capture as much detail as possible in the FE model, many unknowns were introduced in the manufacturing process. For instance, the size and location of fillets were not fully known as they are contained within the sealed wing. Uncertainty in the manufacturing may also be a factor as the final orientation of the carbon fiber layers may vary from manufacturing specifications. Additionally, some uncertainty remains in the modeling of material properties as some data was not supplied by the manufacturer and no experimental data existed that completely characterized the laminate properties. In an effort to validate the predicted results of the FE analysis, a ground based static loading test of the existing RPV platform without the aft wings attached was completed. The test focused on evaluating the strains and deflections of the existing forward wing while loaded. The testing goal was to validate the FE analysis presented. The objectives of the test to meet the overall goal were as follows:

1. Obtain deflection measurement of forward wings;

2. Measure strains on forward wings in the area of interest;

3. Determine in-plane major and minor principal strains; and,

4. Compare resulting principal strains and deflections to FEA results.

3.4.1 Test Apparatus

The cantilever test used a three-component test apparatus comprised of: an overhanging mezzanine structure to provide the hard points for loading; a turnbuckle system to apply the loading; and, a restraining fuselage cage to impose fixed boundary conditions on the vehicle. A digital scale was placed in line with the turnbuckle system to verify the load applied to the structure. Fig. 3.13 shows both the mezzanine and the turnbuckle system. The last component of the test apparatus was the same fuselage cage used for the GSRPV static loading efforts.

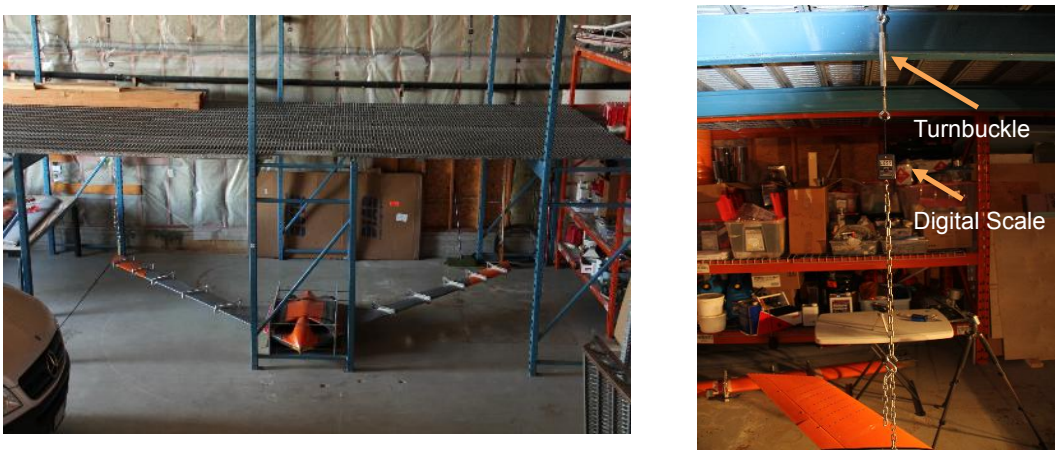

Figure 3.13: Mezzanine structure with RPV in test configuration (left); Turnbuckle system (right)

3.4.2 Vehicle Test Configuration and Load Profile

The vehicle used for the cantilever tests was the GSRPV without the aft wings attached (Fig. 3.13). A point load was applied which produced a root bending moment at the forward wing/fuselage connection point. The point load was applied symmetrically on each wing at the forward wing/aft wing connection. This location was chosen because a through-hole already existed, which allowed for an easy attachment point. Furthermore, this location avoids compromising the forward wing structure due to fabrication of an additional attachment point which could potentially alter the response of the wing under load.

Finite element analysis (FEA) showed that first ply failure occurs in layer five of the unicarbon at 37.5% of a 3g aerodynamic load distribution. To avoid potential damage to the wing, the final load step was set at 25% of the 3g load. This percentage corresponds to a safety factor of 1.5 from the failure percentage of 37.5%. A load case profile was then determined and is shown in Table 3.3. Zero load step includes gravity.

Table 3.3: Point Load Increments for Cantilever Tests

Load Step	**Load (kg)**
0	0*
1	4.22
2	8.44
3	10.55
4	12.66
5	14.77
6	16.88

*** Includes force of gravity**

3.4.3 Test Instrumentation

The two measurements of interest included strain measurements of the wing box area in the forward wing, and deflection measurements of the forward wing. The deflection measurements were taken for both forward wings at the wing tips and at the leading and trailing edge of the forward wing root (Fig. 3.14). A ruler was used to mark the deflection measurements of the wing tips while four deflection dial gages, each with a 1 inch range and 0.0005-inch graduation, was used for the root measurements.

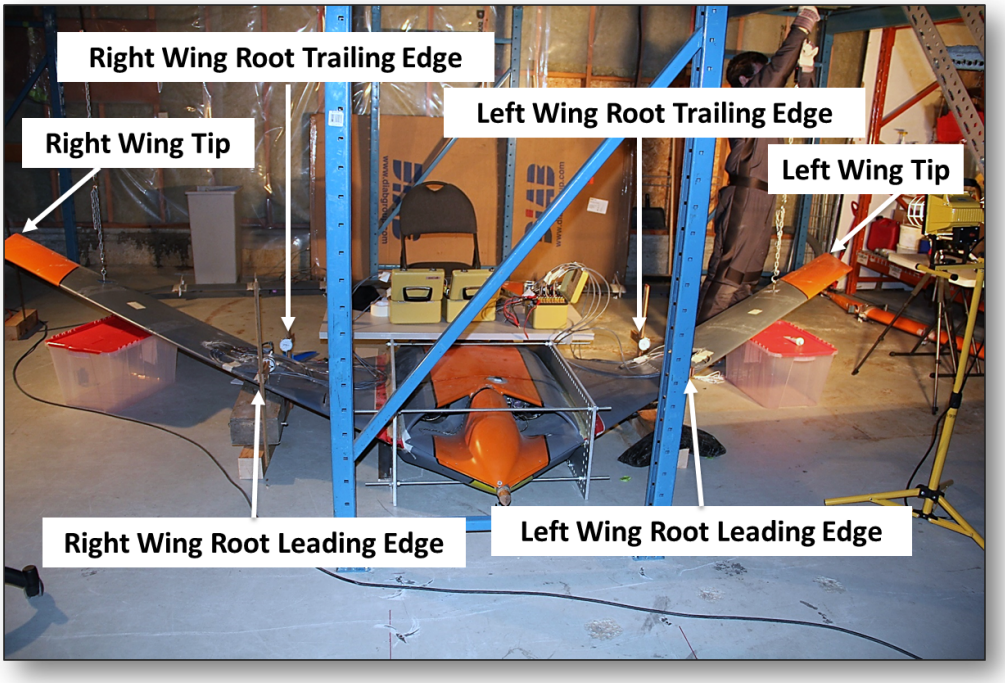

Figure 3.14: Deflection measurement locations

Rectangular strain gage rosettes were used for the strain readings for the forward wings. The rosettes chosen were all model CEA-03-250UR-350 from Vishay Micro-Measurements (Fig. 3.15). The three element rosette was chosen because the wing was subjected to a biaxial strain state, and, more importantly, the principal strain directions were unknown. Utilizing a rectangular rosette allowed for placement of gages without worry of matching principal strain directions, thus alleviating the potential of misalignment error for the strain readings. Gage placement, however, was still a critical decision due to differences in where the areas of failure occurred according to the FEA and as-built wings. One concern was in the modeling of a fillet region within the wing. The fillet region was a region of epoxy and glass microspheres that were smoothed into the fabricated wing to connect the foam spar

cap to the wing skin layers. The thickness of this area was undocumented for the fabricated wings and thus could have been a potential issue in strain comparisons as it has implications on where the maximum strain could have occurred along the area of interest. A further potential problem was that the wing skin was composed of five layers and the ply failure was occurring in layer five, which is of uni-carbon material. Placing the gages onto this layer would have caused unrepairable damage to the forward wing. The only layer accessible was the first layer of woven carbon which was under the outer layer of gel coat. To alleviate these concerns, the rectangular rosettes were placed on the woven carbon layer and all principal strains were compared for the top layer only. The gages were placed based on the areas of highest strain shown in the FEA. Three rectangular rosettes were placed in varying positions along the foam shear web and fillet interface in an effort to alleviate the uncertainty of the filleted region. The results (Section 3.4.6) present comparisons of the highest strain for the region closest to the leading edge, the highest magnitude strain in the concave depression region, and the highest magnitude strain for the region closest to the trailing edge. These regions of interest and placements of the gages are shown in Fig. 3.15. Upon final application of the gages, gages 4 and 14 were damaged and were unable to be used.

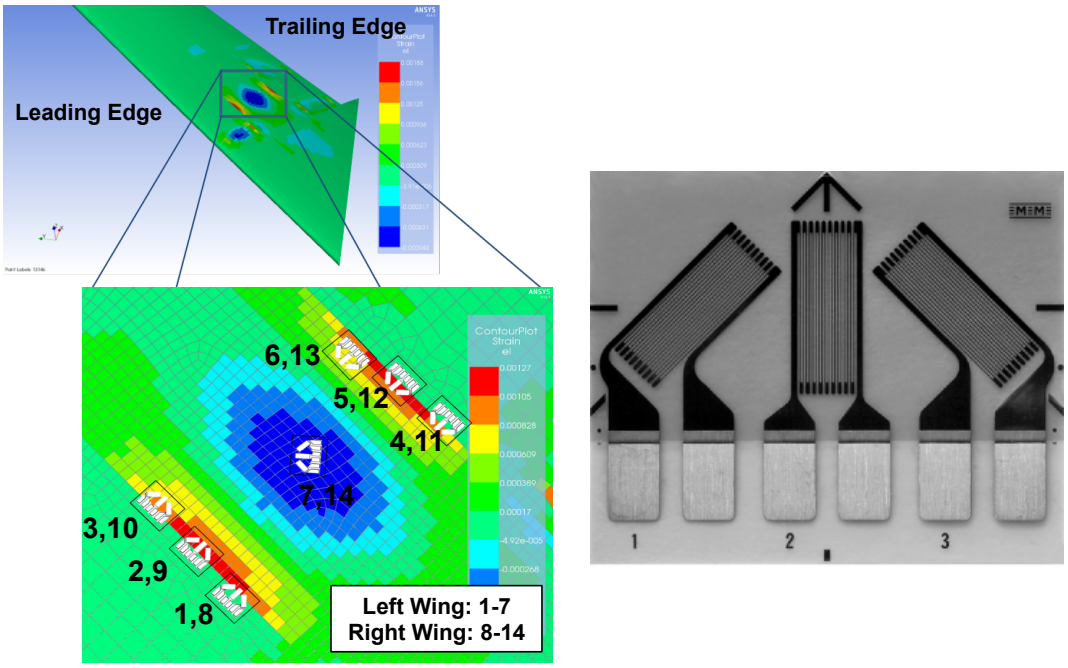

Figure 3.15: Strain gage placement on forward wings and numbering scheme(left); CEA-03-250UR-350, 3 element rectangular rosette (right)

Shielded nine-wire twisted cable was used for the connections between the strain gages and the supporting test equipment. A Vishay Mircro-Measurement P-3500 strain gage reader was used to provide the quarter bridge completion for each strain reading while a Vishay Micro-Measurement SB-10 switch and balance board was connected in series to allow up to three full rosette gages to be read at a time for a total of nine signals. Results of the strain gage application and the supporting test equipment are pictured in Fig. 3.16.

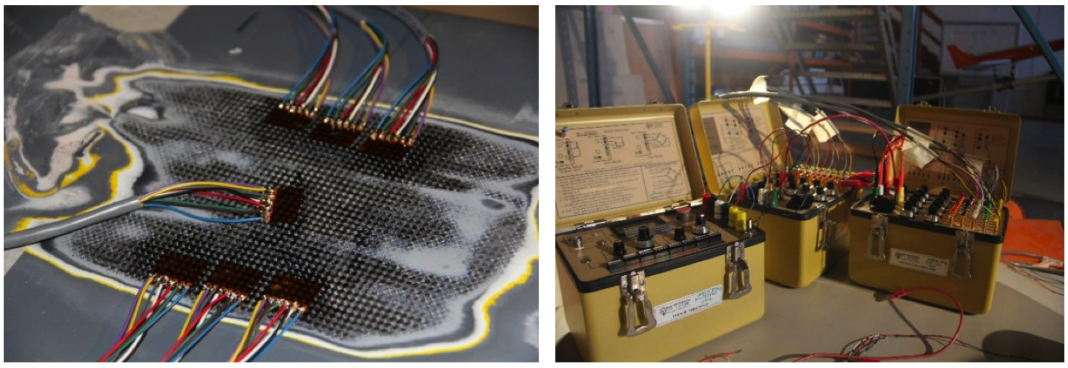

Figure 3.16: Applied strain gages on right wing (left); P-3500 strain gage reader and 2 SB-10 switch boards(right)

3.4.4 Test Procedure

Due to the available equipment for the test, only three gages were able to be measured during any one load cycle. This resulted in four loading cycles. Each loading cycle was performed with the following steps:

1. The wing being measured was taken off the vehicle and laid across a mat to place the gages as close to a zero strain state as possible.

2. The three strain gages being measured were then zeroed utilizing the P-3500 strain reader.

3. The wing was reattached to the RPV and the strain readings were then measured. This reading was comprised of the strain due to gravity and thus the gage trimming point for each load step.

4. A load was then applied to each wing symmetrically matching one of the load steps.

5. The strain at this state was manually measured for each active strain gage at the corresponding gage factor which was manually set on the P-3500 strain reader.
6. The deflection for the wing tip and root measurement points were taken.
7. The load was taken off the RPV.
8. The gages were trimmed to their corresponding strain due to gravity.
9. The load step was repeated once more to assure reproducibility.
10. Steps 4 though 8 were repeated for each load step until the full load cycle was complete.

The load steps within a load cycle are outlined in Table 3.3 shown in the *Vehicle Test Configuration and Load Profile* section. Once one load cycle was completed, the procedure was repeated until all readings were collected for all 12 gages between both wings.

3.4.5 Post Processing Procedures

The use of a three component rectangular rosette served two primary purposes. First, was the ability to determine the strain state at a particular point on the wing by calculating the principle strains. Using the principal strains alleviated the potential of misalignment error when comparing strains between the experiment and the FE results. Secondly, the specific use of a three element rosette addressed the fact that the principle strain directions were unknown. In order to obtain the principal strains from the CEA-03-250UR-350 rosette (Fig. 3.15) used within this experiment, the strain results had to first be corrected to account for

the bi-axial strain state of the material and its effect on the gage. Using the two dimensional strain transformation equations, the corrected strain results were then used to calculate the principle strains of the material.

Each strain gage in the CEA-03-250UR-350 (Fig. 3.15) configuration produces a single strain value (3 in total). However, due to the biaxial strain state of the material produced by the loading of the forward wing, each gage in the rosette is subject to transverse stretching of their respective measuring grid. This produces a small error within the raw strain output of each gage, which subsequently produces error in the principle strains. To correct the raw strain outputs, the results must take into account the transverse sensitivity of each grid (provided by the manufacturer) as well as the Poissons ratio for the material used in calibration of the strain gage (provided by the manufacturer). The equations to correct the raw output are as follows:[26]

$$\epsilon_1 = \frac{\hat{\epsilon}_1(1-\nu_0 K_1) - K_1\hat{\epsilon}_3(1-\nu_0 K_3)}{1-K_1K_3} \tag{3.1}$$

$$\epsilon_2 = \frac{\hat{\epsilon}_2(1-\nu_0 K_2)}{1-K_2} - \frac{K_2[\hat{\epsilon}_1(1-\nu_0 K_1)(1-K_3) + \hat{\epsilon}_3(1-\nu_0 K_3)(1-K_1)]}{(1-K_aK_3)(1-K_2)} \tag{3.2}$$

$$\epsilon_3 = \frac{\hat{\epsilon}_3(1-\nu_0 K_3) - K_3\hat{\epsilon}_1(1-\nu_0 K_1)}{1-K_1K_3} \tag{3.3}$$

where:

- $\hat{\epsilon}_1, \hat{\epsilon}_2, \hat{\epsilon}_3$= indicated strains from respective gage elements;
- $\epsilon_1, \epsilon_2, \epsilon_3$= corrected strains for respective gage elements ;
- K_1, K_2, K_3= transverse sensitivity coefficients for respective gage element (manufacturer); and,
- ν_o= Poissons ratio.

It is important to note the numbering scheme for the strain gage, indicated on the bottom of the gage in Fig. 3.15, as the formulation of the equations are dependent on the configuration. Having obtained the corrected values of each strain output, the principal strains can be calculated utilizing the strain transformation relationships. The strain transformation equations are based on the geometry of the deformation of deformable bodies. This relationship provides the ability to represent normal strain in any direction on a planar surface in terms of the principle strains and the angle from the principal axis to the direction of the specified strain. This relationship, and its use with rectangular rosettes, is most easily represented by the tool known as Mohrs circle (Fig. 3.17, Fig. 3.18).

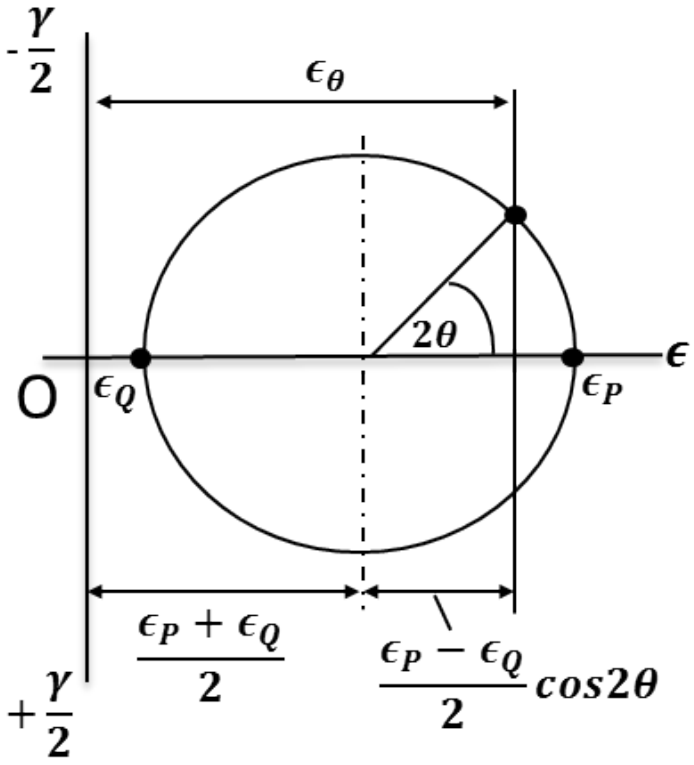

Figure 3.17: Mohr's circle representation of arbitrary normal strain, ϵ_θ, in terms of principal strains(Image adapted from source)[2]

Referring to Fig. 3.17, any arbitrary normal strain, ϵ_θ, obtained from a surface can be expressed as:[2]

$$\epsilon_\theta = \frac{\epsilon_P + \epsilon_Q}{2} + \frac{\epsilon_P - \epsilon_Q}{2} cos2\theta \tag{3.4}$$

where:

- ϵ_P, ϵ_Q= Major and minor principal strains, respectively; and,
- θ=angle normal strain is from principal axis

It is important to note for this formulation that angles in Mohrs circle are double that of physical angles. Furthermore, to calculate a result using this formulation requires knowledge of θ. Using a manufactured, three element rosette provides knowledge of the angles between the three ϵ_θ measurements of normal strain $(\epsilon_1, \epsilon_2, \epsilon_3)$. Fig. 3.18 shows a 45° rectangular rosette configuration (used for this experiment) placed on an arbitrary element and its subsequent strain representation on a Mohrs circle.

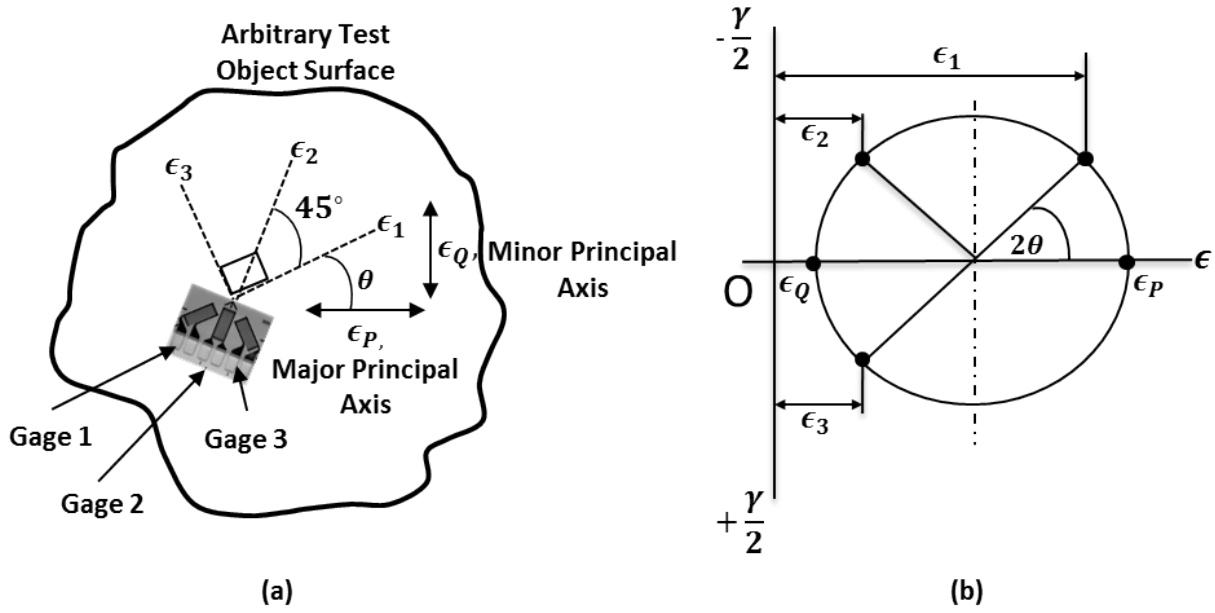

Figure 3.18: (a) 3-element rectangular rosette on an arbitrary test surface; (b) Normal strains of rosette represented on Mohr's circle(Image adapted from source)[2]

Incorporating the geometry presented in Fig. 3.18 into Equation 3.4, the three normal strains from the rosette can be calculated as:[2]

$$\epsilon_1 = \frac{\epsilon_P + \epsilon_Q}{2} + \frac{\epsilon_P - \epsilon_Q}{2} cos2\theta \tag{3.5}$$

$$\epsilon_2 = \frac{\epsilon_P + \epsilon_Q}{2} + \frac{\epsilon_P - \epsilon_Q}{2} cos2(\theta + 45^\circ) \tag{3.6}$$

$$\epsilon_3 = \frac{\epsilon_P + \epsilon_Q}{2} + \frac{\epsilon_P - \epsilon_Q}{2} cos2(\theta + 90^\circ) \tag{3.7}$$

For this experimental setup, the only known quantities are the corrected strain values on the left hand side of the equations. This yields a system of three unknowns and three equations. Solving the equations simultaneously yields,[2]

$$\epsilon_{P,Q} = \frac{\epsilon_1 + \epsilon_3}{2} \pm \frac{1}{\sqrt{2}} \sqrt{(\epsilon_1 - \epsilon_2)^2 + (\epsilon_2 - \epsilon_3)^2} \tag{3.8}$$

$$\theta = \frac{1}{2} tan^{-1}(\frac{\epsilon_1 - 2\epsilon_2 + \epsilon_3}{\epsilon_1 - \epsilon_3}) \tag{3.9}$$

Equation 3.8 is of interest for this experiment where the minimum value represents the minor principal strain, ϵ_Q, and the maximum represents the major principal strain, ϵ_P.

3.4.6 Results

The linear region of initial deflection data for the wing tips was used to calibrate a global stiffness parameter linked to material stiffnesses. This resulted in the FE and experimental deflection data matching well within the linear region. This was done based on the mentioned

uncertainties in the material properties. The deflection results are presented first for both wing tips followed by the root deflections of the leading and trailing edges for the forward wings (Fig. 3.19 and Fig. 3.20).

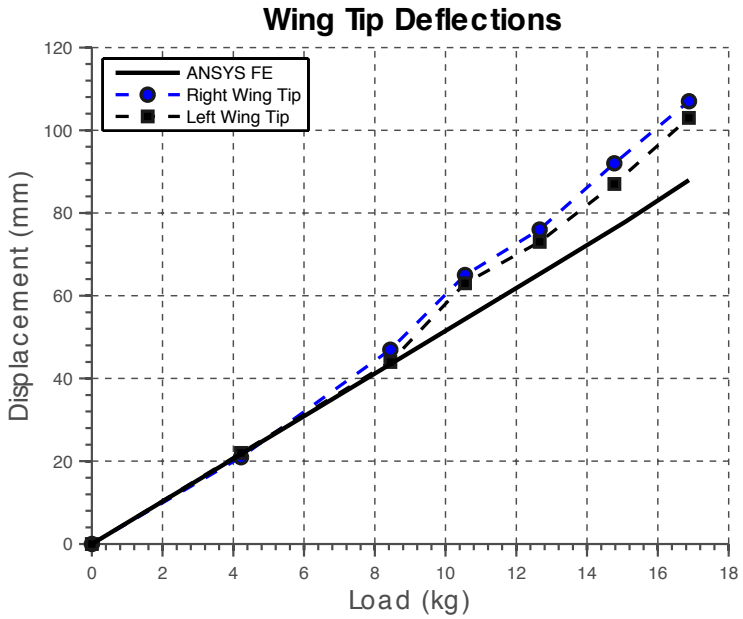

Figure 3.19: Wing tip deflections for each wing

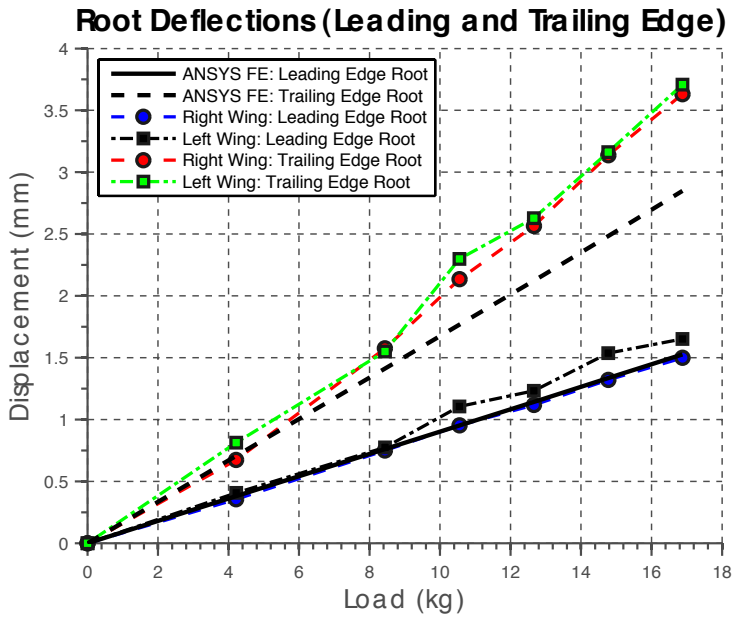

Figure 3.20: Root deflection results at the leading and trailing edges of each wing

The experimental wing tip deflections indicate a linear region up to a load of approximately 8.44 kg (Fig. 3.19). Comparing the slope of this linear region to the predicted FE model yields a difference of 5%. Some discrepancies exist at the higher load cases, but since the FE is under predicting the deflections at these higher load cases, any conclusions drawn from the FE model will likely be conservative. In other words, the FE model is likely stiffer than the actual article due to uncertainties in material properties. Similar results are shown for the root deflections (Fig. 3.20). Defining the linear region of each set of experimental data up to a load of approximately 8.44 kg, the slope of the linear region to the FE model yields a difference of 10% for the trailing edge measurements. Comparing the slopes for the leading edge region yields a 1% difference between the FE model. Some discrepancies exist at the higher load cases, which is likely due to the uncertainty in material properties and

the range of deflection at which these measurements were taken.

The following experimental results reflect strain readings for a sample of the applied strain gages. The strain gages not used in comparison efforts were strain gages 1,2, and 3 on the left wing closest to the leading edge. These gages laid along an area of the left wing where a crack had developed. This crack was visually noticeable in the paint layer but not the woven carbon layer where the gages were applied. Though the crack did not visually appear in the woven carbon layer, there was a concern that an area of high strain existed here. Post processing verified these concerns showing the strain in this area to be overly large, therefore these gage results were treated as outliers. For completeness, the results of these gages are included in Appendix B. The remaining gages were those that provided the most confidence for comparison to the finite element analysis (FEA). The FEA results shown in Figs. 3.21-3.23 represent the highest magnitude principal strains along each of the three regions mentioned in the test instrumentation section (i.e. interface closest to the leading edge of the wing, interface closest to the trailing edge of the wing, and the concave depression). Each resulting plot in Figs. 3.21-3.23 show one FE result compared to the strain gages spanning the the corresponding area of interest. The comparison to multiple gages was an effort to reduce the uncertainty in gage placement mentioned in previous sections. The principal strain results from both experimental measurement and the FEA are presented in the subsequent figures.

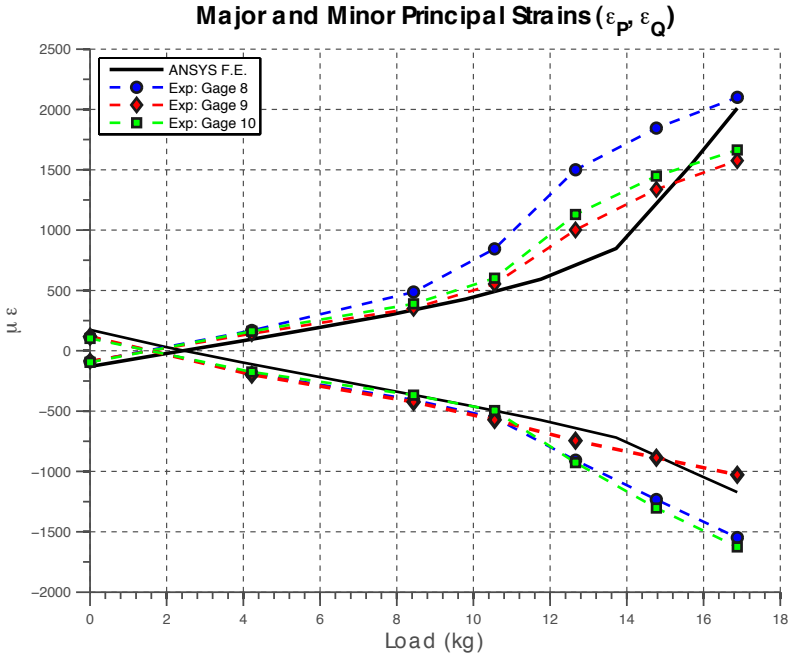

Figure 3.21: Principal strain results for the interface closest to the leading edge of the forward wing

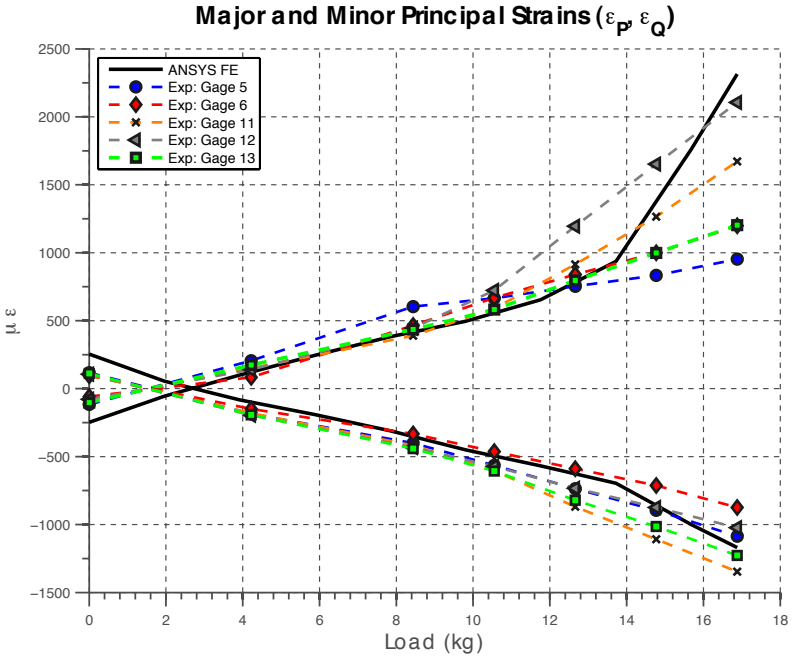

Figure 3.22: Principal strain results for the interface closest to the trailing edge of the forward wing

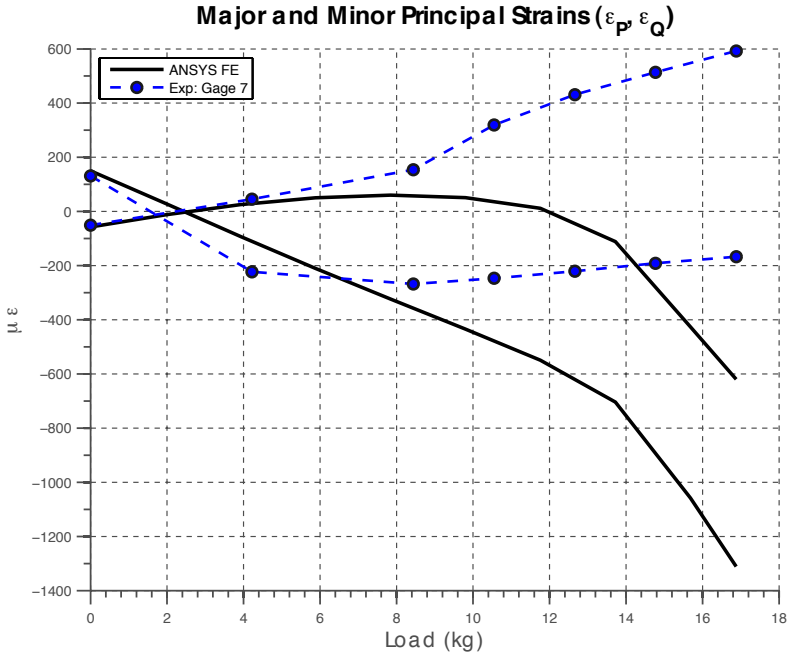

Figure 3.23: Principal strain results for the panel buckling region

The strain gages closest to the leading and trailing edges of the forward wing match well with what the calibrated FE analysis predicts, especially in the linear region at the lower loads. Here a close correlation can be seen between the slopes of the predicted and measured responses. Fig. 3.21 shows the measured and calculated strain response for the area nearest the leading edge. Again the agreement is very good in the linear region up to a load of approximately 10 kg at which point the experimental data show an increase in slope for the principle strains. This response is expected due to the nonlinear behavior of the buckled panel and its effect on the local response of the region. At a load step of approximately 12 kg, an inflection appears in the strain and the slope begins to reduce. This effect is likely due to the shifting of the local concave depression to a more inboard location, thereby moving the high strain state away from the strain gages. This phenomenon was also observed in

the FE model which predicted an increase in slope and subsequent strain relief of the strain rate. The FE results presented in Fig. 3.22 show the onset of this increasing slope at a load of approximately 14 kg. The subsequent strain rate relief characterized by a decrease in slope is not presented as it occurs beyond the limits of the plot. The gages closest to the trailing edge follow a similar trend as the gages closest to the leading edge but the inflection and subsequent decrease in slope is not as apparent. This could be a result of the spatial uncertainty with the placement of the gages should they have been placed aft with respect to the trailing edge interface of interest.

The experimental measurements from gage 7 (Fig. 3.23) did not coincide with the predicted response. This is likely due to the fact that the gage was not located in the bottom of the concave depression where the FE results were queried. This was later verified visually by observing the panel while under higher loads and noting that the gage was outboard of the desired location. This discrepancy was due largely to both spatial uncertainty of the exact location for the minimum of the concave depression at the time of applying the gages, as well as the concave depression being observed to migrate with increasing load. One useful observation can be made from the data, as it indicates the migration phenomenon of the concave depression. The data shows that up to approximately 4 kg in load, the experimental results match well with the linear region of the FE model. Following 4 kg load step, the results diverge from each other. The FE model shows a compression of the material indicating a region of concavity. However, the experimental results show the opposite effect where the material is seemingly expanding in the principal directions. Because the local concave

depression moves inboard for increasing load step, the data suggests gage 7 began in the local concave depression but was on an outboard slope of the depression after the migration of the depression inboard towards the root. This observation was again verified visually.

3.4.7 Conclusions

The objective of this work was to determine if the existing forward wing could be reused with an aeroelastically tuned aft wing to demonstrate the geometric nonlinearities that have been predicted for the JWSC configuration. A high fidelity FE model was used to determine the maximum allowable root bending moment and this value was used to constrain the design space of the compliant aft wing. The FE model predicts that the aft wing required to support the existing forward wing would have to be so stiff that the corresponding nonlinear response would be too small to measure in flight.

Because there exist uncertainties in the FE, due to unknown material properties and fabrication techniques, an experimental analysis was performed. Displacement and strain measurements were taken for the forward wing and compared to the FE results. The linear region of initial deflection data for the wing tips was used to calibrate a global stiffness parameter linked to material stiffnesses in the FE model. The FE model was then validated against measured strains. Enough agreement existed between experimental and FE data to provide confidence in the FE model. The calibrated and validated FE model predicts failure in the forward wing due to root bending moment outside the usable aft-wing design space

for the ATRPV. It is recommended that a new forward wing be designed.

Future work will involve the design of a new forward wing which is compliant enough to allow a nonlinear aft wing response while still being capable of sustaining the required flight loads. The requirement to build a new forward wing will also allow improved tailoring of the aft wing response. By not having to work within the constraints of using an existing wing, the optimization process can now tune both forward and aft wings simultaneously.

Chapter 4

Aeroelastic Response Program Flight Tests

4.1 Approach

The aeroelastic response program is the second phase in the overall flight test program (Section 2.1). Involved with this phase is the design, fabrication, and eventual flight test of an Aeroelastically Tuned RPV. The design of such a vehicle is an ongoing effort as highlighted in the previous chapter, and fabrication of the vehicle will commence once a design has been decided. However, the development of the flight test plan for the aerelastic response program was completed. It was determined that the aeroelastic response program will have two flight test plans developed: one for a Mini SensorCraft, and one for the final ATRPV. The Mini

SensorCraft is a 37% scale model of the previously flown GSRPV and, subsequently, the follow-on ATRPV.

An incremental approach to testing was instrumental to the success of the flight demonstration program. This involved the development of a series of aircraft, each of increasing complexity and risk, which were used to address a variety of key design concerns and challenges such as the marginal stability of the configuration. This approach and mindset was applied for the aeroelastic response program.

The introduction of flexibility into a $1/9^{th}$ scale RPV platform requires a sufficient understanding of the resulting dynamic responses. Specific focus must be placed on the handling quality, control (possible binding of elevator on aft wing), and the ability to capture the static nonlinear aeroelastic response. To minimize risk and increase potential for later success in the ATRPV tests, a test program was developed for the Mini SensorCrafts to investigate these potential dynamic effects. Furthermore, previous test efforts in the flight demonstration program did not perform maneuvers necessary to achieve the required loading on the aft wing to excite the nonlinear aeroelastic response. These maneuver investigation tests were written into the GSRPV flight demonstration program flight test plan (Aeroelastic Response Preparation Tests), but only as a tertiary objective.[20] A final benefit outside the primary goals of the Mini SensorCraft Flight Tests is to simulate operational procedures. Because the Mini SensorCraft will be utilizing a Piccolo autopilot (also used in GSRPV/ATRPV), the control of the vehicle and all other system utilized, including the ground station and flight personnel communication, will be identical allowing for real operational flight simulation.

Following the successful completion of the Mini SensorCraft FTP, the ATRPV FTP will proceed.

4.2 Methodology

To develop a flight test plan for both the Mini SensorCraft and ATRPV platforms, the design methodology adopted by Aarons[20] was implemented. This design methodology was based on the work of Kimberline.[27] This methodology presents a logical organization of a flight test plan based on developing the overall program goals, development of test objectives aimed at meeting those goals, development of tests to be implemented within the objectives, and establishing the metrics of success for the flight test program. This methodology is presented in the following sections for both the Mini SensorCraft FTP and the ATRPV FTP.

4.3 Mini SensorCraft Flight Test Plan

The following section highlights the overall test organization of the Mini SensorCraft FTP including the goals and objectives of the test effort. The full rough draft of the Mini SensorCraft Flight Test Plan can be seen in Appendix C.

4.3.1 Test Goals

The overall test goals for the Mini SensorCraft are aimed at providing transitional guidance for the aeroelastically tuned RPV follow-on platform. The Mini SensorCraft provides a reduced risk vehicle to investigate the introduction of flexibility along the length of the aft wing for the Boeing JWSC configuration. The Mini Sensorcraft Flight Test Plan goals are as follows:

1. Determine achievable loading conditions during flight for the follow-on ATRPV;
2. Validate safe flight characteristics with a flexible aft wing; and,
3. Investigate aeroelastic response of the flexible aft wing from flight data.

4.3.2 Test Objectives

Using the aforementioned goals as a driver, a series of primary and secondary objectives were developed. These objectives are listed below. The test (or series of tests) that corresponds to each objective is shown after that objective in parentheses.

Primary Objectives:

1. Demonstrate accurate and successful data acquisition/ logging of instrumentation system ***(Static Loading Tests, Flight Tests)***.
2. Safely demonstrate and capture geometric nonlinearities of the JWSC in flight utilizing

the Mini SensorCraft ***(Flight Tests***).

Secondary Objectives:

1. Validate appropriate nonlinear static deflection of target aeroelastic responses for three tuned flexible aft wings on the ground ***(Static Loading Test)***.
2. Validate rigid body mass moments of inertia ***(Bifilar Pendulum Test)***.
3. Verify EDF performance ***(Static Thrust Testing.)***
4. Validate control surface deflections and mixing ***(System Calibration Test)***.
5. Validate appropriate flight critical system communications ***(EMI/RF Test)***.
6. Accurately tune Piccolo SL Autopilot ***(Simulation)***.
7. Verify control hierarchy and fail safe scenarios ***(Safety Tests)***.
8. Verify appropriate take off procedures ***(Launcher Test)***.

Tertiary Objectives:

1. Perform flight maneuvers with full autopilot ***(Maneuver Control Investigation Tests)***.

4.3.3 Metrics for Success

In order for the Mini SensorCraft flight tests to be considered a success, all primary objectives must be met along with a majority of the secondary objectives. The tertiary objective for the Mini SensorCraft has no bearing on the success of the overall flight test effort. A successful completion of the listed objectives, based on the the weighting applied to them, promotes the success for the follow-on ATRPV platform effort.

4.3.4 Testing Breakdown

The Mini SensorCraft FTP is divided into four phases, meant to facilitate a prudent progression of testing to meet the overall objectives. Phase 1, Flight Readiness System Tests, includes the integration and testing of all onboard systems. The tests involved in this phase include a bifilar pendulum test, thrust test, SIL simulation, system calibration tests, HIL simulation, EMI and RF tests, launcher tests, and safety tests. Phase 1 will be concluded with a check out flight test of the Mini SensorCraft. Phase 2, Test Point Investigation Tests, will involve an incremental approach towards a chosen test point for the aft wing designs. The variables to be incremented include static margin and test point weights. Phase 3, Maneuver Control Investigation Tests, contains planned flight tests to investigate in flight control handover between both pilots. The final result of this phase will determine the most feasible means of performing an accurate flight maneuver (primary pilot or back up pilot with first person video from vehicle). The tertiary objective of exploring

the full autopilot mode of the piccolo SL autopilot will also be attempted during this phase. Phase 4, Flexible Flight Tests, will involve a static loading test for three flexible aft wing designs and flight tests with the aft wings configured onto the Mini SensorCrafts. The testing planned for this final phase of the Mini SensorCraft FTP will provide better understanding of the JWSC aeroelastic response with respect to controllability, flying quality, and geometric nonlinearities. The Mini SensorCraft flight test phase breakdown is summarized in 4.1

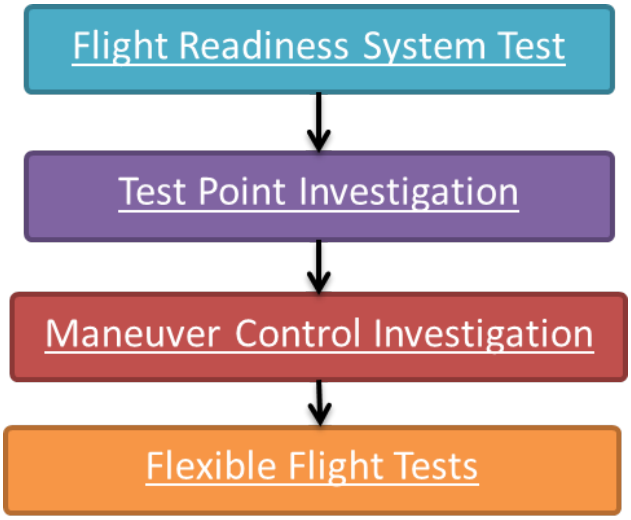

Figure 4.1: Mini SensorCraft phase testing breakdown

All manufactured Mini SensorCraft will perform phase 1 of testing in order to verify airworthiness. Phase 2 and 3 will be attempted by one model of the Mini SensorCraft fleet, since these tests have no bearing on the airworthiness of the aircraft. However, phase 2 and 3 must be completed by a Mini SensorCraft before any subsequent manufactured models may perform phase 4.

4.4 Aeroelastically Tuned RPV Flight Test Plan

The following section highlights the overall test organization of the $1/9^{th}$ scale ATRPV FTP. Included are the goals and objectives of the final test effort. The full rough draft of the ATRPV FTP can be seen in Appendix D.

4.4.1 Test Goals

The overall program goals of the Aeroelastically Tuned RPV Flight Test Plan are to validate the target static aeroelastic response of the vehicle, and safely demonstrate and accurately capture the geometric nonlinearities of the JWSC in flight.

4.4.2 Test Objectives

Using the previously mentioned goals as a driver, a series of primary, secondary, and tertiary objectives were developed. There are three planned phases (Validation Tests, Flight Readiness System Tests and Flight Tests) aimed at meeting at least one of the objectives listed below. The test (or series of tests) that corresponds to each objective listed below is shown after that objective in parentheses.

Primary Objectives:

1. Validate appropriate nonlinear static deflection of target aeroelastic response of the ATRPV ***(Static Loading Test)***.

2. Safely demonstrate and accurately capture geometric nonlinearities of the JWSC in flight utilizing the ATRPV ***(Flight Test)***.

Secondary Objectives:

1. Demonstrate accurate and successful data acquisition/ logging of instrumentation system ***(Ground Tests***).
2. Verify achievable flight maneuvers and loading of ATRPV ***(Simulation)***.
3. Determine key endurance parameters ***(Simulation, Usable Fuel Tests)***.
4. Validate rigid body mass moments of inertia for each test point ***(Bifilar Pendulum Test)***.
5. Determine flight mass and CG location for each test point ***(Mass and CG Verification)***.
6. Verify turbine performance ***(Installed Static Thrust Testing)***.
7. Validate control surface deflections and mixing ***(Control Surface Phase Margin Test, Control Surface Scheduling Test)***
8. Validate appropriate flight critical system communications ***(EMI/RF Test, Safety Tests)***.

For the ATRPV FTP, and subsequently the entire flight test program, the metrics of

success are that all outlined primary objectives must be met along with a majority of the secondary objectives.

4.4.3 Testing Breakdown

The Aeroelastic Response FTP is divided into three phases, meant to facilitate a prudent progression of testing to meet the overall objectives and goals of the program. Phase 1, Validation Tests, includes ground testing of the ATRPV. The tests involved in this phase include a static structural loading test and a bifilar pendulum test of the RPV. Phase 2, Flight Readiness System Tests, includes the integration and testing of all onboard systems. The tests involved in this phase include instrumentation testing, turbine testing, verifying control surface deflections and mixing, mass and center of gravity verification, and EMI/RF testing. Phase 3, Flight Tests, includes all flight test operations of the ATRPV. This includes taxi tests, a check out flight, and finally the maneuver flight tests of the ATRPV to measure the target aeroelastic response.

Chapter 5

Conclusions and Future Work

This research focused on investigating geometric nonlinearities for the Boeing Joined-Wing SensorCraft through the use of a $1/9^{th}$ scale RPV model. Specifically, this thesis presented experimentation based design exploration for an aeroelastically tuned RPV. The first test performed was a ground based static load test of the GSRPV. The overall goal of this testing was to explore the possibility of existing geometric nonlinearities in an already airworthy vehicle. Furthermore, the static loading test of the GSRPV was meant to provide data for FE model calibration and validation for follow-on design efforts. Results from this investigation yielded asymmetric loading in the deflection measurements due to unaccounted friction within the load application system (pulley system). Despite the asymmetric results, it was determined that the deflections did not indicate visible nonlinearities meaning the GSRPV was too stiff for the follow-on ATRPV effort and a redesign of the lifting surfaces had to occur.

Jenner Richards[25] produced a design in which flexibility was introduced along the length of the aft wing in order to produce geometric nonlinearities within the aft wing. Richards analysis, coupled with perceived results of the previous static loading test, indicated that the existing GSRPV forward wing provided adequate flexibility if an optimized aft wing and a stiff vertical boom were employed. However, there were concerns that introduction of flexibility into the aft wing would correspond to a reduction in its load carrying capability and as a result more load would be carried by the forward wing. A high fidelity FE model was used to investigate the forward wing root bending moment that would result from a compliant aft wing for a given 3g maneuver. The high fidelity FE analysis concluded that the forward wing was sufficient to carry loads in the GSRPV, which was supported by very rigid aft wings, but the forward wings were not capable of supporting loads required if a sufficiently compliant aft wing was chosen.[25] The analysis showed that failure occured at a load step of 241 N which corresponded to $1.43x10^5 Nm$, which was only 37% of the required design limit load. This result overly constrained the design space for the aft wing. In order to validate this result, a second ground based static loading test was performed on the existing GSRPV without the aft wings attached.

The overall goals and objectives of this second static loading experiment was to first calibrate the FE model by obtaining deflection measurements in key locations along the forward wing. Secondly, principal strains were measured along the area where the failure occured within the FE model and the results of both models were compared. The linear region of initial deflection data for the wing tips was used to calibrate a global stiffness

parameter linked to material stiffness. The youngs modulus and shear stiffness of all carbon laminates within the model were multiplied by the global stiffness parameter. This resulted in good comparative results between the FE and experimental deflection data within the linear region (0-8.44kg). The percent difference in slopes for this region between the FE and experimental results was 10% for the trailing edge root deflection measurements, 5% for the wing tip measurements, and 1% for the leading edge root measurements. The resulting strain measurements compared well especially within the linear region defined from 0-10kg. The strain gage results predicted similar behavior for the shear web and spar cap region of interest where the failure had been predicted. This provided confidence in the FE model predictions, leading to the conclusion that a new forward wing must be designed along with new aft wing.

The remaining work within this research involved the design and development of two flight test plans in support of the Aeroelastic Response Program. It was determined that the introduction of flexibility into a $1/9^{th}$ scale RPV platform requires a sufficient understanding of the resulting dynamic responses. Specific focus must be placed on the handling qualities, control (possible binding of elevator on aft wing), and the ability to capture the static nonlinear aeroelastic response. To reduce risk, a Mini SensorCraft flight test plan was developed and presented with the goal of providing needed transitional guidance for the ATRPV platform. Following this flight test plan was the presentation of the aeroelastically tuned RPV flight test plan aimed at fulfilling the overall goals for the entire flight test program of demonstrating and capturing geometric nonlinearity within the JWSC in flight.

Future work will involve the design of a new forward wing for the ATRPV which is compliant enough to allow a nonlinear aft wing response while still being capable of sustaining the required flight loads. The requirement to build a new forward wing will also allow improved tuning of the aft wing response. By not having to work within the constraints of using an existing wing, the optimization process can now tune both forward and aft wings simultaneously.

Further future work will involve the implementation of the drafted Aeroelastic Response Flight Test Plans. This will immediately begin with the Mini SensorCraft Flight Test Plan. Successful completion of the Mini SensorCraft flights and a finalized design for the ATRPV will authorize the fabrication and testing of the $1/9^{th}$ scale ATRPV. A successful implementation of the ATRPV flight test plan will result in the overall conclusion of the Joined-Wing SensorCraft Flight Test Program.

Bibliography

[1] Canfield, R., "Sensorcraft Research Projects at AFIT 2001-2008," Tech. rep., AF-VT Collaborative Center, September 2009.

[2] "Strain Gage Rosettes: Selection, Application, and Data Reduction," Tech. rep., Vishay-Micromeasurements, Tech Note TN-515.

[3] "RQ-4 Block Global Hawk," Tech. rep., Northrop Grumman, 2010.

[4] Rasmussen, C. C., Canfield, R. A., and Blair, M., "Optimization Process for Configuration of Flexible Joined-Wing," *10th AIAA/ISSMO Multidisciplinary Analysis and Optimization Conference*, No. September, Albany, New York, 2004, pp. 1–9.

[5] Lucia, D., "The SensorCraft Configurations: A Non-Linear AeroServoElastic Challenge for Aviation," *AIAA 2005-1943, 46th AIAA/ASME/ASCE/AHS/ASC Structures, Structural Dynamics & Materials Conference*, No. April, Austin, Texas, 2005, pp. 1–7.

[6] Wolkovitch, J., "The Joined Wing: An Overview," *Journal of Aircraft*, Vol. 23, No. 1, 1986, pp. 161–178.

[7] Blair, M. and Canfield, R. A., "A Joined-Wing Structural Weight Modeling Study," *43rd AIAA/ASME/ASCE/AHS/ASC Structures, Structural Dynamics, and Materials Conference*, No. April, Denver, Colorado, 2002.

[8] Blair, M., Canfield, R. A., and Roberts, R. W., "Joined-Wing Aeroelastic Design with Geometric Nonlinearity," *Journal of Aircraft*, Vol. 42, No. 4, July 2005, pp. 832–848.

[9] Bond, V., *Flexible Twist for Pitch Control in a High Altitude Long Endurance Aircraft with Nonlinear Response*, Ph.D. thesis, AIR FORCE INSTITUTE OF TECHNOLOGY, 2008.

[10] Kroo, I., Gallmant, J., and Smith, S., "Aerodynamic and Structural Studies of Joined-Wing Aircraft," Vol. 28, No. 1, 1990, pp. 74–81.

[11] Gallman, J. W., Smith, S. C., and Kroo, I. M., "Optimization of Joined-Wing Aircraft," *Journal of Aircraft*, Vol. 30, No. 6, Nov. 1993, pp. 897–905.

[12] Gallman, J. W. and Kroo, I. M., "Structural Optimization for Joined-Wing Synthesis," *Journal of Aircraft*, Vol. 33, No. 1, Jan. 1996, pp. 214–223.

[13] Livne, E., "Aeroelasticity of Joined-Wing Airplane Configurations: Past Work and Future Challenges- A Survey," *42nd AIAA/ASME/ASCE/AHS/ASC Structures, Structural Dynamics, and Materials Conference,*, No. April, Seattle, WA, 2001, pp. 16–19.

[14] Patil, M. J., "Nonlinear Aeroelastic Analysis of Joined-Wing Aircraft," *44th AIAA/ASME/ASCE/AHS Structures, Structural Dynamics, and Materials Conference*, No. April, Norfolk, Virginia, 2003, pp. 1–7.

[15] Ricciardi, A., Patil, M., Canfield, R., and Lindsley, N., "Evaluation of Quasi-Static Gust Loads Certification Methods for HALE Aircraft," *Journal of Aircraft*, Vol. 50, No. 2, 2013, pp. 457–468.

[16] Roberts, R. W., Canfield, R. A., and Blair, M., "Sensor-Craft Structural Optimization and Analytical Certification," *46th AIAA/ASME/ASCE/AHS/ASC Structures, Structural Dynamics & Materials Conference*, No. April, Austin, Texas, 2005.

[17] Richards, J., Suleman, A., Canfield, R., and Blair, M., "Design of a Scaled RPV for Investigation of Gust Response of Joined-Wing Sensorcraft," *50th AIAA/ASME/ASCE/AHS/ASC Structures, Structural Dynamics, and Materials Conference*, No. May, Palm Springs, California, 2009, pp. 1–14.

[18] Richards, J., Suleman, A., Aarons, T., and Canfield, R. A., "Multidisciplinary Design for Flight Test of a Scaled Joined Wing SensorCraft," *13th AIAA/ISSMO Multidisciplinary Analysis Optimization Conference*, No. September, Fort Worth, Texas, 2010, pp. 1–25.

[19] Richards, J., Aarons, T., Suleman, A., Canfield, R. A., Woolsey, C., Lindsley, N., and Blair, M., "Design for Flight Test of a Scaled Joined Wing SensorCraft," *52nd AIAA/ASME/ASCE/AHS/ASC Structures, Structural Dynamics and Materials Conference*, No. April, Denver, Colorado, 2011, pp. 1–30.

[20] Aarons, T. D., *Development and Implementation of a Flight Test Program for a Geometrically Scaled Joined Wing SensorCraft Remotely Piloted Vehicle* , Master's thesis, Virginia Polytechnic Institute and State University, 2011.

[21] Richards, J., Aarons, T., Garnand-Royo, J., Suleman, A., Canfield, R. A., and Woolsey, C., "Airworthiness Evaluation of a Scaled Joined-Wing Aircraft 1," *53rd AIAA/ASME/ASCE/AHS/ASC Structures, Structural Dynamics and Materials Conference*, No. April, Honolulu, Hawaii, 2012, pp. 1–37.

[22] McClelland, W. A., *Inertia Measurement and Dynamic Stability Analysis of a Radio-Controlled Joined- Wing Aircraft* , Master's thesis, Graduate School of Engineering and Managament, Air Force Institute of Technology, 2006.

[23] "Xianglong Unmanned Reconnaissance Aerial Vehicle," Tech. rep., February 2009, http://www.sinodefence.com/airforce/uav/xianglong.asp.

[24] "Xianlong UAV - China," Tech. rep., http://airforceworld.com/pla/english/Xianglong-UAV-china.html.

[25] Richards, J., Garnand-Royo, J., Ricciardi, A., Suleman, A., Canfield, R. A., and Woolsey, C., "Design and Evaluation of Aeroelastically Tuned Joined-Wing SensorCraft Flight Test Article," *54th AIAA/ASME/ASCE/AHS/ASC Structures, Structural Dynamics and Materials Conference*, No. April, Bostan, Massachusetts, 2013, pp. 1–18.

[26] "Transverse Sensitivity Errors," Tech. rep., Measurements Group, Inc., 1993, MicroMeasurements Group Technical Note TN-509.

[27] Kimberlin, R. D., *Flight Testing of Fixed-Wing Aircraft*, American Institute of Aeronautics and Astronautics, Inc, Reston, Virginia, 2003.

Appendices

Appendix A

GSRPV Static Loading Test Results

The following are the full results of the GSRPV static loading test. The first plots (Fig.A.1 and A.2) only represent the Z-deflection of the measurable points along the aft wing and boom for the 3g load test. Figs. A.3 and A.4 represent the mean z deflections of the forward wing for the point load test for F3 and F5 (no aft wings attached). The tables proceeding These figures represent the 3D motion of the points of interest for all point load tests of the forward wing completed.

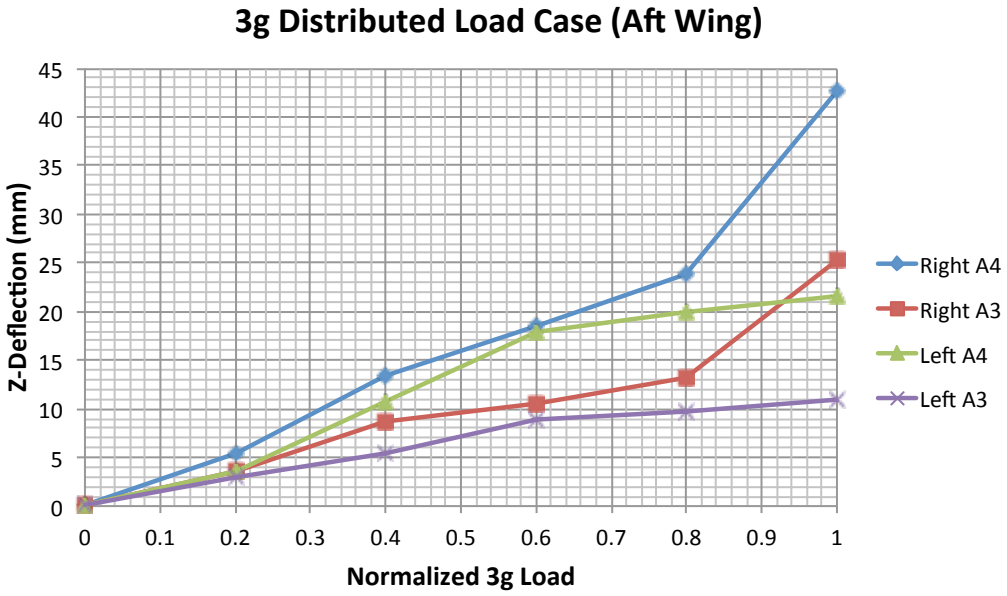

Figure A.1: Z-deflection results for specific points of aft wing for the 3g distributed load case.

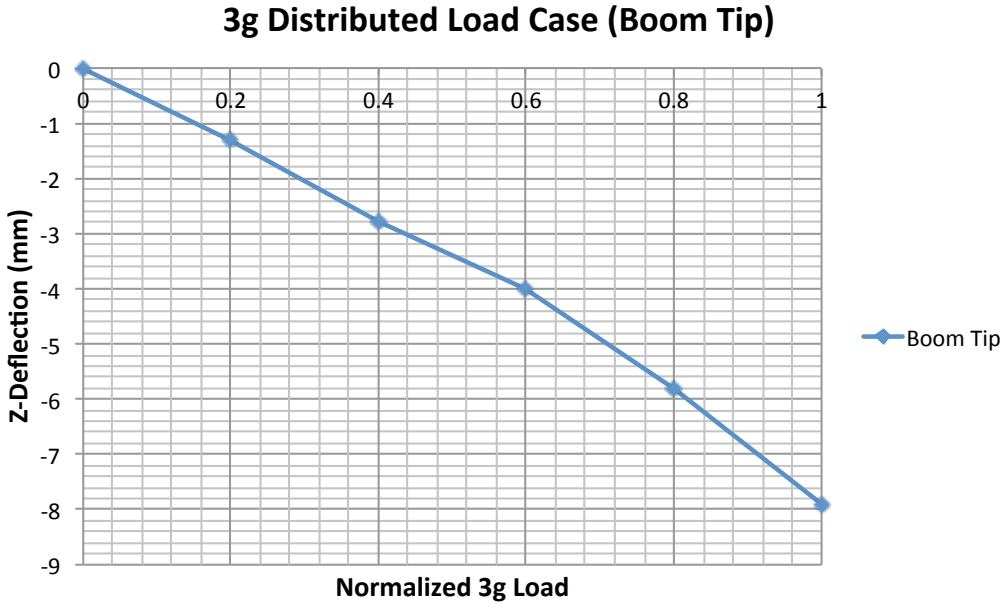

Figure A.2: Z-deflection results for boom tip during 3g load case.

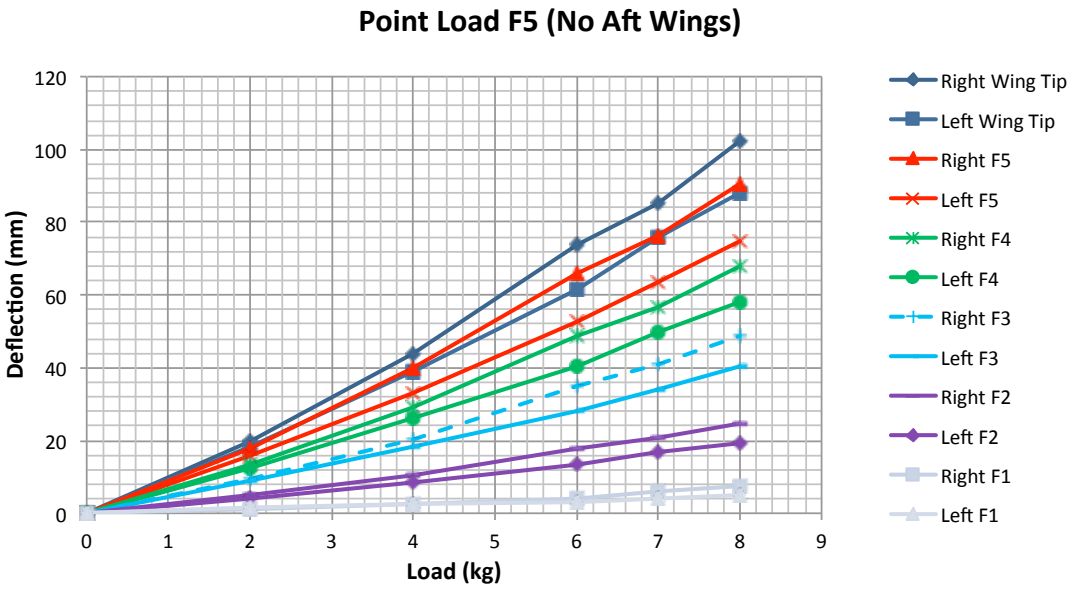

Figure A.3: Mean of forward wing z-deflection for point load application at F5 location (no aft wings attached)

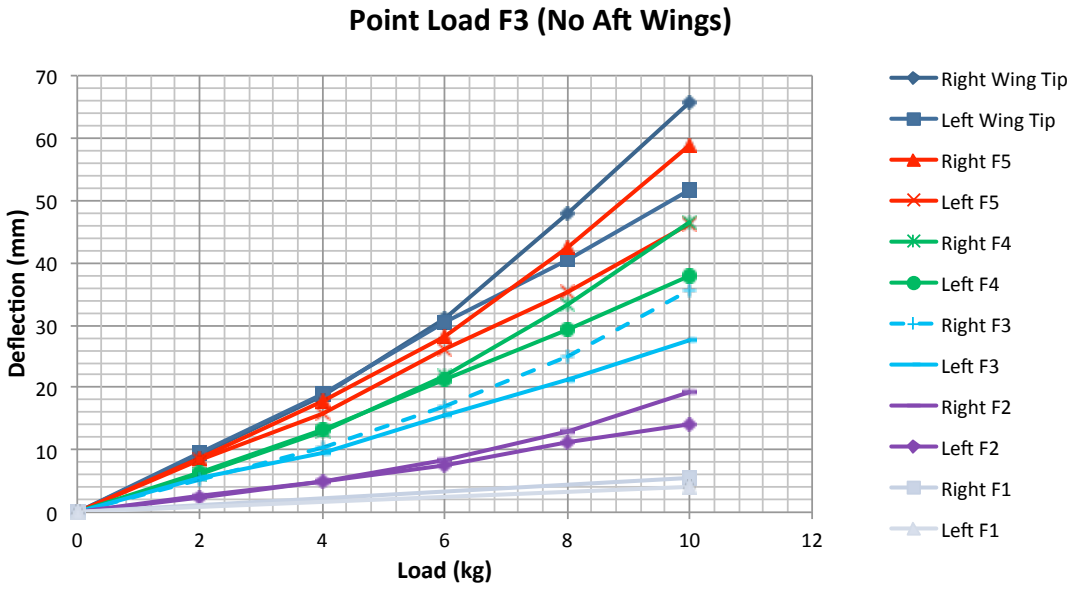

Figure A.4: Mean of forward wing z-deflection for point load application at F3 location (no aft wings attached

Table A.1: 3D displacement measurements for point load test 1 of point load application at F5 location

Right Wing																		
	Position Measurements [mm]																	
	Wing Tip			F5			F4			F3			F2			F1		
Loading Weights [kg]	x	y	z	x	y	z	x	y	z	x	y	z	x	y	z	x	y	z
0	0	0	0	0	0	0	0	0	0	0	0	0	0	0	0	0	0	0
2	2.47	0.8	19.03	1.41	3.32	15.41	1.93	3.07	11.87	0.3	1.67	9.1	0.6		5.11		1.78	1.69
4	6.84	2.4	42.71	3.72	5.57	37.19	3.86	4.49	27.76	2.54	3.26	19.4	1.2		10.72		2.47	2.16
6	11.29	3.4	74.11	7.68	9.8	64.52	6.49	7.3	47.7	5.42	6.13	34.07	2.8	3.64	17.19		3.27	4.53
7	12.36	4.8	84.22	8.68	12.48	74.87	6.79	8.3	54.72	6.12	7.39	40.2	4.4	4.41	21.02		3.3	6.47
8	15.19	4.8	103.19	9.98	14.46	89.58	9.19	10.2	68.25	8.17	8.73	48.44	5.07	6.32	25.84	2.54	3.8	8.63
Left Wing																		
	Position Measurements [mm]																	
	Wing Tip			F5			F4			F3			F2			F1		
Loading Weights [kg]	x	y	z	x	y	z	x	y	z	x	y	z	x	y	z	x	y	z
0	0	0	0	0	0	0	0	0	0	0	0	0	0	0	0	0	0	0
2	2.65	0	16.28	1.47	2.23	16.48	0.71	1.77	12.53	0.8	0.7	9.2	0.5	0.74	3.98			1.8
4	4.92	2.4	36.62	3.27	3.41	31.61	1.71	2.52	25.2	1.8	1	18.05	1	1.31	7.54			2.2
6	9.72	2.4	60.31	5.32	5.99	51.72	3.01	4.45	39.34	2.8	1.83	28.38	2.13	2.6	12.62			3
7	12.46	3.2	73.74	6.22	7.95	62.65	4.01	6.61	48.1	3.3	3.86	34.03	2.73	2.9	15.65			4.2
8	15.96	4	86.48	7.56	8.76	73.96	5.67	7.11	56.8	3.8	5.3	40.23	3.03	3.87	18.12	1	2.2	5.27

Table A.2: 3D displacement measurements for point load test 2 of point load application at F5 location

Right Wing																		
	Position Measurements [mm]																	
	Wing Tip			F5			F4			F3			F2			F1		
Loading Weights [kg]	x	y	z	x	y	z	x	y	z	x	y	z	x	y	z	x	y	z
0	0	0	0	0	0	0	0	0	0	0	0	0	0	0	0	0	0	0
2	3	0.8	23.58	1.1	2.86	18.53	2.3	2.28	15.25	0.7	1.23	9.97	0.3	1.4	5	0.5		0.7
4	7.16	1.6	49.61	3.6	6.2	42.61	3.46	4.97	33.25	2.9	3.9	22.15	1.4	1.8	12.08			2.49
6	12.07	3.2	75.21	5.6	10.74	65.65	5.53	7.9	50.13	4.38	6.07	35.61	2.2	3.87	17.74			3.63
7	14.37	3.2	91.52	7.4	12.56	79.35	6.93	10	60.94	5.48	8.19	43.34	2.5	5.2	21.93			5.86
8	17.83	4	105.74	8.8	14.91	92.29	7.93	11.57	70.48	6.64	9	49.61	2.8	6	24	2.28	2.97	7.84
Left Wing																		
	Position Measurements [mm]																	
Loading Weights [kg]	Wing Tip			F5			F4			F3			F2			F1		
	x	y	z	x	y	z	x	y	z	x	y	z	x	y	z	x	y	z
0	0	0	0	0	0	0	0	0	0	0	0	0	0	0	0	0	0	0
2	2.55	0.8	20.9	1	2.12	15.29	1.6	1.38	12.4	1	1	9.8		0.4	4.88			1.34
4	5.71	1.6	41.94	3.36	4.27	36	3.5	2.9	28.42	2	2.15	19.94		1.3	10.2			2.5
6	9.97	1.6	64.94	4.93	6.18	54.83	5.2	3.38	41.76	2.54	3.6	28.63		2.4	15.2			3.6
7	12.77	3.2	79.17	6.13	8.14	66.46	6.2	4.56	52.8	3.84	4	34.86		3	18.2			4
8	14.77	3.2	91.81	6.93	8.33	77.32	7.15	7.02	61	3.94	4.7	41.15	4	4.3	20.4	1	1.7	4.7

Table A.3: 3D displacement measurements for point load test 3 of point load application at F5 location

Right Wing																		
	Position Measurements [mm]																	
	Wing Tip			F5			F4			F3			F2			F1		
Loading Weights [kg]	x	y	z	x	y	z	x	y	z	x	y	z	x	y	z	x	y	z
0	0	0	0	0	0	0	0	0	0	0	0	0	0	0	0	0	0	0
2	1	0.8	17.33	3	2.71	19.23	2	1.75	12.81	2.19	1.7	8.63	0.5	1	4.62			
4	4	1.6	39.56	5	5.42	39.72	6.6	4.09	26.92	4.79	2.99	18.65	1	2.3	8.24			
6	11	2.4	72.47	8.4	9.67	67.49	8.6	7.57	48.24	6.43	6.57	35.36	2.2	3.8	17.99			
7	12.8	3.2	79.39	9.4	12.58	75.02	10.6	8.95	53.93	7.31	7.62	39.41	2.5	4.48	19			
8	16.4	4	98.61	12.8	14.23	90.27	12.65	9.81	65.11	7.96	8.85	47.96	3.2	5.45	23.82	2.1	2.13	5.82
Left Wing																		
	Position Measurements [mm]																	
	Wing Tip			F5			F4			F3			F2			F1		
Loading Weights [kg]	x	y	z	x	y	z	x	y	z	x	y	z	x	y	z	x	y	z
0	0	0	0	0	0	0	0	0	0	0	0	0	0	0	0	0	0	0
2	2.76	0.8	18.37	1.57	2.3	15.04	1.81	1.8	11.85	1.26	2.42	8.47	0.3	2	3.7			
4	6.96	0.8	38.64	3.4	4.2	31.67	3.26	3.95	24.85	2.63	3.64	16.98	1.3	2.15	8			
6		1.6	60	5.17	6.54	51.42	4.51	4.95	40.32	3.83	5.67	27.63	2.62	2.75	12.83			
7	14.36	2.4	73.93	6.89	7.45	62.18	5.76	6.66	48.19	4.73	6.46	33	2.72	3.6	16.72			
8	17.76	3.2	86.67	8.13	8.5	73.48	6.66	8.1	56.39	5.63	7.16	40	3.22	4	19.54	1.2	2.43	5

Table A.4: 3D displacement measurements for point load test 1 of point load application at F3 location

Right Wing																		
	Position Measurements [mm]																	
	Wing Tip			F5			F4			F3			F2			F1		
Loading Weights [kg]	x	y	z	x	y	z	x	y	z	x	y	z	x	y	z	x	y	z
0	0	0	0	0	0	0	0	0	0	0	0	0	0	0	0	0	0	0
2	1.77	0	10.14	0	2.3	9.3	1.5	1.31	6.22	1.01	2.15	5.43	1.24	0.4	2.58			
4	4.67	0.8	19.63	1.42	3	18.17	3.13	2	12.8	1.61	2.5	10.13	1.24	1.22	5.27			
6	5.96	1.6	31.34	2.55	4.76	28.24	4.93	4.07	21.67	3.02	3.74	16.94	2.17	1.5	8.28			
8	9.34	2.4	46.76	3.82	7.76	41.38	6.02	5.84	31.7	3.95	5.1	24.55	2.65	1.94	12.57			
10	14.03	3.2	68.84	7.05	10.77	61.26	7.11	8.3	48.29	5.76	6.52	37.26	3.6	3.3	19.64	2.81	1	5.95
Left Wing																		
	Position Measurements [mm]																	
	Wing Tip			F5			F4			F3			F2			F1		
Loading Weights [kg]	x	y	z	x	y	z	x	y	z	x	y	z	x	y	z	x	y	z
0	0	0	0	0	0	0	0	0	0	0	0	0	0	0	0	0	0	0
2	0.4	0	8.95	1.2	1.08	8.84	0.89	1.47	6.54	0.9	0.9	5.2	1.56	0.7	3.04			
4	2.82	0.8	18.18	2.25	1.6	17.25	1.93	2.3	13.65	1.62	1.24	10.11	2.42	1	4.86			
6	4.68	1.6	31.25	3.24	3.8	27.86	3.51	3.3	21.89	2.32	2.15	16.11	3.14	1.3	8.29			
8	6.54	2.4	42.16	3.94	4.2	37.5	4.29	3.62	31.23	3.02	2.87	21.96	3.89	1.7	11.86			
10	8.37	2.4	51.17	4.34	5.9	47.52	5.04	4.72	38.03	4.21	3.7	27.79	4.7	2.2	14.79	1	1	4.4

Table A.5: 3D displacement measurements for point load test 2 of point load application at F3 location

Right Wing																		
	Position Measurements [mm]																	
	Wing Tip			F5			F4			F3			F2			F1		
Loading Weights [kg]	x	y	z	x	y	z	x	y	z	x	y	z	x	y	z	x	y	z
0	0	0	0	0	0	0	0	0	0	0	0	0	0	0	0	0	0	0
2	1.14	0	9.57	1.39	1.53	7.93	0.87	1.69	5.85	0.67	1.3	4.47	0.81	1	1.92			
4	2.33	0.8	17.59	1.76	3.37	16.98	1.18	2.43	12.63	1.14	1.8	10.14	1.4	1.1	4.48			
6	4.38	0.8	31.85	2.53	4.98	26.77	2.49	3.9	21.46	1.61	3.25	16.33	2.04	1.6	7.48			
8	6.43	1.6	47.6	4.28	7.38	41.92	4.13	5.54	33.26	3.1	3.86	25.22	2.83	2.1	12			
10	9.88	2.4	64.76	6.03	10.1	56.92	5.77	7.78	45.31	4.96	5.3	34.58	3.43	2.5	18.27	1.45	1.11	4.78
Left Wing																		
	Position Measurements [mm]																	
	Wing Tip			F5			F4			F3			F2			F1		
Loading Weights [kg]	x	y	z	x	y	z	x	y	z	x	y	z	x	y	z	x	y	z
0	0	0	0	0	0	0	0	0	0	0	0	0	0	0	0	0	0	0
2	0.9	0	10.43	0.97	0.85	9.06	0.58	1.14	7.32	1.04	1	5.51	0.85		2.42			
4	3.62	0	19.69	1.72	2	15.35	1.13	1.48	13.71	1.83	1.3	9.7	1.27		4.88			
6	5.24	0.8	30.16	2.29	3.34	25.93	2.17	2.54	20.8	2.54	2.2	14.96	1.95		7.53			
8	7.59	0.8	40.04	3.63	5.31	34.98	2.85	3.75	29	3.25	3.45	21.16	2.89		11.88			
10	9.19	1.6	53.59	4.97	6.3	46.41	4.78	4.57	38.74	4.86	4	28.2	3.55	1.7	14.03	1.17	1.25	4.11

Table A.6: 3D displacement measurements for point load test 3 of point load application at F3 location

Right Wing																		
	Position Measurements [mm]																	
	Wing Tip			F5			F4			F3			F2			F1		
Loading Weights [kg]	x	y	z	x	y	z	x	y	z	x	y	z	x	y	z	x	y	z
0	0	0	0	0	0	0	0	0	0	0	0	0	0	0	0	0	0	0
2	2.33	0.8	4.98	1.52	1.78	8.87	0.3	1.11	6.5	0	1.23	5.6	1	1.25	3.67			
4	3.92	0.8	19.26	2.64	3.24	17.94	1.23	2.68	13.75	0.67	2	10.6	1	2.06	5.31			
6	5.05	1.6	29.59	3.76	5.2	29.53	2.93	3.7	22.25	1.84	2.64	17.42	1.88	2.8	9.51			
8	10.03	2.4	49.35	5.48	7.84	44.34	4.25	6	34.81	3.24	4.8	25.58	3.25	3.3	14.36			
10	14.53	3.2	63.37	7.61	10.64	58.49	5.58	7.8	46.12	4.94	6.16	34.68	4.25	4.5	19.7	1.71	2.3	5.48
Left Wing																		
	Position Measurements [mm]																	
	Wing Tip			F5			F4			F3			F2			F1		
Loading Weights [kg]	x	y	z	x	y	z	x	y	z	x	y	z	x	y	z	x	y	z
0	0	0	0	0	0	0	0	0	0	0	0	0	0	0	0	0	0	0
2	0.92	0.8	9.47	0.75	1	7.45	0.62	1.2	5.65	0.34	1	6.22	0.39	1.17	1.63			
4	3.31	0.8	19.04	1.7	1.8	14.83	1.78	2.25	12.1	0.82	1.5	8.82	1.01	2	4.93			
6	5.03	1.6	30.3	2.38	3	25.09	2.49	3.2	21.08	1.26	2.2	15.3	1.4	2.4	6.99			
8	6.64	2.4	39.19	2.74	4.6	33.28	2.99	3.7	28.09	2.4	3	21.02	0.59	3.2	10.07			
10	8.14	2.4	50.06	3.92	6.3	44.49	3.88	4.54	36.56	3.05	3.6	26.45	0.91	3.8	13.88	0.5	2	4.06

Appendix B

Cantilever Loading Test Results

The following plot represents the gages applied to the shear web interface closest to the leading edge of the left forward wing. These gages laid along an area of the left wing where a crack had developed. This crack was visually noticeable in the paint layer but not the woven carbon layer where the gages were applied. Though the crack did not visually appear in the woven carbon layer, there was a concern that an area of high strain existed here. The results in Fig.B.1 confirm this concern.

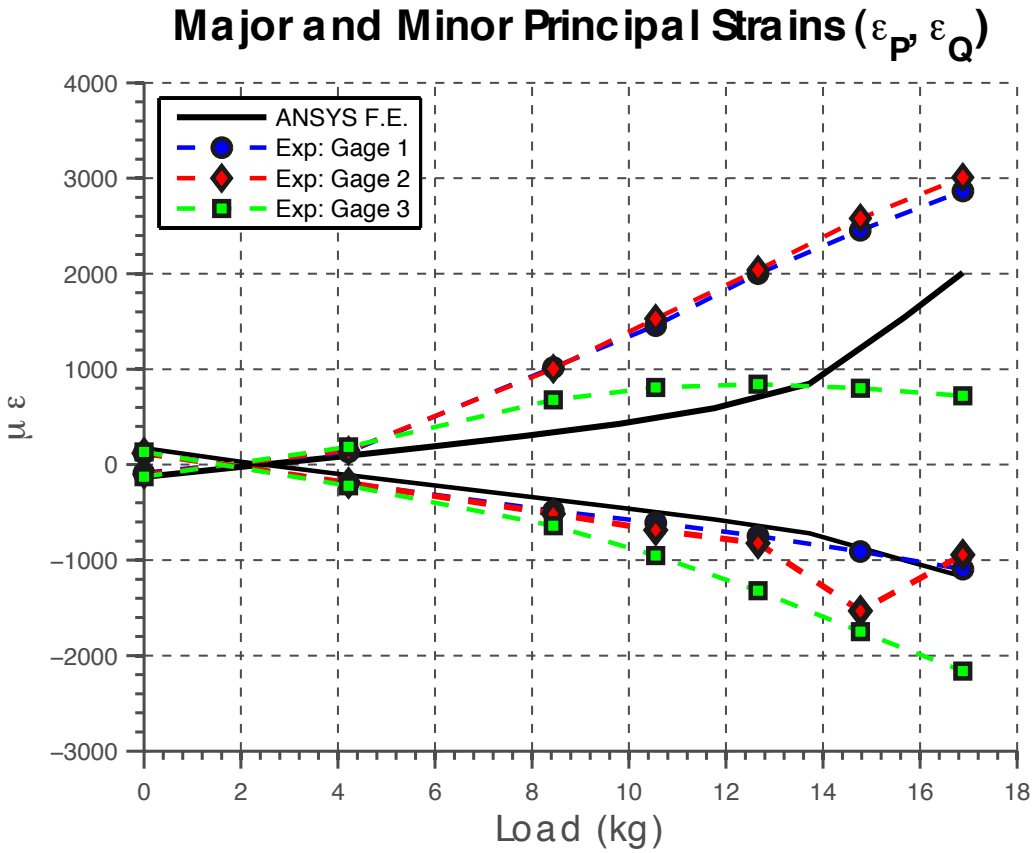

Figure B.1: Principal strain results for gages along the shear web interface closest to the leading edge of the left forward wing

Appendix C

Mini SensorCraft Flight Test Plan

This appendix presents the rough draft of the Mini-SensorCraft Flight Test Plan. This is the first of two flight test plans proposed for the Aeroelastic Response Program. This flight test plan is presented as a stand-alone document. The primary author of this document is the author of this thesis, Jeffrey Garnand-Royo. Two co-authors assisted in this document including Tyler Aarons and Jenner Richards.

Joined-Wing SensorCraft Aeroelastic Response Program Mini-SensorCraft Flight Test Plan

Blacksburg, VA — Victoria, BC — Foremost, AB

Security Classification: Unclassified

AFRL Program Manager: Ned Lindsley

Virginia Tech POC: Robert Canfield

University of Victoria/ Quaternion Engineering POC: Afzal Suleman

CCUVS POC: Sterling Cripps

Version 1

Executive Summary

The aeroelastic tuning of the Boeing Joined-Wing SensorCraft (JWSC) and flight testing of the tuned model is the topic of an ongoing international collaboration between Virginia Tech and The University of Victoria (Canada). The program leverages the resources of Quaternion Engineering Inc. (Victoria, Canada), the Canadian Centre for Unmanned Vehicle Systems (CCUVS), and the Air Force Research Lab (AFR)L/ Virginia Tech/ Wright State Collaborative Center for Multidisciplinary Sciences (CCMS) at Virginia Tech. This ambitious program has two primary objectives. The first objective is to develop a cost-effective, aeroelastically tuned, remotely piloted vehicle (RPV) to investigate the geometrical nonlinear behavior associated with the JWSC configuration. The second objective is to design and perform flight test experiments to demonstrate, measure, and characterize the nonlinear behavior in flight.

The JWSC Flight Test Program is divided into two distinct phases: the flight demonstration program, and the aeroelastic response program. The flight demonstration program involved the design and flight testing of the Geometrically Scaled RPV with equivalent rigid body dynamics, but with no aeroelastic tuning, and was the subject of the previous flight test program. Once the Geometrically Scaled RPV flight tests were completed in October 2011, the aeroelastic response program began. This program includes the re-design of the Geometrically Scaled RPV to include flexibility within the structure. The aeroelastic response program extends to include construction methods for a more flexible configuration, design and integration of a robust flight worthy measurement system, and flight test program development and execution.

The introduction of flexibility into a 1/9th scale RPV platform requires a sufficient understanding of the resulting dynamic responses. Specific focus must be placed on handling qualities, control, and the ability to capture the static nonlinear aeroelastic response. To minimize risk and increase potential for later success when using a 5 meter RPV platform, a test program was developed for the Mini SensorCrafts to investigate these potential effects. The Mini Sensorcraft flight efforts, will be the subject of this report. The Mini SensorCraft FTP is divided into 4 testing phases the scope of which is meant to facilitate the appropriate progression to the follow on ATRPV efforts.

Phase 1: **Flight System Readiness Tests** - This phase includes the Integration and testing of all onboard systems including simulation, system calibration, EMI/RF tests, launcher testing safety testing, and a bifilar test. This phase of testing will conclude with a checkout flight of the Mini SensorCraft Platform

Phase 2: **Test Point Investigation Tests** - Phase 3 of testing focuses on implementing an incremental testing approach to reach a decided test point configuration for the Mini SensorCraft.

Phase 3: **Maneuver Control Passover Tests** – This phase will investigate the most feasible means of performing accurate flight maneuvers based on the hardware set up for operations.

Phase 4: **Flexible Flight Tests** - This phase includes the introduction of 3 flexible aft wings to the Mini SensorCraft configuration. A static loading test and subsequent flights with the interchangeable wings will provide better understanding of the JWSC aeroelastic response with respect to controllability and flying quality on a reduced risk platform. Insights from these tests will provide valuable insight to the follow on ATRPV effort.

Attribution

The primary author of this document is Jeffrey Samuel Garnand-Royo. Jeffrey Garnand-Royo will act as flight test director for the efforts presented in this document. Jeffrey Garnand-Royo is a master's graduate of the Aerospace Department working out of the Nonlinear Systems Lab at Virginia Tech.

A co-author to this document is Jenner Richards. Jenner Richards is a doctoral candidate of the Mechanical Engineering Department at the University of Victoria and is tasked with aeroelastic tuning of the next phase JWSC RPV as well as overseeing the design and construction of the test platform itself. Jenner Richards is responsible for the design and fabrication of the previous Geometrically Scaled JWSC RPV including the Mini SensorCrafts and is responsible for developing a computational framework for performing aeroelastic scaling of aerospace vehicles and applying this to the SensorCraft.

The second co-author to this document is Tyler Aarons. Tyler Aarons is a master's graduate of the Aerospace Department who worked out of the Nonlinear Systems Lab at Virginia Tech. He acted as the previous flight test director for the Flight Demonstration Program and is responsible for providing a well-organized test document template for which this test plan is based.

Table of Contents

List of Figures

List of Tables

1 Introduction

1.1 Motivation

High altitude, long endurance (HALE) unmanned aerial vehicles (UAVs) are capable of providing revolutionary intelligence, surveillance and reconnaissance (ISR) capabilities over vast geographic areas when equipped with advanced sensor packages. The aeroelastic responses, specifically aft wing buckling and gust load response, associated with the Joined Wing SensorCraft (JWSC) have been demonstrated and investigated in numerous computational and wind tunnel studies[1-3]; however, these phenomena have never been successfully tested in a flight test program. The Air Force has determined that an aeroelastically tuned Remotely Piloted Vehicle (RPV) provides a low cost and effective way to investigate these nonlinear aeroelastic responses. By experimentally demonstrating, investigating and measuring these responses, future flight test programs will be able to test active aeroelastic control and gust load alleviation systems to reduce the structural and aerodynamic effects of the nonlinear responses. In addition, the testing of the RPV will support management planning for future tests of SensorCraft technologies.

1.2 Background Information

The SensorCraft is a concept initiated by the Air Force Research Laboratory (AFRL) to serve as a next-generation, HALE reconnaissance system. The SensorCraft is envisioned to fill the role of the next generation HALE ISR platform to contribute to persistent battle space awareness capabilities .[4] The Boeing JWSC, shown in Fig. 2, represents the top of this flight test plan.[4] The Boeing Joined Wing Concept, shown in Figure 2, represents the topic of this flight test plan.

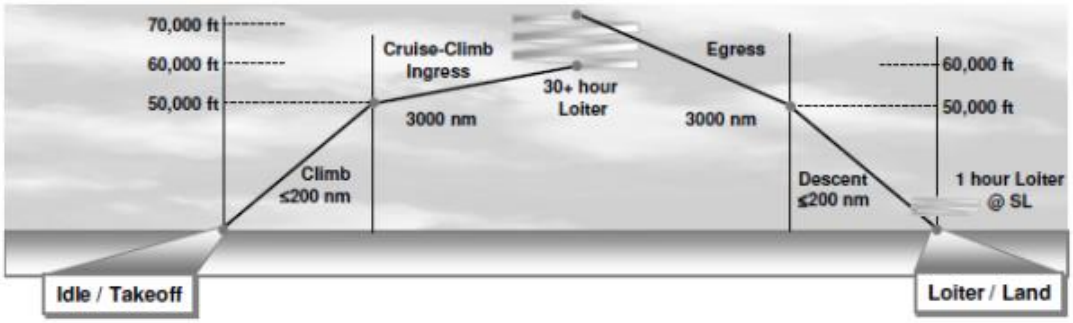

Figure 1 – Full scale SensorCraft mission profile[4]

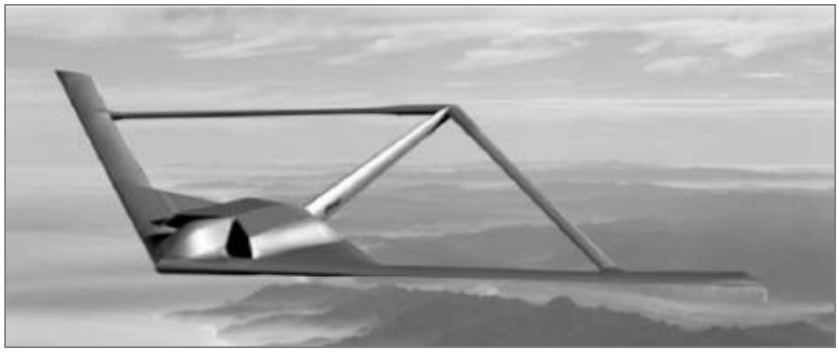

Figure 2- Joined-wing SensorCraft concept[4]

The primary driver behind this departure from conventional aircraft design is the ability to incorporate conformal radar antennas in the fore and aft wings to provide persistent 360 degree, foliage penetrating surveillance. This ability is of great benefit to the ISR mission, but it does come with a price. Previous computational studies of joined-wing aircraft configurations have shown the importance of structural geometric nonlinearity due to large deflections and follower forces that may lead to buckling of the aft wing[1,5]. This potential buckling represents a unique and challenging aeroelastic design problem. The non-linear behavior, which is a result of the joined wing configuration and advanced, lightweight structural design, could be removed by strengthening the wing to a point where these non-linear behaviors vanish; however, this would result in large penalties in aspect ratio and structural weight, greatly reducing the performance of the aircraft. To avoid these penalties, non-linear aeroelastic design, analysis and testing are required to ensure that the JWSC is able to sustain the non-linear responses required to complete the proposed ISR mission. An aeroelastically tuned RPV provides a low cost and effective way to investigate these nonlinear aeroelastic responses.

A necessary step towards flight of an aeroelastically tuned RPV, is the development and execution of a stringent Mini SensorCraft flight test program. Previous efforts utilizing the Mini SensorCraft have seen 5 airframes fabricated and tested in over 40 successful flights. These reduced complexity flight tests originally provided a range of necessary investigations from initial proof of concept flights for the JWSC configuration to more advanced performance characterization including stall speed tests and investigation into Dutch roll tendencies for the JWSC configuration. The most important contribution of the reduced complexity flight tests have been invaluable insight into the flight performance and handling qualities of the JWSC configuration. A relative sizing from the full scale Boeing design to the Mini SensorCraft is presented in Fig. 3.

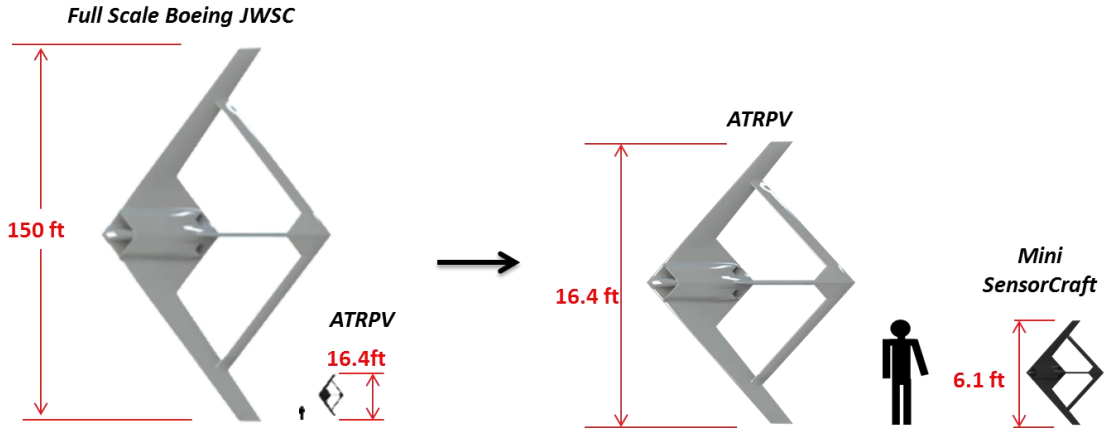

Figure 3 - Relative size of full scale Boeing JWSC, aeroelastically tuned RPV, and Mini SensorCraft[6]

1.3 Program Overview

The aeroelastic tuning of the JWSC and flight testing of the scaled model is the topic of an ongoing international collaboration between Virginia Tech and The University of Victoria (Canada). The program leverages the resources of Quaternion Engineering Inc. (Victoria, Canada), the Canadian Centre for Unmanned Vehicle Systems, and the AFRL/ Virginia Tech/ Wright State Collaborative Center for Multidisciplinary Sciences (CCMS) at Virginia Tech.

1.3.1 Program Breakdown

Due to the unique JWSC geometry, the relative large scale of the RPV and the challenge of fabricating aeroelastically tuned, flight worthy components, the JWSC Flight Test Program (FTP) is divided into two distinct phases: a Flight Demonstration Program which was the topic of the previous flight test plan and an Aeroelastic Response Program, the topic for this flight test plan. The Flight Demonstration Program involved the design of a Geometrically Scaled RPV, GSRPV (one with equivalent rigid body dynamics, i.e. preserved aerodynamics, overall mass and moments of inertia)including construction methods, flight test instrumentation selection and integration, control system tuning and flight test program development. This also includes the construction and flight testing of several preliminary models to determine flying qualities and trim requirements[1]. The Flight Demonstration Program concluded October 15, 2011 following the successful flight of the GSRPV.

Once the GSRPV flight test was completed, attention was shifted to the second phase of the JWSC FTP; The Aeroelastic Response Program. The Aeroelastic Response Program involves the design of an Aeroelastically Tuned RPV, ATRPV (one with equivalent rigid body dynamics, i.e. preserved aerodynamics, overall mass and moments of inertia) including construction methods for a more flexible configuration, design and integration of a robust flight worthy measurement system, and flight test program development. Following the success of utilizing small scale models in the form of Mini-

[1] All preliminary, reduced complexity flight models were designed, tested and flown using private funding from Quaternion Engineering as internal research and development (IRAD) to promote the success of both programs.

SensorCrafts , the Aeroelastic Response Program will include the construction and flight testing of Mini SensorCrafts to explore appropriate flight maneuvers and aircraft parameters that will induce the expected nonlinear structural response in the ATRPV platform. Furthermore, Mini-SensorCraft testing will provide a platform for test procedure development and fine-tuning of autopilot parameters. The Mini SensorCraft flight tests will concludes with the successful completion of the tests described in section 3.3.

1.3.2 Participating Organizations

The major organizations playing roles in this project are Virginia Tech, The University of Victoria, Quaternion Engineering Inc., the Canadian Centre for Unmanned Vehicle Systems (CCUVS), and the AFRL/ Virginia Tech/ Wright State Collaborative Center for Multidisciplinary Sciences (CCMS) at Virginia Tech. Virginia Tech is the primary contractor. Quaternion Engineering is the subcontractor, and also the owner of the test articles. The University of Victoria employs the founders and employees of Quaternion Engineering Inc. AFRL is the lead test organization (LTO) and provides funding and guidance for the project. CCUVS is a participating test organization (PTO), and provides support for the execution of all planned tests.

2 Test Item Description

This section provides a description of the Mini-SensorCraft. A general description of the vehicle, including overall dimensions will be presented first. This will be followed by descriptions of the predicted performance, control surface layout, propulsion system, control scheme, and instrumentation.

2.1 General Description

The test item for the Aeroelastic Response Program Mini SensorCraft flight test plan is the Mini SensorCraft. To reduce risk in the overall program, the Mini SensorCraft will be used as an incremental stepping stone toward the flight of ATRPV. The Mini SensorCraft is a 37% scale model of the previously flown GSRPV and the follow on ATRPV. The RPV has been designed and manufactured by Jenner Richards of the University of Victoria. A CAD rendering of the Mini SensorCraft is presented in Figure 4.

Figure 4 - CAD rendering of Mini SensorCraft[7]

The Mini SensorCraft is a joined wing configuration consisting of a center body housing twin electric ducted fans (EDF), a vertical tail boom and four lifting surfaces. The forward wings have positive dihedral and are swept aft. The aft wings have negative dihedral and are swept forward to

join with the forward wings at approximately 56% span (measured from the centerline) forming a diamond. Figure 5 presents a dimensioned 3-view drawing of Mini SensorCraft, highlighting key design parameters. A summary of these parameters is presented below in Table 1.

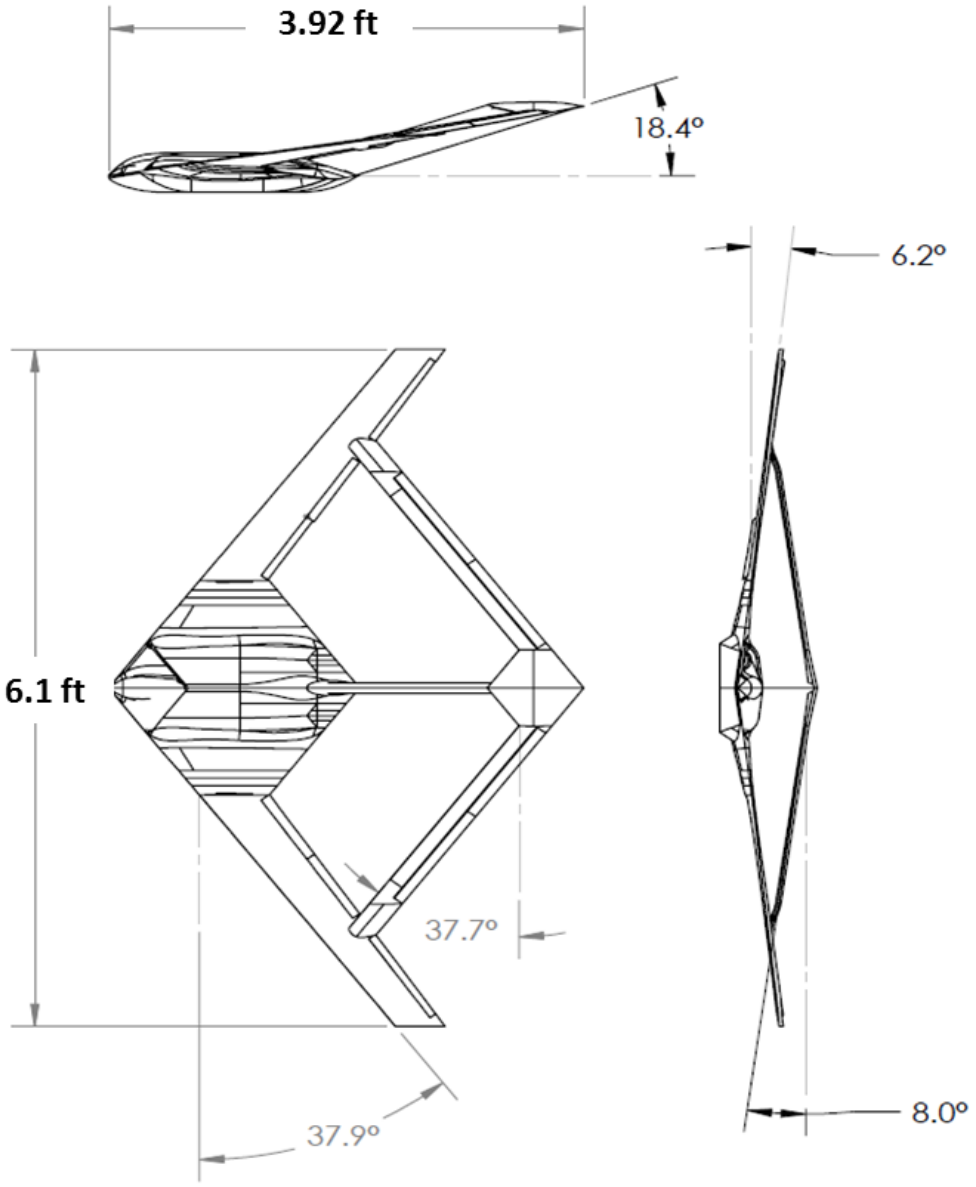

Figure 5 - Overall dimensions of Mini SensorCraft (dimensions shown in ft)

Table 1-Mini SensorCraft specifications

Parameters	English	Metric
Wing Span	6.1 ft	1.86 m
Wing Area	5.55 ft^2	0.52 m^2
Length	3.92 ft	1.19 m
Aircraft Weight (min-max)	7.7-10.1 lbs	3.5-4.6 kg
Total Thrust	8.38 lbs	3.8 kg
Front Wing Sweep	37.9°	-
Front Wing Dihedral	6.2°	-
Front Wing Sweep	-37.9°	-
Aft Wing Dihedral	-8.0°	-

2.2 Performance

Key measures of performance for the Mini SensorCraft are presented below in Table 2 for the largest planned flight weight. A typical mission profile is presented in Figure 6. Note that all performance parameters are estimates based on Fluent CFD analysis of the JWSC configuration in free stream conditions, simulations, reduced complexity flights, and the previous GSRPV flight.

Table 2 - Performance parameters for the maximum considered Mini SensorCraft take off weight (10.1 lbs, 4.6 kg)

Parameter	English	Metric
Stall Speed, V_{stall}	27.4 knots	14.1 m/s
Takeoff Speed, V_{TO}	32.9 knots	16.9 m/s
Nominal Cruise Speed, V_{cruise}	53.8 knots	27.7 m/s
Do Not Exceed Speed, V_{NE}	80.7 knots	41.5 m/s
Approach Speed, V_A	35.6 knots	18.3 m/s
Operating Altitudes, AGL	328 ft	100 m
Maximum Altitude, AGL	394 ft	120 m

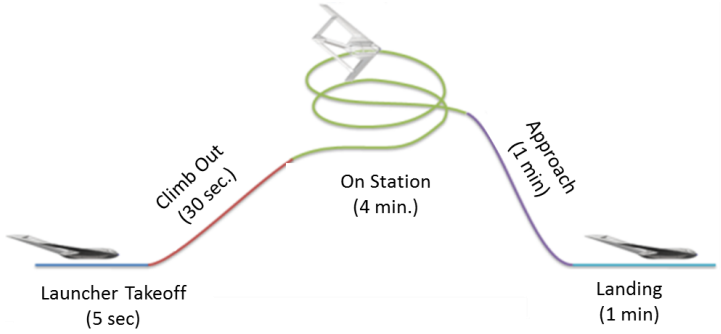

Figure 6 - Mini SensorCraft Mission profile[6]

The Mini SensorCraft will fly at a range of weights and static margin positions in order to incrementally approach a test point configuration for the follow on ATRPV platform. To accommodate for this, Fig. 7 and 8 present the operating speeds and stall speeds for the range of weights under investigation for the Mini SensorCraft. These figures will be used for operational limits when performing flight testing of the Mini SensorCrafts.

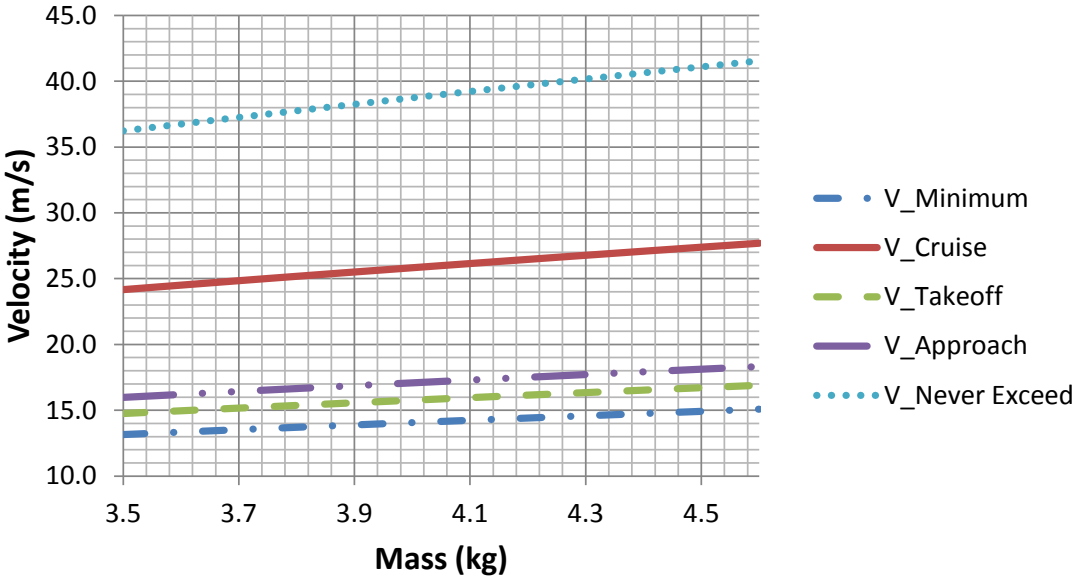

Figure 7- Operational speeds for the Mini SensorCraft at various aircraft weights

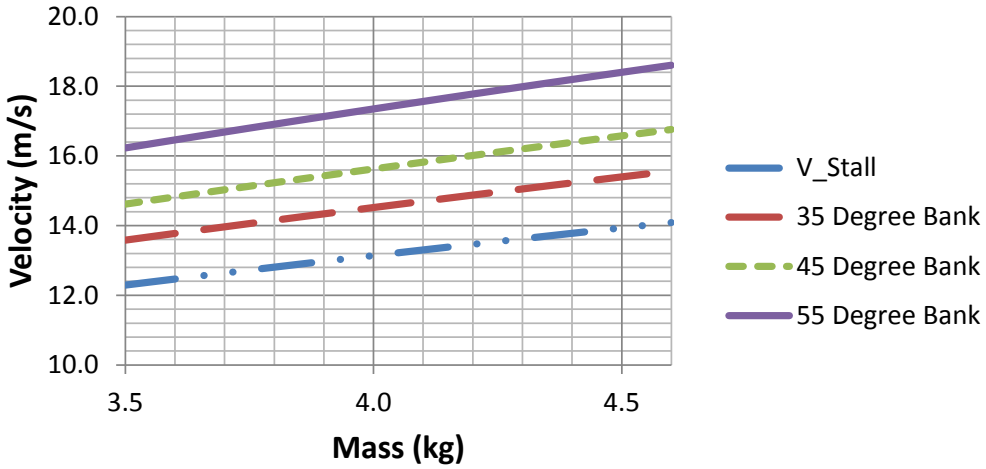

Figure 8- Stall speeds for the Mini SensorCraft at various aircraft weights

2.3 Control Surface Layout

2.3.1 Control Surface Scheduling

The control surface locations are slightly altered from the supplied full size aircraft geometry and the previous flown GSRPV. The primary change for this configuration is the movement of the elevators inboard onto the boom strake. There is a concern that the introduction of flexibility along the length of the aft wing could result in controllability consequences should the rigid elevator control surface remain in its original position.

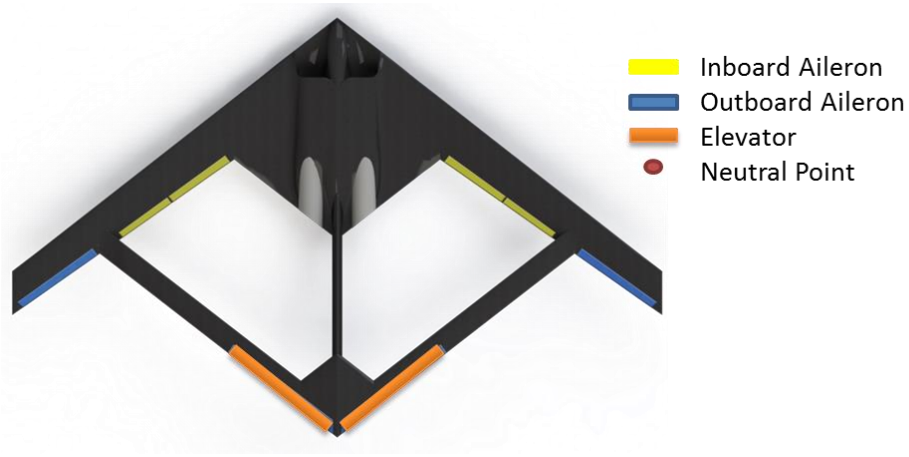

Figure 9 – Control Surface Layout[7]

Several control surface scheduling schemes have been both simulated and tested using reduced scale aircraft, previous Mini SensorCraft, and the GSRPV. The scheduling that will be used in the initial flight test of the Mini SensorCraft is summarized in Table 3. For the primary control surface schedule,

roll command uses the outboard ailerons, and pitch command uses the elevators. The primary ailerons will utilize aileron differential (40% down, 60% up mixing).

Table 3 - Control Surface Scheduling

Surface	Function
Inboard Aileron	Flap or Secondary Aileron
Outboard Aileron	Primary Aileron
Elevator	Primary Elevator

The redundant control surfaces can be utilized in many ways, the choice of which will depend on the need of the flight test specifically. One option is utilizing the inboard aileron as a flap (if more flap area is desired by the pilot) or as an aileron for additional roll control. This change is accomplished via mixing in the transmitter, and it has no effect on the placement of servos. Another option is to fix these control surfaces so they do not move and are unused entirely during the flight

2.4 Propulsion

Two alloy dynamic power series (DPS) 72mm electric ducted fans (EDF), located within the fuselage as shown in Fig. 10, power the Mini SensorCraft. The EDF chosen offers a ready to fly package (propeller and motor) providing a combination of huge power with reliability and efficiency. Table 4, shown below, provides the manufactures specified performance parameters for a single alloy DPS 72mm EDF unit with 2550kv motor.

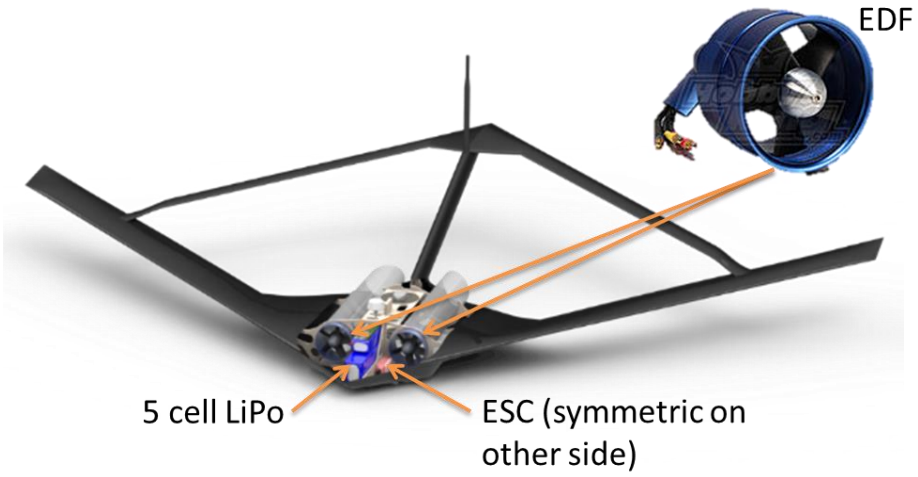

Figure 10 – Component location for Mini SensorCraft propulsion system[7]

Table 4 – Alloy DPS, 72mm EDF unit with 2550kV motor[8]

Component	Metric
EDF Rotor Diameter	72 mm
Outer Diameter	74.4 mm
Weight	276 g
Max RPM	55,000
Max Power	1200 W
Continuous Power	1150 W
Max Voltage	22.2 V (6S)
Max Amps	54 A
Max Thrust	1.9 kg

The EDF's are placed at the front of each pass-through of the Mini SensorCraft to allow for the most air intake. Hollow tubing, extending from the intake to the end of the fuselage, directs the air out. The remaining components of the propulsion system include the power source and two electronic speed controllers (ESC).The two EDF's each utilize a separate ESC to regulate the voltage from the battery to the motor. The two ESC's are connected in parallel to one 5 cell lithium polymer (LiPo) battery located in the front payload hatch. One switch located on top of the fuselage regulates the voltage from this battery therefore providing an on and off function for the full propulsion system.

2.5 Payload

Due to the nature of the Mini SensorCraft flight tests, the required payload consists of 2 Turnigy nano-tech LiPo batteries (5 cell and 3 cell), flight critical avionics (Piccolo SL Autopilot,GPS), Instrumentation, video feed transmitter, and trimming weights. The 5 cell 18.5 volt LiPo battery as shown in Fig. 10, powers the entire propulsion system. The 3 cell 11.1 volt LiPo battery within the same compartment powers the Piccolo SL Autopilot, the servos, and the emergency onboard flight camera. There are two switches on top of the fuselage that control the on and off functionality for the two batteries. Manufacturer specifications for both batteries are shown in Table 5.

Table 5- Manufacturer specifications for propulsion and avionics battery

Parameter	Propulsion Battery	Avionics Battery
Capacity(mAh)	5000	2200
Configuration (S)	5	3
Discharge (c)	75	35
Weight (g)	712	199
Max Charge Rate (C)	8	8
Voltage (V)	18.5	11.1

The fuselage has two main compartments for payload. The first is located at the very front of the vehicle and contains the two batteries. This front hatch is easily accessible in order to provide access to the batteries at all times when handling the vehicle. The second compartment is accessible from the underside of the Mini SensorCraft. This bay is where the remaining components of the payload will be placed. Fig. 11 shows the layout of the fuselage payload section along with positioning of key payload components.

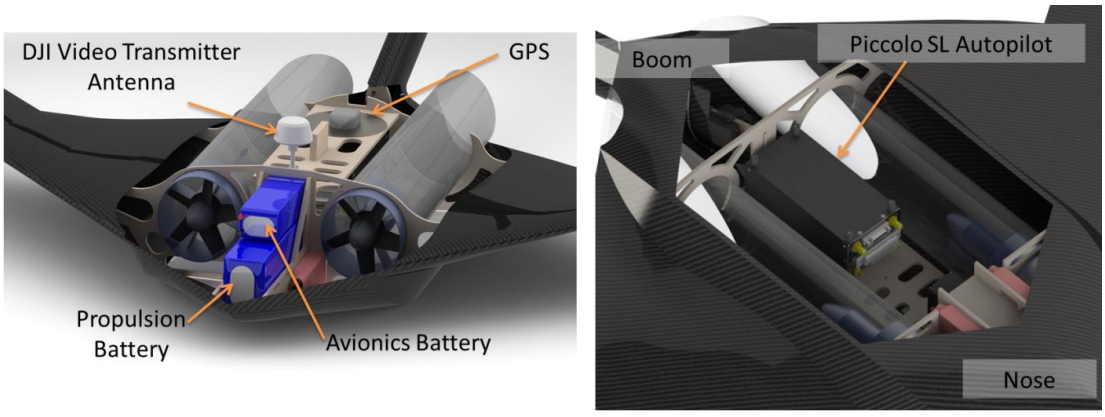

Figure 11 – Inside payload layout from top (left) and bottom perspective (right)[7].

2.6 Takeoff and Landing

All takeoff operations of the Mini SensorCraft will involve the use of a pneumatic launcher as shown in Fig. 12. The first component of the launcher system is the accumulator tank that is connected to a metal piping tube containing an internal plunger. Connected to the plunger is a guide wire where the other end is attached to an external launcher cart. When the pressure is released from the accumulator, the plunger moves down the length of the metal tubing pulling the launcher cart the opposite direction. The external launcher cart has attachments which fit a specialized platform used to hold the Mini SensorCraft. When the launcher cart reaches the end of the launcher, stoppers will prevent the cart from continuing but will result in a launch of the vehicle and launcher platform for the Mini SensorCraft. Sand bags are utilized to prevent any backward movement of the launcher when the pressure is released from the accumulator.

Landing of the Mini SensorCraft will involve belly landings onto the grass flying field. The test location does not have cement or asphalt within its boundaries. As a result, all aircraft flown must have the underside clear of protruding objects.

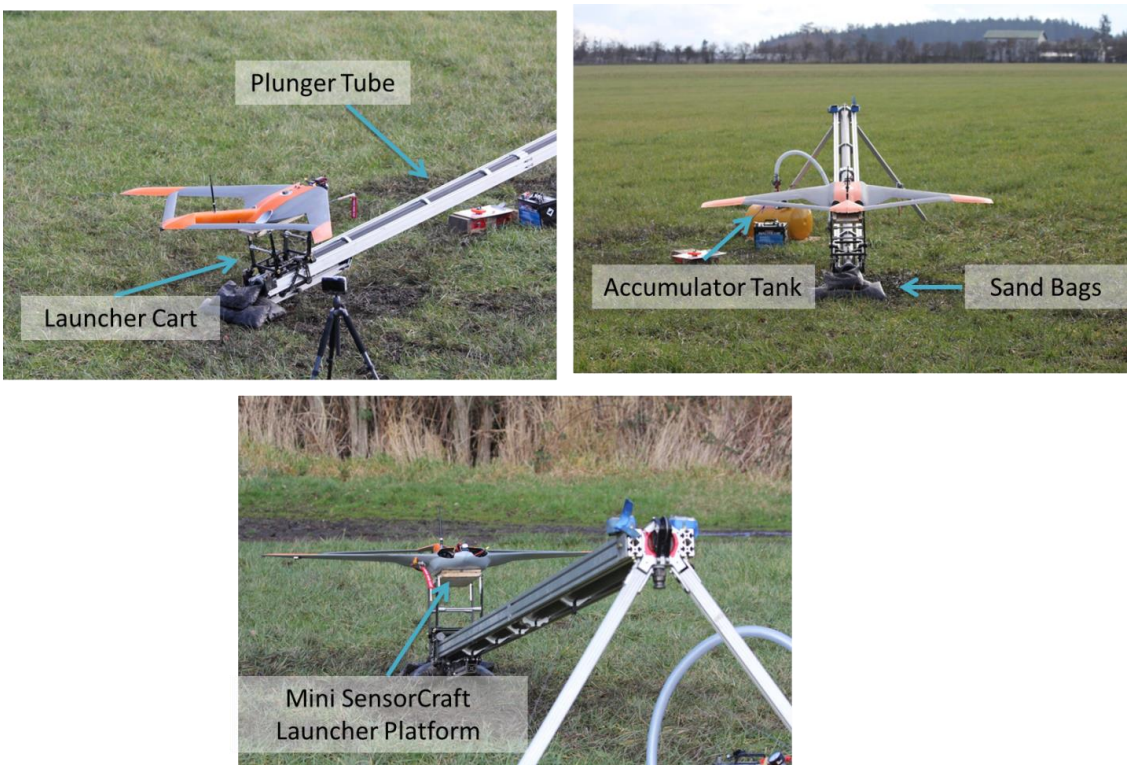

Figure 12-Launcher and Mini SensorCraft in takeoff operational setup

2.7 Control

Control of the Mini SensorCraft is accomplished via the onboard Cloud Cap Technology piccolo SL autopilot. The piccolo SL is used primarily as a data acquisition system and as a means of establishing reliable control of the Mini SensorCraft. A JR level shifter board provides the ability to incorporate a second transmitter and thus a second pilot into the control scheme for the Mini SensorCraft. A schematic of the control system used for the Mini SensorCraft is shown in Fig. 13.

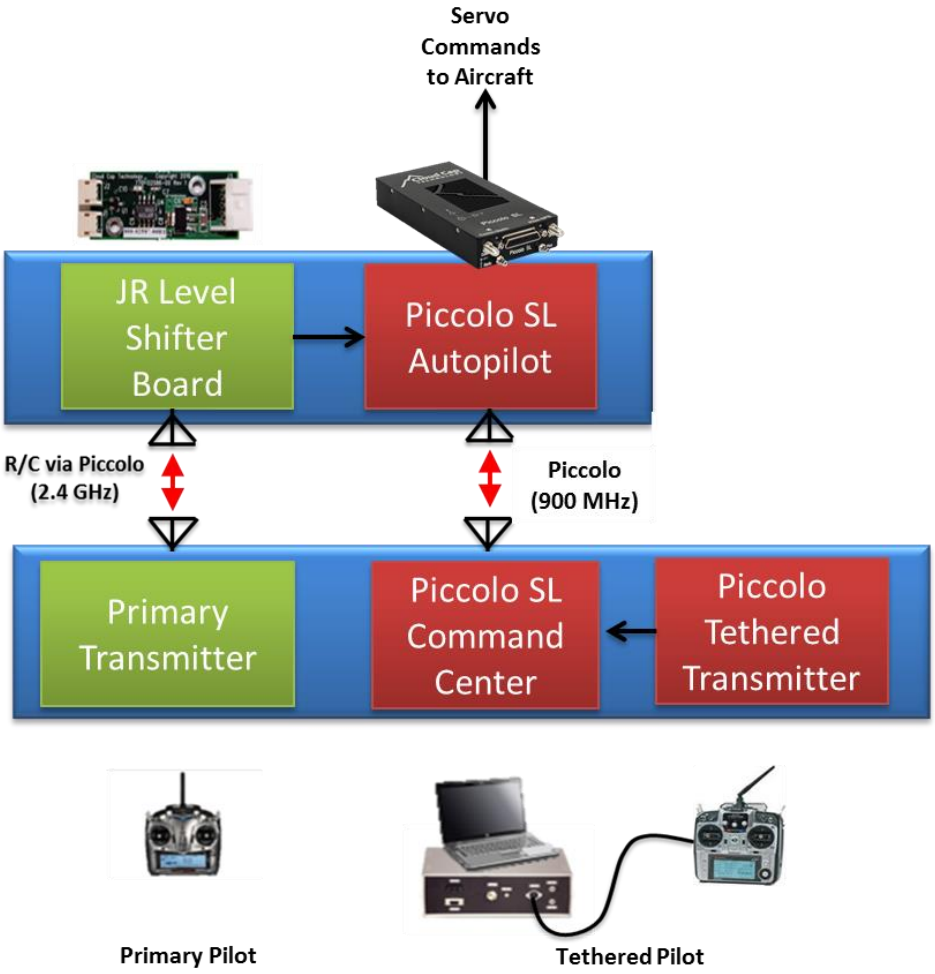

Figure 13 – Piccolo SL system architecture

Primary control of the RPV is provided through a JR 12X 2.4 GHz transmitter labeled above as the Primary Transmitter. Control signals sent via a 2.4 GHz RF link are received using the JR Level Shifter Board, and processed by the onboard Piccolo SL autopilot. The use of the JR Level shifter board allows the incorporation of multiple satellite receivers, improving RF communication to the aircraft. The primary control is allocated to the primary pilot whose role is to takeoff, place the Mini SensorCraft on station for test maneuvers, and then land. The second transmitter, labeled Piccolo Tethered Transmitter, will be used for 2 purposes. Its primary function is to provide a backup control should the primary experience a loss of link or the primary pilot commands a handover of control. The second function is to provide the ability for the inclusion of a test pilot who will perform all flight maneuvers in a controlled and meticulous manner from a first person point of view camera on the vehicle itself. The feasibility of this tethered pilot acting as the test pilot will be explored in the Flight Control Passover Tests for the Mini SensorCraft (Section 3.3.2). For more information about the control hierarchy, see Section 6.4.2.1. For a Frequency Usage Chart see Section 4.2.2.1.

Stability augmentation provided by the autopilot will be used to enhance yaw stability. The JWSC exhibits strong roll-yaw coupling, and previous flight tests with reduced complexity models and the GSRPV have shown that a "fly by wire" system, such as that provided by the Piccolo SL, can greatly assist in removing pilot workload during the flight by improving undesired coupling. Stability augmentation does not take any control authority away from the pilot, it simply uses the built in instrumentation in the autopilot to correct undesired coupling. The stability augmentation provided by the autopilot can be switched off via a switch on the transmitter at any point during the flight, and the pilot can regain full, unassisted control.

2.8 Instrumentation

2.8.1 Piccolo SL

The Piccolo SL serves as the primary data logging and data acquisition system on board of the aircraft. Aircraft altitude, attitude, airspeed, groundspeed and servo commands (which can be correlated, for a given mixing scheme, to control surface deflections) are all recorded and transmitted to the ground station in real time during the flight, along with GPS position. The Piccolo SL also has built in gyros/accelerometers which allow for the incorporation of stability augmentation.

2.8.2 Geometric Nonlinearity Measurements

Capturing the geometric nonlinearity introduced by the addition of flexibility along the length of the aft wing of the JWSC configuration is the overall technical objective of the Aeroelastic Response Program. In order to fulfill the overall technical objective, two measuring techniques have been identified and will be implemented. A traditional strain gage instrumentation of the internal structure of the aft wing will be implemented to not only measure strains in flight but also in ground based testing like the static structural loading test (Section 3.3.4.1). A photogrammetric measuring technique will also be utilized for ground based testing to obtain deflection measurements directly from multiple images. This technique will also be explored for inflight measurements. The Mini SensorCraft platform offers a reduced risk environment to develop these measuring techniques and systems.

2.8.2.1 Strain Gages

For the Aeroelastic Response Program (Mini SensorCraft FTP and ATRPV FTP), a digital strain gage measuring technique will be utilized. This technique is known as the picostrain concept [9]. The picostrain technology provides resistance-to-digital converters based on ratio-metric time-interval measurements. Conventional strain gage measurement includes constant excitation of a Wheatstone bridge circuit where the differential voltage output is amplified and converted by an A/D converter. The change in voltage, and thus strain, is captured by the mechanical deformation of the strain gages causing a change in resistance in the circuit thus varying the voltage output. However, these subsequent voltage outputs can be in the millivolt range and is consequently susceptible to random noise, which if present to an extent can render the measurement useless. The picostrain concept uses a simple RC circuit that excites the bridge only when the capacitor is discharged. The voltage is discharged through each strain gage in the bridge setup (ours will utilize a half bridge for each location) and the time it takes to discharge is measured using a time to digital converter which converts the measurement directly to digital thereby avoiding conventional noise in the measurement. The High Resolution module with

which the picostrain microchip is attached supports up to 4 half bridges and is capable of bridge trimming and temperature/gain drift compensation internally. Keeping all compensation internal and automatic on the stand alone board offers the advantage of less flight line operational time expenditure on trimming each bridge. The board is shown below in Fig. 14, and will be used as the intermediate step between the half bridges in the aft wing and the onboard data logger/ strain gage telemetry downlink unit.

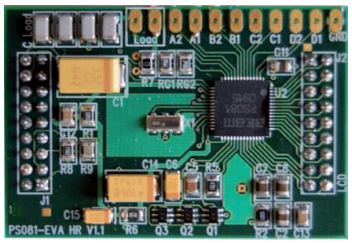

Figure 14- High resolution quattro bridge digital front end module[9]

The picostrain technique will utilize traditional strain gages placed in a half bridge configuration. The strain gages used are Micro-Measurements EA-13-125BZ-350 Option W. These linear pattern strain gages were selected based on form factor (width less than 4 mm) and availability. The high resolution module, which will be located within the fuselage, will be directly connected to the strain gages and output results in digital SPI format. The output from the high resolution module will be streamed into the piccolo SL autopilot through a digital I/O. The data will be telemetered via the piccolo 900 MHz downlink to the ground control station. This data will be monitored live in the sprinter van ground control station. Furthermore, the piccolo command center will save the data automatically along with all other sensor data within the piccolo SL autopilot. The strain gage system setup is shown below in Fig. 15 and the proposed measuring locations are displayed in Fig. 16. It is important to note, that to obtain 8 separate gage measurements the components for the measuring system was doubled.

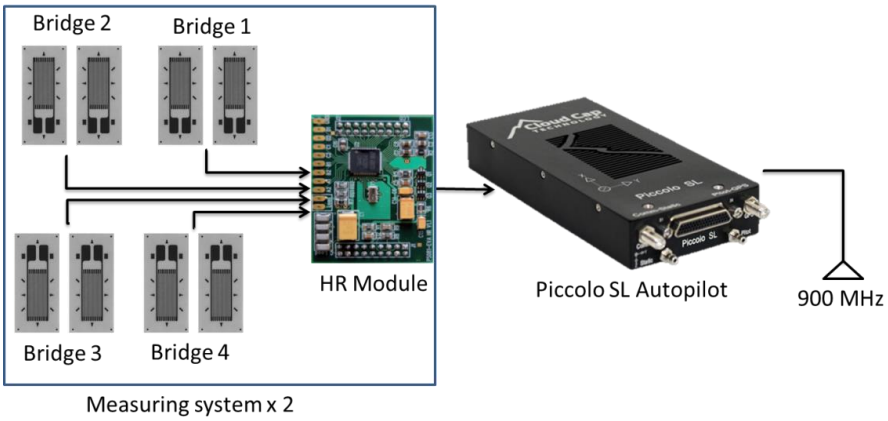

Figure 15- Strain gage system concept

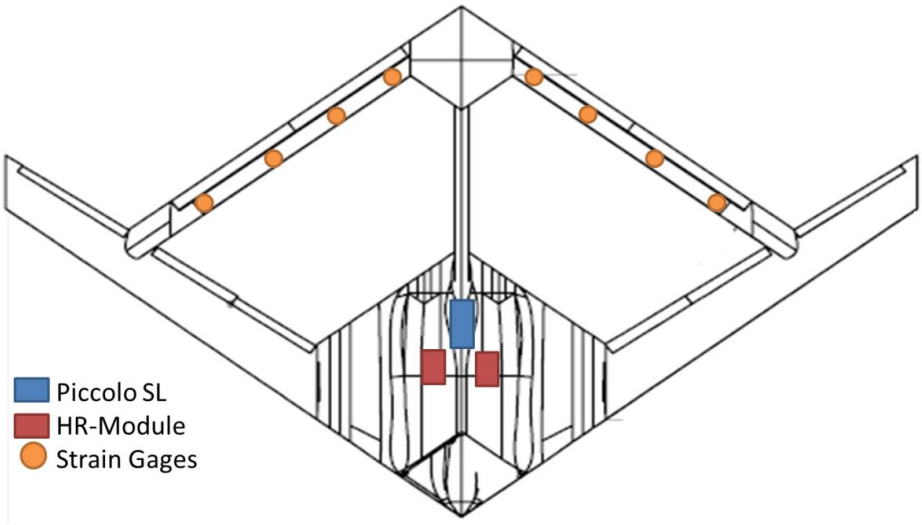

Figure 16- Strain gage system distribution and proposed measuring locations.

2.8.2.2 Photogrammetry Measurements

Photogrammetry is a measuring technique that can determine the geometric properties of objects from photographic images. Using multiple images of the object at various angles and distances provides the ability to triangulate 2D points into a 3D space through simple coordinate transformations to create a 3D model of the object. Tracking these points through multiple image sets for various deflection states provides the ability to obtain the 3D displacement of these points when referenced from an un-deflected set of images. This ability to obtain direct deflection measurements will be utilized specifically in the static loading test (Section 3.3.4.1). A common DSLR camera will be used along with post processing software known as PhotoModeler[10]. The process to obtain images for measurement is shown below in Fig. 17.

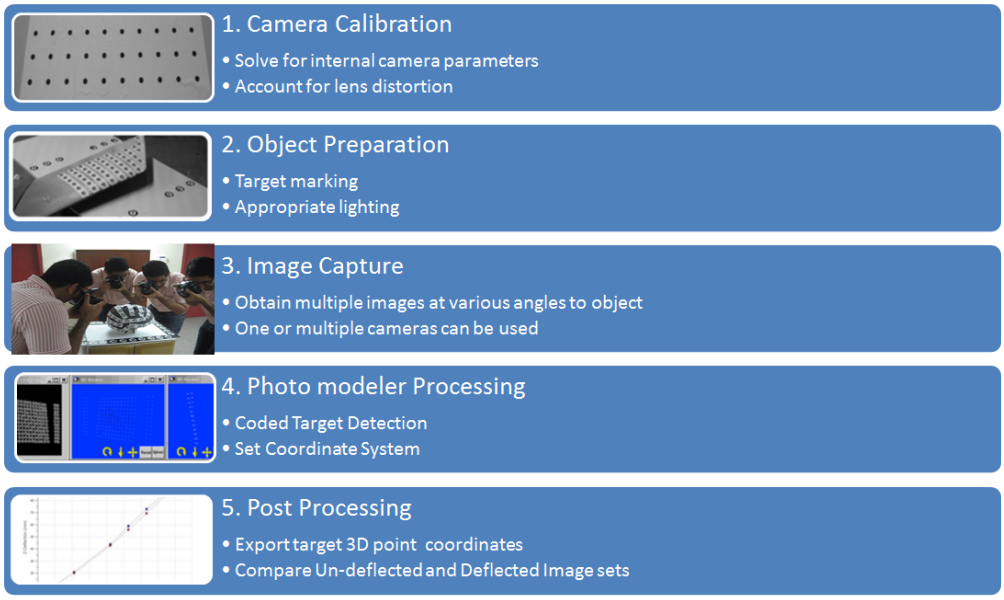

Figure 17- Photogrammetry process using PhotoModeler[10]

The first step within this process is to perform camera calibration. Images may be post processed without calibrating the camera, but this would result in less accurate measurements. The camera calibration stage will require the camera of interest obtain 12 photos of a calibration sheet (Fig. 18) on each axis of the camera. Importing these images into PhotoModeler will result in solved internal camera parameters including lens distortion. These factors are then used in PhotoModelers solving process to triangulate target markers from 2D to 3D space for a set of images. The calculated max residual dictates the quality of the calibration. The max residual is the pixel difference between the marked target points in the images and the 3D position solved by PhotoModeler. For a high quality calibration, the max residual should be less than 1 pixel.

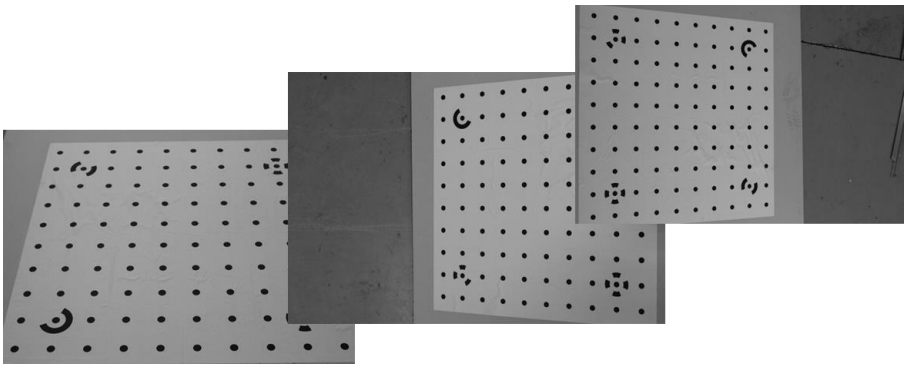

Figure 18 – Calibration images with calibration sheet used in PhotoModeler.

Preparing the object of interest is the next step in this photogrammetry procedure. PhotoModeler is capable of creating up to 99 individual coded targets to be placed onto the target for accurate referencing when post processing. However, due to glare and inappropriate light, these targets can be washed out and hinders the solving process which results in inaccurate measurements. A chemical spray to reduce glare must be utilized. After placing the targets onto the object, one camera can be used to obtain images at various angles and positions. These images are post processed through PhotoModeler which automatically marks the targets, and triangulates the points to create a 3D model of the object. The user must define a coordinate system manually to create a set of 3D points for the target markers that are reference to a similar origin for various load step image sets. (Fig. 19). PhotoModeler then provides the ability to export the solved 3D coordinates for targets. This data is referenced to the un-deflected data to obtain the 3D deflection results for the test (Fig. 20).

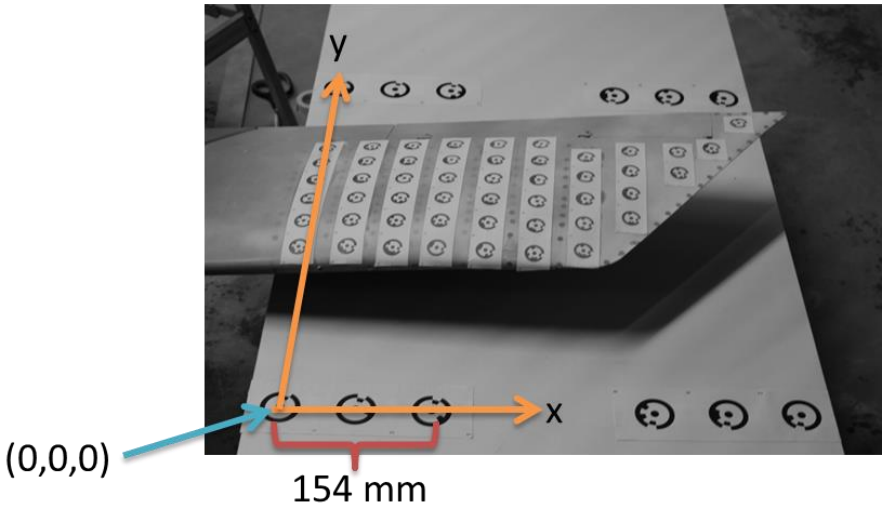

Figure 19- Defined reference plane to be common between separate loading image sets.

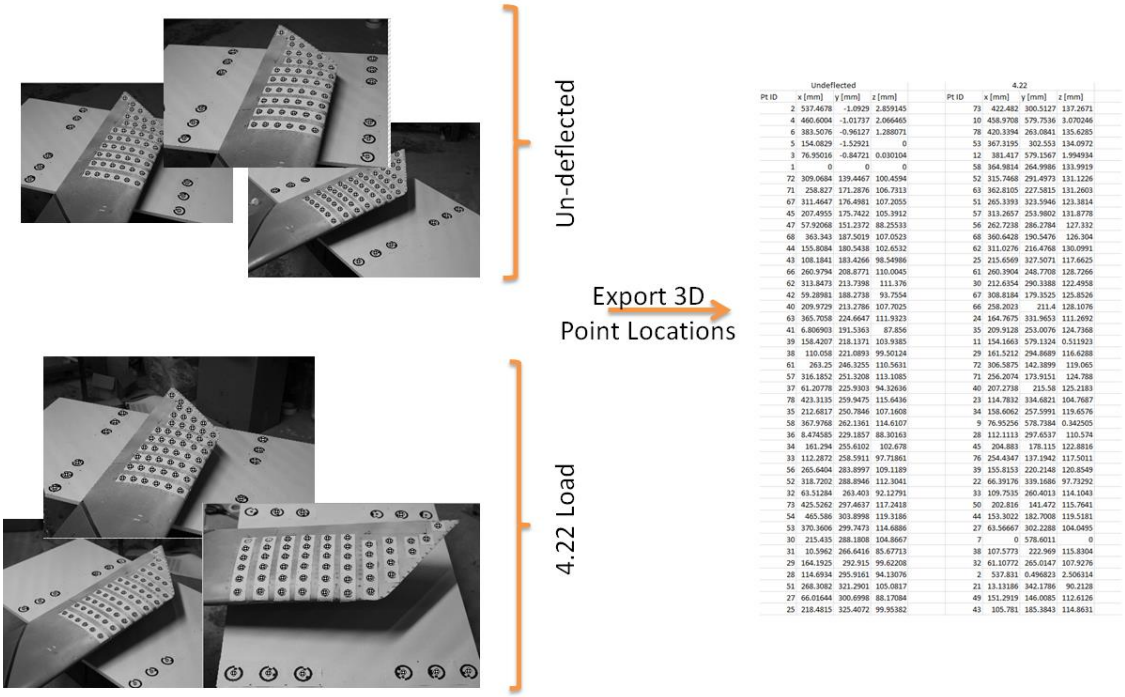

Undeflected				4.22			
Pt ID	x [mm]	y [mm]	z [mm]	Pt ID	x [mm]	y [mm]	z [mm]
2	537.4678	-1.0929	2.859145	73	422.482	300.5127	137.2671
4	460.6004	-1.01737	2.066465	10	458.9708	579.7536	3.070246
6	383.5076	-0.96127	1.288071	78	420.3394	263.0841	135.6285
5	154.0829	-1.52921	0	53	367.3195	302.553	134.0972
3	76.95016	-0.84721	0.030104	12	381.417	579.1567	1.994934
1	0	0	0	58	364.9814	264.9986	133.9919
72	309.0684	139.4467	100.4594	52	315.7468	291.4973	131.1226
71	258.827	171.2876	106.7313	63	362.8105	227.5815	131.2603
67	311.4647	176.4981	107.2055	51	265.3393	323.5946	123.3814
45	207.4955	175.7422	105.3912	57	313.2657	253.9802	131.8778
47	57.92068	151.2372	88.25533	56	262.7238	286.2784	127.332
68	363.343	187.5019	107.0523	68	360.6428	190.5476	126.304
44	155.8084	180.5438	102.6532	62	311.0276	216.4768	130.0991
43	108.1841	183.4266	98.54986	25	215.6569	327.5071	117.6625
66	260.9794	208.8771	110.0045	61	260.3904	248.7708	128.7266
62	313.8473	213.7398	111.376	30	212.6354	290.3388	122.4958
42	59.28981	188.2738	93.7554	67	308.8184	179.3525	125.8526
40	209.9729	213.2786	107.7025	66	258.2023	211.4	128.1076
63	365.7058	224.6647	111.9323	24	164.7675	331.9653	111.2692
41	6.806903	191.5363	87.856	35	209.9128	253.0076	124.7368
39	158.4267	218.1371	103.9385	11	154.1663	579.1324	0.511923
38	110.058	221.0893	99.50124	29	161.5212	294.8689	116.6288
61	263.25	246.3255	110.5631	72	306.5875	142.3899	119.065
57	316.1852	251.3208	113.1085	71	256.2074	173.9151	124.788
37	61.20778	225.9303	94.32636	40	207.2738	215.58	125.2183
78	423.3135	259.9475	115.6436	23	114.7832	334.6821	104.7687
35	212.6817	250.7846	107.1608	34	158.6062	257.5991	119.6576
58	367.9768	262.1361	114.6107	9	76.95256	578.7384	0.342505
36	8.474585	229.1857	88.30163	28	112.1113	297.6537	110.574
34	161.294	255.6102	102.678	45	204.883	178.115	122.8816
33	112.2872	258.5911	97.71861	76	254.4347	137.1942	117.5011
56	265.6404	283.8997	109.1189	39	155.8153	220.2148	120.8549
52	318.7202	288.8946	112.3041	22	66.39176	339.1686	97.73292
32	63.51284	263.403	92.12791	33	109.7535	260.4013	114.1043
73	425.5262	297.4637	117.2418	50	202.816	141.472	115.7641
54	465.586	303.8998	119.3186	44	153.3022	182.7008	119.5181
53	370.3606	299.7473	114.6886	27	63.56667	302.2288	104.0495
30	215.435	288.1808	104.8667	7	0	578.6011	0
31	10.5962	266.6416	85.67713	38	107.5773	222.969	115.8304
29	164.1925	292.915	99.62208	32	61.10772	265.0147	107.9276
28	114.6934	295.9161	94.13076	2	537.831	0.496823	2.506314
51	268.3082	321.2901	105.0817	21	13.13186	342.1786	90.2128
27	66.01644	300.6998	88.17084	49	151.2919	146.0085	112.6126
25	218.4815	325.4072	99.95382	43	105.781	185.3843	114.8631

Figure 20- Post processing of PhotoModeler results

2.8.3 FPV and Emergency Navigation Camera

The Mini SensorCraft will be equipped with a camera pointing out from the boom to provide first person view (FPV) navigation for performing test maneuvers and in the event that the aircraft inadvertently travels out of visual range. This camera will transmit real-time video feed to the ground station at all times during the flight. The forward facing camera is a GoPro HD Hero 3 digital camera. The camera offers up to as much as a 170 ° field of view and records to flash memory (1080p at 60fps). This camera will also output a standard definition video stream to a DJI onboard video transmitter. The video transmitter link has a power rating of 600mW, and transmits at 5.8 GHz to a receiver integrated into the sprinter van ground control station. Live feed of the video transmission will be streaming at an operation station within the ground control station.

3 Test and Evaluation

This section opens with a discussion of the hierarchy of the program objectives and success criteria that will be used to assess the success of the Mini SensorCraft flight test. This is followed by a detailed description of all four phases of tests proposed for the Mini SensorCraft FTP including descriptions of all of the tests that make up each phase. This section closes with a table summarizing all proposed tests, their respective location and objective level.

3.1 Goals and Objectives

The aeroelastic responses, specifically aft wing buckling and gust load response, associated with the JWSC have been demonstrated and investigated in numerous computational and wind tunnel studies[1-3,5]; however, these phenomena have never been successfully tested in a flight test program. **The Air Force has determined that a 1/9th scaled Remotely Piloted Vehicle (RPV) is needed to serve as a low cost and effective way to experimentally investigate nonlinear aeroelastic responses.** By demonstrating, investigating and measuring these responses, future joined-wing demonstrator flight test programs will be able to test active aeroelastic control and gust load alleviation systems to reduce the structural and aerodynamic effects of the nonlinear responses.

The introduction of flexibility into a 1/9th scale RPV platform requires a sufficient understanding of the resulting dynamic responses. Specific focus must be placed on handling qualites, control, and the ability to capture the static nonlinear aeroelastic response. To minimize risk and increase potential for later success in the 5 meter RPV program, a test program was developed for the Mini SensorCrafts to investigate these potential dynamic effects.

3.1.1 Overall Program Goal

The overall program goals of the Mini SensorCraft FTP are as follows:

1. Determine achievable loading conditions during flight for the follow on ATRPV;
2. Validate safe flight characteristics with a flexible aft wing; and,
3. Investigate aeroelastic response of aft wing from flight data.

3.1.2 Program Objectives

Using the aforementioned goals as a driver, a series of primary, secondary, and tertiary objectives were developed. These objectives are listed below. There are four planned phases (Flight Readiness System Tests, Test Point Investigation Tests, Maneuver Control Investigation Tests, and Flexible Flight Tests) aimed at meeting at least one of the objectives listed below. The test (or series of tests) that corresponds to each objective listed below is shown after that objective in parentheses. For more information about these tests, see Section 3.3.

3.1.2.1 Primary Objectives

1. Demonstrate accurate and successful data acquisition/ logging of Instrumentation system ***(Static Loading Tests, Flight Tests)***.
2. Safely demonstrate and capture geometric nonlinearities of the JWSC in flight utilizing the Mini SensorCraft ***(Flight Tests)***.

3.1.2.2 Secondary Objectives

1. Validate appropriate nonlinear static deflection of target aeroelastic responses for three tuned flexible aft wings on the ground ***(Static Loading Test)***.
2. Validate rigid body mass moments of inertia ***(Bifilar Pendulum Test)***
3. Verify EDF performance ***(Static Thrust Testing)***
4. Validate control surface deflections and mixing ***(System Calibration Test)***
5. Validate appropriate flight critical system communications ***(EMI/RF Test).***

6. Accurately tune Piccolo SL Autopilot ***(Simulation)***
7. Verify control hierarchy and fail safe scenarios ***(Safety Tests)***
8. Verify appropriate take off procedures ***(Launcher Test)***

3.1.2.3 Tertiary Objectives

1. Perform flight maneuvers with full autopilot ***(Maneuver Control Investigation Tests)***.

3.2 Success Criteria

In order to be considered a success, all primary objectives must be met, along with a majority of the secondary objectives. Below is a list explaining the relative importance of the secondary objectives. The tests are listed from most to least important, and this hierarchy will be used when evaluating the completion of "a majority" of the secondary objectives. Each test presented in Section 3.3 is labeled with a (P) or (S) corresponding to a primary or secondary objective, respectively. The successful completion of these tests will be used to quantify meeting the objectives. The tertiary objective has no waiting on the success of the overall flight test effort.

1.) The Static Structural Loading Test is the most important ground test in the FTP. The success of this test will validate the static structural target response of the flexible aft wings for the Mini SensorCraft. Furthermore, the static loading tests will validate the tuning procedure for the follow on ATRPV. Verifying the appropriate response of the aft wing on the ground provides confidence that the Mini SensorCraft will demonstrate the resulting dynamic responses of concern. This test provides the ability to investigate the controllability of the vehicle and verify the vehicles handling characteristic in a reduced risk environment. This test is directly related to ensuring the success of the final goal of the Mini SensorCraft flight tests which will provide confidence in moving to the ATRPV.

2.) Second to the Static Structural Loading Test is the Bifilar Pendulum Test. The Bifilar Pendulum Test provides experimental validation of the rigid body mass moments of inertia. The results of the Bifilar Test provide confidence in tuning the avionics.

3.) Static Thrust Testing, Safety Tests, Simulation, System Calibration Tests, and EMI/RF Tests are all critical to ensuring the success of flight testing of the Mini SensorCraft. These tests are responsible for preparing the internal avionics of the Mini SensorCraft. These tests have been performed successfully for previous flight vehicles including previous Mini SensorCrafts and the GSRPV.

4.) The Launcher Test, which includes verifying launching range using a dummy weight and verifying clean separation of the platform and dummy mass, is the least important of the tests. This low rank is due to the success with previous vehicles, including the Mini SensorCraft, and the fact that a launch test is performed before every flight as outlined in the launcher operational checklist in Appendix A. As a result, the need to do a standalone test outside of the tests completed for each flight becomes redundant.

3.3 Test Breakdown (4 Phases)

The Mini SensorCraft FTP is divided into four phases, which are meant to facilitate a prudent progression of testing to meet the overall objectives. Phase 1, Flight Readiness System Tests, includes the integration and testing of all onboard systems. The tests involved in this phase include bifilar pendulum testing, thrust testing, SIL simulation, system calibration tests, HIL simulation, EMI and RF

tests, launcher tests, and safety tests. Phase 1 will be concluded with a check out flight test of the Mini SensorCraft. Phase 2, Flight Control Passover Tests, contains planned flight tests to investigate in flight control handover between both pilots. The final result of this phase will determine the most feasible means of performing an accurate flight maneuver (primary pilot or back up pilot with first person video from vehicle). Phase 3, Test Point Investigation Tests, will involve an incremental approach towards a chosen test point for the aft wing designs. The variables to be incremented include static margin and test point weights. If the test point configuration chosen for the vehicle is a configuration the Mini SensorCraft has previously flown successfully, this testing phase will not be required. Phase 4, Flexible Flight Tests, will involve a static loading test for three flexible aft wing designs and flight tests with the aft wings configured onto the Mini Sensorcrafts.

All manufactured Mini SensorCraft will perform phase 1 of testing in order to verify airworthiness. Phase 2 and 3 will be attempted by one model of the Mini SensorCraft fleet, since these tests have no bearing on the airworthiness of the aircraft. However, phase 2 and 3 must be completed by a Mini SensorCraft before any subsequent manufactured models

3.3.1 may perform phase 4.Phase 1 –Flight Readiness System Tests

These tests serve to validate the functionality of all internal avionics and flight critical systems of the complete, flight worthy Mini SensorCraft.

3.3.1.1 Bifilar Pendulum Test (S)

A bifilar pendulum test will be used to experimentally determine the moments of inertia about each axis of the Mini SensorCraft. The bifilar pendulum test configuration for each axis is shown below in Fig. 21. The fuselage cage utilized for the static loading rig will be used as the suspension cage for the RPV in the bifilar pendulum test.

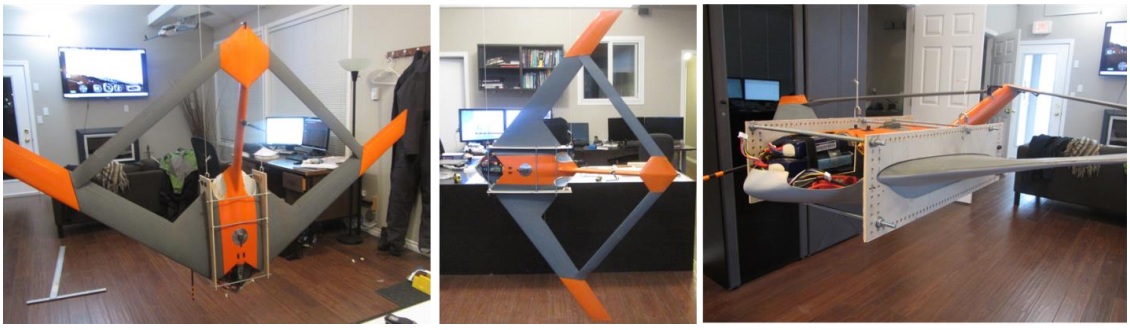

Figure 21- Bifilar pendulum test configurations for roll (left), pitch (middle), and yaw (right).

Tests will include the measurement of the moments of inertia for each configuration in which the RPV will fly. Trimming weights will be used to match the required scaled moments of inertia. A primary goal of this test is the investigation of the use of ballast to reach the maximum test point weight at the correct scaled moments of inertia for the Mini SensorCraft. During phase 1, this test will lay the foundation for the tuning of the piccolo SL autopilot.

3.3.1.2 Static Thrust Test (S)

The Static Thrust Test will be used to ensure that the full propulsion system is running properly. Installed thrust testing will verify that the EFD's are able to produce the required static thrust for safe operability at all scheduled test points.

Installed static thrust will commence with a simple startup, variable throttle run and cool down to ensure that all EDF mounts and ducting are functioning properly. Once this initial testing is complete, throttle sweeps will be completed. Throttle percentage, throttle command (pulse width), and current draw, will be recorded for each engine during each test run. Additionally, the thrust reading from a load cell attached to a custom apparatus will be recorded. The custom apparatus was built for the GSRPV to reduce the magnitude of the measured thrust by 50% to compensate for the theoretical maximum of both engines of the GSRPV (100 lbs) to the maximum of the load cell (50 lbs). To accomplish this aim, a hinged test apparatus was constructed (Fig. 22). Results will be compared to data from the manufacturer to validate full functionality of the EDFs.

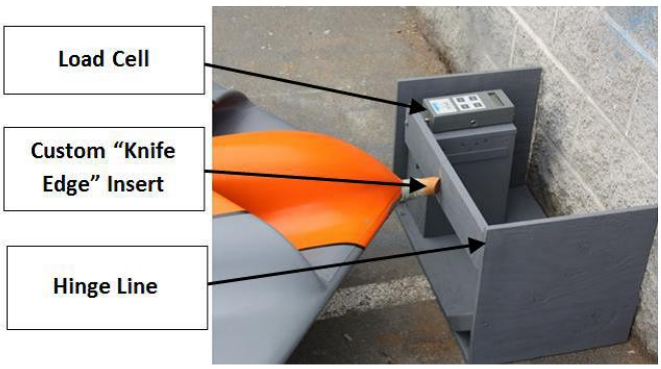

Figure 22- Static thrust test rig[11]

3.3.1.3 EMI /RF Test (S)

The electromagnetic interference and radio frequency (EMI/RF) test is meant to validate sufficient communication between the piccolo command center (PCC) integrated into the ground station and the onboard piccolo SL autopilot. This will be done through an inline hardwire test in which the signal to the piccolo will be attenuated to simulate range. This inline hardwire test will be repeated as a free space test in which the direct hardline will be removed between the ground station and vehicle. During both tests the Ack Ratio (Telemetry Downlink strength), RSSI (Receive Signal Strength Indicator), and Pilot Uplink will be monitored to verify sufficient gain margin for communications (Gain Margin of 10 dB at least). The Ack Ratio is a ratio measure of the number of good telemetry packets to the total number of telemetry packets sent from the piccolo SL autopilot to the ground station. The Ack ratio is an indication of downlink telemetry strength and must be kept within 90-100% strength throughout attenuation to stay within the flight test plan limits. RSSI indicates the radio frequency signal strength and must be greater than -108 dB through all attenuations. The most important measure is the pilot uplink which is the rate at which the autopilot reads the pilot input and is a direct indication of pilot

controllability. For all attenuations, the Pilot Uplink must stay at 40-50 Hz. The vehicle in each test will be orientated at various angles and heights to simulate any possible shielding due to aircraft attitude as well. The final portion of the EMI/RF test is to validate antenna tracking from the ground station to the aircraft location as it is in motion.

3.3.1.4 Launcher Test (S)

The launcher test will validate the launch range of a simulated dummy weight representing the Mini SensorCraft. Furthermore, the test will verify the clean separation of the launch platform and dummy weight upon launch. The launch platform is the platform the Mini SensorCraft will rest on prior to and throughout launch procedures. A clean separation of the dummy weight and launch platform is necessary for appropriate launch operations and to avoid damage of the vehicle. For the given range of Mini SensorCraft mass to be explored, a Simulink model of the complete propulsion system will be used to calculate minimum required range for a given mass as well as the pressure required in the accumulator to produce that range. In order for the test to be a success, the dummy mass must be within 3 meters of this calculated range. The inclination of the ramp is 10 degrees.

3.3.1.5 System Calibration Test (S)

The system calibration tests consist of a surface calibration of the control surfaces and a throttle calibration to the piccolo SL autopilot. For the surface calibration, an inclinometer (or other device) is needed to measure the angular deflection of the control surface from the neutral position. This is done for each surface by commanding a pulse width from the piccolo command center, then measuring the physical deflection. The angle deflection values are then entered into a corresponding table (Fig. 23) and saved to the avionics. The operator must take care to avoid binding within the control surfaces when performing this test. Once complete, the pilot should be able to run through a complete controls check. All surfaces should respond accordingly. The calibration data accounts for sign convention, surface neutral, travel limits, and any existing nonlinearities in the surface motion. A similar procedure is performed for the throttle calibration.

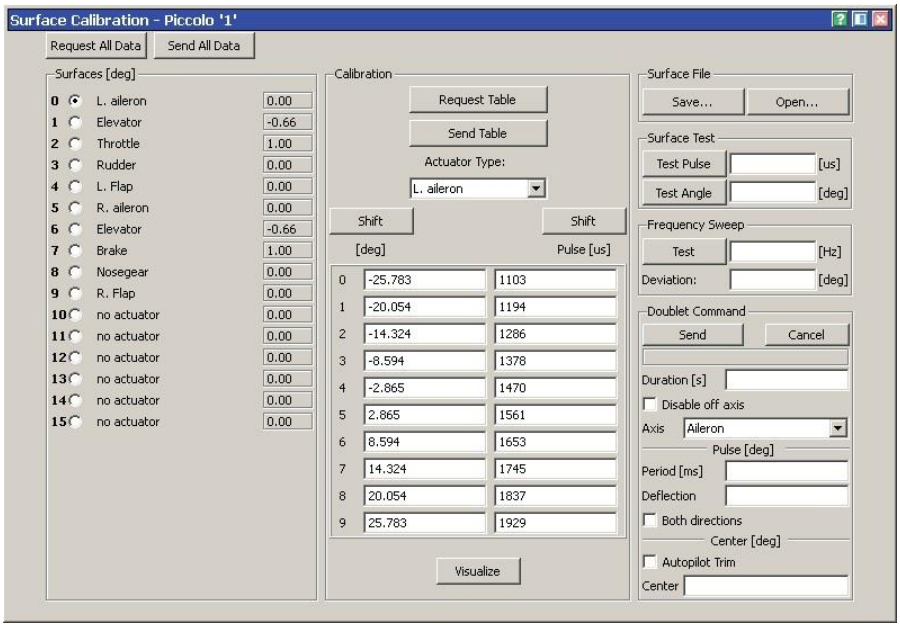

Figure 23- Surface calibration window.

3.3.1.6 Simulation(S)

Simulation will involve both software in the loop (SIL) and hardware in the loop (HIL) simulation of the Mini SensorCraft. These simulation systems are a product of Piccolo's development environment. SIL simulation provides the ability to simulate operations and flight maneuvers in an environment where the avionics are virtualized and utilized within a simulator. HIL provides the ability to simulate operations and flight maneuvers in an environment where the avionics are directly connected to the simulator meaning that all Mini SensorCraft systems and control surfaces are in the loop. The ultimate goal of HIL simulation efforts is to develop a better understanding of the power system endurance for the vehicle (since all systems are operational). If the EDFs are operational during the HIL simulation, the Mini SensorCraft will be restrained from any possible movement. Furthermore, the Mini SensorCraft will be placed in an open area with little possibility of FOD ingestion. The common goals between the SIL and HIL simulation efforts are to provide further operational training for flight critical personnel and tuning of the piccolo SL autopilot prior to the first flight.

3.3.1.7 Safety Tests(S)

These safety tests involve the verification of all safety measures implemented within the Mini SensorCraft. This includes a camera transmission test to verify the emergency navigation camera and connectivity, a controller hierarchy test to validate all control switch permutations, and finally all fail safe conditions pre-programmed within the piccolo SL autopilot.

3.3.1.7.1 Camera Transmission (S)

The ground station operator will begin transmission of the emergency navigation camera on the Mini SensorCraft. The video streams as viewed on the ground station will be checked for signal loss or

gaps in the transmission. For more information about camera placement and purpose, see Section 2.8.3.

3.3.1.7.2 Control Hierarchy Tests (S)

The RPV will be prepared for flight, including the propulsion system. With the aircraft firmly secured, all onboard systems will be running (including instrumentation and propulsion) and control will be passed between the primary controller and the tethered controller. A flow chart of the control hierarchy between both controllers is presented in Section 6.4.2.1.

3.3.1.7.3 Fail Safe Test (S)

Loss of link will be simulated for both the primary and tethered controller to ensure that the "failsafe" condition is operational and that the loss of link hierarchy is operating as planned. This includes the pre-programmed autonomous flight path in the event of primary link loss. The failsafe condition is executed during full loss of link, and corresponds to a controlled crash: full up elevator, full right rudder, full right aileron, turbines at idle or shutdown if possible. The failsafe condition is designed to minimize residual damage in the event of total loss of link. For more information about the failsafe procedure, see Section 6.4.3.1.2.

3.3.1.8 Checkout Flight (P)

The final test to be performed in phase 1 is a checkout flight for the Mini SensorCraft. The goals of this flight are to successfully take off from the launcher (manual mode), tune the inner loop gains while on station performing race track patterns (Fly-by-Wire Mode), perform landing approaches, and successfully belly land. Resulting success metrics of this flight in order to move onto the next phase in testing are reliable endurance data, the aircraft is deemed controllable based on the cooper harper (Appendix A) scale, and the airframe state after the flight is less than 2. The airframe state represents the state of the aircraft upon completion of the mission. The aircraft levels are presented below.

1. No Damage: Aircraft requires no repairs or modifications other than configuration modifications required by subsequent mission.
2. Light Damage: Some light damage sustained by aircraft due to unavoidable operational "wear and tear". Required repairs can be performed in-field.
3. Significant Damage: Aircraft requires new components or more significant repairs that can't be performed in-field.
4. Catastrophic Damage: Aircraft is destroyed or damaged beyond repair. Over 50% of structure requires repair and replacement.

The flight test card for the Checkout flight of the Mini SensorCraft is presented in Appendix B.

3.3.2 Phase 2 –Test Point Investigation Tests (P)

Phase 2 of testing focuses on incrementally approaching the test point configuration of the Mini SensorCraft for follow on flights. The flights within this phase of testing will focus on incrementing test point weight and static margin. The test point will be chosen based on outside investigations of the aeroelastic tuning of the aft wings for the follow on ATRPV efforts. Flights at the test point configuration will be evaluated by the test pilot based on the cooper harper scale listed in Appendix A. Should the test

point configuration chosen for the vehicle be a configuration the Mini SensorCraft has flown successfully, this testing phase will not be required.

The success metrics to move onto phase 3 of testing include demonstrating the Mini SensorCraft is controllable in maneuvers at the test point configuration, the test pilot can consistently perform these maneuvers, and the airframe state remains less than 2 for the flight at the determined test point.

3.3.3 Phase 3 –Maneuver Control Investigation Tests (P)

Phase 3 of testing is meant to investigate feasible means of performing flight maneuvers. The flight goals of this testing are to successfully demonstrate control handover between the primary and tethered pilot and test all possible permutations of this control handover in flight. Further goals include the tethered pilot performing racetrack patterns while on station in first person view from within the ground station van via the onboard video camera.

The two maneuvers (approved in the previous GSRPV flight test plan) that will be performed are a push-over pull-up and a windup turn. These maneuvers each present a unique method of reaching the required wing loading to eventually demonstrate geometric nonlinearity of the aft wing. The push-over pull-up requires the pilot to put the aircraft into a controlled dive and then pull-up, causing the aircraft to encounter positive loading at the bottom of the maneuver and negative loading at the top of the maneuver. The windup turn is performed when the pilot maintains constant speed and flies the aircraft through a spiral pattern. As the radius of the turn decreases, the wing loading increases. This approach allows for a gradual increase in wing loading, but it can only accomplish positive asymmetric loading.

Should time permit, the tertiary objective of using the fully autonomous mode of the piccolo SL autopilot to perform flight maneuvers will be investigated. The success metrics of these subsequent flights are that there must be 3 consecutive flights with safe control handover, 3 consecutive flights where the airframe state remains less than 2, and the most feasible method of performing a controlled maneuver must be determined

3.3.4 Phase 4- Flexible Flight Tests (P)

Having decided on a test point, 3 flexible aft wings will be designed to exhibit geometric nonlinearity. These designs will be implemented interchangeably onto the Mini SensorCraft platform. The resulting configurations will first go through an extensive ground based static loading test to verify the target aeroelastic response on the ground and then flights will be performed with each flexible aft wing where the aeroelastic response of the flexible structure will be monitored.

3.3.4.1 Static Loading Test (P)

The static structural loading test has 4 goals. The first is to validate the manufacturing of the Mini SensorCraft to produce the designed target static nonlinear aeroelastic response. Secondly, this test will validate the structural integrity of the RPV and ensure that all wing loadings experienced during flight can be safely sustained. Another goal is to verify there is no binding of the control surfaces when the Mini SensorCraft is under a loaded condition. Lastly, this test provides a controlled method to tune the strain gage system. Measurements will be taken using the tuned strain gage system and the developed photogrammetry process (see section 2.8.2).

The test will utilize a 3 component test rig composed of outer rib casings, a restraining fuselage cage, and a turnbuckle system to provide the loading. A concept of the outer rib casings to be employed is shown in Fig.24.

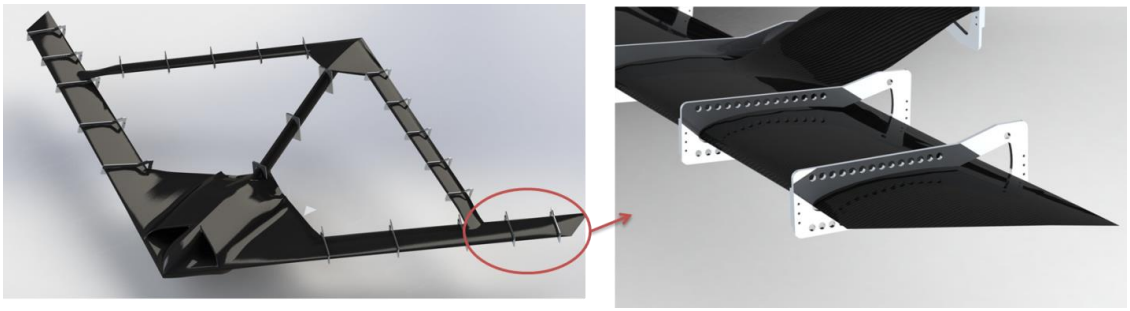

Figure 24-Outer rib casings distributed across platform (left); Zoomed in view at wing tip (right)

The second component to the test rig is the fuselage cage. The fuselage cage is composed of 2 ½" thick wooden pieces held together with threaded rods. The cage is then bolted to the ground using angled steel brackets to prevent rotation of the fuselage during load applications. Fig. 25 shows the developed fuselage cage while Fig. 21 in Section 3.3.1.1 shows the Mini SensorCraft within the fuselage cage.

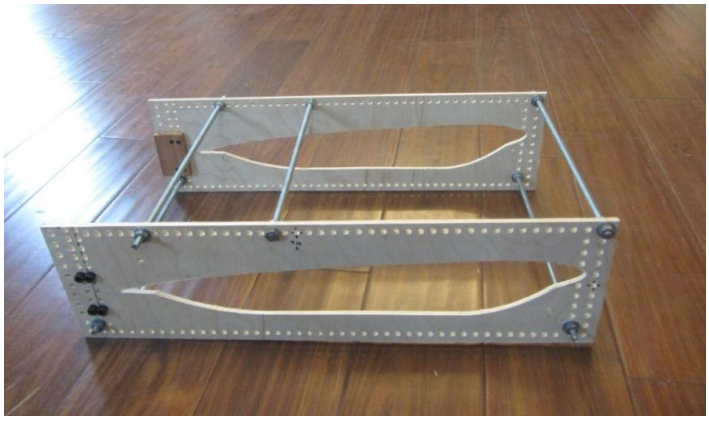

Figure 25- Fuselage cage used to prevent rotation of the RPV during load tests

The final component of the static loading rig will be a turnbuckle system used to transfer loads to the external rib casings and thus to the vehicle. The turnbuckle is attached to an overhanging structure and is placed directly in line with the point load location desired along the length of the outer rib casings. A force gage is placed in line between the turnbuckle and the outer rib casings to verify the loading at that point. The set up utilized for the GSRPV effort demonstrates this concept below in Fig. 26.

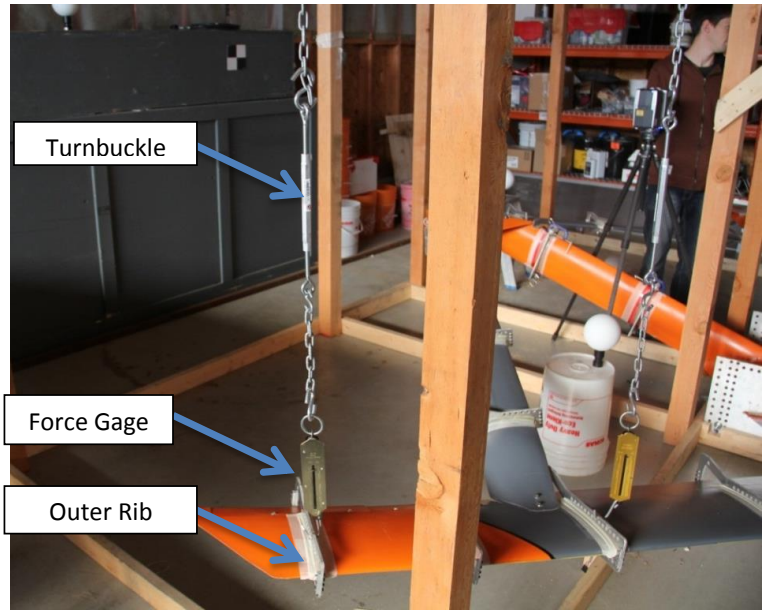

Figure 26- Turnbuckle system used for static loading tests

3.3.4.2 *Aeroelastic Response Flights (P)*

The goal of these flights is to fly 3 various flexible aft wings on the Mini SensorCraft. The overall goal of these tests is to monitor the resulting dynamics of introducing a flexible aft wing specifically focusing on controllability and flight handling characteristics. Furthermore, a strain gage system will be implemented along the internal structure of the aft wing in order to monitor and capture the static strain of the aft wing in flight. The success metrics that lead to the completion of the overall Mini SensorCraft FTP are there must be at least 3 consecutive flights with save operations, 3 consecutive flights where the airframe state remains less than 2, post processing of flight data yields aeroelastic response of aft wing, and finally the aircraft is controllable and exhibits good flying qualities (Cooper Harper Scale).

3.3.5 Overall Flight Test Summary

The following table summarizes all planned tests, the phase of testing that each test falls into, and the classification (primary objective, secondary objective or tertiary objective) which corresponds to the success criteria mentioned in Section 3.2

Table 6- Overall Flight Test Summary

Phase 1-Flight Readiness System Tests	Objective Level
Bifilar Pendulum Test	Secondary
System Calibration Tests	Secondary
Simulation	Secondary
EMI/RF Tests	Secondary
Static Thrust Test	Secondary
Launcher Test	Secondary
EMI/RF Test	Secondary
Piccolo Data Transmission Test	Secondary
Antenna Motion Test	Secondary
Safety Tests	Secondary
Camera Transmission Test	Secondary
Control Hierarchy Test	Secondary
Fail Safe Tests	Secondary
Checkout Flight	Primary
Phase 2- Test Point Investigation Tests	**Objective Level**
Test Point Investigation Flight Tests	Primary
Phase 3- Maneuver Control Investigation Tests	**Objective Level**
Flight Tests	Primary
Phase 4-Flexible Flight Tests	**Objective Level**
Static Loading Test	Secondary
Aeroelastic Response Flights	Primary

4 Test Logistics

This section outlines the infrastructure in place to ensure that the Mini SensorCraft flight testing of the vehicle has the highest chance of success. The section begins discussing the two primary test locations for the FTP efforts. Test resources, including the ground station and all Mini SensorCraft control systems will then be presented, along with a frequency usage chart. Safety requirements will follow and a description of all flight test personnel, including each participant's qualifications will close this section.

4.1 Test Locations

All tests will be performed in Victoria, British Columbia, Canada. Ground based testing will be done at UVics Centre for Aerospace Research (Cfar) located in Sydney, British Columbia Canada. All flight tests will take place at the Cfar flying site.

4.1.1 Cfar Flying Site, Victoria Canada

The Cfar flying site, is a large farm space approximately five minutes away from Cfar. Fig. 27**Error! Reference source not found.** below presents a satellite view of the Cfar airspace overlaid the normal flight operations boundary and safety boundaries.

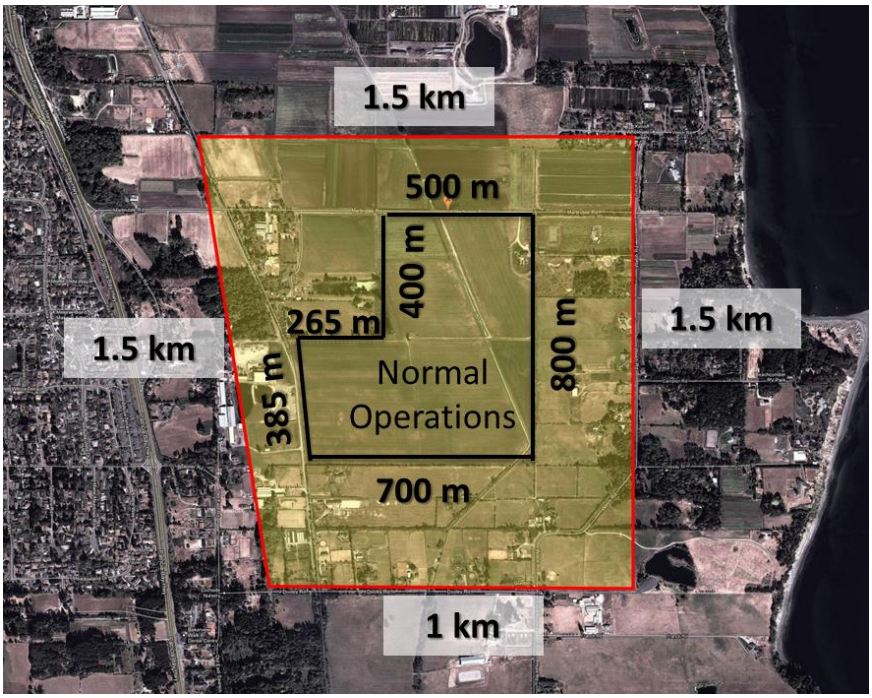

Figure 27– Approved Airspace (Cfar Flying Site).

The airspace available for this site is sufficient for all planned flight tests and has proven to be so for outside flight test efforts. The airfield is centered at N 48˚33'28", W123˚ 22'47". The airspace shown in Fig. 27 has been approved by Transport Canada for the flight testing of the Mini SensorCraft. The "Safety Template," or the airspace in which all flight operations are allowed to continue uninterrupted, is shown in Fig. 27 as the normal operations area. All planned flight tests will remain well within this Safety; however, should unanticipated flight conditions and/or problems cause the aircraft to leave this normal operations area, appropriate measures will be taken. Immediately outside of the normal operations area, the rest of the approved airspace is known as the Caution Zone. Should the Mini SensorCraft travel into the caution zone, a return to lost communications (lost comm.) way point will be automatically activated and performed by the piccolo SL autopilot. The lost comm. way point will be situated within the normal operations area.

Immediately outside of the Caution Zone is the Kill Zone, shown in red. If the Mini SensorCraft exits the approved airspace (which includes the normal operations area and Caution Zone), failsafe via aerodynamic termination will be automatically executed. In other words, should the aircraft enter the kill zone, the failsafe will be automatically executed to terminate the flight. Note that the safety envelope, caution and kill zones will be programmed into the ground station computer and overlaid over

the real-time vehicle position information. Within the normal operations area exists a further safety template level which is shown in Figures 28 and 29. The maximum permitted flight altitude is 120 meters (394 ft).

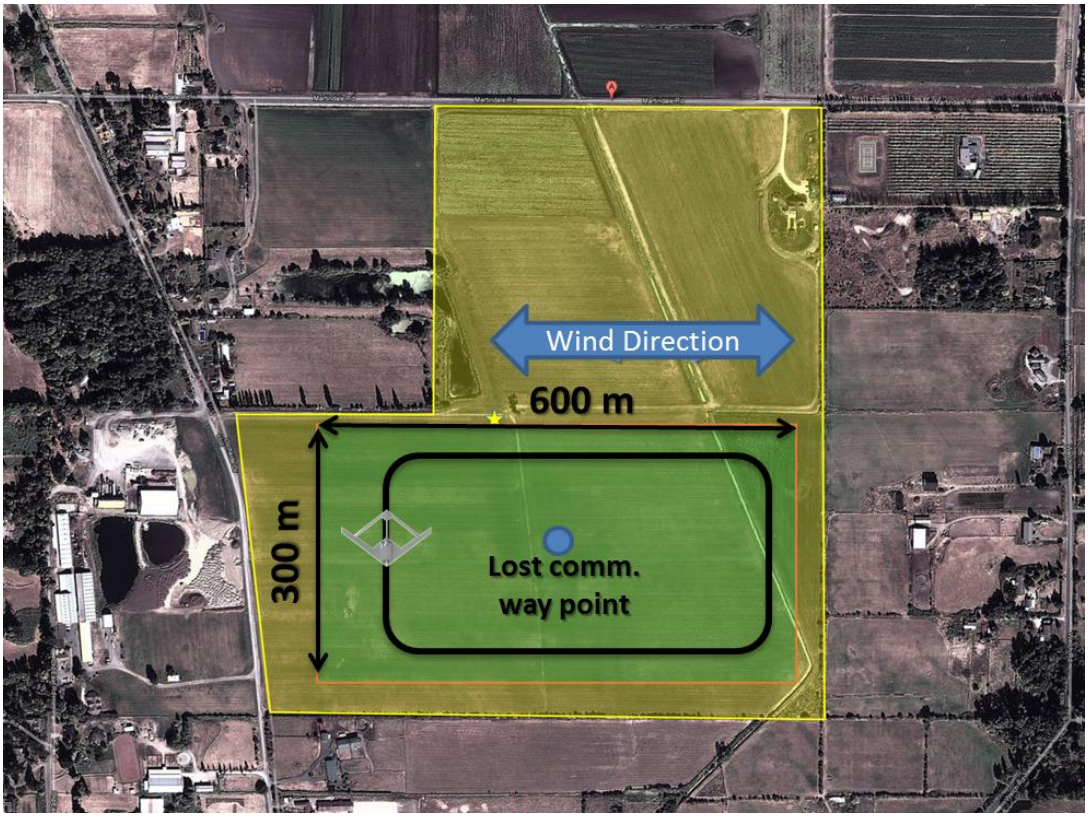

Figure 28-Operations area for test day with wind directions west and/or east.

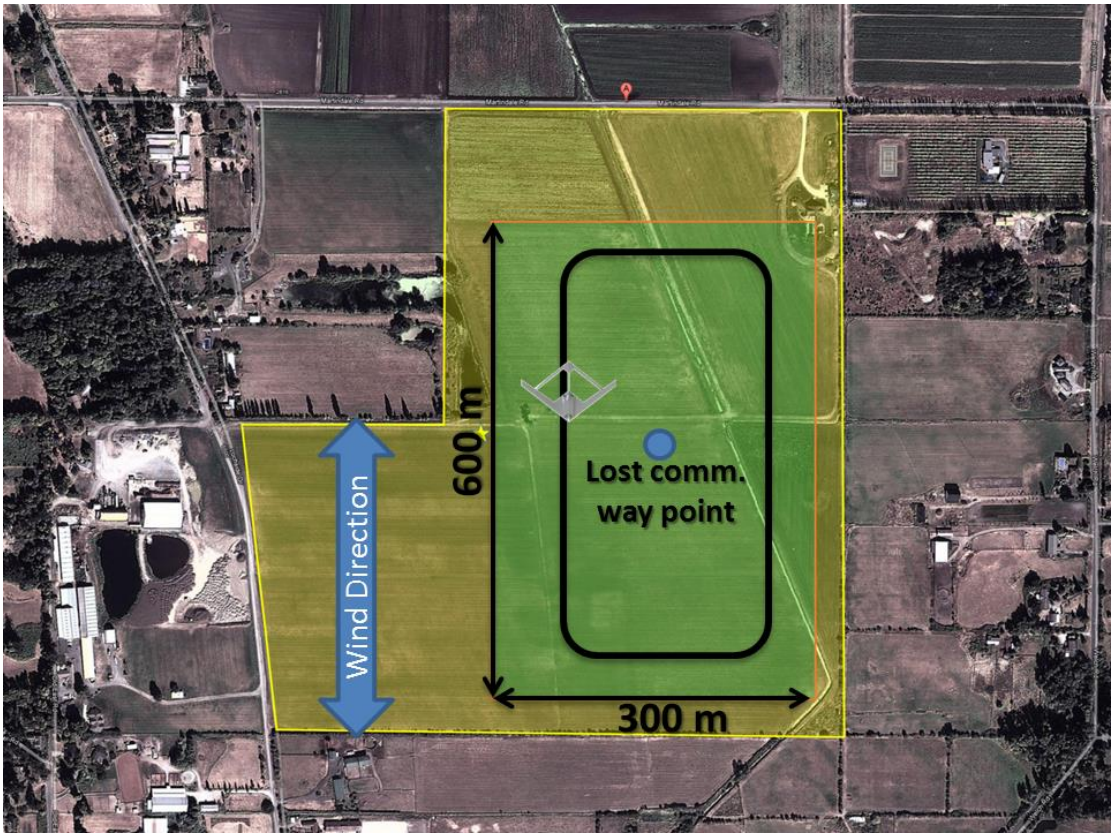

Figure 29- Operations area for test day with wind directions north and/or south.

There are two possible test day configurations for the normal operations area. The wind direction for the day of the flight test will determine which to use. For a given flight test, the green area in Figures 28 and 29 indicate the flight operations area. It is defined as a 600 meter by 300 meter box, which allows for enough area for all flight patterns planned to be performed by the Mini SensorCraft. As an example, both figures indicate a 500 meter by 250 meter race track pattern. The lost communications way point is defined in the middle of each of these areas. The Mini SensorCraft will be commanded to the lost comm. way point and enter an orbital pattern until control is taken back by the primary pilot. Return to the lost comm. way point will only occur should the Mini SensorCraft exit the normal operations area. The yellow area shown within the normal operations area is a buffer caution zone. Should the Mini SensorCraft enter this zone, the pilot will immediately bring the aircraft back into the green zone.

4.1.2 Special Flight Operations Certificate

A Special Flight Operations Certificate (SFOC) approved by Transport Canada for the operation of the Mini SensorCraft is active for this flying site. All flight operations will abide by the guidelines set forth in this document, including airspace, operational and safety requirements (Appendix E).

4.2 Test Resources

4.2.1 Mini SensorCraft

The Mini SensorCraft is the main component to the Mini SensorCraft Flight Test plan. Reference Section 2 for a full description of the Mini SensorCraft and supporting systems.

4.2.2 Ground Station

The ground station used for all test operations will be the UVic Sprinter Van-UAV Command Station (Fig. 30). The ground station, which is used for real time data monitoring as well as post-flight data download and reduction, has the following features:

1. Two computer workstation each with a 30” monitor and two 17” monitors
2. Additional 40” Plasma/LCD screen
3. 120 VAC and 12 VDC power throughout vehicle
4. Custom wall plates with power outlets, HDMI, USB, RS232, etc.
5. Internet router with Wi-Fi network and access to 3/4G
6. External Connection including several 120 VAC outlets, shore power hookup, and payload pass through connectors for miscellaneous hookups.
7. Video switch/matrix (8-12 inputs by 8 outputs)
8. Pneumatic antenna mast and compressor
9. Easy Integration of the Piccolo Command Center into ground station
10. Two portable Honda EU2000KC2 generators (2000 watts, 120VAC power)
11. Stabilizing Jacks to prevent excessive rocking and movement of Van

Figure 30 – Mobile Ground Station (Left), Internal (Right)

4.2.2.1 Frequency Usage Chart

Radio frequencies are shown in Table 7, and all frequency usage will be coordinated with the test range prior to testing.

Table 7- Frequency Usage

Form of Communication	Frequencies Used During the Test
R/C Communications	2.4 GHz Spread Spectrum (JR 12x)/ 900 MHz (Piccolo SL)
Data Transmission	900 MHz (Piccolo SL)
Emergency Navigation Camera	5.8 GHz
Team Communications	Clark Head Sets 2-Way Radio system (125 Hz)

4.3 Security Requirements

This program is UNCLASSIFIED and NOT restricted by ITAR regulation. The Piccolo SL is ITAR equipment, but Quaternion Engineering has received all required approval to operate with the Piccolo SL.

4.4 Test Project Management

This section will outline all personnel who will participate in the tests. At a minimum, the following people are required to be present during flight tests: Test Director, Ground Station Operator, Ground Support, Range Safety Officer, Primary Pilot, and Tethered Pilot. Efforts will be made to have at least 2 additional people on site during flight testing to serve as observers or additional ground crew.

Table 8 - Flight Test Personnel

Name	Title	Responsibilities
Dr. Ned Lindsley	AFRL Program Manager	Oversee the administration of the program. Point of Contact (POC) at AFRL.
Jeff Garnand-Royo	Test Director	Plan, coordinate and oversee all tests. Awareness of test area, equipment and procedure. Exercise Go/No Go authority as well as direct pilot during testing (including termination of flight if necessary). Communicates all information to pilot.
Jenner Richards	Ground Station Operator	Operate the ground station. Monitor and oversee data collection and storage. Provide real-time aircraft state and health information to the test director.
Kelly Williams	Primary Pilot	Perform flight maneuvers listed on the test cards under direct direction from the test director. The pilot will control the RPV through the primary

		transmitter.
Jon Harwood	Tethered Pilot	The Tethered Pilot will be in charge of the second, tethered transmitter. He will act as a Backup Pilot who will take control of the aircraft if he is directly directed to do so by the primary pilot in the event of a primary link failure or if the pilot becomes incapacitated. The Backup Pilot will also provide assistance to the pilot as required (trim assistance, range assessment, visual orientation, etc.). May also act as test pilot who performs later test maneuvers.
Gord Cooney	Range Safety Officer (RSO)	Intimately aware of the flying site as well as all safety requirements imposed by the flying site. Provides safety briefing at the beginning of each Phase 3 testing day. Authority to call an immediate stop to testing (abort flight) in the event that an unsafe situation arises.
(TBD)	Observers	Observe test operations and provide assistance as required by other personnel.
Wanjohi Mugo	Ground Support	Observe test operations, help with RPV operations as required and provide assistance as required by other personnel.
Dr. Robert Canfield	Virginia Tech Technical Advisor	Advisor to Jeff Garnand-Royo, provide technical guidance and expertise throughout the program.
Dr. Afsal Suleman	University of Victoria Technical Advisor	Advisor to Jenner Richards, provide technical guidance and expertise throughout the program.
Dr. Craig Woolsey	Virginia Tech Technical Advisor	Advisor to Jeff Garnand-Royo, provide technical guidance and expertise throughout the program.

4.4.1 Qualifications of Pilots

Kelly Williams is a Mechanical Engineer and has been flying R/C aircraft since 1989, including flying turbine powered R/C jets since 1998. He serves as the Committee Chair on the R/C Jet Committee of The Model Aeronautics Association of Canada. Prior to flying the Mini SensorCraft platforms for this test effort, Kelly will have trained on the 6DoF simulator. Furthermore, he was the Primary Pilot for the Flight Demonstration Program and was the first to fly the GSRPV. Kelly has also flown previous models of the Mini SensorCraft.

Jon Harwood has 15 years' experience as a R/C pilot and holds his private pilot's license. He has served as the primary test pilot during the majority of Quaternion Engineering's previous Mini SensorCraft flight tests. He holds his CCUVS UAS Operator Certificate. Jon will also continue training on the 6DoF simulator. Furthermore, Jon served as the tethered pilot of the GSRPV for the Flight Demonstration Program.

4.4.2 Other Qualifications

Jeff Garnand-Royo, Jenner Richards, Gord Kooney, Wanjohi Mugo, and Jon Harwood have all taken and passed the Transport Canada Radio Operator Certificate Exam. The Transport Canada Radio Operator Certificate gives each the authority to monitor airfield air traffic. Jenner Richards and Jon Harwood have both taken and pass the CCUVS UAS Operators course. The CCUVS UAS Operator Certificate recognizes each as an official CCUVS UAS Operator.

5 Operational Day Procedures

On any operational flight day, the specific testing procedure will consist of the following steps:

Pre-Operations :

1. Pre-Operations Checklist
    a. Airframe Checklist
    b. Ground Station Checklist
    c. Pre-Ops Preparation Checklist
2. Test Day Overview Briefing
    a. Full Day Mission Briefing
    b. Safety Briefing
    c. AFRL SUAS Test Ops ORM Assessment
    d. Pre-Ops Preparation Checklist

Flight Operations:

1. **Pre-Flight:**
    a. Pre-Flight Mission Briefing
    b. Pre-Flight Log
    c. Pre-Flight checklists:
        1. Aircraft
        2. Launcher
        3. Piccolo
        4. Ground Station
        5. Instrumentation
    d.Go/No-go Decision
2. **In-Flight (Test Execution)**
3. **Post-Flight:**

a. Post-Flight Log
b. Post-Flight Checklists
    1. Post Flight-Aircraft Checklist
    2. Post Flight Data Checklist
c. Post-Flight Briefing

Post-Operations:

1. Post Operations Briefing

5.1 Pre-Operations

The pre-operations procedures encompass the entire test day and are completed the night prior and at the beginning of each operational day. The night before operations, the Pre-Operations checklists are completed. The pre-ops checklist also has a component (test article packing) that is completed the day of operations before leaving for the flying field. Pre-Operations include the test day overview briefing which contains a full day mission briefing and a safety briefing specific for the current test day. This is followed by the test director completing the AFRL SUAS Test Ops ORM Assessment (Appendix C). A safety briefing is then conducted by the range safety officer. Having completed administrative duties, a full airframe and ground station inspection are completed. These inspections are meant to be the most comprehensive of the checklists to verify full operational readiness of critical flight test articles before flight test operations begin.

5.1.1 Pre-Operations Checklist

The pre-operations Checklist will be completed the night before the test day. The pre-operations checklists are located in Appendix A. There are separate pre-operation checklists for:

1. Airframe
2. Ground Station

The pre-operations airframe checklist will check all mechanical aspects of the flight vehicle, including verifying all internal avionics connections. The pre-operations ground station checklist will verify ground station power and operation before test day. A preparation checklist is performed the night before and also the day of operations. The pre-ops preparation checklist ensures appropriate execution of the Aircraft and ground station checklist and further encompasses the packing lists for all flight critical components to be brought to the flying field.

Flight critical personnel will be responsible for portions of the pre-operations checklists as outlined in Appendix A. All pre-operations checklists are located in Appendix A.

5.1.2 Test Briefing

The test briefing will be conducted by the Test Director and will consist of an overview of all tests planned for the current test day. All personnel present for the days testing will be required to attend. The briefing will serve to allow everyone on site to unify their understanding of the goals for that particular day. The test briefing shall consist of:

1. A review of results of the previous days test, if any
2. Proposed test schedule for the given operational day
3. Weather report
4. Complete the AFRL SUAS ORM form and brief participants on ORM level (AFRL SUAS ORM Form shown in Appendix C)
5. Security issues

5.1.3 Safety Briefing

The safety briefing will be conducted by the Range Safety Officer and will include the following:

1. Test boundaries for the day
2. Safety concerns for any of the planned tests
3. Review of Test Hazard Analysis, THA

5.2 Flight Operations

The flight operations procedures will include pre-flight, in-flight, and post-flight operations and is meant to be repeated for as many tests indicated in the full day mission briefing completed in pre-operations.

5.2.1 Pre-Flight

The pre-flight portion of the flight operations segment is the flight line preparation of a planned individual test outlined in the full day mission briefing. The pre-flight procedure will be conducted at the onset of any new flight of the Mini SensorCraft within a given test day. All items outlined in the subsequent sections must be completed to move on to actual in-flight operations and test execution.

5.2.1.1 Pre-Flight Mission Briefing

The pre-flight mission briefing will be conducted by the test director prior to each test. The Pre-flight mission briefing will consist of:

1. Brief description of the test item configuration (if any changes have been made since any previous tests)
2. Overview of the test objective(s) and procedure
3. Review of Test Cards (Test Card Template shown in Appendix B)
4. Weather report (visibility, wind direction and strength, precipitation forecast)

5.2.1.2 Pre-Flight Log

The flight log is an operational document meant to be filled out by the test director for an individual flight. The document contains sections for both pre-flight and post-flight. The pre-flight sections include logistics of the current test to be conducted including a summary of the aircraft configuration for the current test. Most important in the pre-flight section is the checklist completion verification. The pre-flight checklists are outlined in the subsequent section. Each checklist is the responsibility of one or more flight critical personnel. Once completed and signed by the responsible personnel, the test director must indicate on the flight log the checklist has been performed without

complication. This provides the test director with necessary knowledge to perform the Go/No-go decision before in-flight operations begin.

5.2.1.3 Pre-Flight Checklist

Pre-Flight Checklists will be completed prior the start of each test. There are separate pre-flight checklists for:

1. Aircraft
2. Launcher
3. Piccolo
4. Ground Station
5. Instrumentation

Flight critical personnel will be responsible for portions of the Pre-Flight checklists as outlined in Appendix A. All Pre-Flight checklists are located in Appendix A.

5.2.1.4 Go/No-go Decision

The Go/No-go decision will be made by the Test Director. The Range Safety Officer has the authorization to terminate testing at any time should a safety concern arise. The following are the required conditions:

1. Weather
    a. Daylight VFR conditions
    b. No current precipitation with favorable forecast
    c. No lightning within a 10 mile radius
    d. Visibility: >3 miles
    e. Ceiling: >1000 feet (AGL)
    f. Wind: Calm, gusting to no more than 5 kts
    g. Sustained Maximum Crosswind: 4 kts
2. AFRL SUAS Test Ops ORM Assessment must be complete.
3. All pre-flight checklists must be complete with no concerns

5.2.2 In-Flight (Test Execution)

All flight operations will be conducted based on the provided information within the flight test cards for the particular test. An example of a flight test card is shown in Appendix B. All communications will be ceased except for the communication between the test director, primary pilot, tethered pilot, RSO, and GSO.

5.2.3 Post-Flight

The post-flight procedure is conducted following the completion of each flight. Each Post-Flight operation is meant to finalize the current test and prepare the vehicle for any follow on tests left within an operational day. If another test is to be performed, following the post-flight procedure, there will be a preflight procedure for the following test. If the current-test was the final test of the day, post-flight procedures will be followed by post-operations.

5.2.3.1 Post-Flight Log

The flight log is an operational document meant to be filled out by the test director for an individual flight. The document contains sections for both pre-flight and post-flight. The Post-Flight section includes a summary of the in-flight test, including post-flight comments from the acting pilots and other flight critical personnel.

5.2.3.2 Post-Flight Checklists

Post-Flight checklists will be completed after the completion of the recently completed in flight test execution. There are separate post-flight checklists for:

1. Aircraft
2. Data
3. Instrumentation

Each flight critical personnel will be responsible for portions of the Post-Flight checklists. Their corresponding obligations are outlined in Appendix A. All post-flight checklists are located in Appendix A.

5.2.3.3 Post-Flight Briefing

The post-flight briefing will be conducted by the flight test director and will include:

1. System status
2. System performance
3. Overall review of the test
4. Action items
5. Preliminary results from completed flight.

5.3 Post-Operations

Post-Operations will be conducted after all tests for the operational day are completed or after outside influences prevent further flight for that operational day.

5.3.1.1 Post-Operations Briefing

The Post-Operations briefing will be conducted by the Flight Test Director and will include:

1. System status
2. System performance
3. Overall review of the test
4. Lessons learned
5. Action items
6. Preliminary results from full test day.
7. Brief overview of tests for the next testing day

5.4 Operational Day Procedure Summary

The overall operational day test procedure is sequentially organized and summarized in Fig. 31. This high order organization is meant to facilitate an efficient and safe flight test procedure.

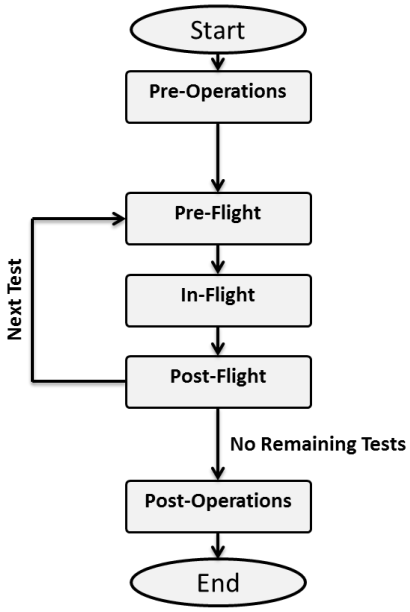

Figure 31- Operational day flowchart

Figure 32 presents an organizational structure indicating the documents needed for each operation within an operational day. In general, operational documents are found in Appendix A. Administrative documents are found in Appendix C, D, and E. The example flight test card is located in Appendix B.

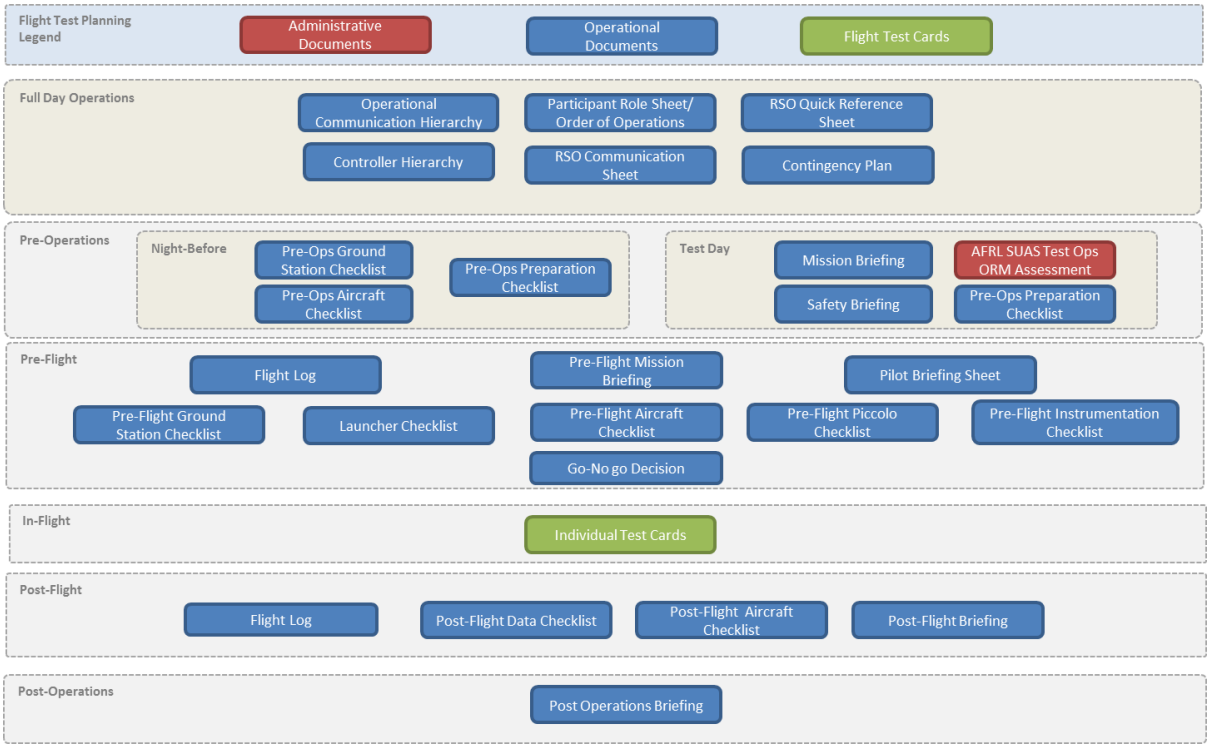

Figure 32- Document organizational structure

6 Risk Minimization and Safety Considerations

All testing, both ground testing and flight testing, will be conducted in accordance with this approved test plan. If any changes are necessary, the test team will contact the Safety Review Board for approval prior to completing the test. If, at any point during the test, a conflict between technical and safety issues should arise, safety concerns will always take precedence.

The following sections will outline safety considerations and risk minimizing procedures for several key risks during flight operations.

6.1 Required Test Conditions

All ground tests will be conducted indoors when possible. All outdoor tests, both ground tests and flight tests, during which the Mini SensorCraft is in motion, will take place in daylight, with VFR conditions. The following weather conditions must exist at all times for testing to continue:

1. No current precipitation with favorable forecast
2. No lightning within a 10 mile radius
3. Visibility: >3 miles
4. Ceiling: >1700 feet (AGL)
5. Wind: Calm, gusting to no more than 5 kts
6. Sustained Maximum Crosswind: 4 kts

The weather will be evaluated at the beginning of each test to satisfy the Go/No-Go determination, and the test director will monitor the weather throughout the test. The test director will confirm his assessment of the weather with the primary pilot prior to all flights. If at any time the primary pilot, test director or range safety officer raises any concerns about current conditions, testing will be immediately suspended until all 3 parties agree it is safe to continue. If these conditions are exceeded during a flight test, the pilot will be asked to land the RPV as safely and quickly as possible.

6.1.1 Personnel Locations During Testing

During all flight tests, all personnel will be positioned behind the primary pilot to ensure that the primary pilot has an unobstructed view of the air field and all personnel are accounted for. During takeoff, all personnel except the launcher operator, test director and primary pilot will be required to remain around the ground station. Once the RPV has reached a safe altitude, spotters may move to other locations in the field, as required, but they will return to the ground station for landing. The desired location for each person involved in the testing will be communicated prior to beginning testing.

6.1.1.1 Safe Zone

A pre-defined safe zone will be established at the flying site to serve as a gathering point in the event that the aircraft is in danger of impacting on or near personnel. This safe zone will be at the ground station which is at least 50 feet behind the launcher. The safe zone will be kept unobstructed during all flight operations.

6.2 Hazardous Materials

The Mini SensorCraft is electrically powered. The power is provided by lithium polymer (LiPo) batteries. Only LiPo approved chargers will be used and all batteries will never be charged at a rate greater than 1C. LiPo batteries will also be stored carefully and are located at the easily accessible front hatch bay of the Mini SensorCraft.

6.3 Risk Minimization to Technical Objectives

The overall technical objectives of the Mini SensorCraft FTP is outlined in Section 3.1. Achieving these goals thus requires safe flight and robust measurements and data logging from the onboard avionics. Therefore, the primary risks to achieving the overall test goal and technical objectives are failure in these two aspects.

6.3.1 Loss of Downlink Telemetry

The Piccolo SL provides the GSO with real time data including GPS position, GPS altitude, barometric altitude, attitude, airspeed information and so on. Additional modifications however will provide real time monitoring of strain (strain gage system for final flights). The data is sent via telemetry packets at a user specified rate during flight and is automatically saved by the ground station to the computer. A loss of downlink signal from the autopilot to the ground station thus represents a loss of telemetry and will present a loss in data for that period of time. It is important to note this does not represent a loss in communication between the Piccolo SL and the pilot, and thus does not present a hazardous situation. To combat this potential loss in data due to loss of downlink telemetry, the eventual strain gage system will have onboard logging capability.

6.4 Failure Protocol

All testing of the Mini SensorCraft performed is aimed at not only achieving technical objectives but also minimizing the potential for failures. Should there be a failure during flight operations of the vehicle, the flight test director will guide all flight critical personnel to respond to the failure in an appropriate manner. To respond to a failure, a logical stepwise response decision tree has been implemented to all flight operations. This hierarchal decision process is presented below in Fig. 33. It is important to note that all flight critical personnel will be versed in this procedure. The procedure should not last more than a few seconds.

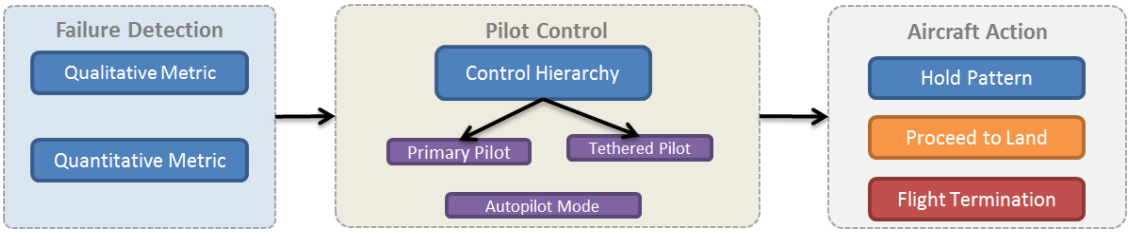

Figure 33- Three step failure protocol

6.4.1 Failure Detection

The first step in the failure protocol is the detection of a failure during flight. A failure can be detected based on a breach of an established qualitative metric, or a breach of an established quantitative metric. The qualitative metrics are based on the pilot input and GSO input. The pilot in control will indicate a failure should there be an undesirable change in control characteristics for the vehicle. The GSO will continually monitor all telemetered aircraft parameters to the ground station serving as a quantitative metric to detect failure. Should the vehicle venture outside an established target or the ground station indicates a failure of a monitored system, the failure will be relayed to the flight test director.

6.4.2 Pilot Control

The first act following the detection of a failure is establishing which pilot will be in control of the Mini SensorCraft. This decision will be made based on the control hierarchy and the perceived failure.

6.4.2.1 Control Hierarchy

The control hierarchy is as follows:

Primary Controller → Piccolo SL Tethered Controller → Failsafe

To safely hand over control between the two pilots without introducing the potential for additional failures, a protocol has been developed. When the primary pilot hands over control to the tethered pilot, the primary pilot must be in auto mode and vice versa. Should the tether pilot take control from the primary pilot, the primary pilot must be in Auto mode. If the Tethered pilot hands control back to the primary it will be in manual mode. All possible permutations of control switch are shown in the control hierarchy flowchart (Fig. 34).

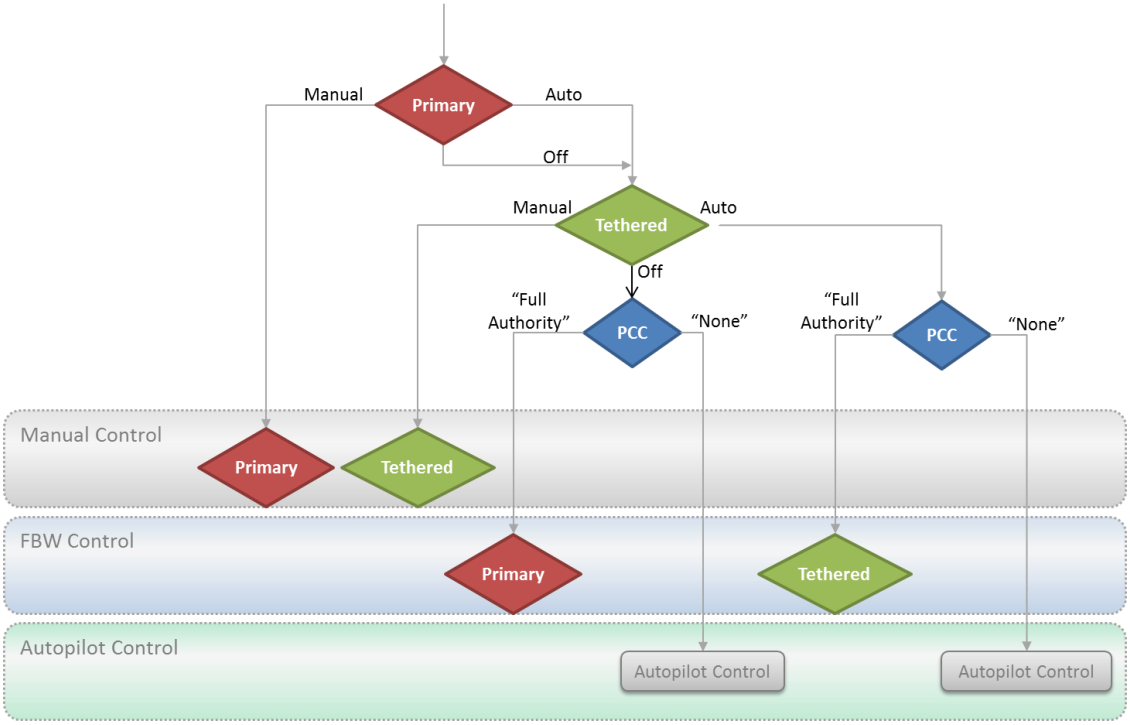

Figure 34 –Control hierarchy

The horizontal blocks indicate the three potential modes of control; manual, FBW, or full autopilot. The Piccolo Command Center (PCC) is integrated into the ground station and provides the capability of switching between FBW mode ("Full Authority") and full autopilot mode ("none") for the primary and tethered transmitters.

6.4.2.2 Link Loss

Link loss is a communication failure occurring between a transmitter and the Mini SensorCraft. For a link loss, the Piccolo SL will flash a warning on the ground station and the GSO will relay this information to the test director and primary pilot. In the event of primary controller link loss a warning is given on the ground station display. Should this happen during the flight of the Mini SensorCraft, the tethered pilot will immediately take control. In the event that that the aircraft is within visual range and the primary pilot can comfortably fly the aircraft, the tethered pilot will take control. In the event that the Mini Sensorcraft leaves visual range, the last effort to control the aircraft will be using the Piccolo SL tethered controller. Using the emergency navigation camera as well as the Piccolo SL telemetry (which includes an artificial horizon), the tethered pilot will steer the aircraft back into visual range at which point the primary pilot will take control. Flying the aircraft using the emergency navigation camera is the last option, and should this prove unsuccessful, the failsafe protocol will be executed.

In the event of total communication loss with the RPV (primary and tethered controls all fail), a failsafe procedure will automatically be executed. For more information about the failsafe procedure, see section6.4.3.1.2. This automatic failsafe procedure will be tested *at full range* at the flying site.

6.4.3 Mini SensorCraft Action

There are three primary actions for the aircraft to take once the appropriate pilot has taken control of the RPV. The action will be decided on based upon the perceived failure. The first is to hold a racetrack pattern over the flying field near the lost comm. way point in an attempt to work at correcting the failure. The aircraft must be fully controllable for this to occur. Should fixing the failure in air not be possible, the aircraft will safely proceed to land. Should the aircraft be in a situation where neither of the previous actions are possible, the flight termination system will be utilized.

6.4.3.1 Flight Termination System

The flight termination system (FTS) consists of a failsafe procedure that will be executed manually (commanded kill) in the event that the RPV is uncontrollable or if it travels outside of visual range and the backup navigation systems fail. The failsafe procedure will be executed automatically in the event of a total loss in link or in the event that the Mini SensorCraft travels outside of approved airspace.

6.4.3.1.1 Flight Termination Criteria

The following list consists of situations in which the failsafe procedure would be executed:

1. Unresponsive flight controls
2. Total loss of link
3. Mini SensorCraft travels outside of the approved airspace boundary
4. Complete visual contact is lost and the backup navigation systems (GPS, emergency navigation camera, artificial horizon) fails

6.4.3.1.2 Failsafe Procedure

The failsafe condition is executed during full loss of link, and corresponds to a controlled crash: full up elevator, full right aileron, throttle idle. The failsafe condition is designed to minimize residual damage and results in the aircraft experiencing a tip stall on the right wing and entering a tight, downward spiral until impact.

6.4.3.1.3 Commanded Kill

In the event that the Mini SesnorCraft is uncontrollable or travels outside of visual range and the backup navigation systems fail, a manual kill command will be executed. A manual kill corresponds to a commanded executed failsafe condition. The manual kill can be executed via both the tethered controller and the ground station.

6.5 General Safety Mitigating Considerations

This section will elaborate on several topics relating to general safety.

6.5.1.1 RF Masking/ Shielding

The use of carbon fiber composite materials and the unique shape of the JWSC creates a situation where RF masking and/or shielding is a concern. To combat these issues, remote receivers are placed with the antennas outside of the fuselage to avoid masking. Additionally, the placement of these receivers allows communication to be maintained with the Mini SensorCraft in any attitude. All servo extension wires will be braided to avoid EMI issues. Note that all onboard systems will be rigorously tested for interference/masking/shielding issues during phase 1 tests (EMI/RF Tests).

The Piccolo SL ground station contains a 900MHz spectrum analyzer. Through the user interface on the ground station, the Ground Station Operator can generate a spectrum analysis table that provides an indication of other RF users and potential sources of interference across the 900MHz band. The spectrum analyzer will be used to survey the spectrum before all flight operations and during range/EMI testing.

6.5.2 Airspace

All flights will take place at the Cfar flying site. All flights will take place in the approved airspace. For more details about the airspace, see section 4.1.1.

6.5.2.1 Midair Collision

In the event of a midair collision (bird strike, FOD ingestion in flight), the pilot will land the aircraft as quickly and safely as possible. Spotters will be used to help locate possible collision risks, and inform the test director if necessary.

6.5.2.2 Geo-Fence Failsafe Protocol

The geo-fence programmed into the Piccolo SL Autopilot is defined as the Kill Zone shown in red on the airspace requirements figure (Fig . 27) in section 4.1.1. The aircraft upon entering the Kill Zone and reaching the geo-fence will failsafe via aerodynamic termination. The failsafe enacted depends on the current mode control of the RPV (Manual, FBW, or Autopilot) as it reaches the geo-fence. The failsafe enacted are summarized for the different flight modes below (Table 9).

Table 9- Failsafe protocol for geo fence in various control modes

Situation	Protocol
Aircraft encounters Geo-Fence in manual mode	Manual Failsafe executed by the ground station operator
Aircraft encounters Geo-Fence in FBW mode	Manual Failsafe executed by the ground station operator
Aircraft Encounters Geo-Fence in Autopilot	Automatic Failsafe executed

6.5.3 Unresponsive Flight Controls

In the event that flight controls are unresponsive, the tethered controller will be activated and the tethered pilot will take control of the aircraft. If the tethered controller is unable to control the aircraft due to a total loss in uplink, the failsafe procedure will automatically execute.

6.5.4 Loss of Vehicle Position Data

A loss of vehicle position information (GPS) while the vehicle is flying within visual contact represents a loss of downlink telemetry, and not a hazardous situation. At all times during the flight, the pilot, tethered pilot, and test director will keep visual reference on the aircraft. The ground station operators will monitor the telemetry feeds from the aircraft and the spotters will assist in visual referencing of the aircraft.

If the Mini SensorCraft inadvertently travels outside of visual contact, but remains within the allotted airspace, the ground station operator will take control of the aircraft using the live feed from the emergency navigation camera to navigate the aircraft back into visual contact. The camera feed will be placed next to the artificial horizon (from the Piccolo SL) on the ground station to assist with maintaining constant altitude while flying using the emergency navigation camera. In the event that the emergency navigation camera fails, the artificial horizon and GPS information available in real time on the Piccolo ground station display can be used to navigate the aircraft. In the event that the emergency navigation camera feed fails and either the GPS or artificial horizon fails, the failsafe procedure will be executed.

6.5.5 Malfunction/ Failure During Takeoff

A malfunction/ failure during takeoff could be caused by improper launcher functioning, a total loss of link with the aircraft, pilot error during takeoff or FOD ingestion. The effects of a malfunction or failure during takeoff could include damage to or loss of the vehicle as well as property damage, personal injury or death.

In order to minimize the risk of a malfunction or failure during takeoff, both the primary and backup pilot have trained on several reduced complexity flight models in preparation for their roles in this project. Additionally, the Test Director will ensure that all checklists and procedures are complete as described in this flight test plan and the flying site will be examined for FOD prior to each flight. The control hierarchy will be tested prior to every flight to verify appropriate pass over of control. Finally, the primary pilot will be ready at all times to re-direct the aircraft away from people or property.

In the event that a malfunction or failure occurs, the pilot will perform evasive maneuvers if required to avoid personnel and property damage and landing the aircraft as quickly and as safely possible. Once the Mini SensorCraft is back on the ground, the ground crew and RSO will approach the aircraft from the nose of the aircraft and unplug all LiPo batteries. Remaining personnel are free to approach the aircraft only after Test Director and Range Safety Officer confirm that the aircraft is powered down and call “all clear.” Any available personnel will perform first aid if needed and inform proper facilities personnel as necessary.

6.5.6 Fire

A fire could be caused by faulty/malfunctioning electronics, or improper charging of batteries. The effects of a fire could include damage to or loss of the vehicle, property damage or personal injury or death.

In order to minimize the risk of a fire, all batteries will be charged according to manufacturer specifications. Electrical connections will be checked for frayed wires and possible short circuits before flight. The Test Director will ensure that all checklists and procedures are complete as described in this flight test plan and a fire extinguisher will be present at the test site at all times.

In the event that a fire occurs, the local fire department will be contacted immediately. If the fire is small enough, a single member of the ground crew will carefully approach the aircraft and attempt to put out the fire with the fire extinguisher. If in doubt, personnel will wait and let the fire patrol take care of the fire.

6.5.7 Structural Damage

Structural damage could be caused by loss of control and the resulting dive causing the pilot to fly outside of safe flight speed range, failure of one or more structural components during flight, a hard impact on landing, a mid-air collision, or mishandling of the vehicle. The most important structural component to monitor during flight is the aft wing. The effects of structural damage could include loss of the vehicle, property damage or personal injury or death.

In order to minimize the risk to structure, the primary and tethered pilots will have extensive simulator training before flying the Mini SensorCraft, including training for degraded modes of flight, such as structural failure. To prevent a mid-air collision, spotters will actively search the airspace for collision hazards, and inform the test director who will in turn inform the primary pilot if necessary. In order to prevent mishandling of the vehicle, all personnel who will be in contact with the aircraft at any time during the test procedures will be trained by either the flight test director or GSO before arriving at the test site. During flight, the pilot will be prepared for inadvertent flight maneuvers due to loss of link, stuck control surfaces, or other degraded modes of flight and the backup pilot will be prepared to take control in the event that the tethered pilot loses control. Finally, the aircraft structure will be checked for wear and tear before each flight in pre-flight operations.

In the event that structural damage occurs in transport or during ground operations, the appropriate repairs will be made and checked before testing is resumed. If damage occurs in flight, the pilot will perform an emergency landing (if possible) as quickly as possible to minimize collateral damage. In the event that the structural damage renders the aircraft uncontrollable, all personnel will keep eyes on the aircraft at all times.

6.5.8 Malfunction/ Failure during Landing

A malfunction or failure during landing could be caused by a loss of control during approach or landing, heavy crosswind or adverse weather conditions, pilot error during approach or landing or a total loss of link. The effects of such a failure include damage to or loss of the vehicle, property damage and personal injury or death.

In order to minimize the risk of such a malfunction or failure, the flight test director will ensure that all checklists and procedures are complete as described in this flight test plan. Additionally, the primary pilot will be ready at all times to re-direct the aircraft away from people or property and the tethered pilot will have the backup transmitter in his hands at all times during test operations, ready to

take control if a loss of primary link situation arises. The backup controller will be tested prior to each flight for reliable link with the aircraft as well as the ability to take control of the aircraft at any time.

Should a failure occur while still upon approach, the pilot will perform evasive maneuvers if required to avoid personnel and property damage. If possible, a "go around" maneuver will be performed to avoid a hard landing and give the pilot more time to assess the situation: the pilot will then land the aircraft as soon as safely possible. After landing, a single member of the ground crew will carefully approach and unplug both LiPo Batteries. Remaining personnel are free to approach the aircraft only after flight test director and RSO confirm that the aircraft is powered down and call "all clear." Flight testing will resume only after the test director, GSO, and primary pilot approve any/all repairs.

6.6 Test Hazard Analysis

A detailed test hazard analysis will be completed in the following drafts of the document.

6.7 Mishaps

For the purposes of this test, a mishap will be defined as:

> ***Mishap:*** An event that results in damage to the aircraft (outside of normal wear and tear from operations), injury to personnel, damage to private property and/or damage to airfield property at the flight location in Victoria.

In the event of a mishap, the Test Director will contact the AFRL Flight Test and Evaluation Office as well as the AFRL Flight Safety point of contact as soon as possible (within 8 hours) to inform them of the event. The decision to continue, postpone or cancel testing will be made in collaboration with the flight test director, pilots, ground station operator, range safety officer, and AFRL Safety Review Board. Immediately after the RPV is recovered and damage is assessed, AFRL Form 29 – AFRL Test Safety Mishap Form will be completed. The unfilled form is located in Appendix D. Efforts will be made to be as detailed and descriptive as possible about the cause and effects (both short and long term) of the mishap, as well as its implications on future testing.

6.7.1 Emergency Personnel

Emergency Personnel, including the fire department, will be local to flying site and available by phone during all flight operations.

Flight Test Plan References

[1]Blair, M., Canfield, R. A., and Roberts Jr., W., "Joined-Wing Aeroelastic Design with Geometric Nonlinearity," Journal of Aircraft, Vol.42, No.4, 2005, pp. 832-848.

[2]Bond, V., "Flexible Twist for Pitch Control in a High Altitude Long Endurance Aircraft with Nonlinear Response," Ph.D. Dissertation Prospectus, Department of the Air Force, Air Force Institute of Technology, Wright-Patterson AFB, Dayton, OH, 2007.

[3] The Boeing Company. "Selected Results from Test of Model on Sting", Presentation Excerpts, NASA Langley, Hampton VA, slides 2-5.

[4] Lucia, David J., "The SensorCraft Configurations: A Non-Linear AeroServoElastic Challenge for Aviation," AIAA Paper 2005-1943, 2005.

[5]Roberts, R. W., Jr., Canfield, R. A., and Blair, M., "Sensor-Craft Structural Optimization and Analytical Certification," AIAA Paper 2003-1458, April 2003.

[6]Richards, J., Suleman, A., Aarons, T. and Canfield, R.A., "Multidisciplinary Design for Flight Test of a Scaled Joined Wing SensorCraft," AIAA Paper 2010-9351, Sep. 2010.

[7]CAD work completed by Jenner Richards of Quaternion Engineering/ University of Victoria

[8]http://www.hobbyking.com/hobbyking/store/__17221__Alloy_DPS_Series_72mm_EDF_unit_with_2550kv_Motor_1200watt.html >, Hobby King

[9]"PS081 Single Chip Solution for Strain Gauges," ACAM mess electronic, 2010, DP_PS081_en VO.7.

[10]PhotoModeler[C] Manual

[11]Richards, J., Aarons, T., Suleman, A., Can_eld, R. A., and Woolsey, C., \Airworthiness Evaluation of a Scaled Joined-Wing Aircraft 1," 53rd AIAA/ASME/ASCE/AHS/ASC Structures, Structural Dynamics and Materials Conference, April, Honolulu,Hawaii, 2012, pp. 1-37

Appendix A. Operational Flight Documents

Pre Ops Preparation List

Item	Checked
Night Before Operations	
Charge Batteries (and check for memory cards)	
- Gopro x2	
- SLR	
- Video Camera	
- Canon SX220 GPS	
Aircraft Preparation	
- JR Transmitter and back up battery x 2	
-Charge flight packs X6	
- Charge Piccolo Pack x2	
-Futaba Transmitter	
-Charge Launcher Battery	
Pre-Ops AC Checklist	
Van Preparation	
- Maps downloaded for mission	
- Fuel level > 50%	
- Items on roof secured	
-Charge Dave Clarke Headsets	
-Check that van starts	
Day Of Operations	
Launcher Packing	
Media Kit	
Tool Kit	
Transmitter Box	
Battery Box	
Van	
Documentation	
Load Everything	
Mission Briefing	

Figure A1- Pre-Operations preparation list

Pre-Operations Aircraft Checklist

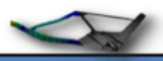

SENSORCRAFT VT

Version1 (1/7/13) *Grey (Indicates that must be performed after AC State >2)*

Flight Number: Date:	Checked By:		INITIALS
Airframe Free of Damage			
Verify Pitot Static Tubes connected to Piccolo II			
Ensure that all wiring is secure within Avionics Bay			
Ensure avionics cable connected			
Attach telemetry antenna wire and GPS to Piccolo			
Attach satellite Rx wire x2 (JR Switch Board I/O 2 & 3)			
Attach and secure Right Elev. Connection to Elev.			
Attach and secure Left Elev. Connection to Rudder			
Check wing servo linkage/Servo Horns/Aft Wing Keepers etc....			
Inspect launcher hook			
Ensure Pitot Static Tube Secure and in Appropriate Position			
Ensure Camera is mounted and secure			
Ensure TX Secure			
Ensure EDF's are Secure and Intake Free of debris			
Ensure Satellite Recievers are Secure/connected			
Ensure 900MHz antenna is vertical and Secure			
Verify Avionics cover secure			
Switches in OFF position.			
Install and secure all batteries (Do Not Plug In)			
EDF Battery (>95%)	Level:	%	
Autopilot/ Servo Battery (>70%)	Level:	%	
CG Check			
Measure Aircraft Mass	Distance:	cm/%	
	Mass:	Kg	
TX switched on			
Check for Correct Model in TX (Mini PicII)			
TX Battery level >9.8V			
Install Pitot Cover	Level:	V	
Secure Wiring in EDF Intake Area			
Plug in Batteries			
Turn ON Autopilot Switch			
Turn ON Servo Switch			
Jr Tx range test			
==> PICCOLO CHECKLIST			
Turn on Camer and Reciever			
Verify transmission to ground station			
Verify Video Storage			
Delete old video			
Turn off Camera and Reciever			
==> Pre-Flight Mission Briefing to Full Crew			
Start Video Devices			
REMOVE PITOT COVER			
CLEAR FLIGHTLINE			
Review Control Hierarchy			
Check control surface directions			
Check AP state (ALL GREEN) with GCS operator			
Verify correct autopilot state (Full Authority, None, Steering etc..)	State: Full Authority		
Verify Teathered Controller unplugged (Primary has control in FBW)			
Airspace Clear			
Simulate			

Figure A2- Pre-Operations aircraft checklist

Pre-Operations Ground Station Checklist

Version1 (1/7/13)

Flight Number:	Date:	Checked By:	INITIALS
Unpack Van			
Plug in Headset Batteries			
Turn on Clark Base Station			
Distribute Head Sets			
Verify Communication			
Turn Stereo to NAV			
Put down stabilizer legs			
Put up Antenna Mast			
Ensure Inverter is on			
Turn on Computers			
Turn on Piccolo Ground Station			
Open PCC			
Plug in Futaba Pilot Console			
Check for Correct Model in TX (Mini PicII)			

Figure A3- Pre-Operations ground station checklist

Pre-Flight Ground Station Checklist

Version1 (1/7/13)

Flight Number:	Date:	Checked By:	INITIALS
Unpack Van			
Plug in Headset Batteries			
Turn on Clark Base Station			
Distribute Head Sets			
Verify Communication			
Turn Stereo to NAV			
Put down stabilizer legs			
Put up Antenna Mast			
Ensure Inverter is on			
Turn on Computers			
Turn on Piccolo Ground Station			
Open PCC			
Plug in Futaba Pilot Console			
Check for Correct Model in TX (Mini PicII)			

Figure A4- Pre-Flights ground station checklist

Launcher Checklist

Version2 (1/9/13)

Flight Number:	Date:	Checked By:		INITIALS
Assembly				
Place Cart on Fore Section				
Join Aft and Fore Section				
Fasten 4 Joining Lugs				
Fold Down Legs				
Check Wind Direction and line up launcher into wind				
Attach Cart to Cable				
Attach Hose to Accumulator Tank				
Attach Hose to Launcher				
Place Sand Bags on Aft Launcher Foot				
Test Fire				
Launch Valve in Open Position				
Lookup/Estimate Target Pressure		Pressure:	PSI	
Dummy Mass		Mass:	kg	
Lookup Minimum Distance for Desired Velocity		Distance:	m	
Pull Cart Full Aft				
Ensure Cable Seated in Pully				
Insert Safety Pin to Lock Cart				
Esnure Cable is Free of Ware				
Launch Valve in Close Position				
Start Compressor and Stop at Desired Accumulated Pressure				
Place Dummy Mass Securely on Cart				
Verify Launch Area is Safe (All personnel behind launcher)				
Attach Hose and Remove Safety Pin				
Announce: "Test Fire in 3,2,1..."				
Return Launch Valve to Closed Position Remove Hose				
Record Distance		Distance:	m	
Distance Satisfactory? **(Min. Dist.)<DIST<(Min.Dist. +3m)**				
Inspect Launcher for Damage				
R.S.O Performs FOD Sweep of Aircraft Landing Zone				
Launching Instructions				
Launch Valve in Open Position				
Pull Cart Full Aft				
Ensure Cable Seated in Pully				
Insert Safety Pin to Lock Cart				
Esnure Cable is Free of Ware				
Launch Valve in Close Position				
Start Compressor and Stop at Desired Accumulated Pressure				
Stop Compressor at Desired Accumulated Pressure				
Place Aircraft Securely on Cart				
Verify Launch Area is Safe (All personnel behind launcher)				
Attach Hose and Start Camera				
Remove Safety Pin				
Announce: "Launch in 5,4,3,2,1, Pull"				
Return Launch Valve to Closed Position and Remove Hose				

Figure A5- Launcher checklist

Pre-Flight Aircraft Checklist

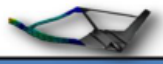

SENSORCRAFT VT

Version2 (1/9/13)

Flight Number: Date:	Checked By:		INITIALS
Airframe Free of Damage			
Check wing servo linkage/Servo Horns/Aft Wing Keepers etc....			
Inspect launcher hook			
Ensure Pitot Static Tube Secure and in Appropriate Position			
Ensure Camera is mounted and secure			
Ensure TX Secure			
Ensure EDF's are Secure and Intake Free of debris			
Ensure Satellite Recievers are Secure/ Connected			
Ensure 900MHz antenna is vertical and Secure			
Verify Avionics cover secure			
Switches in OFF position.			
EDF Battery (Servo)(>95%)	Level:	%	
Autopilot/Servo Battery (>70%)	Level:	%	
Install and secure all batteries (Do Not Plug In)			
CG Check	Distance:	cm/%	
Measure Aircraft Mass	Mass:	Kg	
TX switched on			
Check for Correct Model in TX (Mini PicII)			
TX Battery level >9.8V	Level:	V	
Install Pitot Cover			
Secure Wiring in EDF Intake Area			
Plug in Piccolo/Serov Battery			
Turn ON Autopilot Switch			
Turn ON Servo Switch			
Jr Tx range test (30 paces away)			
==> PICCOLO CHECKLIST			
Turn on Camer and Reciever			
Verify transmission to ground station			
Verify Video Storage			
Delete old video			
Turn off Camera and Reciever			
==> Pre-Flight Mission Briefing to Full Crew			
Start Video Devices			
REMOVE PITOT COVER			
CLEAR FLIGHTLINE			
Review Control Hierarchy			
Check control surface directions			
Check AP state (ALL GREEN) with GCS operator			
Verify correct autopilot state (Full Authority, None, Steering etc..)	State: Full Authority		
Verify pilot console unplugged (Primary has control in FBW)			
JR TX: Switch to Auto and verify CS movement in Auto			
JR TX: Switch to manual and verify CS movement in Manual			
Plug in EDF Battery			
Perform Thrust Test			
Airspace Clear			
Ready to launch			

Figure A6- Pre-Flight Aircraft checklist

Pre-Flight Piccolo Checklist

Version2 (1/9/13)

Flight Number: Date:	Checked By:	INITIALS
Configure PCC for mission (Open System, Telemetry and Controller Config Screens)		
Verify and/or load flight plans.		
Verify correct command loops (Flaps, Altitude, Airspeed all auto)		
Take aircraft to landing site		
Open GCS\DGPS window and average satellites (ensure "enable DGPS" not checked)		
Verify working aircraft GPS, check number of satellites and PDOP (>6 sats <3 PDOP)	# sats >6 PDOP <3	
Verify working GCS GPS, check number of satellites and PDOP (>6 sats <3 PDOP)	# sats >6 PDOP <3	
Return aircraft to launch site		
Verify mission limits including deadman status and lost comm waypoint.	Min/Max Alt _____m	
Flight Timer Set to 5 minutes.		
Verify that modem power level is set to 1W for GCS and Avionics.		
Set Avionics telemetry to > 5Hz.		
Verify Avionics Battery Level >11.1V		
Verify Servo Battery Voltage (4.8V< Voltage< 6.55V)		
Control Surface Tests		
JR Tx -- !!! Set to auto mode !!!		
Pilot Console -- Select manual control and verify "AP Off" indicated in autopilot page		
Pilot Console -- Verify control surface trims in manual mode. Adjust using pilot console		
Pilot Console -- Verify manual control, both magnitude and direction, for all surfaces.		
Pilot Console -- Verify reported controls match the actual control positions.		
Check Pilot Sample Rate and frequency (>95% >14Hz)		
Pilot Console -- !!! Set to Auto Mode !!!		
JR Tx -- Select manual control and verify manual control indicated in autopilot page.		
JR Tx -- Verify control surface trims in manual mode. Adjust using pilot console.		
JR Tx -- Verify manual control, both magnitude and direction, for all surfaces.		
JR Tx -- Verify reported controls match the actual control positions.		
Check Pilot Sample Rate and frequency (>95% >14Hz)		
JR Tx -- Set to auto mode and ensure AP is indicated in autopilot page		
Preflight Tab		
Preflight Tab -- Perform Control Surface Test		
Preflight Tap -- Set altimeter to local base pressure (1 inHg = 3376.85 Pa)	LBP _____ Pa	
Preflight Tab -- Set the battery charge state of the vehicle. (480000 Whr)		
Preflight Tab -- Set Payload mass and check aircraft MTOW		
Ensure pitot cover installed		
Preflight Tab -- Check sensor readings and zero air data if needed.		
Remove pitot cover and check Pitot (Thumb press ***ONLY***)		
Check the operation of the gyros and accelerometers by rotating the aircraft.		
Place Aircraft on Launcher		
Preflight Tab -- Ensure altitude reading is correct		
JR Tx-- Set to manual mode and enusre AP OFF indicated in autopilot page		
Plug in EDF Batteries		
Perform thrust test and ensure sensors work throughout throttle range		
Unplug EDF Batteries		
Check comms at the far end of the runway. RSSI should be at maximum (-71 dBm)	RSSI _____	
Check aircraft LINK is 100 (95-100 at least)	ACK _____	
!!! Determine the takeoff direction and **set the initial waypoint.**	W.P. _____	
Verify lost comm waypoint	W.P. _____	
Verify correct autopilot state **(Full Authority, None, Steering etc)**	State: *Full Authority*	
Pilot Console--Verify unplugged (JR Tx has control)		
Pilot Console-- Set to auto mode		
JR Tx -- Verify CS Movement in Auto Mode		
JR Tx -- Switch to Manual and verify CS Movement in Manual Mode		
Final checks: Battery voltage and current, GPS health, RSSI, and sensors.		
ENSURE ALL AP STATES ARE GREEN (GPS, GYRO,ATT ETC)	Yes _____ No_____	
Replace pitot cover		
Preflight Tab		
==>AIRCRAFT CHECKLIST		

Figure A7- Pre-Flight Piccolo SL checklist

Post-Flight Data Checklist

Version1 (1/7/13)

Flight Number: Date:	Checked By:	INITIALS
Create Folder with Flight # (Day/Time) on Desktop		
Place Piccolo Telemetry File inside folder		
Place Dublet Data inside (Labeled Sequentially)		
Place a copy of the Configuration File used for Flight Inside folder		
Place media from video camera in folder then delete off SD Card		
Place media from DSLR Slow Motion in folder then delete off SD Card		
Place media from GoPro's in folder then delete off SD Card		
Place media from wing camera in folder then delete off SD Card		
Transfer Hard Drive Media into folder		

Figure A8- Post-Flight data checklist

Post-Flight Aircraft Checklist

Version1 (1/7/13)

Flight Number: Date:	Checked By:	INITIALS
Retrieve Aircraft		
Turn Piccolo Switch off		
Turn Servo Switch off		
Unplug and remove all batteries		
Assist Test Director with Flight Duration Calculations		
Place Batteries on Charge (if needed)		
Replace Flight Packs and Piccolo Batteries		
Verify Aircraft State <2		

Figure A9- Post-Flight aircraft checklist

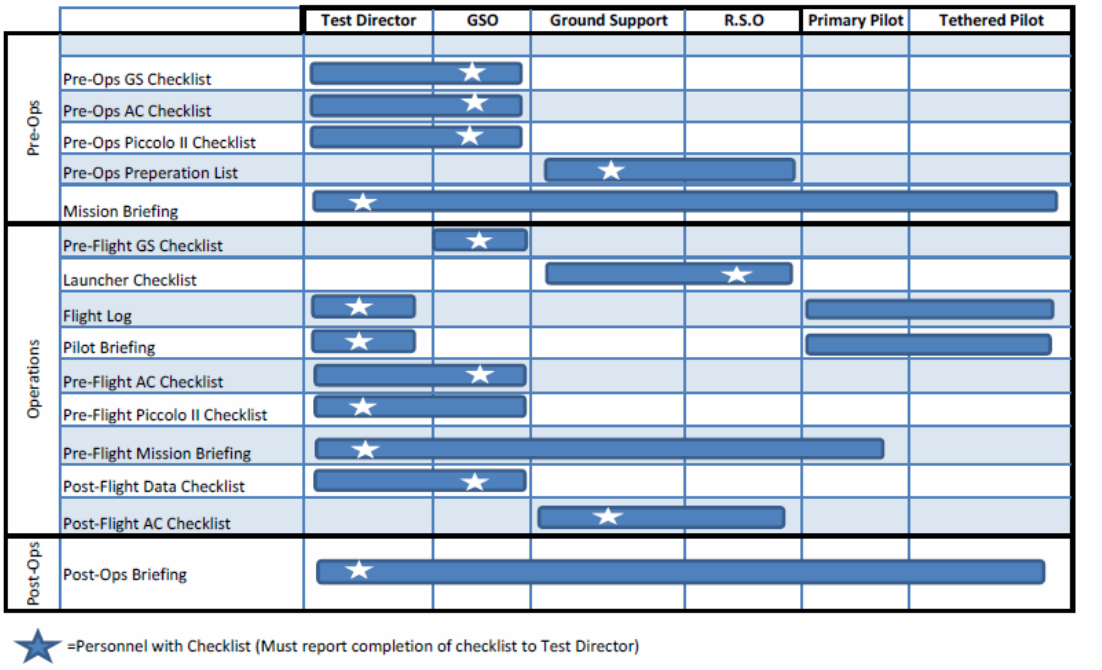

Figure A10- Flight critical personnel responsibility sheet

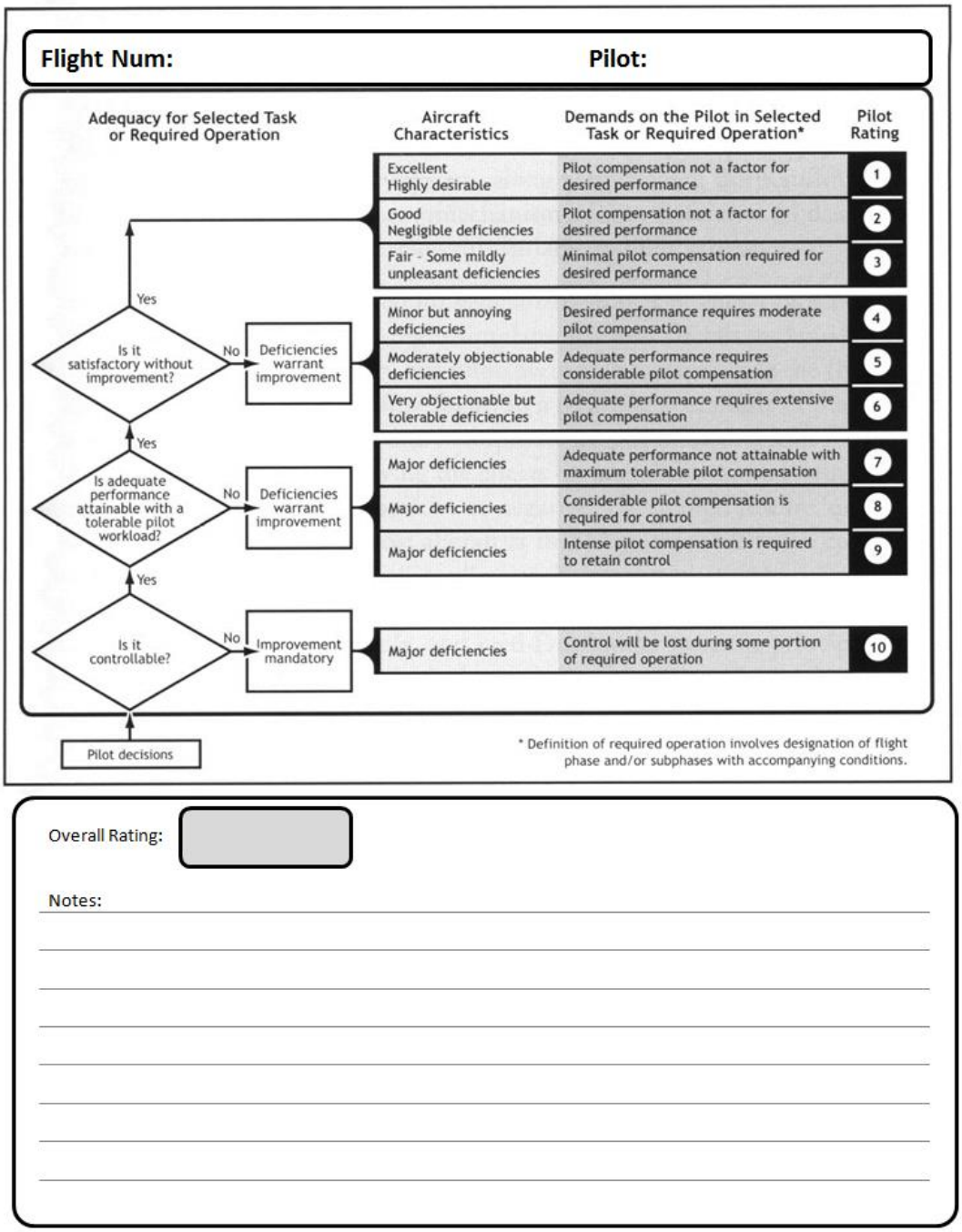

Figure A11- Cooper Harper Scale

Appendix B. Example Flight Test Card

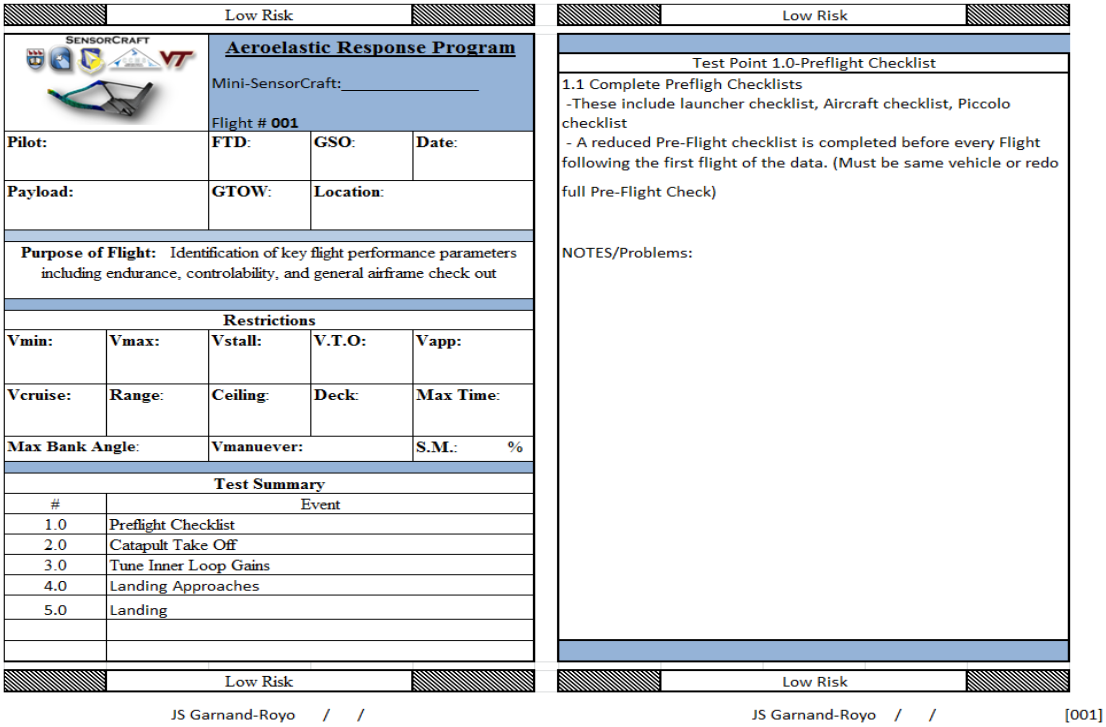

Low Risk

Aeroelastic Response Program

Mini-SensorCraft:_____

Flight # **001**

Pilot:	**FTD**:	**GSO**:	**Date**:
Payload:	**GTOW**:	**Location**:	

Purpose of Flight: Identification of key flight performance parameters including endurance, controlability, and general airframe check out

Restrictions

Vmin:	**Vmax:**	**Vstall:**	**V.T.O:**	**Vapp:**
Vcruise:	**Range**:	**Ceiling**:	**Deck**:	**Max Time**:
Max Bank Angle:		**Vmanuever:**		**S.M.**: %

Test Summary

#	Event
1.0	Preflight Checklist
2.0	Catapult Take Off
3.0	Tune Inner Loop Gains
4.0	Landing Approaches
5.0	Landing

Low Risk

JS Garnand-Royo / /

Low Risk

Test Point 1.0-Preflight Checklist

1.1 Complete Prefligh Checklists
-These include launcher checklist, Aircraft checklist, Piccolo checklist
- A reduced Pre-Flight checklist is completed before every Flight following the first flight of the data. (Must be same vehicle or redo full Pre-Flight Check)

NOTES/Problems:

Low Risk

JS Garnand-Royo / / [001]

Low Risk

Test Point 2.0-Catapult Take Off

2.1 Ensure all personnel are in position
2.2 Check with Pilot for go-ahead and manual mode is engaged
2.3 Signal for Launch Operator to start 5 second countdown
2.4 Increase throttle to 20% at 3 seconds
2.5 Once Launched, increase to max throttle and proceed climb out to 100 meters altitude Following tangential trajectory
2.6 Switch to FBW mode 50% across field (>= 50m AGL)

If Behavior Suitable proceed to T.P. 3.0

If Undesired behaviour, Switch to manual and land

Launch Positions:

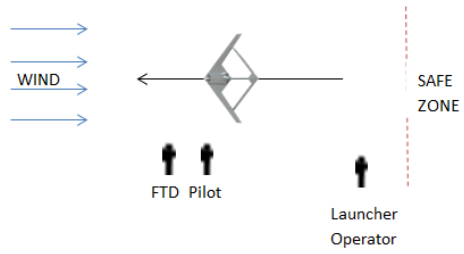

Low Risk

JS Garnand-Royo / /

Low Risk

Test Point 3.0-Tune Inner Loop Gains

3.1 Pilot will climb aircraft to a indicated altitude and fly in racetrack pattern (2 to 3 laps) at Vcruise (**Fig. 1**)

Vcruise=_____ m/s

Desired Altitude_____ m

Figure 1. RaceTrack Pattern

3.3 Ground Station Operator will tune gains based on pilot input. (Relayed via Test Director)

3.4 Pilot will indicate when control is satisfactory

Flight Time:_____

Flight Time > 3 Minutes: Move to TP4
Flight Time > 4 Minutes: Move to TP5

Low Risk

JS Garnand-Royo / / [001]

Low Risk

Test Point 4.0-Landing Approaches

4.1 Ensure Aircraft is at least 300m away from landing zone and at 50m AGL.

5.2 Start a shallow approach while not reducing airspeed below Vmin

Vmin=_____ m/s

5.3 Aim to be 20 m AGL by the time the aircraft reaches the landing zone

5.4 Repeat (2 times) (NOTE: Number of repeats will depend on time elapsed)

Flight Time:_____

Test Point 5.0-Landing

5.1 Ensure base leg will be at least 300m away from the designated landing zone

5.2 On Downwind leg, reduce altitude to 50m

6.3 On Base leg reduce to 40m.

5.4 Turn on Final leg and try to maintain a constant glide slope

5.5 Belly land the aircraft

Flight Time:_____

Low Risk

JS Garnand-Royo / /

Low Risk

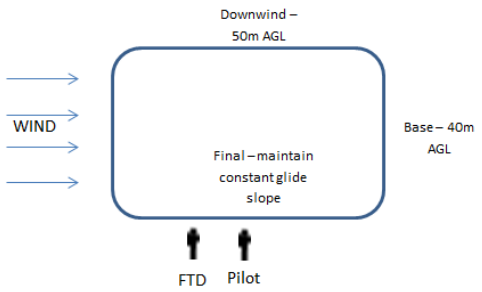

Flight Time:_____

Notes/Problems:

Low Risk

JS Garnand-Royo / / [001]

Appendix C. AFRL SUAS ORM Assessment Form

Date: _____ Program: _____ Vehicle: _____ Flight # ____

	GREEN	YELLOW	RED
HUMAN		Place "X" in appropriate box	
Vehicle Operator			
Qualified *	Fully Qualified	In-Training	No Training at All
Currency (this vehicle) *	< 30 Days	30-60 Days	> 60 Days
Sleep (Crew Rest)	≥ 8 Hours	6 – 8 Hours	≤ 6 Hours
Ground Control Station (GCS) Operator			
Qualified	Fully Qualified	In-Training	No Training at All
Currency (this GCS/vehicle)	< 30 Days	30-60 Days	> 60 Days
Sleep (Crew Rest)	≥ 8 Hours	6 – 8 Hours	≤ 6 Hours
Payload Operator			
Qualified	Fully Qualified	In-Training	No Training at All
Currency (this payload/vehicle)	< 30 Days	30-60 Days	> 60 Days
Sleep (Crew Rest)	≥ 8 Hours	6 – 8 Hours	≤ 6 Hours
Launch Crew			
Qualified	Fully Qualified	In-Training	No Training at All
Currency (this launch system/vehicle)	< 30 Days	30-60 Days	> 60 Days
Sleep (Crew Rest)	≥ 8 Hours	6 – 8 Hours	≤ 6 Hours
Observers			
Qualified (if flying in the National Airspace	Fully Qualified	In-Training	No Training at All
Sleep (Crew Rest)	≥ 8 Hours	6 – 8 Hours	≤ 6 Hours
Crew/Personal Concerns	None	Minor	Major
MISSION/OPS		Place "X" in appropriate box	
Test Location Familiarity	> 3 Previous Tests at this Location	1 - 3 Previous Tests at this Location	First Time at this Location
Test Location Weather	All Criteria Acceptable	1-2 Criteria Within 30% of Limits	1-2 Criteria Within 10% of Limits or > 2 Criteria Within 30% of Limits
Mission Duration	< 30 minutes	30-120 minutes	> 120 minutes
Takeoff Times	Between Sunrise & Sunset	All Other Times	At Night
Landing Times	Between Sunrise & Sunset	All Other Times	At Night
Bird Activity (check US Avian Hazard Advisory System at www.usahas.com, verify on-site, prior to start of testing)	Low	Moderate	Severe
Duration of Duty Day	< 8 Hours	8 - 12 Hours	> 12 Hours
Mission Complexity	Low/Normal	Demanding	Extremely Demanding
Safety Risk	Low	Medium	High
Check AFRL Flight Crew Information Folder (Flight Crew Information Folder)	0 Notices pertaining to systems under test or all relevant issues have been satisfactorily addressed		Relevant notices exist and not yet complied with
VEHICLE/GCS/LAUNCH SYSTEM/RECOVERY SYSTEM		Place "X" in appropriate box	
Config Changes (hardware/software)	None	Minor or first flight after down time > 30 days	Major modifications or Functional Check Flight or down time > 90 days
Maintenance Write-ups	0 Write-ups outstanding	≤ 3 Minor Write-ups outstanding – no impact on meeting test objectives and/or compromising safety	≥ 1 Major Write-up(s) outstanding impacting meeting test objectives and/or compromising safety or > 3 Minor Write-ups outstanding
Service Bulletins/Safety Supplements **	0 New Bulletins / Supplements outstanding; all existing complied with and reviewed/approved by SRB and TAA		Bulletin/Supplement exists, applicable to system under test, and not yet complied with

TOTAL ORM LEVEL		GREEN (< 3 Total Yellows/Reds, with no more than 1 Red)		YELLOW (≥ Total 3 Yellows/Reds, with no more than 1 Red)		RED (2 or More Reds)

AFRL Form 33A DRAFT 4 Aug 10
Prescribing Directive AFRLI 61-103, Volume 1

*** Review FAA Interim Operational Approval Guidance 08-01, dated 13 Mar 08, Section 9.0 Personnel Qualifications, for specific requirements.**

**** Mandatory for all commercial products used in test (vehicle, ground control station, launch system, and recovery system). If using an in-house system designed and developed by another organization, check with that organization for any cautions and warnings. Assessment only needs to be completed prior to first flight of each week's testing.**

Test Director: Discuss How ORM Which Shows Up as Yellow or Red Was Addressed/Mitigated/Who Was Notified (use continuation page as needed)

This is a preliminary form filled out in anticipation of the first flight of the Geometrically Scaled RPV. The pilots will have both flown at the test site prior to the first flight of the RPV, and the Virginia Tech/Quaternion Engineering crew will have performed ground operations at the test site (as part of this test plan) before the aircraft goes wheels up. The only yellow ORM level comes from the fact that this is the first flight of a new aircraft. The pilots will have both flown reduced scale models of this aircraft prior to flying the full 1/9th scale RPV.

Mission Completed (y/n): _____

If Not, Why:

Initials _____

GREEN ORM: If any specific area is Red, look at ways to lower risk in that area. Test Director or Test Safety Officer discretion to continue test.

YELLOW ORM: Try to mitigate to Green ORM. Work with Test Director, Vehicle Operator, and Test Safety Officer to lower ORM risk. If unable to lower risk, AFRL Branch Chief must be notified and approve test start.

RED ORM: Try to mitigate to Green or Yellow ORM. Work with Test Director, Vehicle Operator, and Test Safety Officer to lower ORM risk. If unable to lower risk, AFRL Division Chief must be notified and approve test start.

INSTRUCTIONS:

1. Complete this assessment prior to each flight or like series of consecutive sorties.
2. Maintain completed forms in test log book.
3. If Total ORM level is Yellow or Red, notify AFRL/SEF and AFRL/RBCT that approval to continue with testing was sought/garnered by the appropriate level of authority. Notification should be made within 4 hours of the start of the test. Preferred method of notification is by e-mailing the completed form to Afrl.se.workflow@wpafb.af.mil and AFRLDL.flighttestandevaluation@wpafb.af.mil
4. Provide copy of completed forms to AFRL/SEF and AFRL/RBCT upon the completion of the test program.

AFRL Form 33A DRAFT Aug 10
Prescribing Directive AFRLI 61-103, Volume 1

Appendix D. AFRL Form 29 – AFRL Test Safety Mishap Worksheet

AFRL Test Safety Mishap Worksheet

Complete General Information and Mishap Notification Contacts in advance.
Mishap to be reported within 8 hours of occurrence.

General Information

		AFRL Costs	Non-AFRL Costs
Program Title:	Vehicle:		
Program Manager/Symbol/Phone: Dr. Ned Lindsley	Non-Vehicle		
	Total System		

Mishap Notification Contacts/Record

Name/Office	Phone/Cell	Email	Date/Time Notified
AFRL Det Safety:			
Branch Chief:			
Division Chief:			
SRB Chair:			
AFRL Flight Safety:			
Host Safety Office:			

For use only in the case of a Class A, B, or C mishap.

TD Executive Officer: _____

Tech Director: _____

Mishap Information: Class A, B, or C? (See instructions on Page 2) ☐ Yes ☐ No

Location of Mishap: _____ Date of Mishap: _____

Brief Narrative: _____ Time of Mishap: _____

Personnel

Injuries? ☐ Yes ☐ No If Yes: ☐ Military ☐ Gov't ☐ Civilian ☐ Contractor ☐ Non Gov't

How many people were injured? _____ Hospitalization Required? _____

Extent of Injuries (be as specific as possible):

Name of responding emergency organization:

Point of contact at organization (name & number):

Name of clinic or hospital where injured was taken:

Property

Property Damage? ☐ Yes ☐ No If Yes: ☐ Gov't ☐ Contractor ☐ Non Gov't

Approx dollar cost:

Extent of Damage:

Additional Notes:

FOR OFFICAL USE ONLY (FOUO) When Form is Completed

AFRL Form 29, Previous Editions Obsolete
Prescribing Directive: AFRLI 61-103, Volume 1

As a reminder, in case a mishap occurs the test team should follow the initial responses listed below:

- Ensure everyone is safe and contact emergency services, if needed.
- Minimize fire damage to wreckage, if applicable.
- Do not disturb the accident scene – preserve all wreckage and surrounding areas in their original state.
- Only move or change things at the scene in the interest of safety. Photograph the site before and after anything is disturbed. Take lots of pictures so an investigator can easily retrace the situation before it was changed.
- Gather pertinent personal information from everyone at the scene (name, duty, title, office symbol, contact information).
- Gather witness statements as soon as possible to ensure clarity and freshness of memory. Write down exactly what was personally witnessed.
- Follow the contact procedures on the front of the AFRL Form 29. Report mishap to identified contacts as soon as possible but no later than 8 hours after occurrence.
- **For Class A, B, or C mishaps, notify the Tech Directorate's Executive Officer or Tech Director to initiate OPREP-3 reporting procedures IAW AFI10-206 AFMCSUP 1.** (See below for additional information on OPREP reporting.)
- Wait for guidance from range safety, a trained safety investigator, or HQ safety personnel before removing, cleaning, or disturbing a crash site.

If in doubt, wait and ask AFRL Safety. Remember that all safety investigations are non-retribution in nature and are conducted for mishap prevention purposes only.

OPREP-3 Reporting Matrix

Event/Incident	Submit Report When (Description)	Type Report
Aircraft Mishap	Any AF aircraft mishap involving civilian causalities or damage to civilian property	PINNACLE
Aircraft Mishap Class A	A. aircraft destroyed, B. damage of $2,000,000 or more, C. mishap resulting in an AF fatality	BEELINE
Aircraft Mishap Class B	A. damage of $500,000 but less than $2,000,000, B. aircraft mishap resulting in a permanent partial disability, C. aircraft mishap resulting in inpatient hospitalization of three or more personnel	BEELINE
Aircraft Mishap Class C	Damage of $50,000 or more but less than $500,000 not reportable under BEELINE criteria	HOMELINE
Civil Aircraft Mishap	Any civil aircraft mishap that occurs on AF property or under the control of/in airspace controlled by an AF air traffic control facility	HOMELINE

For Determining Vehicle and Non-vehicle Costs:

For "Vehicle" cost consider providing quantity and cost of each vehicle, chase aircraft, or unmanned aerial vehicle.

For "Non-vehicle" cost consider infrastructure, ground control station, trailers, ground equipment, etc.

Note 1: Vehicle and Non-vehicle costs shall be mutually exclusive.
Note 2: Non-AFRL and AFRL costs shall be mutually exclusive.

AFRL FORM 29, Prescribing Directive: AFRLI 61-103, Volume 1 PREVIOUS EDITIONS OBSOLETE

Appendix E. Special Flight Operations Certificate (SFOC)

Transport Canada / Transports Canada
Civil Aviation / Aviation Civile

620 - 800 Burrard Street
Vancouver, BC
V6Z 2J8

Your file Votre référence

Our file Notre référence
5812-9

15 April 2013

University of Victoria
Department of Mechanical Engineering
PO Box 3055, Stn CSC
Victoria, BC
V8W 3P6

Phone: 250-721-6039
Cell: 250-516-1972

TAR U 2013 - 37

Attention Jenner Richards

Dear Sir:

Pursuant to section 603.67 of the Canadian Aviation Regulations, this constitutes your Special Flight Operations Certificate (SFOC) for the operation of the Mini SensorCraft, QT1.1 Skyanna, Siobahn, DJI S800, and the Penguin-B unmanned air vehicles (UAV) as described in your SFOC application emailed 26 March 2013.

This Certificate:

1. is issued to the University of Victoria, Department of Engineering, Center for Aerospace Research—Jenner Richards;
2. is not transferable and is valid from 16 April 2013 to 30 April 2014; and
3. is for the operation of the UAV for the purpose of training and testing, centered at N48°33'28." W123°22'47", as indicated in the application emailed 26 March 2013.

This Certificate may be suspended or cancelled at any time by the Minister for cause, including failure on the part of the authorized holder, its servants or agents to comply with the provisions of the Aeronautics Act and the Canadian Aviation Regulations, or the terms of this Certificate.

Nothing in this Certificate shall be held to relieve the Certificate holder from requirements to comply with the provisions of such Canadian Aviation Documents as may have been issued to him/her pursuant to the Aeronautics Act or the Canadian Aviation Regulations.

RDIMIS # **8321832**
Application RDIMS # **8321817**

This Certificate is valid for the operation of the UAV without the requirement for aircraft markings, aircraft registration, an airworthiness authority or a transponder.

Issued under the authority of the Minister pursuant to the Aeronautics Act, this document certifies that the Certificate holder is adequately equipped and able to conduct a safe operation, subject to the observance and performance by the Certificate holder of the following conditions:

1. Except where otherwise referred to in this Certificate, the Certificate holder shall comply with the applicable provisions of the Aeronautics Act and the Canadian Aviation Regulations (CARs).

2. The Certificate holder shall maintain an adequate management organization that is capable of exercising supervision and operational control over persons participating in the UAV operations.

3. The Certificate holder shall ensure that all persons connected with this operation are a minimum of eighteen years of age.

4. The Certificate holder shall conduct the operation of the UAV in a safe manner.

5. The Certificate holder shall have subscribed to adequate liability insurance covering risks of public liability at the levels described in subsection 606.02 (8) of the Canadian Aviation Regulations for the period of the UAV operations. A copy of the insurance certificate/policy shall be onsite during all operations.

6. The Certificate holder shall adhere to the security plan for the selected areas of operation in accordance with the data provided in the SFOC application, emailed 26 March 2013, or as agreed to between the University of Victoria, Department of Engineering and Transport Canada.

7. The normal and emergency procedures for the selected areas of operation shall be conducted in accordance with data provided in the University of Victoria, Department of Engineering SFOC application emailed 26 March 2013, or as agreed to between the University of Victoria, Department of Engineering and Transport Canada.

8. The Certificate holder is responsible for ensuring that the applicable authority (i.e. aerodrome Operator, landowner, tenant, MAAC local field Operator etc.) governing over the land over which flights of the UAV will take place, has been advised of the proposed operations and has no objections.

9. Throughout flight operations, the Certificate holder shall ensure that the UAV is flown over areas that would permit a safe landing on the surface, without hazard to persons or property, in the event of any emergency requiring immediate descent.

10. The UAV shall give way to manned aircraft.

RDIMIS # **8321832**
Application RDIMS # **8321817**

11. The UAV shall only be operated during the day, and remain within continuous unaided visual contact of the Operator/Observer team, or by Observer(s) who are in direct communication with the Operator at all times.

12. The UAV shall be operated with a minimum crew of two qualified persons: 1) The UAV Operator (Pilot) of the UAV, who's sole responsibility is the operation of the UAV; 2) The Observer(s) who's sole responsibility shall be notifying the Operator of any hazards that pertain to the operation of the UAV.

13. The UAV shall be operated by the Chief (Primary) Pilot, Jenner Richards, or any person authorised by the Chief Pilot to act as a UAV Operator.

14. No more than one UAV shall be operated by a single UAV Operator at any one time.

15. The UAV shall only be operated with an Observer(s), who has been briefed and determined to be qualified by the UAV Operator. The number of Observers required will be determined by the Certificate holder, based upon the circumstances associated with the UAV's Operation.

16. The UAV shall be operated with the minimum visibility of 3 nm (5.5 km) and a minimum ceiling of 1000 feet AGL. The UAV shall remain clear of cloud.

17. The UAV operations shall be limited to a maximum altitude of 120 meters above ground level (AGL).

18. Notwithstanding the requirements of paragraph 602.14 (2) (b) of the Canadian Aviation Regulations, the UAV shall not be operated (including take-offs, landings and flight demonstrations) at a horizontal distance of less than 30 meters away from inhabited structures such as buildings, vehicles, vessels and other persons who are not associated with the operation.

19. Flight of the UAV over spectators is prohibited.

20. The control station operator shall maintain constant communication with the UAV pilot at all times while the UAV is in operation.

21. The Certificate holder shall not require any person to operate the controls of the UAV if either the person, or the Certificate holder, has any reason to believe that the person is suffering, or is likely to suffer from, fatigue, that would result them being unfit to perform their duties.

22. No person shall operate the UAV within eight hours after consuming an alcoholic beverage, or while under the influence of alcohol, or while using any drug that impairs the person's faculties to the extent that the safety of the operation is endangered in any way.

23. The Certificate holder shall not operate the UAV in controlled airspace or within the Mandatory Frequency/Air Traffic Frequency area specified in the Canadian Flight Supplement of a certified aerodrome, unless the Certificate holder has contacted the applicable authority responsible for the airspace, and has received permission to operate within it.

    The test area as detailed in the SFOC application, at N48°33'28." W123°22'47" is within the control zone of Victoria International Airport. All UAV operations will be cleared with Victoria International Airport and Nav Canada Air Traffic Control Services prior to all operations. The Operator shall maintain a continuous listening watch on the appropriate Tower Frequency to maintain situational awareness of manned aircraft that may be transiting the zone.

24. The Certificate holder shall report to this office, on the first working day following the occurrence, the details of any of the following occurrences:
    - any injury to persons requiring medical attention,
    - unintended contact between the UAV and person(s), livestock, vehicle(s) or other structure(s),
    - unanticipated damage incurred by the UAV, control station, payload or communications links.
    - Unintentional loss of control of the UAV by the Operators.
    - Any time the UAV is not kept within the geographic and altitude limits as outlined in this Certificate.

25. The Certificate holder shall not operate the UAV following any of the occurrences listed in Condition 24, without further written approval of this office.

26. All persons connected with this operation shall be familiar with the contents of this Certificate.

27. A copy of this Certificate and a copy of the application emailed 26 March 2013 shall be on site any time the UAV is in operation.

28. The Certificate holder shall:
    1. Document their flight planning and procedures for each flight.
    2. Document a post flight report on performance and any deviations from the intended plan.
    3. Shall keep records and make available for inspection if requested by this office.

Yours truly,

John Milligan,
Superintendent, Flight Operations,
Transport Canada, Civil Aviation, Pacific Region

RDIMIS # **8321832**
Application RDIMS # **8321817**

Appendix D

Aeroelastically Tuned RPV Flight Test Plan

This appendix presents the rough draft of the Aeroelastic Response Program's final flight test plan, the Aeroelastically Tuned RPV Flight Test Plan. The test plan is presented as a stand-alone document. The primary author of this document is the author of this thesis, Jeffrey Garnand-Royo. Two co-authors assisted in this document including Tyler Aarons and Jenner Richards.

Joined-Wing SensorCraft
Aeroelastic Response Program Flight Test Plan
Aeroelastically Tuned RPV

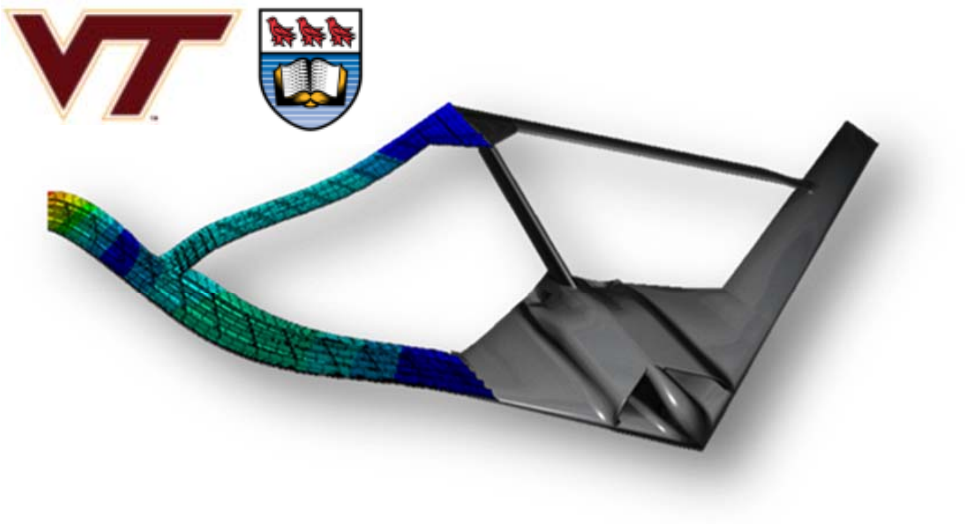

Blacksburg, VA — Victoria, BC — Foremost, AB

Security Classification: Unclassified

AFRL Program Manager: Ned Lindsley

Virginia Tech POC: Robert Canfield

University of Victoria/ Quaternion Engineering POC: Afzal Suleman

CCUVS POC: Sterling Cripps

Version 1

Executive Summary

The aeroelastic tuning of the Boeing Joined Wing SensorCraft (JWSC) and flight testing of the tuned model is the topic of an ongoing international collaboration between Virginia Tech and The University of Victoria (Canada). The program leverages the resources of Quaternion Engineering Inc. (Victoria, Canada), the Canadian Centre for Unmanned Vehicle Systems (CCUVS), and the AFRL/ Virginia Tech/ Wright State Collaborative Center for Multidisciplinary Sciences (CCMS) at Virginia Tech. This ambitious program has two primary objectives. The first is to develop a cost-effective, aeroelastically scaled, remotely piloted vehicle (RPV) to investigate the geometrical nonlinear behavior associated with the JWSC configuration. The second objective is to design and perform flight test experiments to demonstrate, measure, and characterize the nonlinear behavior in flight.

The JWSC is a high aspect ratio, joined wing aircraft. It features four lifting surfaces forming a diamond shape with a fuselage and vertical tail along the longitudinal axis of symmetry. The JWSC RPV has a 16.4ft span (5m) and is powered by twin JetCat P200-SX turbine engines.

The JWSC Flight Test Program (FTP) is divided into two distinct phases: the Flight Demonstration Program and the Aeroelastic Response Program. The Flight Demonstration Program involved the design and flight testing of the Geometrically Scaled RPV with equivalent rigid body dynamics, but with no aeroelastic tuning, and was the subject of the previous FTP. Once the Geometrically Scaled RPV flight tests were completed, the Aeroelastic Response FTP began. This program includes the re-design of the Geometrically Scaled RPV to include flexibility within the structure. The program extends to include construction methods for a more flexible configuration, design and integration of a robust flight worthy measurement system, and flight test program development and execution. The re-designed RPV, known as the Aeroelastically Tuned RPV (ATRPV), will be the subject of this report. This document supports the approval process for the Aeroelastic Response Program, including all ground and flight tests related to the Aeroelastically Tuned RPV.

The Aeroelastical Response Program FTP is divided into three phases the scope of which is meant to facilitate the appropriate progression to the flight test.

Phase 1: **Validation Tests –** This phase includes ground testing of the completed Aeroelastically Tuned RPV. A Static Loading Test will be utilized to validate the appropriate nonlinear static deflection of the designed target response. A bifilar pendulum test will be implemented to ensure the ATRPV has equivalent aerodynamic characteristics.

Phase 2: **Flight System Readiness Tests -** This phase includes the Integration and testing of all onboard systems, including instrumentation, static thrust testing, verification of control surface mixing and center of gravity placement.

Phase 3: **Flight Tests -** This phase includes all flight test operations of the RPV. Taxi tests, phasing tests and maneuvering tests are all included in this phase.

Attribution

The primary author of this document is Jeffrey Samuel Garnand-Royo. Jeffrey Garnand-Royo will act as flight test director for the efforts presented in this document. Jeffrey Garnand-Royo is a master's graduate of the Aerospace Department working out of the Nonlinear Systems Lab at Virginia Tech.

A co-author to this document is Jenner Richards. Jenner Richards is a doctoral candidate of the Mechanical Engineering Department at the University of Victoria and is tasked with aeroelastic tuning of the next phase JWSC RPV as well as overseeing the design and construction of the test platform itself. Jenner Richards is responsible for the design and fabrication of the previous Geometrically Scaled JWSC RPV including the Mini SensorCrafts and is responsible for developing a computational framework for performing aeroelastic scaling of aerospace vehicles and applying this to the SensorCraft.

The second co-author to this document is Tyler Aarons. Tyler Aarons is a master's graduate of the Aerospace Department who worked out of the Nonlinear Systems Lab at Virginia Tech. He acted as the previous flight test director for the Flight Demonstration Program and is responsible for providing a well-organized test document template for which this test plan is based.

Table of Contents

List of Figures

List of Tables

1 Introduction

1.1 Motivation

High altitude, long endurance (HALE) unmanned aerial vehicles (UAVs) are capable of providing revolutionary intelligence, surveillance and reconnaissance (ISR) capabilities over vast geographic areas when equipped with advanced sensor packages. The aeroelastic responses, specifically aft wing buckling and gust load response, associated with the Joined Wing SensorCraft (JWSC) have been demonstrated and investigated in numerous computational and wind tunnel studies[1-3]; however, these phenomena have never been successfully tested in a flight test program. The Air Force has determined that an aeroelastically tuned Remotely Piloted Vehicle (RPV) provides a low cost and effective way to investigate these non-linear aeroelastic responses. By experimentally demonstrating, investigating and measuring these responses, future flight test programs will be able to test active aeroelastic control and gust load alleviation systems to reduce the structural and aerodynamic effects of the nonlinear responses. In addition, the testing of the RPV will support management planning for future tests of SensorCraft technologies.

1.2 Background Information

The SensorCraft is a concept initiated by the Air Force Research Laboratory (AFRL) to serve as a next-generation, HALE reconnaissance system. The SensorCraft is envisioned to fill the role of the next generation HALE ISR platform to contribute to persistent battle space awareness capabilities .[4] The Boeing Joined Wing Concept, shown in Fig. 2, represents the topic of this flight test plan. [4]

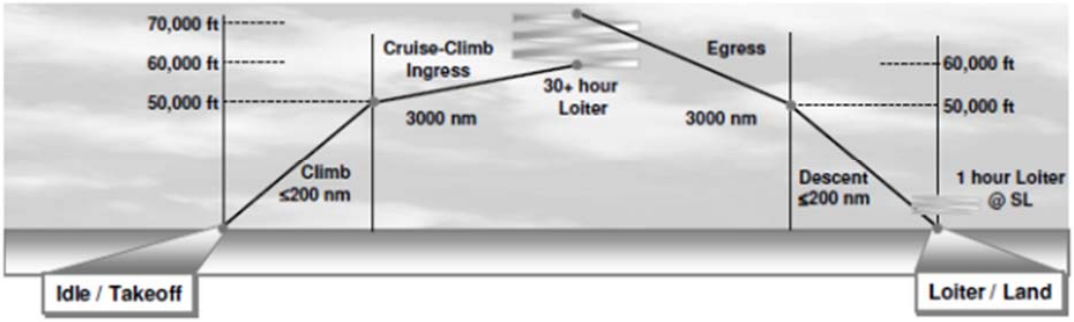

Figure 1 – Full scale SensorCraft mission profile[4]

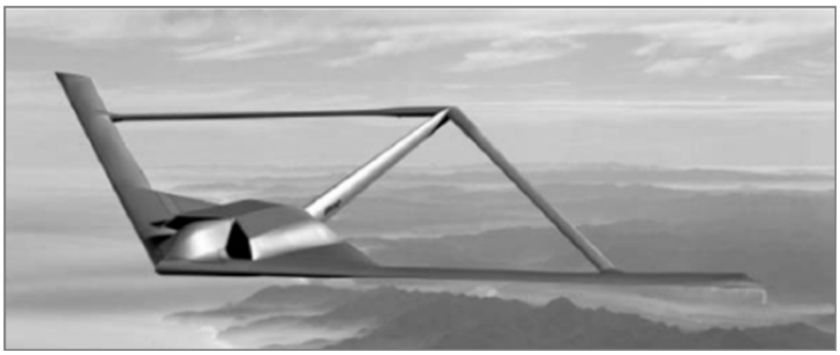

Figure 2. Joined-wing SensorCraft Concept[4]

The primary driver behind this departure from conventional aircraft design is the ability to incorporate conformal radar antennas in the fore and aft wings to provide persistent 360 degree, foliage penetrating surveillance. This ability is of great benefit to the ISR mission, but it does come with a price. Previous computational studies of joined-wing aircraft configurations have shown the importance of structural geometric nonlinearity due to large deflections and follower forces that may lead to buckling of the aft wing[1,5]. This potential buckling represents a unique and challenging aeroelastic design problem. The non-linear behavior, which is a result of the joined wing configuration and advanced, lightweight structural design, could be removed by strengthening the wing to a point where these non-linear behaviors vanish; however, this would result in large penalties in aspect ratio and structural weight, greatly reducing the performance of the aircraft. To avoid these penalties, non-linear aeroelastic design, analysis and testing are required to ensure that the JWSC is able to sustain the non-linear responses required to complete the proposed ISR mission. An aeroelastically tuned RPV provides a low cost and effective way to investigate these nonlinear aeroelastic responses. Fig. 3 illustrates the size of the full scale and RPV airframes.

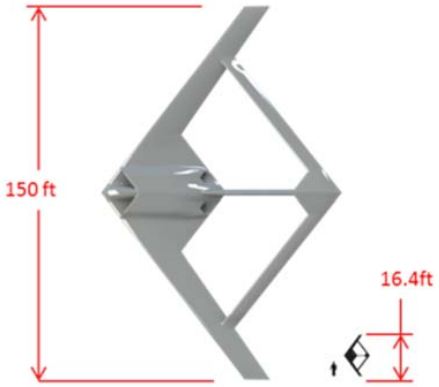

Figure 3 - Relative size of full scale JWSC and RPV[6]

1.3 Program Overview

The aeroelastic tuning of the JWSC and flight testing of the scaled model is the topic of an ongoing international collaboration between Virginia Tech and The University of Victoria (Canada). The

program leverages the resources of Quaternion Engineering Inc. (Victoria, Canada), the Canadian Centre for Unmanned Vehicle Systems, and the AFRL/ Virginia Tech/ Wright State Collaborative Center for Multidisciplinary Sciences (CCMS) at Virginia Tech.

1.3.1 Program Breakdown

Due to the unique JWSC geometry, the relative large scale of the RPV and the challenge of fabricating aeroelastically tuned, flight worthy components, the JWSC Flight Test Program (FTP) is divided into two distinct phases: a Flight Demonstration Program which was the topic of the previous flight test plan and an Aeroelastic Response Program, the topic for this flight test plan. The Flight Demonstration Program involved the design of a Geometrically Scaled RPV, GSRPV (one with equivalent rigid body dynamics, i.e. preserved aerodynamics, overall mass and moments of inertia)including construction methods, flight test instrumentation selection and integration, control system tuning and flight test program development. This also includes the construction and flight testing of several preliminary models to determine flying qualities and trim requirements[1]. The Flight Demonstration Program concluded October 15, 2011 following the successful flight of the GSRPV.

Once the GSRPV flight test was completed, attention was shifted to the second phase of the JWSC FTP; The Aeroelastic Response Program. The Aeroelastic Response Program involves the design of an Aeroelastically Tuned RPV, ATRPV (one with equivalent rigid body dynamics, i.e. preserved aerodynamics, overall mass and moments of inertia) including construction methods for a more flexible configuration, design and integration of a robust flight worthy measurement system, and flight test program development. Following the success of utilizing small scale models in the form of Mini-SensorCrafts , the Aeroelastic Response Program will include the construction and flight testing of Mini SensorCrafts to explore appropriate flight maneuvers and aircraft parameters that will induce the expected nonlinear structural response in the ATRPV platform. Furthermore, Mini-SensorCraft testing will provide a platform for test procedure development and fine-tuning of autopilot parameters.

1.3.2 Participating Organizations

The major organizations playing roles in this project are Virginia Tech, The University of Victoria, Quaternion Engineering Inc., the Canadian Centre for Unmanned Vehicle Systems (CCUVS), and the AFRL/ Virginia Tech/ Wright State Collaborative Center for Multidisciplinary Sciences (CCMS) at Virginia Tech. Virginia Tech is the primary contractor. Quaternion Engineering is the subcontractor, and also the owner of the test articles. The University of Victoria employs the founders and employees of Quaternion Engineering Inc. AFRL is the lead test organization (LTO) and provides funding and guidance for the project. CCUVS is a participating test organization (PTO), and provides support for the execution of all planned tests.

[1] All preliminary, reduced complexity flight models were designed, tested and flown using private funding from Quaternion Engineering as internal research and development (IRAD) to promote the success of both programs.

2 Test Article Description

This section provides a description of the Aeroelastically Tuned RPV (ATRPV). A general description of the vehicle, including overall dimensions will be presented first. This will be followed by descriptions of the control surface layout, structural design and propulsion system. A description of the internal layout of the fuselage and the location of all trimming weights will close this section.

2.1 General Description

The test item for the Aeroelastic Response Program is the Aeroelastically Tuned RPV. The tests of the ATRPV will include flight maneuvers to induce the geometric nonlinearity within the JWSC configuration. Having verified the airworthiness and controllability of 1/9th scale RPV, the GSRPV, focus has been shifted modifying the wings to include flexibility. The Aeroelastically Tuned RPV is a 1/9th scale model of the Boeing JWSC concept, and the RPV has been designed and manufactured by Jenner Richards of the University of Victoria to include flexibility. Jenner Richards is also responsible for the design and manufacturing of the Mini-SensorCraft's and the GSRPV platform. A CAD rendering of the Aeroelastically Tuned RPV is presented in Fig. 4.

Figure 4- CAD Rendering of the Aeroelastically Tuned RPV[7]

The Aeroelastically Tuned RPV is a joined wing configuration consisting of a center body housing twin JetCat P200-SX turbine engines, a vertical tail boom and four flexible lifting surfaces. The forward wings have positive dihedral and are swept aft. The aft wings have negative dihedral and are swept forward to join with the forward wings at approximately 56% span (measured from the centerline) forming a diamond. Fig. 5 presents a dimensioned 3-view drawing of the ATRPV highlighting key design parameters. A summary of these parameters is presented below in Table 1.

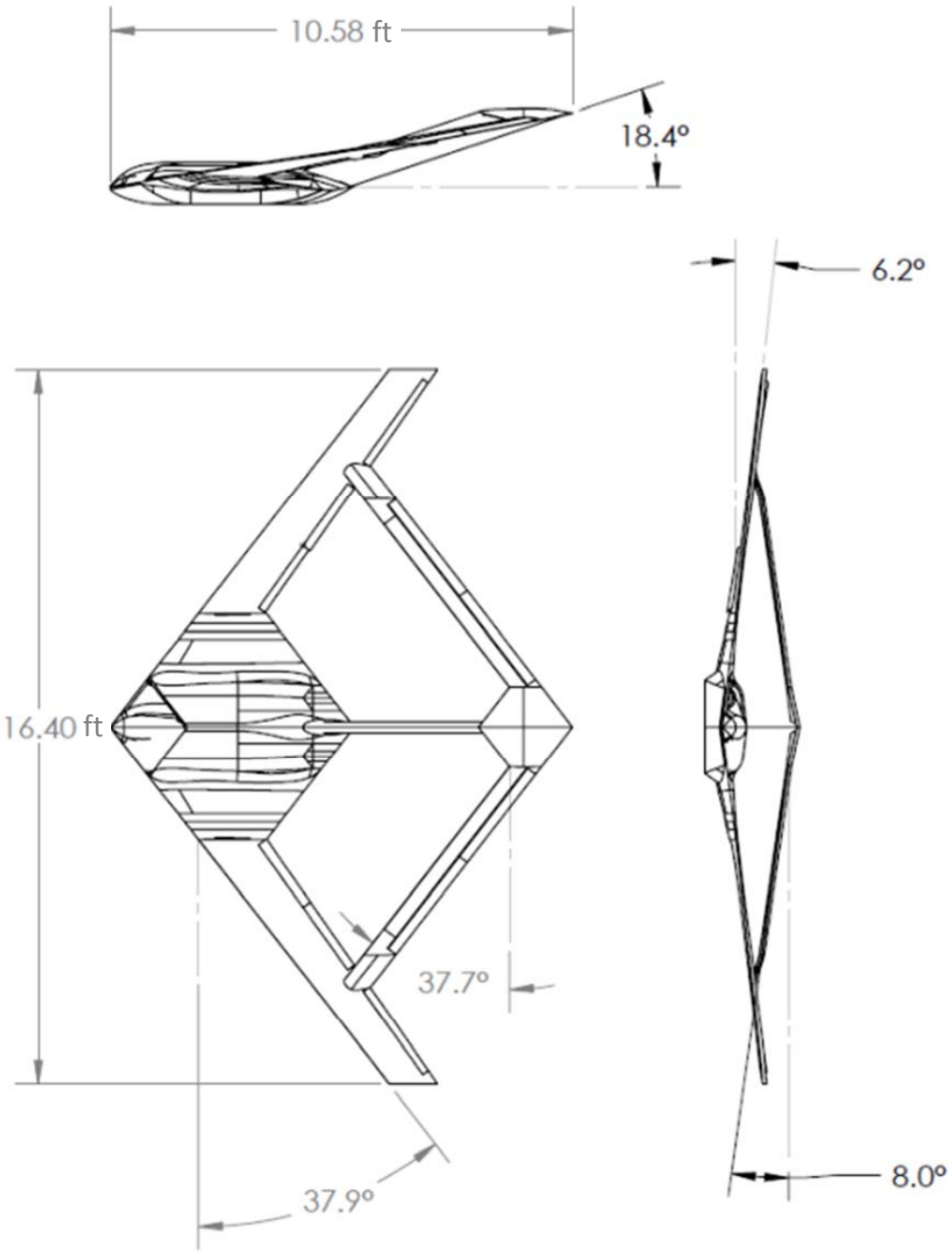

Figure 5- Overall Dimensions of the Aeroelastically Scaled RPV (dimensions shown in ft)[8]

Table 1- ATRPV specifications

Parameters	English	Metric
Wing Span	16.4 ft	5 m
Wing Area	15.0 ft^2	1.4 m^2
Length	10.58 ft	3.22 m
Aircraft Weight (min-max)	152-204.5 lbs	69-92.8 kg
Total Thrust	104 lbs	47.17 kg
Front Wing Sweep	37.9°	-
Front Wing Dihedral	6.2°	-
Front Wing Sweep	-37.9°	-
Aft Wing Dihedral	-8.0°	-

2.2 Performance

Performance parameters for the Aeroelastically Tuned RPV represent target limits for which the pilot will operate within while flying the ATRPV. The performance parameters for the ATRPV at the theoretical maximum possible weight (204.5 lbs) is presented below in Table 2 and a typical mission profile is presented in Fig. 6. The parameters are estimates based on Fluent CFD analysis of the JWSC configuration in free stream conditions, simulations, reduced complexity flights, and the previous GSRPV flight.

Table 2- Performance Parameters (204.5 lbs, 92.8 kg)

Parameter	English	Metric
Stall Speed, V_{stall}	41.6 knots	14.1 m/s
Takeoff Speed, V_{TO}	49.8 knots	16.9 m/s
Nominal Cruise Speed, V_{cruise}	68-87.5 knots	27.7 m/s
Do Not Exceed Speed, V_{NE}	126.4 knots	41.5 m/s
Approach Speed, V_A	49.8 knots	18.3 m/s
Operating Altitudes, AGL	328.1-698.8 ft	100-213 m
Max Distance from Operator	4921.3 ft	1500 m

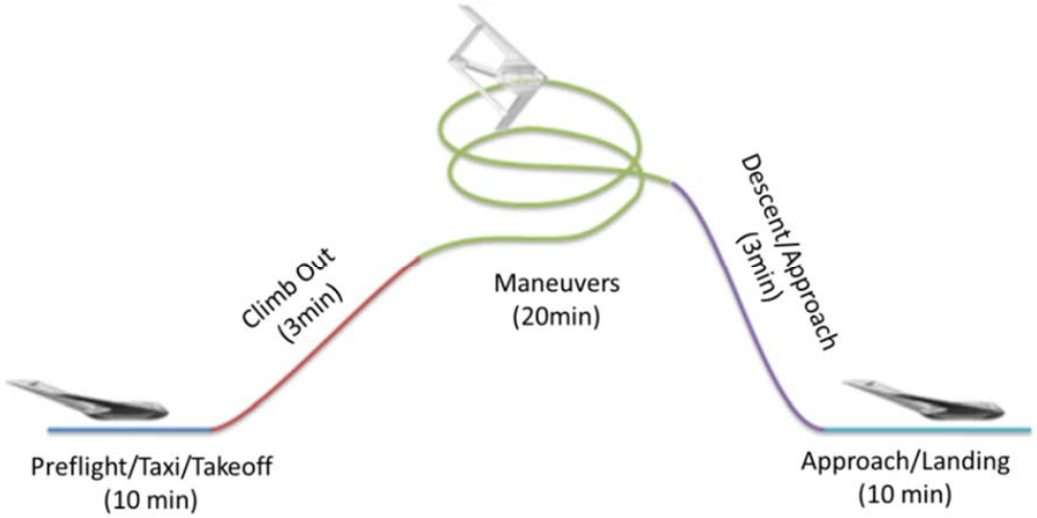

Figure 6- Aeroelastically Tuned RPV Mission profile[6]

The Key Performance Parameters, KPP's, for the ATRPV represent a target region for which the pilot will operate within during maneuvers. This includes maneuver speeds, pitch rates, bank rates, and most importantly a target objective/threshold strain reading that will indicate if the aft wing has reached the nonlinear geometric target. The pilot will stay within the KPP's and once the target strain has been reached during a maneuver, the pilot will safely cease the maneuver in order to unload the vehicle. The KPP's for the ATRPV must still be developed based on the finalized design of the vehicle.

2.3 Control Surface Layout

2.3.1 Control Surface Scheduling

The control surface locations are specified in the supplied full size aircraft geometry. Surface sizing and locations are unchanged with two exceptions. First, the outboard ailerons are split into two separate surfaces due to a complex hinge line as the wing twists towards the tip. The second change is the movement of the elevators inboard into the boom strake. This configuration will be tested on the Mini SensorCraft platform prior to implementation onto the ATRPV. Fig. 7 shows the control surface layout.

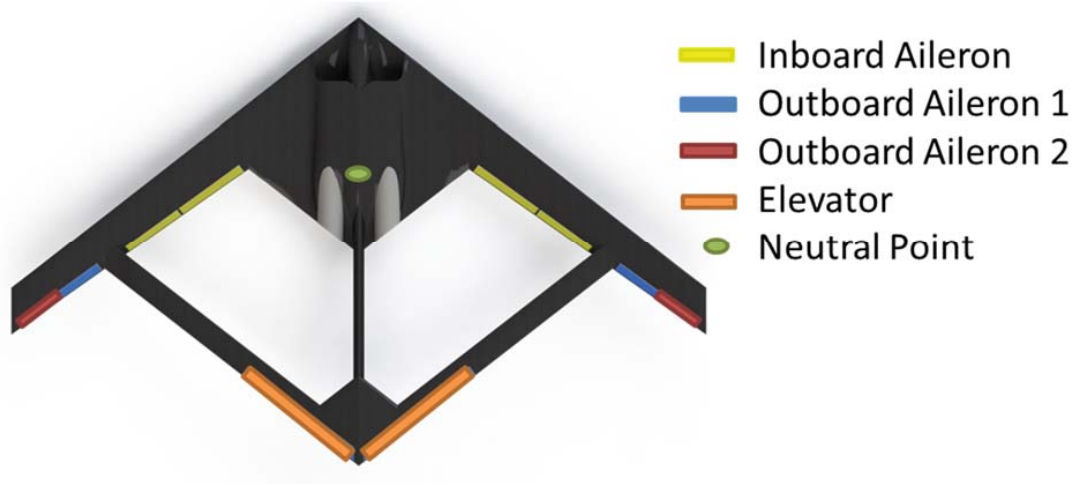

Figure 7– Control Surface Layout[8]

Several control surface scheduling schemes have been both simulated and tested using reduced scale aircraft. The scheduling that will be used in the initial flight test of the ATRPV is summarized in Table 3.

Table 3- Control Surface Scheduling

Surface	Function
Inboard Aileron	Redundant
Outboard Aileron 1	Primary Aileron
Outboard Aileron 2	Primary Aileron
Elevator	Primary Elevator

Multiple surfaces are used to control the aircraft in each axis to provide redundancy for all critical control modes in case of in-flight failure of any surface. For the primary control surface schedule, roll command uses both outboard ailerons deflecting together as one pseudo surface; a pitch command uses the elevators. The redundant control surfaces can be utilized in many ways, the choice of which will depend on the need of the flight test specifically. One option is utilizing the inboard aileron as a flap (if more flap area is desired by the pilot) or as an aileron for additional roll control. This change is accomplished via mixing in the transmitter, and it has no effect on the placement of servos or the use of the Power Box Royals. Another option is to fix the inboard ailerons so they do not move and are unused entirely during the flight.

2.3.2 Servo Selection and Control Surface Flutter Reduction.

In order to reduce the possibility of control surface flutter, each surface is actuated using two servos. An aluminum rib at each hinge point acts both as the hinge attachment and also as a hard point for attaching the control horn. This reduces any flex to mitigate the possibility of flutter. Each control

surface is hinged in two locations using a spherical joint. This ensures that minimal loading is transferred to the control surface and prevents binding due to excessive wing bending.

In order to size servos for the Aeroelastically Tuned RPV, hinge moments will be calculated using VLM analysis for ±30° control surface deflections at the never exceed speed (worst case calculations) for the decided test point configuration. Computed hinge moments will be compared with the rated torque of candidate servos (as specified in kg-cm).

Servos operate using a high-gain feedback controller to monitor and maintain commanded position. As long as the servo is not pushed beyond its maximum torque rating, the servo is able to maintain the commanded position with little variation due to loading. This, coupled with two servos per control surface (two points of contact with the main wing) minimizes the risk of control surface flutter.

2.4 Structure

2.4.1 General Arrangement

The overall structural design of the RPV was driven by several factors including sufficient structural strength, component space reservations, modularity, and the addition of flexible components to produce the target nonlinear aft wing response

The structure, of the ATRPV uses conventional rib/spar construction excluding the aft wing and a majority of the forward wing. The fuselage employs a construction with conformal spar caps running across the span. All bulkheads, spars and ribs are designed to interlock to ensure accurate location and simple assembly, as shown in Fig. 8**Error! Reference source not found.**.

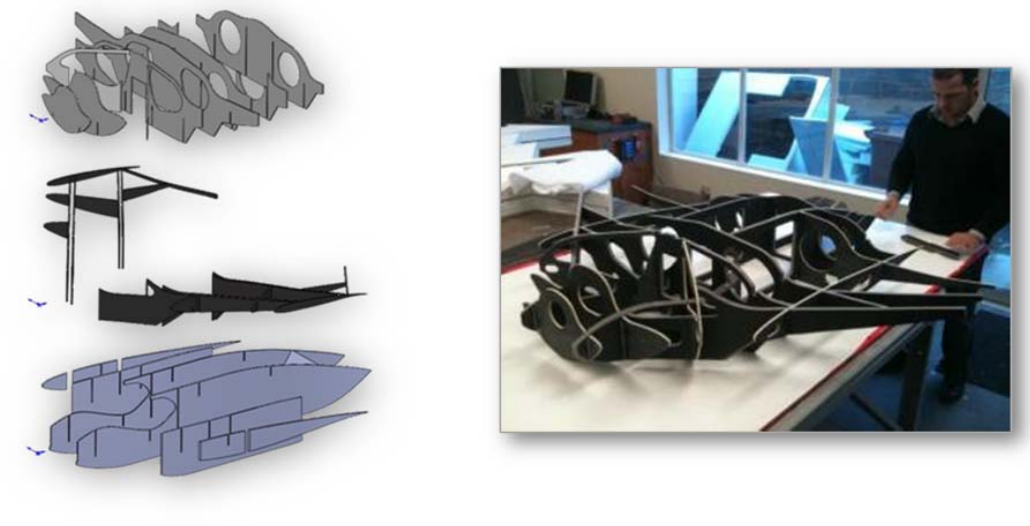

Figure 8- Exploded View Showing Interlocking Components of the Fuselage Design (Left) Final Product (Right)[8]

The aircraft breaks down for transport and this modularity also allows quick refitting in the case of damage during flight testing. The forward wing attaches to the fuselage with a series of aircraft fasteners that transfer load from the wing spar caps into the fuselage skins. The rear wings attach to the forward wings using two aircraft grade fasteners. The aft wing spars terminate with a partial main wing airfoil cross section. This allows the rear wing to mate into the forward wing between two aluminum ribs. A gusset plate is employed on the underside of the wing to anchor the fasteners and tie joint loads into the aluminum ribs. The rear wings attach to the vertical boom using four aircraft grade fasteners. Finally the boom attaches to the fuselage by means of main boom spar passing through into a receiving compartment in the fuselage. A torque wrench will be used to ensure that all bolts are properly secured during aircraft assembly.

In order to produce the nonlinear aft wing response, the forward wing must produce a larger deflection. This can be achieved through the implementation of a leaf spar into the forward wings. This additional compliant internal structure is introduced just outboard of the existing forward wing root/fuselage joint. The spar is tied into an aluminum slot which connects to the root/fuselage joint. The other end of the spar is tied into a similar connection joint at the aft/forward wing connection. Outboard of the aft/forward wing joint, the structure will remain unchanged from the previous design of the GSRPV. The leaf spar stiffness will be based on the target response analysis. The introduction of the leaf spar is shown in Fig. 9.

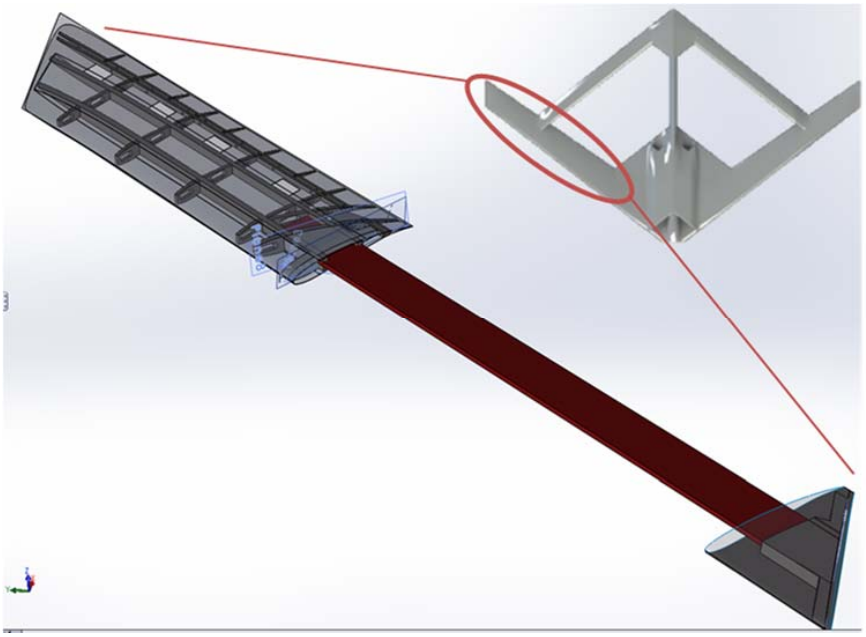

Figure 9- Leaf spar implementation[8]

Coupled with the need to produce larger deflections in the forward wing, a complete redesign of the aft wings to introduce flexibility must occur. This is accomplished by introducing a tailored ladder-spar internal structure in which the cross sectional members will be optimized to match a desired stiffness, based on the target response analysis. This structure is shown below in Fig. 10.

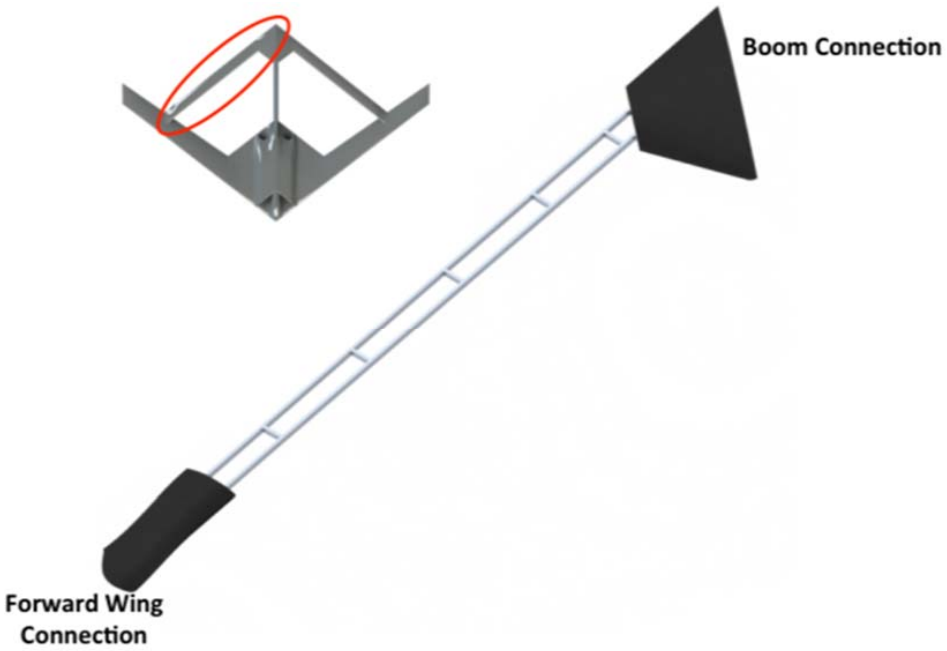

Figure 10- Internal Ladder Spar Structure[9]

A composite outer skin will be fabricated utilizing existing molds of the aft wing in order to preserve the aerodynamic shape of the aft wing. Each portion of the composite outer skin will be attached to the structure utilizing rapid-prototype rib sections placed on each torsional bar of the ladder structure. Relief cuts will be introduced into the composite outer skin, so that each subsequent outer skin panel will be attached to one rib only. This technique will avoid the possibility of introducing additional stiffness by the skin, when the aft wing is under load. This overall design choice means the composite outer skin serves only simply as aerodynamic fairings. The proposed manufacturing of the aerodynamic fairings is summarized in Fig. 11.

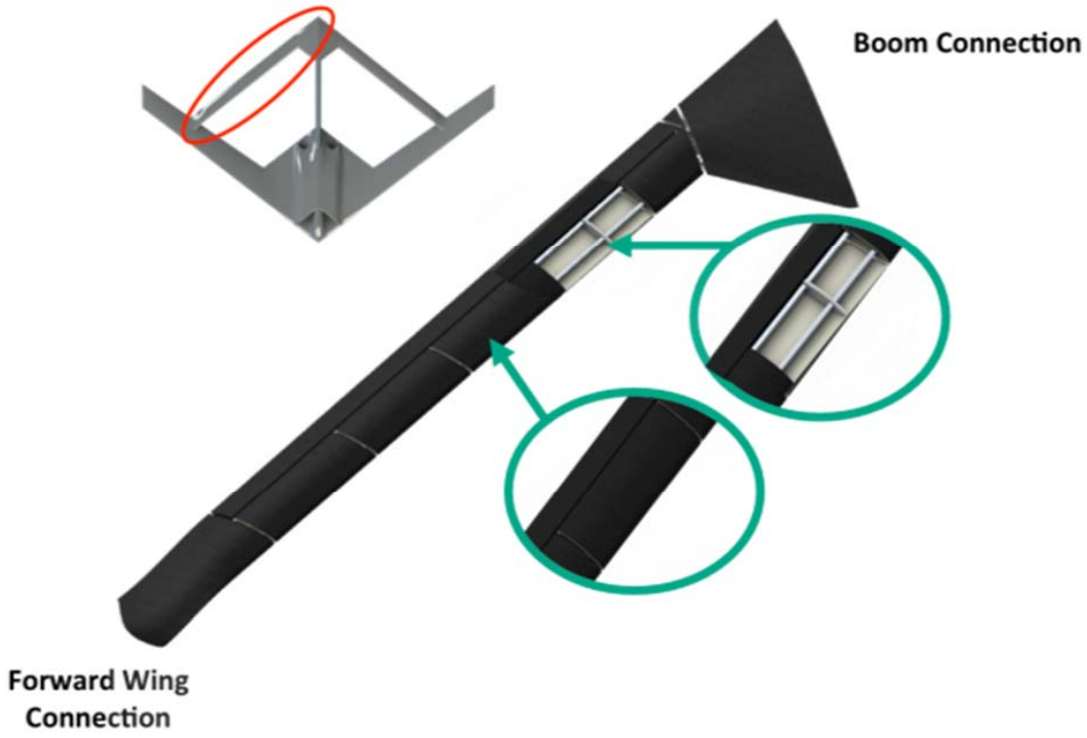

Figure 11- Aerodynamic Outer Skin for Aft Wing (Attached to One Prototype Rib) [8]

There are advantages associated with this design due to the ability of accessing the internal structure. One advantage is the ability for control of mass distribution in the aft wing to assist in producing the target nonlinear aft wing response. Secondly, access to the internal structure allows for the ability to access any instrumentation or wiring within the aft wing. Furthermore, the aluminum rectangular cross section of the internal ladder spar structure allows for a convenient strain gage instrumentation system.

2.5 Propulsion

Two JetCat P200-SX turbine engines, located within the fuselage as shown in Fig. 12, power the ATRPV.

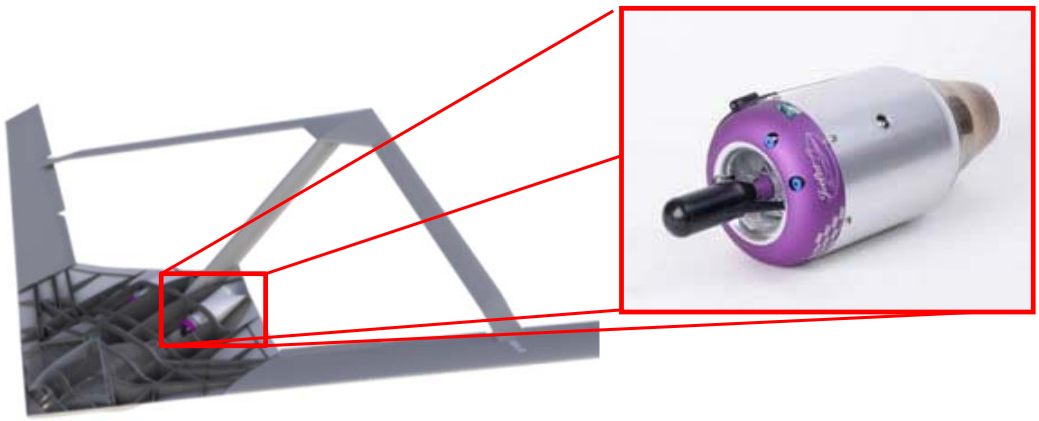

Figure 12- Location of JetCat P200-SX Turbines in the Fuselage [8,10]

The P200-SX is the largest turbine available from JetCat turbines. Table 4, shown below, provides the manufactures specified performance parameters for a single JetCat P200-SX turbine.

Table 4- JetCat P200-SX Specifications[11]

Thrust	52 lbs @ 112,000 RPM
Weight	5 lbs
Diameter	5.12 in
RPM Range	32,000 - 112,000 RPM
Exhaust gas temperature	580°C-690°C
Fuel consumption	24 oz per/min at full power
Fuel	Jet A1 or 1-K kerosene
Lubrication	5% synthetic Oil in the fuel
Maintenance interval	25 hours

The JetCat P200-SX has many features which make it a safe and reliable choice for powering the JWSC RPV including a heavy duty starter, onboard RPM and exhaust gas temperature sensors and JetCat's industry leading customer service; however, two of the most important features are the Electronic Control Unit (ECU) and the Ground Support Unit (GSU). Below is a description of these features:

1. **JetCat Electronic Control Unit (ECU)** - The JetCat Jet-tronic ECU provides real-time closed loop control of the turbine, resulting in better starts, smoother idle and more reliable performance. The ECU, which features a Hitachi H8 16 bit microcontroller, has a fully automatic starting sequence which promotes safe, reliable starts. The ECU also monitors turbine RPM and exhaust gas temperature during flight via sensors in the turbine. Additionally, the ECU monitors fuel pump voltage, battery voltage and calculates statistical data including total fuel consumption, total turbine time, maximum RPM, run time. The ECU also monitors total turbine runtime. This is especially useful as JetCat requires each turbine to be sent in for maintenance every 25 hours

of runtime. The total engine time will be checked and noted before each start of the engine. The data provided by the ECU will be passed through the Piccolo II Autopilot and thus transferred via telemetry to the ground station to be monitored real time and promote further flight safety during flight operations.

2. **Ground Support Unit (GSU):** Used for monitoring or prescribing (within operational limits) key parameters such as maximum RPM and minimum RPM, in real time, during startup and ground testing. The GSU may be connected or disconnected from the ECU at any time.

The inlet and hot gas passages within the fuselage have been directly scaled for the RPV with the exception of a slight narrowing of the section around the turbines. This portion has been narrowed to create the required 0.75 inch clearance around the perimeter of each turbine to allow air passage for cooling. Fig. 13 shows a cross section of the modified fuselage ducting.

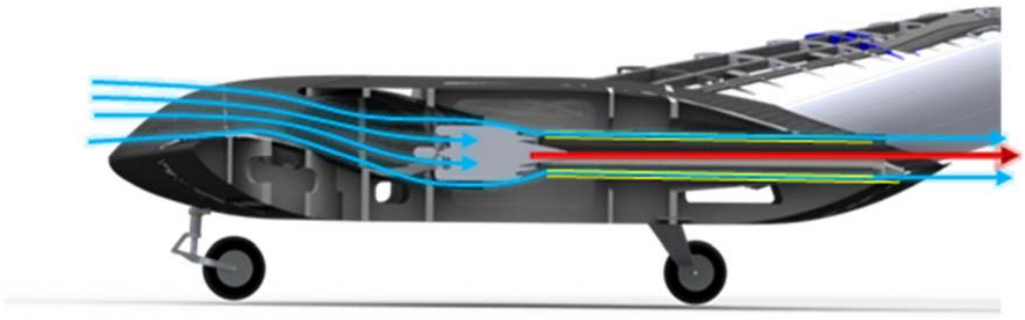

Figure 13 - Fuselage Cross-section Showing Inlet and Exhaust Routing[7]

The engines are placed near the rear of each pass-through for two reasons. The first is to directly route the hot exhaust out the fuselage, minimizing heat transfer, and the other reason is to increase the cooling airflow around the engine. Placing the engine at the point where the duct begins to constrict sets up a venturi effect which helps to draw cooling air around the outside of the engine. This is especially important when the aircraft is stationary, as in taxi and startup. Due to the danger posed by ingesting foreign objects into the turbine, mesh strainer screen is placed across the inlet to the fan opening as shown in Fig. 14.

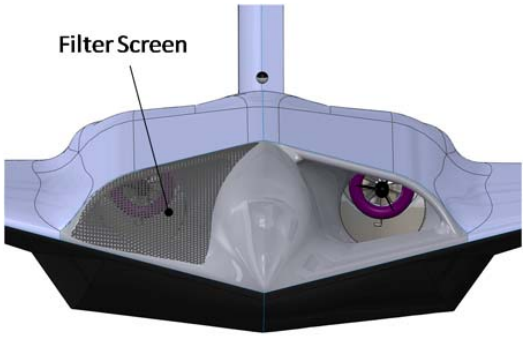

Figure 14- Strainer Screen to Prevent Ingestion of Debris[6]

2.6 Payload

Due to the nature of the Aeroelastically Tuned RPV flight tests, the required payload consists of fuel, flight critical avionics (Piccolo II Autopilot), Instrumentation, and trimming weights (used to ballast to the test point weight as well as provide the proper moments of inertia about each axis). No fuel is stored in the wings of the aircraft. Variance in the weight of the wings due to fuel burn would result in time varying aeroelastic characteristics. Accordingly, the fuel is stored in a large tank on the centerline of the aircraft near the center of gravity.

2.7 Tricycle Landing Gear

Takeoff of the ATRPV is accomplished via a tricycle style landing gear with steerable nose gear. The use of a tricycle arrangement of wheels gives stability during taxi testing and during the takeoff roll. **Error! Reference source not found.** 15 shows the landing gear for the ATRPV, including the custom designed oleo strut for the steerable nose gear. Fig. 16 presents the custom designed oleo strut. Both parts of the landing gear were used successfully on the previous GSRPV platform (Fig. 17).

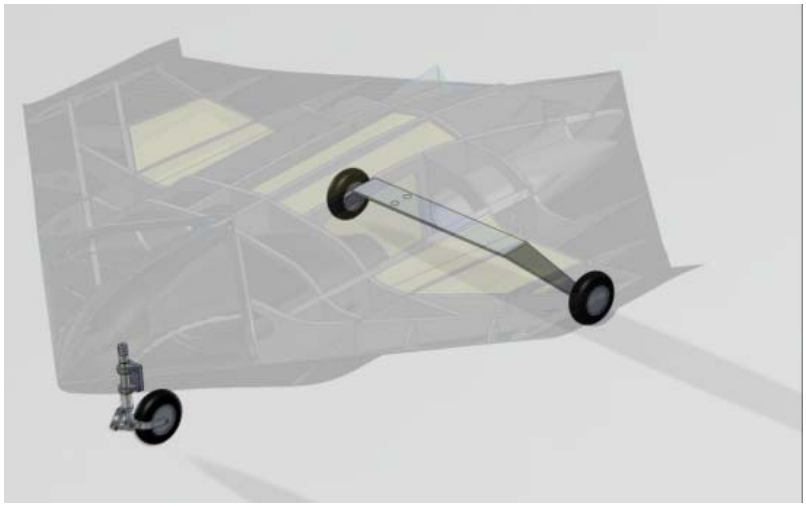

Figure 15– Aeroelasticatlly Tuned RPV Tricycle Landing Gear[8]

Figure 16- Custom Designed Oleo Strut for Nose Gear

Figure 17- Tricycle Landing Gear on GSRPV

2.7.1 Structural Design Validation using ANSYS Finite Element Analysis

In order to validate the structural design of the landing gear, a simulated worst case landing load was analyzed by Jenner Richards of Quaternion Engineering using FEA in ANSYS for the GSRPV efforts. The loading tested was a 4.5 g landing load (which corresponds to a 3g landing load with a factor of safety of 1.5) at both the forward CG and aft CG limits. Fig. 18 and Fig. 19 present the meshed models of the nose gear and rear gear, respectively. These models and all connection points with the main fuselage structure were analyzed. Fig. 20 and Fig. 21 present the results of the landing analysis for the nose gear and rear gear respectively. These figures show the location and magnitude of the maximum and minimum factor of safety (calculated based on a 4.5g loading). Table 5 summarizes the results of these calculations

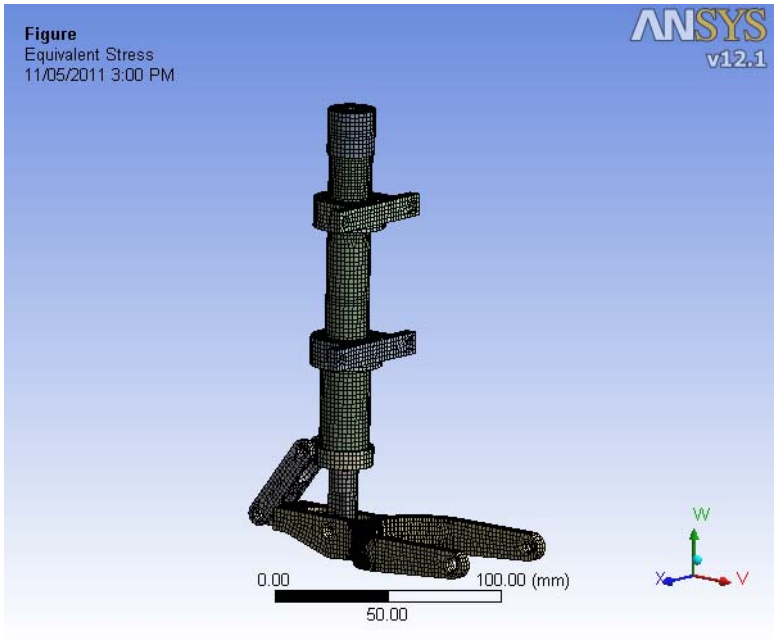

.

Figure 18- Meshed Model of Nose Gear for Testing in ANSYS[8]

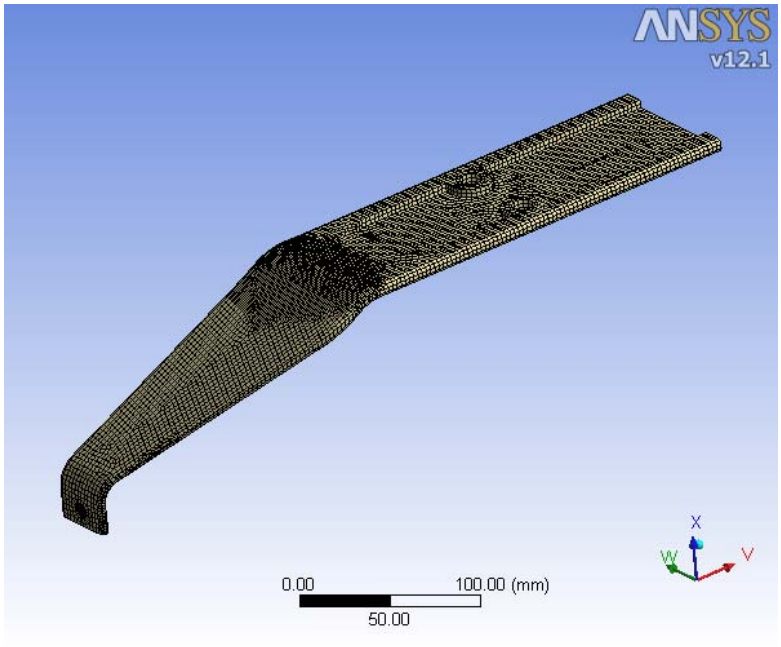

Figure 19- Meshed Model of Rear Gear (half gear) for Testing in ANSYS[8]

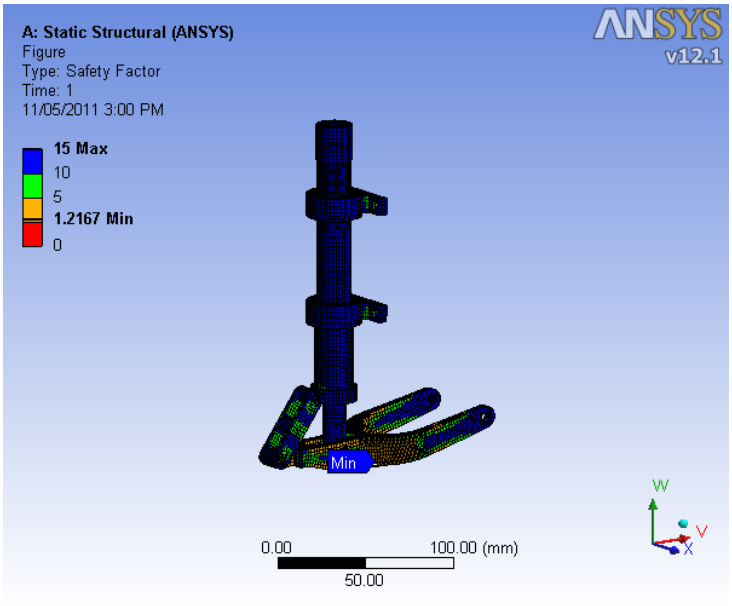

Figure 20- Nose Gear Landing Analysis Results[8]

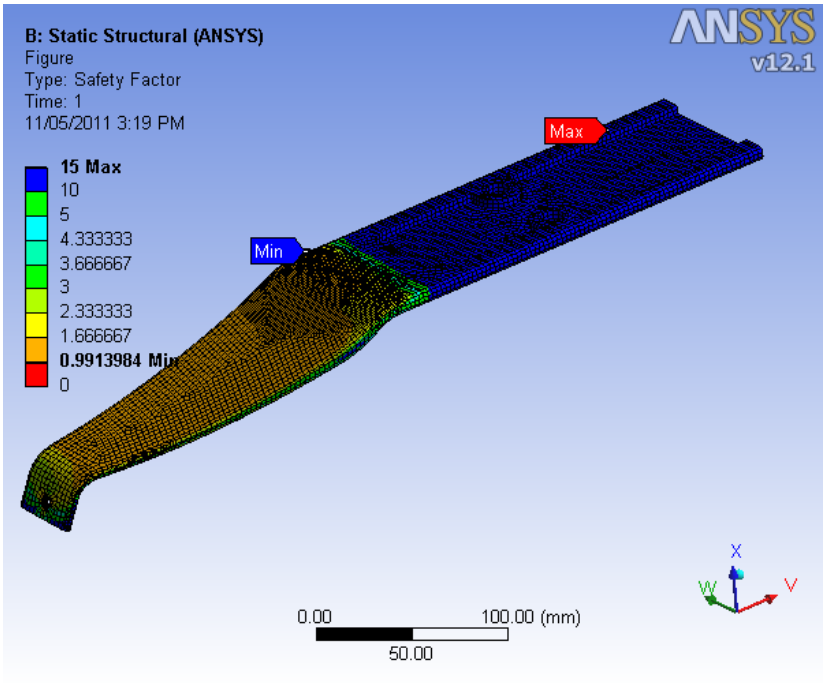

Figure 21- Rear Gear Landing Analysis Results[8]

Table 5– Landing Gear FEA Analysis Results Summary

	Calculated 4.5g FOS	Corresponding 3g FOS
Nose Gear	1.22	1.83
Rear Gear	0.99	1.49

These results show a minimum factor of safety of 1.83 for the nose gear and 1.49 for the rear gear, assuming a 3g landing load. This is acceptable for the flight test of an unmanned aircraft. All connection points with the fuselage were tested as well in the previous Flight Test Demonstration Program, and the resulting factor of safeties were higher than those presented above, indicating that the fuselage structure is capable of handling this worst case landing load.

2.7.2 Experimental Landing Gear Validation

A landing gear drop test was done to evaluate the as-built design of the landing gear to see whether or not it can withstand the required loads upon landing. Utilizing FAR 23 section 725 requirements, a drop height of the landing gear was calculated such that the gear would be at the

required descent rate at the point of impact with the ground for the minimum test point weight indicated in section 2.1, Table 1.

To complete the test, the landing gear was mounted to a solid plywood board in the exact geometric configuration required for the GSRPV and, subsequently, the ATRPV. Weights were added to the board and distributed such that the CG of the system corresponded to the CG of the GSRPV. The loaded rig was raised above the ground and was released utilizing a custom constructed single point release mechanism to assure the proper orientation of the rig at impact. The rig and single point release are shown in Fig. 22.

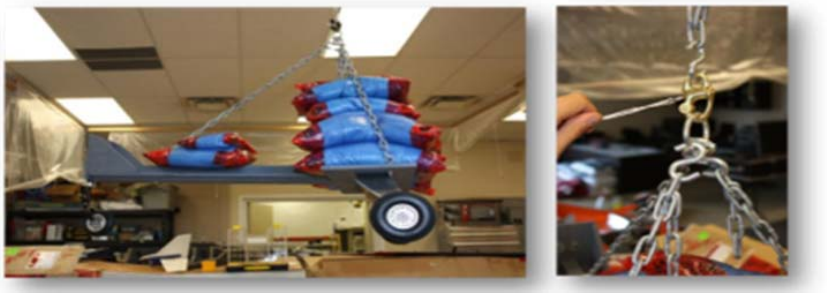

Figure 22- Landing Gear Drop Test Rig[12]

For the test, a worst case condition of level landing (all landing gear touch simultaneously) at a 3g load was done. Fig. 23 shows the landing gear at impact (left) and the landing gear after the test was completed (right).

Figure 23-Landing Gear at Impact (Left); Landing Gear after Test (Right)[12]

The landing gear did not show damage and held well. For a quantitative measurement, the distance between the rear wheel struts before the drop was measured to be 790 mm. After the drop, the distance was again measured and found to be 796 mm showing very little plastic deformation. The front wheel appeared to have hit the bottom of the rig shortly after impact as shown in Fig. 23 but was deemed not to be an issue as the fuselage is quite strong at the location that the front wheel would

have made contact. As per FAR requirements, this test was deemed successful validating the overall design of the tricycle landing gear configuration.

2.8 Control

Control of the ATRPV is accomplished via the onboard Cloud Cap Technology Piccolo II Autopilot coupled with an Acroname Robotics RxMux receiver multiplexer. The Piccolo II is used primarily as a data acquisition system and as a means of establishing reliable control of the RPV. The Acroname Robotics RxMux provides the ability to incorporate a backup, redundant receiver for use in the event that primary control is lost. A schematic of the control system used for the ATRPV is shown in **Error! Reference source not found.**.

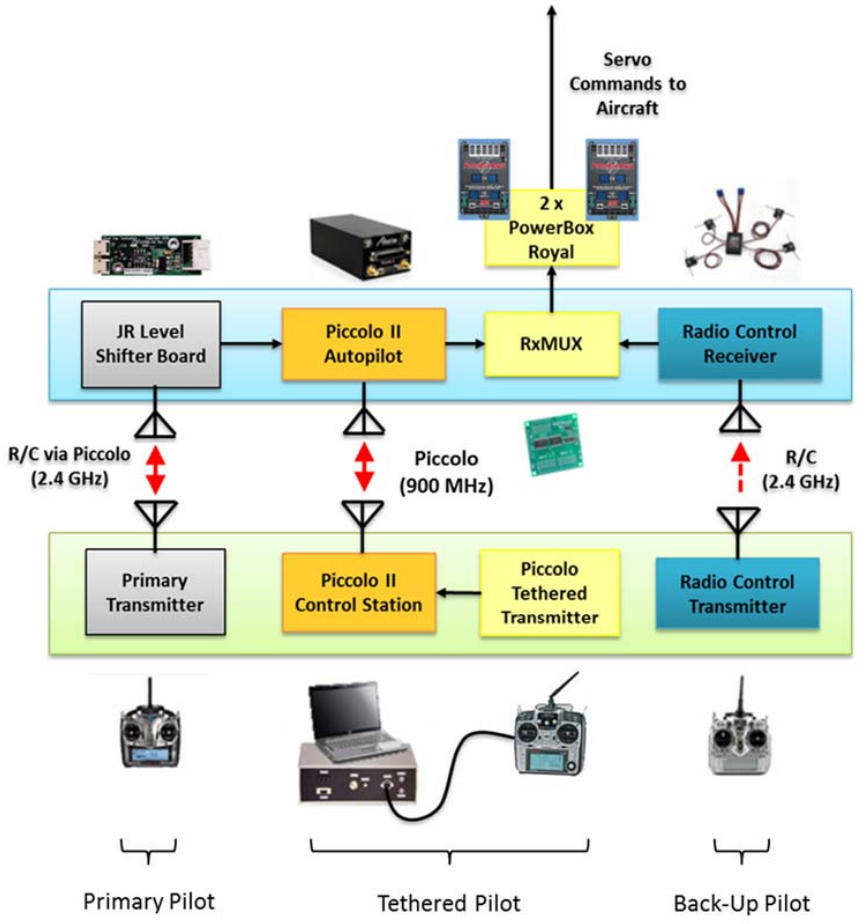

Figure 24– Piccolo II/ RxMUX system architecture

Primary control of the RPV is provided through a JR 12X 2.4 GHz transmitter labeled above as the Primary Transmitter. Control signals are then sent to the RPV via a 2.4 GHz RF link, received using the JR Level Shifter Board, and processed by the onboard Piccolo II autopilot. The use of the JR Level shifter board allows the incorporation of multiple satellite receivers, improving RF communication to the

aircraft. The primary control is allocated to the primary pilot whose role is to takeoff, place the ATRPV on station for test maneuvers, and land the ATRPV. A backup transmitter, a JR 11X (labeled above as the Radio Control Transmitter), provides an entirely independent 2.4 GHz backup RF system in the event of total link loss with the primary transmitter. This backup link can be activated at any time during the flight by simply flipping a switch on the backup transmitter. Flipping this switch changes the active channel on the RxMUX, changing the source of the servo commands to the aircraft. The RxMUX functions by having two inputs and a single output, with the output controlled by a switch on the backup transmitter. The system is designed such that the backup controller can take control of the aircraft at any time, especially in the event of signal loss with the primary controller. Due to the control switch provided by the RxMUX, the Piccolo II Autopilot is taken out of the loop. The radio control transmitter is utilized by the backup pilot whose primary role is to take control of the ATRPV in flight if indicated to by the primary pilot or a loss in signal with the primary controller. The final transmitter, labeled Piccolo Tethered Transmitter, will be used for 2 purposes. Its primary function is to allow the tethered pilot to take flight control of the ATRPV in the event that the aircraft travels out of visual range and neither the primary nor the backup pilot can see the aircraft well enough to fly it. A possible secondary function is to provide control to the tethered pilot to act as the test pilot who will perform all flight maneuvers in a controlled and meticulous manner from a first person point of view camera on the vehicle itself. This role will be investigated in the Mini SensorCraft Flight Test Plan. The use of several 2.4 GHz RF links will not cause interference because of the "binding" process between the transmitter and the receiver. Each transmitter has a unique identifying code, and when the receiver is bound to the transmitter, it will only receive signal from that transmitter. For more information about the backup control hierarchy, see Section **Error! Reference source not found.**. For a Frequency Usage Chart see Section 4.2.2.1.

Stability augmentation provided by the autopilot will be used to enhance yaw stability. The JWSC exhibits strong roll-yaw coupling, and previous flight tests with reduced complexity models and the GSRPV have shown that a "fly by wire" system, such as that provided by the Piccolo II, can greatly assist in removing pilot workload during the flight by improving undesired coupling and reducing pilot workload. Stability augmentation does not take any control authority away from the pilot, it simply uses the built in instrumentation in the autopilot to correct undesired coupling. The stability augmentation provided by the autopilot can be switched off via a switch on the transmitter at any point during the flight, and the pilot can regain full, unassisted control. In order to create a completely independent backup system, the JR 11X system used by the backup pilot does not use the Piccolo II autopilot at all, and therefore does not have stability augmentation.

There are 2 proposed means of control when implementing a test maneuver with the ATRPV during in-flight operations. The first, already mentioned, is to utilize the tethered controller and the emergency navigation camera in FPV mode. This leaves the vehicle in manual control at all times and provides a more advantageous view point to perform a test maneuver. A second option that improves the precision of any performed test maneuver of the ATRPV is to utilize the full autopilot mode of the Piccolo II autopilot. This switch in modes (from FBW to autopilot) is achieved by a switch in the ground station by the primary ground station operator. For each test maneuver, a related mission profile will be loaded into both the GCS and autopilot. Mission profiles are created through the use of way points

within a closed loop configuration. The way points are the defined points for which the RPV will follow under autopilot mode. Any deviation in flight course can be monitored and corrected by the primary GSO. Control can be taken by the primary pilot and back up pilot at all times. Both of these two options will be explored in the prior Mini SensorCraft FTP.

2.9 Instrumentation

2.9.1 Piccolo II

The Piccolo II serves as the primary data logging and data acquisition system on board of the aircraft. Aircraft altitude, attitude, airspeed, groundspeed and servo commands (which can be correlated, for a given mixing scheme, to control surface deflections) are all recorded and transmitted to the ground station in real time during the flight, along with GPS position. The Piccolo II also has built in gyros/accelerometers which allow for the incorporation of stability augmentation.

2.9.2 JetCat P200-SX

The JetCat P200-SX turbines contain built in sensors for engine RPM, exhaust gas temperature and fuel pump voltage. This data is continuously monitored by the JetCat Engine Control Unit (ECU), and this data can be viewed in real time by using the Ground Support Unit (GSU) while the aircraft is on the ground. Current work is aimed at incorporating real-time transmission of these parameters to the ground station during flight operations by reading them using the ECU's RS232 serial connection. JetCat has provided the team with an internal white paper explaining how to transmit this data to the ground station during flight. The goal of the transmission system is to ensure that the data that is recorded with the custom RS232 connection will match the data recorded with the GCU during ground testing of the system.

2.9.3 Geometric Nonlinearity Measurements

Capturing the geometric nonlinearity introduced by the addition of flexibility along the length of the aft wing of the JWSC configuration is the overall technical objective of the Aeroelastic Response Program. In order to fulfill the overall technical objective, two measuring techniques have been identified and will be implemented. A traditional strain gage instrumentation of the internal structure of the aft wing will be implemented to not only measure strains in flight but also in ground based testing like the static structural loading test (Section 3.3.1.1). A photogrammetric measuring technique will also be utilized for ground based testing to obtain deflection measurements directly from multiple images. This technique will also be explored for inflight measurements. These techniques will have been explored in the Mini SensorCraft Flight Test Plan prior to the ATRPV efforts..

2.9.3.1 Strain Gages

For the Aeroelastic Response Program (Mini SensorCraft FTP and ATRPV FTP), a digital strain gage measuring technique will be utilized. This technique is known as the picostrain concept [13]. The picostrain technology provides resistance-to-digital converters based on ratio-metric time-interval measurements. Conventional strain gage measurement includes constant excitation of a Wheatstone bridge circuit where the differential voltage output is amplified and converted by an A/D converter. The change in voltage, and thus strain, is captured by the mechanical deformation of the strain gages

causing a change in resistance in the circuit thus varying the voltage output. However, these subsequent voltage outputs can be in the millivolt range and is consequently susceptible to random noise, which if present to an extent can render the measurement useless. The picostrain concept uses a simple RC circuit that excites the bridge only when the capacitor is discharged. The voltage is discharged through each strain gage in the bridge setup (ours will utilize a half bridge for each location) and the time it takes to discharge is measured using a time to digital converter which converts the measurement directly to digital thereby avoiding conventional noise in the measurement. The High Resolution module with which the picostrain microchip is attached supports up to 4 half bridges and is capable of bridge trimming and temperature/gain drift compensation internally. Keeping all compensation internal and automatic on the stand alone board offers the advantage of less flight line operational time expenditure on trimming each bridge. The board is shown below in Fig. 25, and will be used as the intermediate step between the half bridges in the aft wing and the onboard data logger/ strain gage telemetry downlink unit.

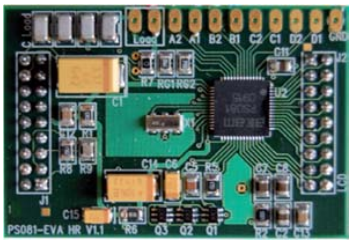

Figure 25- High resolution quattro bridge digital front end module13

The picostrain technique will utilize traditional strain gages placed in a half bridge configuration. The strain gages used are Micro-Measurements EA-13-125BZ-350 Option W. These linear pattern strain gages were selected based on form factor (width less than 4 mm) and availability. The high resolution module, which will be located within the fuselage, will be directly connected to the strain gages and output results in digital SPI format. The output from the high resolution module will be streamed into a PIC24HJ64-Mini Bully to be converted to TTL format. The distance for the digital signal to travel from the wings to the fuselage where the remaining instrumentation components are is over 3 ft. SPI will degrade over this distance, therefore the converstion to a longer distance TTL digital format is required. The data will be streamed to the piccolo II autopilot through a digital I/O and to an onboard datalogger. The data will be telemetered via the piccolo 900 MHz downlink to the ground control station. This data will be monitored live in the sprinter van ground control station. Furthermore, the piccolo command center will save the data automatically along with all other sensor data within the piccolo II autopilot. Onboard logging and telemetry of the data provides redundancy. The strain gage system setup is shown below in Fig. 26. It is important to note, that to obtain 32 separate gage measurements the components for the measuring system must be 8 times what is shown.

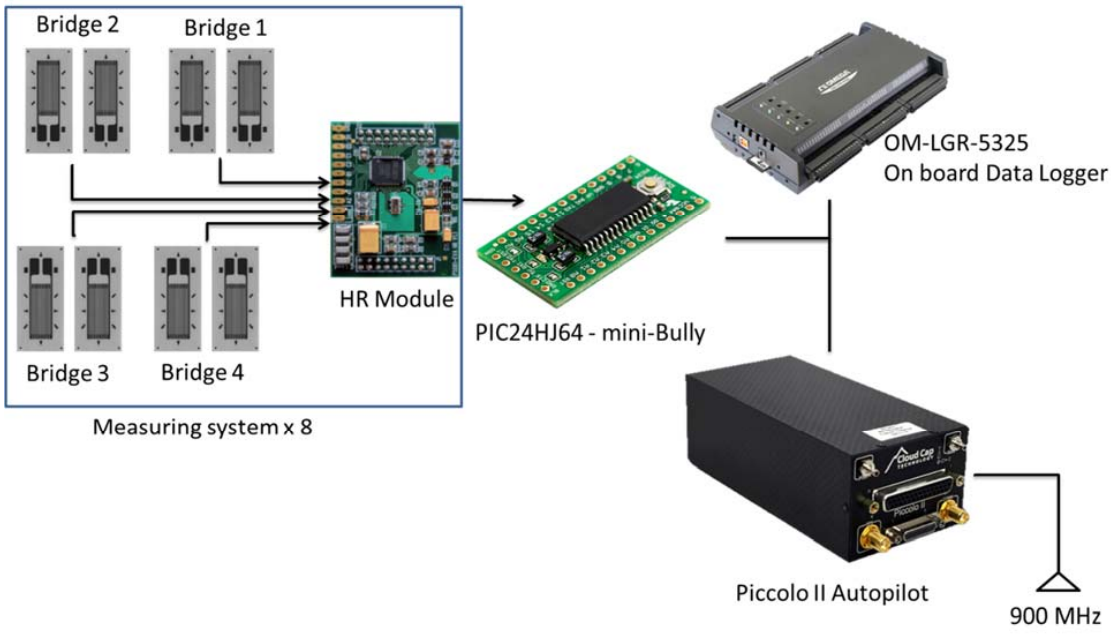

Figure 26- Strain gage system concept

2.9.3.2 Photogrammetry Imaging

Photogrammetry is a measuring technique that can determine the geometric properties of objects from photographic images. Using multiple images of the object at various angles and distances provides the ability to triangulate 2D points into a 3D space through simple coordinate transformations to create a 3D model of the object. Tracking these points through multiple image sets for various deflection states provides the ability to obtain the 3D displacement of these points when referenced from an un-deflected set of images. This ability to obtain direct deflection measurements will be utilized specifically in the static loading test (Section 3.3.1.1). A common DSLR camera will be used along with post processing software known as PhotoModeler[14]. The process to obtain images for measurement is shown below in Fig. 27.

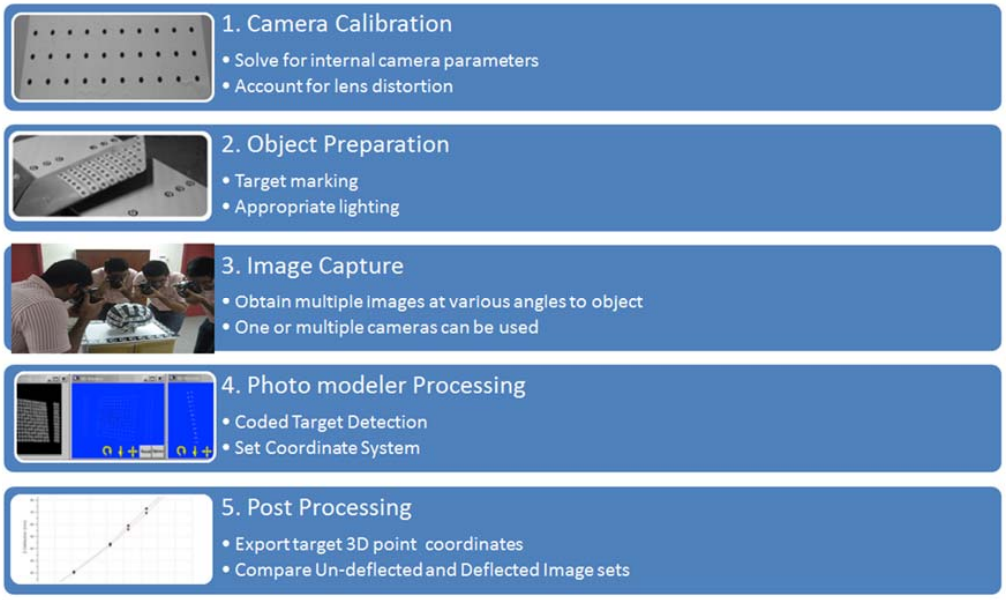

Figure 27- Photogrammetry process using PhotoModeler[14]

The first step within this process is to perform camera calibration. Images may be post processed without calibrating the camera, but this would result in less accurate measurements. The camera calibration stage will require the camera of interest obtain 12 photos of a calibration sheet (Fig. 28) on each axis of the camera. Importing these images into PhotoModeler will result in solved internal camera parameters including lens distortion. These factors are then used in PhotoModelers solving process to triangulate target markers from 2D to 3D space for a set of images. The calculated max residual dictates the quality of the calibration. The max residual is the pixel difference between the marked target points in the images and the 3D position solved by PhotoModeler. For a high quality calibration, the max residual should be less than 1 pixel.

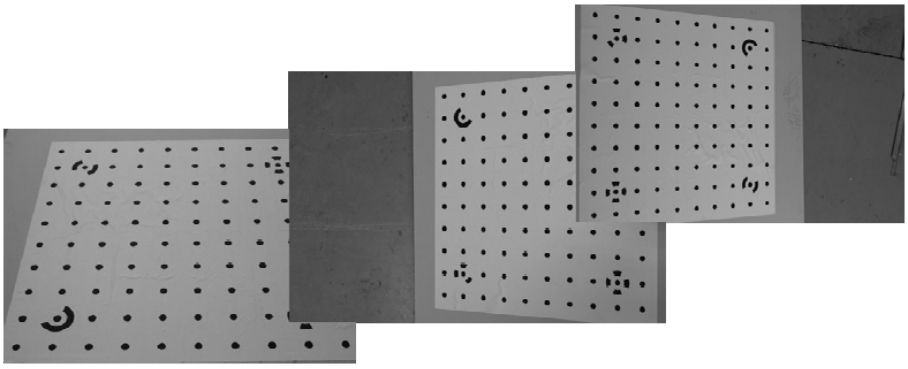

Figure 28 – Calibration images with calibration sheet used in PhotomModeler.

Preparing the object of interest is the next step in this photogrammetry procedure. PhotoModeler is capable of creating up to 99 individual coded targets to be placed onto the target for accurate referencing when post processing. However, due to glare and inappropriate light, these targets can be washed out and hinders the solving process which results in inaccurate measurements. A chemical spray to reduce glare must be utilized. After placing the targets onto the object, one camera can be used to obtain images at various angles and positions. These images are post processed through PhotoModeler which automatically marks the targets, and triangulates the points to create a 3D model of the object. The user must define a coordinate system manually to create a set of 3D points for the target markers that are reference to a similar origin for various load step image sets. (Fig. 29). PhotoModeler then provides the ability to export the solved 3D coordinates for targets. This data is referenced to the un-deflected data to obtain the 3D deflection results for the test (Fig. 30).

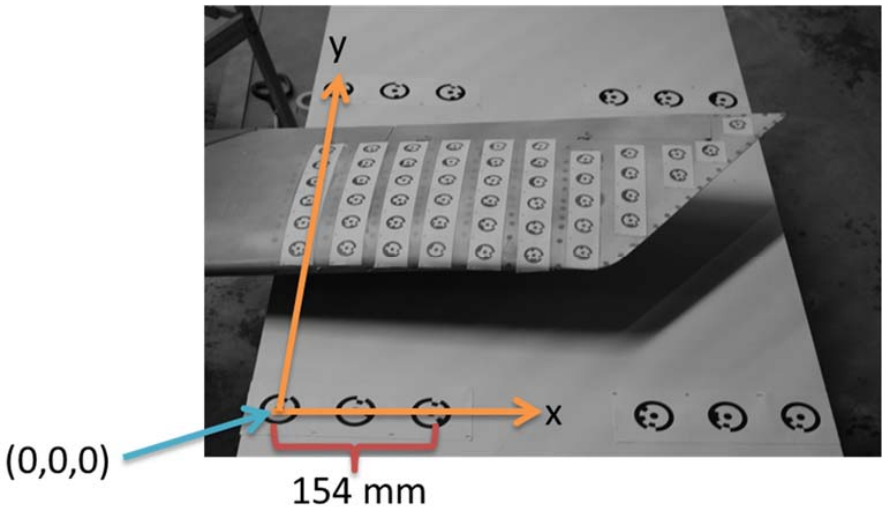

Figure 29- Defined reference plane to be common between separate loading image sets.

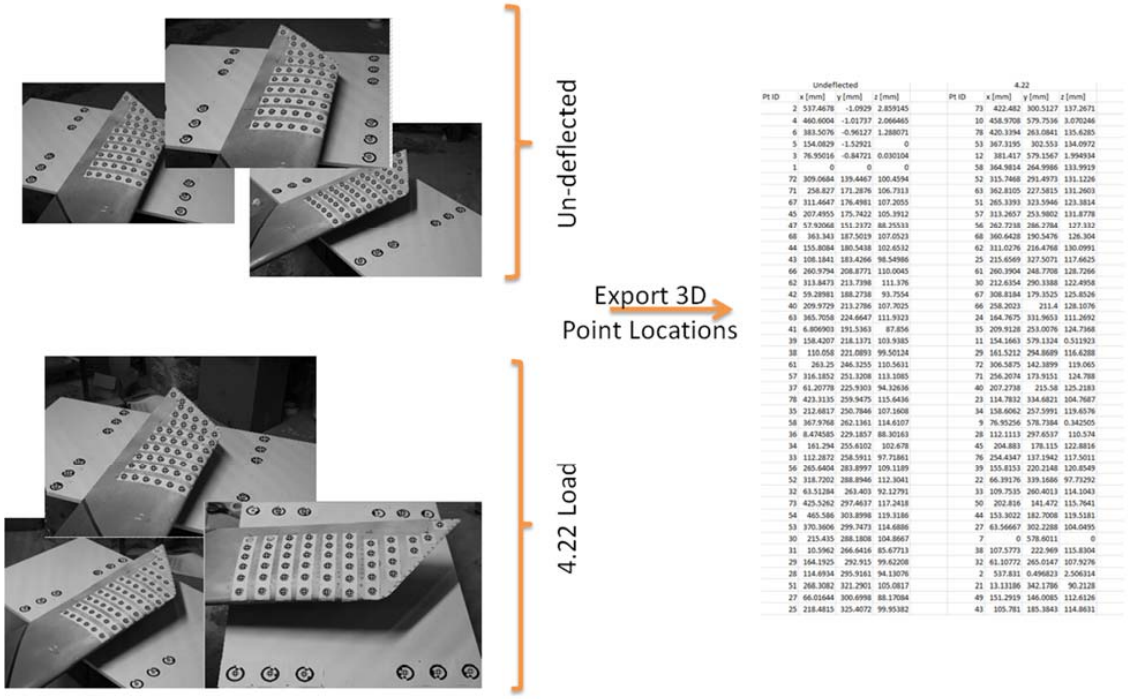

Undeflected				4.22			
Pt ID	x [mm]	y [mm]	z [mm]	Pt ID	x [mm]	y [mm]	z [mm]
2	537.4678	-1.0929	2.859145	73	422.482	300.5127	137.2671
4	460.6004	-1.01737	2.066465	10	458.9708	579.7536	3.070246
6	383.5076	-0.96127	1.288071	78	420.3194	263.0841	135.6285
5	154.0829	-1.52921	0	53	367.3195	302.553	134.0972
3	76.95016	-0.84721	0.030104	12	381.417	579.1567	1.994934
1	0	0	0	58	364.9814	264.9986	133.9919
72	309.0684	139.4467	100.4594	52	315.7468	291.4973	131.1226
71	258.827	171.2876	106.7313	63	362.8105	227.5815	131.2603
67	311.4647	176.4981	107.2055	51	265.3393	323.5946	123.3814
45	207.4955	175.7422	105.3912	57	313.2657	253.9802	131.8778
47	57.92068	151.2372	88.25533	56	262.7238	286.2784	127.332
68	363.343	187.5019	107.0523	68	360.6428	190.5476	126.304
44	155.8084	180.5438	102.6532	62	311.0276	216.4768	130.0991
43	108.1841	183.4266	98.54986	25	215.6569	327.5071	117.6625
66	260.9794	208.8771	110.0045	61	260.3904	248.7708	128.7266
62	313.8473	213.7398	111.376	30	212.6354	290.3388	122.4958
42	59.28981	188.2738	93.7554	67	308.8184	179.3525	125.8526
40	209.9729	213.2786	107.7025	66	258.2023	211.4	128.1076
63	365.7058	224.6647	111.9323	24	164.7675	331.9653	111.2692
41	6.806903	191.5363	87.856	35	209.9128	253.0076	124.7368
39	158.4207	218.1371	103.9385	11	154.1663	579.1324	0.511923
38	110.058	221.0893	99.50124	29	161.5212	294.8689	116.6288
61	263.25	246.3255	110.5631	72	306.5875	142.3899	119.065
57	316.1852	251.3208	113.1085	71	256.2074	173.9151	124.788
37	61.20778	225.9303	94.32636	40	207.2738	215.58	125.2183
78	423.3135	259.9475	115.6436	23	114.7832	334.6821	104.7687
35	212.6817	250.7846	107.1808	34	158.6062	257.5991	119.4576
58	367.9768	262.1361	114.6107	9	76.95256	578.7384	0.342505
36	8.474585	229.1857	88.30163	28	112.1113	297.6537	110.574
34	161.294	255.6102	102.678	45	204.883	178.115	122.8816
33	112.2872	258.5911	97.71861	76	254.4347	137.1942	117.5011
56	265.6404	283.8997	109.1189	39	155.8153	220.2148	120.8549
52	318.7202	288.8946	112.3041	22	66.39176	339.1686	97.73292
32	63.51284	263.403	92.12791	33	109.7535	260.4013	114.1043
73	425.5262	297.4637	117.2418	50	202.816	141.472	115.7641
54	465.586	303.8998	119.3186	44	153.3022	182.7008	119.5181
53	370.3606	299.7471	114.6886	27	63.56667	302.2288	104.0495
30	215.435	288.1808	104.8667	7	0	578.6011	0
31	10.5962	266.6416	85.67713	38	107.5773	222.969	115.8304
29	164.1925	292.915	99.62208	32	61.10772	265.0147	107.9276
28	114.6934	295.9161	94.13076	2	537.831	0.496823	2.506314
51	268.3082	321.2901	105.0817	21	13.13186	342.1786	90.2128
27	66.01644	300.6998	88.17084	49	151.2919	146.0085	112.6126
25	218.4815	325.4072	99.95382	43	105.781	185.3843	114.8631

Figure 30- Post processing of PhotoModeler results

GoPro HD Hero 3 cameras, black edition, such as the one shown in Fig. 31, will be used for the photogrammetry imaging system on the vehicle. The GoPro HD Hero 3 provides a self-contained (battery and memory are internal) camera solution in a ruggedized shock and weatherproof housing.

Figure 31-GoPro HD Hero 3, Black Edition Cameras[15]

The Hero 3 is powered by an internal, rechargeable 1050 mAh rechargeable lithium-ion battery and is capable of records up to 2.5 hours on one charge and up to 9 hours total on a 64GB SD memory

card. It is compact, with dimensions of 1.12" x 1.68" x .84" (H x W x D) and lightweight at 2.6 ounces (only the camera itself). It is capable of taking up to 8 MP video at 12 fps or 12 MP photos at a burst of 30 photos per second. The Hero 3 has built in Wi-Fi, controllable with an included GoPro Wi-Fi remote. The Wi-Fi remote is capable of controlling up to 50 Wi-Fi enabled GoPro's at once providing the ability to synchronize all cameras utilized within the photogrammetry imaging system on the RPV. This is advantageous in post processing efforts following flight operations when correlating images of the deflected aft wing.

2.9.4 Emergency Navigation Camera and FPV

The ATRPV will be equipped with a camera pointing out from the boom to provide first person view (FPV) navigation in the event that the RPV inadvertently travels out of visual range or to assist the tethered pilot in the role of test pilot for performing test maneuvers. This camera will transmit real-time video feed to the ground station at all times during the flight. The forward facing camera is a GoPro HD Hero digital camera. The camera offers a 127^{o} field of view and will record to flash memory (1080p at 30fps). This camera will also output a standard definition video stream to an onboard video transmitter. The emergency navigation camera feed will be telemetered down using a video transmission link which employs a 1 watt, FM analog unit broadcasting at a user selectable frequency (CH1: 5.745GHz or CH4: 5.765GHz) with an omni directional cloverleaf antenna. The receiver unit uses a 24dbi high gain directional dish antenna and the combination has a specified operating range of 25 miles. The emergency navigation camera FPV is shown below in Fig. 32.

Figure 32- Emergency Navigation Camera FPV on Geometrically Scaled RPV [12]

3 Test and Evaluation

This section opens with a discussion of the hierarchy of program objectives and success criteria that will be used to assess the success of the flight test. This is followed by a detailed description of all three phases of tests proposed for the Aeroelastically Tuned RPV FTP, including descriptions of all of the tests that make up each phase. This section closes with a table summarizing all proposed tests, their respective location and objective level.

3.1 Needs, Goals and Objectives

The aeroelastic responses, specifically aft wing buckling and gust load response, associated with the JWSC have been demonstrated and investigated in numerous computational and wind tunnel studies[1-3,5]; however, these phenomena have never been successfully tested in a flight test program. **The Air Force has determined that a 1/9th scaled Remotely Piloted Vehicle (RPV) is needed to serve as a low cost and effective way to experimentally investigate these nonlinear aeroelastic responses.** By demonstrating, investigating and measuring these responses, future joined-wing demonstrator flight test programs will be able to test active aeroelastic control and gust load alleviation systems to reduce the structural and aerodynamic effects of the nonlinear responses.

3.1.1 Overall Program Goal

The overall program goals of the Aeroelastic Response FTP are to validate the target static aeroelastic response of the vehicle, and safely demonstrate and accurately capture the geometric nonlinearities of the JWSC in flight.

3.1.2 Program Objectives

Using the aforementioned goals as a driver, a series of primary, and secondary objectives were developed. These objectives are listed below. There are three planned phases (Validation Tests, Flight Readiness System Tests and Flight Tests) aimed at meeting at least one of the objectives listed below. The test (or series of tests) that corresponds to each objective listed below is shown after that objective in parentheses. For more information about these tests, see Section 3.3.

3.1.3 Primary Objectives

1. Validate appropriate nonlinear static deflection of target aeroelastic response of the ATRPV ***(Static Loading Test)***.
2. Safely demonstrate and accurately capture geometric nonlinearities of the JWSC in flight utilizing the ATRPV ***(Flight Test)***.

3.1.4 Secondary Objectives

1. Demonstrate accurate and successful data acquisition/ logging of Instrumentation system ***(Ground Tests)***.
2. Determine achievable flight maneuvers and loading of RPV ***(Simulation).***
3. Determine key endurance parameters ***(Simulation, Usable Fuel Tests).***
4. Validate rigid body mass moments of inertia for each test point ***(Bifilar Pendulum Test).***

5. Determine flight mass and CG location for each test point ***(Mass and CG Verification).***
6. Verify turbine performance ***(Installed Static Thrust Testing).***
7. Validate control surface deflections and mixing ***(Control Surface Phase Margin Test, Control Surface Scheduling Test).***
8. Validate appropriate flight critical system communications ***(EMI/RF Test, Safety Tests).***

3.2 Success Criteria

In order to be considered a success, all primary objectives must be met, along with a majority of the secondary objectives. Below is a list explaining the relative importance of the secondary objectives. The tests are listed from most to least important, and this hierarchy will be used when evaluating the completion of "a majority" of the secondary objectives.

1.) The Static Structural Loading Test is the most important ground test in the FTP. The success of this test will validate the static structural target response of the ATRPV. To accurately perform the static structural loading test, an investigation into achievable loading conditions on the vehicle to produce the target geometric nonlinear response in flight must be done (Reduced Complexity Flight Tests and Simulation). Verifying the appropriate maneuver and being able to measure the resulting deflection accurately (Ground Tests) is directly related to ensuring the success of the final goal of the Aeroelastic Response Program and thus are considered the most important Tests.
2.) Turbine tests, EMI/RF tests, and the control surface scheduling test are all critical to ensure the success of follow on flights of the ATRPV in Phase 3. These tests are responsible for preparing all internal avionics of ATRPV. These tests have been performed successfully for the previous flight vehicle (GSRPV) but must be performed again prior to flight of the ATRPV.
3.) The Servo Response Test, which includes testing for dynamic actuator properties as well as mapping the control surface deflection angles using the autopilot commands, is the third most important. The real-time knowledge of control surface deflection angles is important, but not flight critical. Additionally, the knowledge of dynamic actuator properties is important to reduce the risk of Pilot Induced Oscillations, but again, this is not flight critical if the pilot is satisfied with the control surface response prior to flight.

Each test presented in Section 3.3 is labeled with a (P) or (S) corresponding to a primary or secondary objective, respectively. The successful completion of these tests will be used to quantify meeting the objectives.

3.3 Test Breakdown (3 Phases)

The Aeroelastic Response FTP is divided into three phases, meant to facilitate a prudent progression of testing to meet the overall objectives. Phase 1, Validation Tests, includes ground testing of the ATRPV which includes a static loading test and a bifilar pendulum test. Phase 2, Flight Readiness System Tests, includes the integration and testing of all onboard systems. The tests involved in this phase include instrumentation testing, Turbine Testing, verifying control surface deflections and mixing, mass and center of gravity verification, and EMI/RF testing. Phase 3, Flight Tests, includes all flight test operations of the ATRPV. This includes taxi tests, a check out flight, and finally the maneuver flight tests of the ATRPV to measure the target aeroelastic response.

3.3.1 Phase 1 –Validation Tests

The following tests will be performed prior to phase 2 and phase 3 tests. The successful completion of these tests will ensure that the designed target static aeroelastic response of the ATRPV has been manufactured correctly. Furthermore, a successful completion to phase 1 will ensure an appropriately tuned instrumentation system.

3.3.1.1 Static Structural Loading Test (P)

The static structural loading test has 4 goals. The first is to validate the manufacturing of the ATRPV to produce the designed target static nonlinear aeroelastic response. Secondly, this test will validate the structural integrity of the RPV and ensure that all wing loadings experienced during flight can be safely sustained. Another goal is to verify there is no binding of the control surfaces when the ATRPV is under a loaded condition. Lastly, this test provides a controlled method to tune the strain gage and photogrammetry imaging instrumentation systems (see section 2.9.3).

The test will utilize a 3 component test rig composed of outer rib casings, a restraining fuselage cage, and a turnbuckle system to provide the loading. The outer rib casings are composed of two, ¼ '' thick extruded aluminum pieces. These pieces are clamped over the skin of the wings along the length of every other internal rib. This allows the load to be transferred evenly chord wise across the internal rib. Each external rib for both the aft wing and forward wing has control surface slots which allows for various trim condition states. Each rib is capable of supporting 220 lb point load. Each forward wing will have 5 external rib casings applied while each aft wing will have 4 external ribs applied. There are holes on each piece of the rib casings to provide various point load locations along the chord length of each wing. The forward wing external rib casings have holes spaced from 0-70% of the chord spaced every 5% of the chord. The aft wing external rib casing have holes spaced from 0-50% along the chord spaced every 10% of the chord. All external rib casings have a top and bottom hole located at 100% of the chord for moment load corrections if needed. A CAD model representation of this design is presented in Fig. 33.

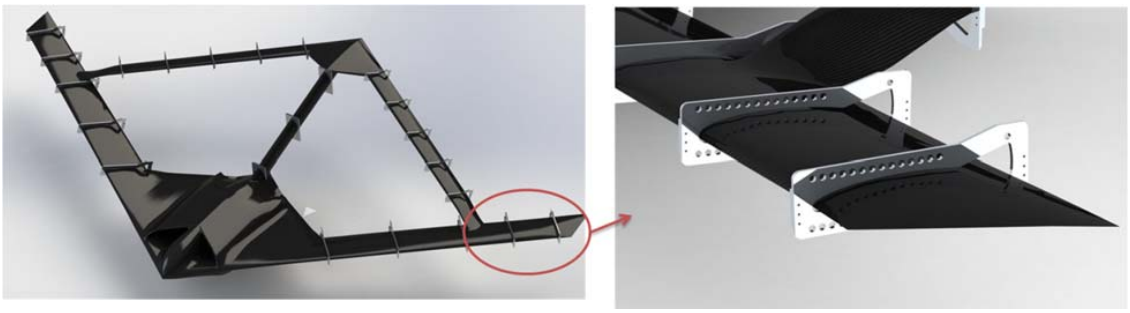

Figure 33- Outer rib casings distributed across platform (left); Zoomed in view at wing tip (right)

The second component to the test rig is the fuselage cage. The fuselage cage is composed of 2 ½" thick extruded aluminum plates sandwiched together with threaded rods. The cage is then bolted to

the ground using angled steel brackets to prevent rotation of the fuselage during load applications. The fuselage cage is shown conceptually in Fig. 34.

Figure 34- Fuselage concept (top); Steel angled bracket for ground restraint (bottom)

The final component of the static loading rig is the turnbuckle system used to transfer loads to the external rib casings and thus the vehicle. The turnbuckle is attached to an overhanging structure and is placed directly in line with the point load location desired along the length of the outer rib casings. A force gage is placed in line between the turnbuckle and the outer rib casings to verify the loading at that point. This set up is shown below in Fig. 35. The full lay out of the static loading rig is shown in Fig. 36.

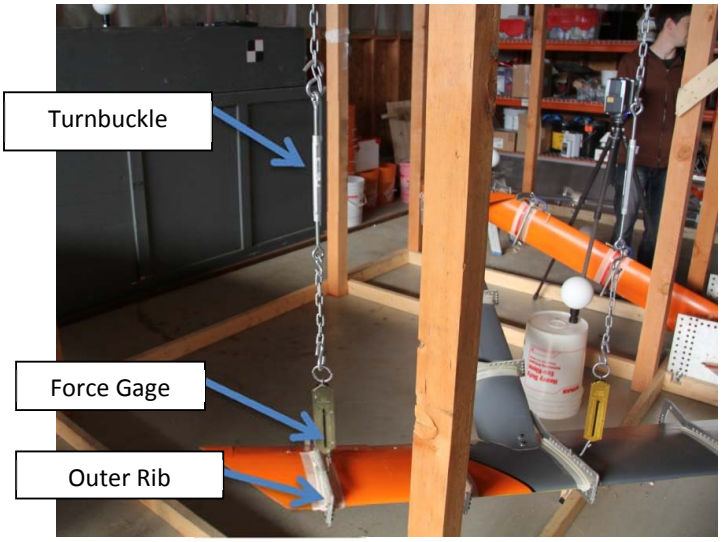

Figure 35- Turnbuckle system used for static loading tests

Figure 36 –Full static loading set up (top); Zoomed in view of load application

Fig. 37 below indicates the loading positions along the ATRPV. The Forward wing and aft wing loading point allocations are carried symmetrically to the left half of the ATRPV.

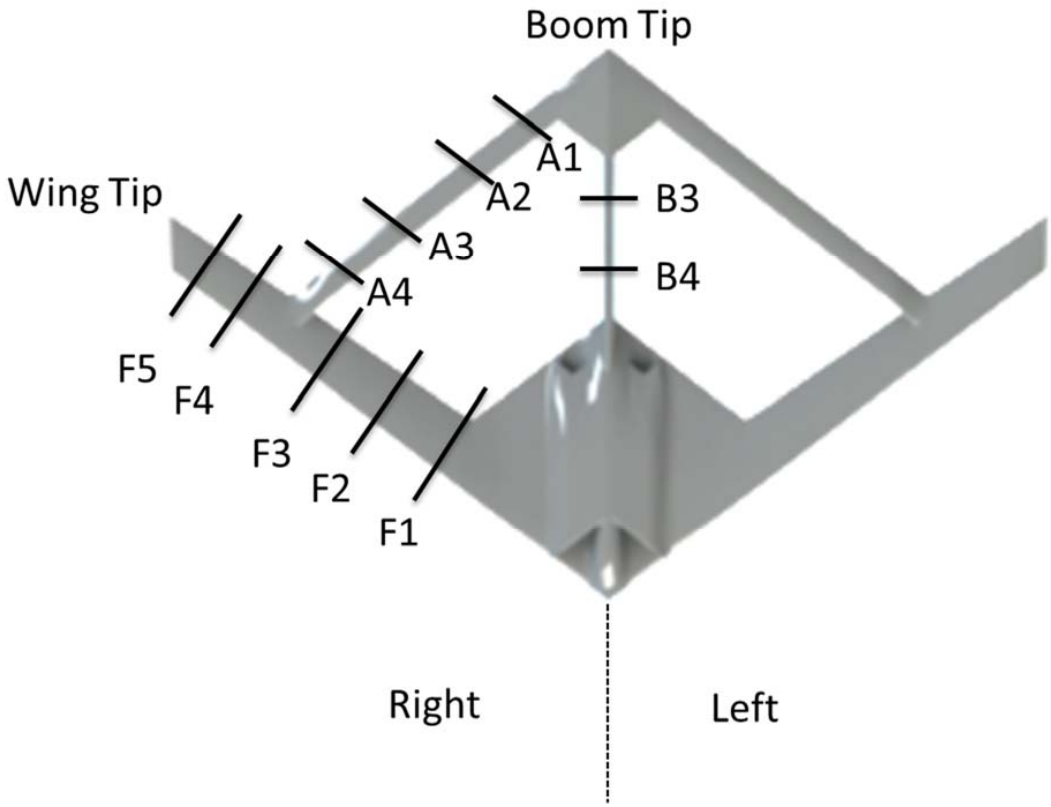

Figure 37- Measurement and load application sites and identification of each. Symmetric on left side

3.3.1.2 Bifilar Pendulum Test (S)

A bifilar pendulum test will be used to experimentally determine the moments of inertia about each axis of the RPV. The bifilar pendulum test configuration for each axis is shown below in Fig.38. The fuselage cage utilized for the static loading rig, will be used as the suspension cage for the RPV in the bifilar pendulum test.

Figure 38- Bifilar pendulum test configuration (GSRPV) for yaw (left), roll (middle), and pitch (right)[10,12]

Tests will include the measurement of the moments of inertia for each configuration in which the RPV will fly. This will include the un-ballasted weight and the test point weight, with varying amounts of fuel. Trimming weights will be used to match the required scaled moments of inertia. A primary goal of this test is the investigation of the use of ballast to reach the maximum test point weight at the correct scaled moments of inertia for the ATRPV.

3.3.2 Phase 2 –Flight Readiness System Tests

These tests serve to validate the functionality of all internal avionics and flight critical systems of the complete, flight worthy RPV.

3.3.2.1 Simulation(S)

Simulation will involve both software in the loop (SIL) and hardware in the loop (HIL) simulation of the ATRPV. These simulation systems are a product of Piccolo's development environment. SIL simulation provides the ability to simulate operations and flight maneuvers in an environment where the avionics is virtualized and utilized within a simulator. HIL provides the ability to simulate operations and flight maneuvers in an environment where the avionics is directly connected to the simulator. This means that all ATRPV systems and control surfaces are in the loop. The ultimate goal of HIL simulation efforts is to develop a better understanding of the power system endurance for the vehicle (since all systems are operational) and the fuel system endurance (when the engines are also operational). If the engines are operational during the HIL simulation, the ATRPV will be restrained from any possible movement. Furthermore, the ATRPV will place in an openly vented area with any possibility of FOD ingestion. The common goal between the SIL and HIL simulation efforts is to provide further operational training for flight critical personnel.

3.3.2.2 Usable Fuel Tests(S)

This test is designed to validate the amount of usable fuel in the as built fuel tank and build a better understanding of fuel system endurance. In other words, this test serves to experimentally determine the clunk effectiveness and assess the amount of fuel in the tank that cannot be attained in adverse attitudes. The clunk was assessed to be effective in lateral travel, so this test will focus on the longitudinal effectiveness. This test will consist of placing the tank at 4 attitudes, siphoning off the fuel in

the tank and assessing the amount of unusable fuel remaining in the tank. The 4 attitudes will be determined based on planned flight maneuvers coupled with limiter values in the autopilot.

3.3.2.3 Installed Static Thrust(S)

This test will be used to ensure that the JetCat P200-SX turbines are running properly. Installed thrust testing will verify that the turbines are able to produce the required static thrust for safe operability at all scheduled test points.

Notes:

1. The JetCat P200-SX turbines used in the Aeroelastically Tuned RPV are mechanically complex and require an understanding of turbine engines as well as a disciplined approach to their operation. All tests will be conducted in accordance with JetCat safety and operational protocol. JetCats manufacturer specified safety protocol is located in Appendix A.
2. The JetCat P200-SX is equipped with onboard sensors (RPM, exhaust gas temperature, fuel pump voltage) and the data is continuously monitored through the ECU. This capability will be extended to transmission while in the air directly through the Piccolo II autopilot.
3. The JetCat P200-SX has a manufacturer's specified 25 hour maintenance interval. Analysis has shown that all planned testing can be completed within the manufacturer's specified maintenance interval. This analysis assumes 3 hours for assembly of the engines and troubleshooting of all associated systems. Planned ground tests then take an additional 12 hours, leaving 10 hours for planned flight maneuvers. Predicted fuel consumption gives a maximum endurance of 40 minutes and a total mission time of 66 minutes. This means that 10 hours of testing would allow for 9 full missions with 6 minutes of run time to spare. This is more than satisfactory, given the planned flight tests.

Installed static thrust will commence with a simple startup, variable throttle run and cool down to ensure that all turbine mounts, ducting and installed JetCat hardware is functioning properly. This will include ensuring that the twin engine setup is functioning properly (i.e. both engines are running at the same RPM throughout the throttle band). Once this initial testing is complete, throttle sweeps will be completed. Throttle percentage, throttle command (pulse width), EGT, fuel flow rate, and RPM will be recorded for each engine during each test run. Additionally, the thrust reading from a load cell attached to a custom apparatus will be recorded. The custom apparatus was built to reduce the magnitude of the measured thrust by 50% to compensate for the theoretical maximum of both engines (100 lbs) to the maximum of the load cell (50 lbs). To accomplish this aim, a hinged test apparatus was constructed. (Fig. 39). Results will be compared to previous data obtained from the Flight Demonstration Program to validate functionality of the turbine engines.

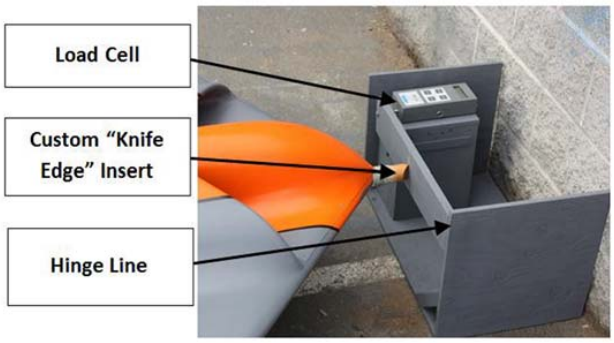

Figure 39- Static thrust test rig[10,12]

3.3.2.4 Landing Gear Drop Test(S)

The landing gear drop test will evaluate the as-built design of the landing gear to see whether or not it can withstand the required loads upon landing. Utilizing FAR 23 section 725 requirements, a drop height of the landing gear will be calculated such that the gear would be at the required descent rate at the point of impact with the ground. The worst case configuration to be tested will be level landing (all landing gear touch simultaneously) at a 3g load for the maximum weight test point configuration of the ATRPV.

3.3.2.5 Instrumentation Tests(S)

The strain gage and photogrammetric image instrumentation will be tuned via the static loading test (section 3.3.1.1). The purpose of the instrumentation tests in phase 2 is to verify full functionality following integration of each instrumentation system and supporting components into the ATRPV. This test will also ensure data transmission of the strain gage system to the ground station to verify a means to monitor the KPP's of the flight test.

3.3.2.6 Control Surface Phase Margin Test(S)

A full range of control input will be provided for each servo and the resulting deflections will be recorded using a standard control surface deflection meter, such as the one shown in Figure 40. A servo tester, which allows for the accurate generation of servo pulse width commands, will be used to establish a correlation between servo pulse width and control surface deflection for each control surface. The Piccolo II, which records commanded servo pulse, will be used as a low fidelity in-flight measurement of control surface deflection through the experimental correlation developed in this test.

http://www.greatplanes.com/accys/gpmr2405.html

Figure 40 - Control surface deflection meter

This test will also serve to identify dynamic actuator parameters including the lag time between command and response and the variation in these parameters with control mode (primary control vs. backup control). In order to be successful, there should be no "pilot perceivable" difference between pure 2.4 GHz control using the backup transmitter (the best possible link, avoids autopilot entirely) and control using the two redundant (900MHz and 2.4GHz) RF links through the Piccolo II. The measurement of the exact delay is not required; however, the pilot should not be able to notice a difference in control response between the primary and backup controls.

3.3.2.7 Control Surface Scheduling Test(S)

A full range of control input will be provided for each receiver channel to verify that the desired control surface scheduling is achieved. The unique and complex control surface layout of the JWSC has been investigated computationally, as well as in flight tests of reduced complexity models and the previously flown GSRPV, and these tests have resulted in a desired control surface scheduling (i.e. which surfaces are used to command roll, pitch and yaw). Additionally, this test will ensure that all control surfaces sharing receiver channels (i.e. those surfaces being controlled via a Y-splitter) experience equal deflections for a given commanded deflection. Finally, the two servos actuating each surface will be checked to ensure that they are not fighting each other and causing binding throughout the entire deflection range of the surface. Care will be taken to test for servo heating (potential servo motor burnout) and servo binding during these ground tests.

3.3.2.8 Mass and CG Verification (S)

These tests serve to develop an understanding of weight distribution and CG location for the configuration the ATRPV will fly. These tests will first take place in Victoria, BC and will result in the development of a look up table of mass distribution and CG location for each test point. The tests will be performed again at Foremost to verify aircraft configurations.

3.3.2.8.1 Dry Mass Test (S)

This test will establish the dry (without fuel) mass of the airframe and all required onboard systems.

3.3.2.8.2 Test Point Mass Test (S)

Once the dry mass is established, fuel and trim weights will be used to ballast the aircraft to the test point weight. This will verify the ability of the RPV structure to safely reach the test point mass. Additionally, this will serve to verify that the ballast chambers can hold the appropriate amount of ballast weight to reach the test point. The result of this test is a look up diagram of weight distribution of each aircraft configuration to fly.

3.3.2.8.3 Center Of Gravity Tests (S)

A dual balance setup will be used to test for the CG. Two vertical supports will be used to support the RPV, and an electronic balance will be used to measure the mass on each support. Using the mass on each support and the distance between the supports, the longitudinal CG location can be calculated. Once the longitudinal center of gravity has been calculated, the aircraft will be put at an angle of attack. The vertical center of gravity can then be calculated by using the known longitudinal CG location, the angle of attack and the measured mass on each support. This test will be used to test the CG shift as ballast weight is added and as fuel is burned for each aircraft configuration.

3.3.2.9 EMI /RF Test (S)

The EMI/RF test is meant to validate sufficient communication between the piccolo command center (PCC) integrated into the ground station and the onboard Piccolo II Autopilot. This will be done through an inline hardwire test in which the signal to the piccolo will be attenuated (to simulate range). This will be repeated as a free space test in which the direct hardline will be removed between the ground station and vehicle. During both tests the Ack Ratio (Telemetry Downlink strength), RSSI (Receive Signal Strength Indicator), and Pilot Uplink will be monitored to verify sufficient gain margin for communications (Gain Margin of 10 dB at least). The Ack Ratio is a ratio measure of the number of good telemetry packets to the total number of telemetry packets sent from the Piccolo II Autopilot to the ground station. This is an indication of downlink telemetry strength and must be kept within 90-100% strength through attenuation to stay within the flight test plan limits. RSSI indicates the radio frequency signal strength and must be greater than -108 dB through all attenuations. The most important measure is the pilot uplink. This is a measure of the rate at which the autopilot reads the pilot input and is a direct indication of pilot controllability. For all attenuations, the Pilot Uplink must stay at 40-50 Hz.

The final portion of the EMI/RF test is to validate antenna tracking from the ground station to the aircraft location as it is in motion. This will be done without the use of an aircraft at first then will be tested with a Mini-SensorCraft

3.3.2.10 Safety Tests(S)

These tests involve the verification of all safety measures implemented within the ATRPV. This includes a camera transmission test to verify the emergency navigation camera and gimbal camera connectivity, a controller hierarchy test to validate all control switch permutations, and finally all fail safe conditions pre-programmed within the Piccolo II autopilot.

3.3.2.10.1 Camera Transmission (S)

The ground station operator will begin transmission of both the gimbal camera and emergency navigation camera on the ATRPV. The video streams as viewed on the ground station will be checked for signal loss or gaps in the transmission. For more information about camera placement and purpose, see Section **Error! Reference source not found.**.

3.3.2.10.2 Control Hierarchy Tests (S)

The RPV will be prepared for flight, including the propulsion system. With the aircraft firmly secured to the ground via padded posts in front of the wings and straps overtop of the fuselage staked into the ground, all onboard systems will be running (including instrumentation and propulsion) and control will be passed between the primary controller, the tethered controller and the backup controller via the RxMUX. A flow chart of the control hierarchy between all three controllers is presented in Section 6.4.2.1.

3.3.2.10.3 Fail Safe Test (S)

Loss of link will be simulated for both the primary and backup controllers to ensure that the "failsafe" condition is operational and that the loss of link hierarchy is operating as planned. This includes the pre-programmed autonomous flight path in the event of primary link loss. The failsafe condition is executed during full loss of link, and corresponds to a controlled crash: full up elevator, full right rudder, full right aileron, turbines at idle or shutdown if possible. The failsafe condition is designed to minimize residual damage in the event of total loss of link. For more information about the failsafe procedure, see Section 6.4.3.1.2.

3.3.2.11 Full System Tests (S)

A full systems test will be completed prior to leaving for the flying site. This test will be performed at the Victoria Airport and will consist of a Low Speed Handling Test and a High Speed Taxi Test.

3.3.2.11.1 Low Speed Handling Test (S)

The pilot will taxi the aircraft with low throttle setting to verify that the Aeroelastically Tuned RPV is stable while taxiing and ground handling characteristics are acceptable. Ground effect calculations have shown that the aircraft has a stall speed of 48.2 knots (at the maximum takeoff weight of 204.5 lbs) and a stall speed of 38.65 knots (at the un-ballasted takeoff weight of 131.8 lbs). Accordingly, all low speed handling testing will restrict the airspeed of the aircraft to 10 knots or less.

3.3.2.11.2 High Speed Taxi Test (S)

During High Speed Taxi testing, the pilot will accelerate the aircraft down the runway to the speeds listed below and then reduce throttle to idle. The pilot will demonstrate the ability to control the Aeroelastically Tuned RPV throughout the takeoff roll. This test will consist of 3 straight line runs down the runway, with the aircraft at the test point configuration weight. The pilot will NOT give the aircraft any pitch input during these runs to eliminate the possibility of unexpected takeoff.

3.3.3 Phase 3 –Flight Tests

Phase 3 Flight Tests represent the final stage of testing for the Aeroelastically Tuned RPV. These are the tests that will take place on site in Foremost. These tests have been designed to use a gradual increase in complexity to minimize risk. All instrumentation will be active and taking data for every test, including taxi tests and ground tests. Additionally, *all* tests will be filmed.

3.3.3.1 EMI/RF Test (S)

This test will be completed as per section 3.3.2.9 at the flying site in Foremost. This test involves the verification of essential communication links between the autopilot onboard the ATRPV and the ground station.

3.3.3.2 Safety Tests (S)

These tests will be completed as per section 3.3.2.10 at the flying site in Foremost. These tests involve the verification of all safety measures implemented within the ATRPV. This includes a camera transmission test to verify the emergency navigation camera and gimbal camera connectivity, a controller hierarchy test to validate all control switch permutations, and finally all fail safe conditions pre-programmed within the Piccolo II autopilot.

3.3.3.3 Full System Test (S)

A full system test will be performed with the ATRPV at the Foremost flying site prior to the first flights. The tests involved in the full system test are outlined in section 3.3.2.11.

3.3.3.4 Phasing Check-Out Flight (S)

This test is the first flight of the ATRPV. It is designed to verify the correlation between pilot command, aircraft response, and instrumentation measurement. The flight is decomposed into 7 segments to illustrate the flow of this test as well as special considerations during each phase. During each phase of this test, aircraft attitude and control surface deflection data will be compared to pilot input to ensure that the aircraft is responding as expected to pilot input and the resulting control surface deflection. Note that this test is considered a success if the aircraft achieves successful takeoff, climb, trim, descent and landing. The in-flight maneuvering tests of the ATRPV will be attempted only after the phasing check-out flight of the ATRPV aircraft is successful at the un-ballast weight of 131.8 lbs.

3.3.3.4.1 Takeoff

The pilot will accelerate the aircraft down the runway. The ground station operator will communicate current airspeed measurements to the pilot, and once takeoff speed is reached, the pilot will provide pitch up input and the ATRPV will become airborne.

3.3.3.4.2 Climb

The pilot will climb the aircraft as quickly as possible to the test altitude. The nominal test altitude is 550 ft to allow ample time for recovery in the event of unanticipated control response, but stay within comfortable visual range for the pilot. Assuming an airspeed of 93 knots during climb and a climb gradient of 0.088 (climb angle of 5°), it will take approximately 39.8 seconds to reach an altitude of

550 ft; however, the actual climb to 550 ft will most likely take much less time as the pilot will be at full throttle during the early stages of climb and will most likely climb at an angle greater than 5°. The pilot will be free to climb at a comfortable rate of his choosing. The final test altitude will be selected by the pilot during this test as a "comfortable" altitude where visibility and aircraft referencing (assessing aircraft attitude) is acceptable. During the first flight of any radio controlled aircraft, the time immediately after the first takeoff is the riskiest portion of the flight because the aircraft is not trimmed and the pilot is not familiar with the handling qualities. Accordingly, the pilot will gain altitude as quickly as possible to the test altitude to avoid problems caused by unexpected aircraft response at low altitude.

3.3.3.4.3 Trim

The pilot will trim the aircraft at the test altitude in a racetrack pattern. Only after the aircraft is fully trimmed will the pilot attempt a figure 8 pattern.

The racetrack pattern will consist of the following 4 legs:

1. 1,500 ft straight line
2. 180°, 750 ft constant radius turn
3. 1,500 ft straight line
4. 180°, 750 ft constant radius turn

Note that this pattern will be completed in each direction, requiring both right and left turns. The Figure 8 will consist of a 750 ft constant radius turn to the left immediately followed by a 750 ft constant radius turn to the right.

3.3.3.4.4 Landing

The pilot will fly the aircraft on a "mock" approach to test the handling characteristics. This will require the pilot to line up the Aeroelastically Tuned RPV for landing while reducing power. Approximately 50% of the way through the approach, the pilot will apply power, and climb back to the test altitude. At no time during this test will the aircraft come lower than 250 ft above the ground, and earlier tests will take place at higher altitudes. Following the "mock" attempts, the pilot will safely land the aircraft on the runway. Care will be taken to keep the airspeed well above the stall speed throughout the entire approach and landing to avoid poor handling at low flight speeds. The aircraft is designed with tricycle landing gear with a steerable nose gear which is controlled via the yaw control channel while on the ground. The aircraft does not have brakes and it is not able to be taxied after landing, so after the aircraft lands and rolls to a stop the ground crew will roll the aircraft back to the ground station.

3.3.3.5 In-Flight Maneuver Tests (P)

The flight test of the ATRPV will commence once all previous tests in Phase 3 have verified appropriate functionality of onboard avionics and all ground operations are functional. The ATRPV flight test will be comprised of multiple flights each following the exact phasing procedure of the previous phasing flight test. Each flight, however will utilize a specifically tested and controlled maneuver while the ATRPV is on station to produce the appropriate loading to force the target geometric nonlinearity

within the structure in a controlled manner. The tested maneuvers include a push-over pull-up maneuver and a windup turn. The two maneuvers (approved in the previous GSRPV flight test plan and investigated in the Mini SensorCraft Flight Test Plan) that will be performed are a push-over pull-up and a windup turn. These maneuvers each present a unique method of reaching the required wing loading to eventually demonstrate geometric nonlinearity of the aft wing. The push-over pull-up requires the pilot to put the aircraft into a controlled dive and then pull-up, causing the aircraft to encounter positive loading at the bottom of the maneuver and negative loading at the top of the maneuver. The windup turn is performed when the pilot maintains constant speed and flies the aircraft through a spiral pattern. As the radius of the turn decreases, the wing loading increases. This approach allows for a gradual increase in wing loading, but it can only accomplish positive asymmetric loading.

3.3.4 Overall Test Summary

The following table summarizes all planned tests, the phase of testing that each test fall into, and the classification (primary objective, secondary objective or tertiary objective) which corresponds to the success criteria mentioned in section 3.2.

Table 6- Overall test summary

Phase 1-Validation Tests	**Objective Level**
Static Structural Loading Test	P
Bifilar Pendulum Test	S
Reduced Complexity Flight Tests	S
Phase 2- Flight Readiness System Tests	
Simulation	S
Usable Fuel Tests	S
Installed Static Thrust Test	S
Instrumentation Test	S
Control Surface Phase Margin Test	S
Control Surface Scheduling Test	S
Autopilot Vibration Test	T
Mass and CG Verification	S
Dry Mass	S
Test Point Mass	S
Center of Gravity	S
Landing Gear Test	S
Landing Gear Dropt Test	S
Wheel/Brakes	S
EMI/RF Test	S
Piccolo Data Transmission Test	S
Antenna Motion Test	S
Safety Tests	S
Camera Transmission Test	S
Control Hierarchy Test	S

Fail Safe Tests	S
Full System Tests	S
Low Speed Handling Test	S
High Speed Taxi Test	S
Phase 3- Flight Tests	
EMI/RF Test	S
Piccolo Data Transmission Test	S
Antenna Motion Test	S
Safety Tests	S
Camera Transmission Test	S
Control Hierarchy Test	S
Fail Safe Tests	S
Full System Tests	S
Low Speed Handling Test	S
High Speed Taxi Test	S
Phasing Check-Out Flight	P
In-Flight Maneuver Tests	P

4 Test Logistics

This section outlines the infrastructure in place to ensure that the ATRPV flight test has the highest chance of success. The section begins discussing the two primary test locations for the FTP efforts. Test resources, including the ground station and all Mini SensorCraft control systems will then be presented, along with a frequency usage chart. Safety requirements will follow and a description of all flight test personnel, including each participant's qualifications will close this section.

4.1 Test Location

This section presents details about the test locations that will be used during the Aeroelastic Response Program. These locations are Quaternion Engineering in Victoria, BC and the Foremost Airstrip in Foremost, AB.

4.1.1 Quaternion Engineering, Victoria, BC

Phase 1 and phase 2 tests will take place in Victoria, BC at Quaternion Engineering, where the Geometrically Scaled RPV and the Aeroelastically Tuned RPV have been fabricated. Quaternion Engineering has a full fabrication shop, and is an ideal location to bench test components, assemble the RPV, and do ground testing on the airframe and instrumentation systems.

4.1.2 Foremost Airstrip, Foremost, AB

The Canadian Centre for Unmanned Vehicle Services (CCUVS) is a non-profit corporation whose purpose is to "facilitate sustained, profitable growth of the Canadian unmanned systems sector."

CCUVS operates small UAV programs at the Foremost airstrip, and provides the required safety support. Foremost, AB is a small town with a population of 524. The Foremost, AB airstrip is a low traffic civilian airstrip off which CCUVS operates small UAV programs. Fig. 41 below presents an aerial view of the Foremost, AB airstrip. According to weatherspark.com, at the time of the planned flights (April), Foremost has an average temperature of 42.75°F (High Mean 54.25°F, Low Mean 31.25°F). Typical wind speeds vary from 2.6 knots to 16.5 knots. The average daily wind speed is 9.6 knots typically from the South or West directions.

Figure 41- Foremost, AB Airstrip Aerial View

Table 7– Foremost, AB Location and Elevation

Coordinates	49°29'N 111°29'W
Elevation	2902 ft

The airspace available at this airfield is sufficient for all planned flight tests and proved to be so during the Flight Demonstration Program. Fig. 42 presents the allotted airspace for flight operations.

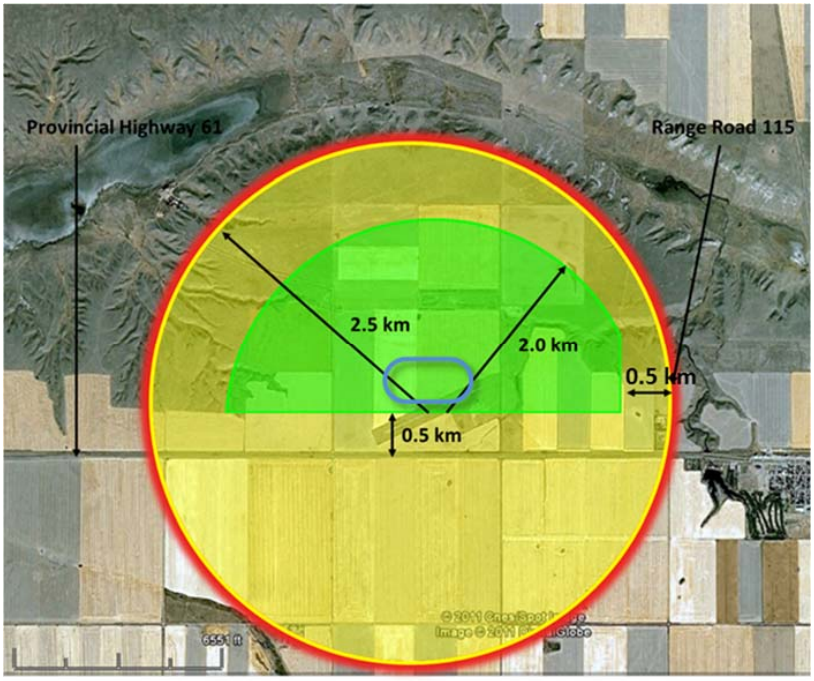

Figure 42- Airspace Requirements (FORMOST AB).

The total approved airspace, shown in Fig. 42, is defined as a 2.5km radius circle centered at the Foremost runway. This is the airspace in which Transport Canada had approved for previous flight operations and will be approached with for the Aeroelastic Response Program. The "Safety Template," or the airspace in which all flight operations are allowed to continue uninterrupted, is shown above in green and is a 2.0 km radius circle centered at the runway truncated 0.5 km west of the approved airspace boundary and 0.5 km north of Provincial Highway 61. All planned flight tests will remain well within the Safety Template (as shown by the racetrack flight path presented above); however, should unanticipated flight conditions and/or problems cause the aircraft to leave the safe zone, appropriate measures will be taken. Immediately outside of this safe zone, the rest of the approved airspace, shown in yellow, is known as the Caution Zone. Normal Operations would avoid flight in this region due to its inclusion of Provincial Highway 61 (with very infrequent traffic). The Mayor of Foremost told the flight test crew that no data exists for the frequency of traffic on this road; however, a reasonable estimate is that traffic varies from 0-20 cars per day. To avoid a potentially hazardous situation with traffic on the road, spotters will be placed at either end of the airspace on the road to inform cars of flight operations in the area. Additionally, takeoff and landing will take place to and from the northeast whenever possible (except in emergency landing situations) to de-conflict with traffic on Provincial Highway 61.

Immediately outside of the Caution Zone is the Kill Zone, shown in red. As a requirement of the previous Special Flight Operations Certificate (see Section 4.1.3), if the RPV exits the approved airspace (which includes the Safety Template and the Caution Zone), failsafe via aerodynamic termination will automatically be executed. In other words, should the aircraft enter the kill zone, the failsafe will be

automatically executed terminating the flight. Note that the Safety Envelope, Caution and Kill zones will be programmed into the ground station computer and overlaid over the real-time vehicle position information (see section 6.5.2.2 for more information).

The maximum permitted flight altitude is 700 ft AGL. Within the airspace is level farmland with no significant terrain elevation change. Immediately outside of the northern boundary of the airspace is a valley containing a small river. This is an elevation drop, and does not pose a threat to flight operations.

The previous flight test operation of the GSRPV has shown that all operations can stay well within the "Safety Template". The GSRPV flight path is tracked in red and overlaid on the airspace template below in Fig. 43.

Figure 43- Flight path (red) of previous GSRPV flight.

4.1.3 Special Flight Operations Certificate

A Special Flight Operations Certificate (SFOC) will be attained following the TRB/SRB procedures from Transport Canada for the operation of the ATRPV at the Foremost test site. All flight operations will abide by the guidelines set forth in this document, including airspace, operational and safety requirements.

4.2 Test Resources

4.2.1 Aeroelastically Tuned RPV

The Aeroelastically Tuned RPV (ATRPV) is the main component to the JWSC Flight Test. A full description of the ATRPV and supporting systems is presented in Section 2 of the FTP.

4.2.2 Ground Station

The ground station used for all test operations will be the UVic Sprinter Van-UAV Command Station: Figure 4444. The ground station, which is used for real time data monitoring as well as post-flight data download and reduction, has the following features:

1. Two computer workstation each with a 30” monitor and two 17” monitors
2. Additional 40” Plasma/LCD screen
3. 120 VAC and 12 VDC power throughout vehicle
4. Custom wall plates with power outlets, HDMI, USB, RS232, etc.
5. Internet router with Wi-Fi network and access to 3/4G
6. External Connection including several 120 VAC outlets, shore power hookup, and payload pass through connectors for miscellaneous hookups.
7. Video switch/matrix (8-12 inputs by 8 outputs)
8. Pneumatic antenna mast and compressor
9. Easy Integration of the Piccolo Command Center into ground station
10. Two portable Honda EU2000KC2 generators (2000 watts, 120VAC power)
11. Stabilizing Jacks to prevent excessive rocking and movement of Van

Figure 44 – Mobile Ground Station (Left), Internal (Right)

4.2.2.1 *Frequency Usage Chart*

Radio frequencies are shown in Table 8, and all frequency usage will be coordinated with the test range prior to testing.

Table 8- Frequency Usage

Form of Communication	Frequencies Used During the Test
R/C Communications	2.4 GHz Spread Spectrum (JR 12x)/ 900 MHz (Piccolo II)
Data Transmission	900 MHz (Piccolo II)
Emergency Navigation Camera	5.8 GHz
Team Communications	Clark Head Sets 2-Way Radio system (125 Hz)

4.3 Security Requirements

This program is UNCLASSIFIED and NOT restricted by ITAR regulation. The Piccolo II is ITAR equipment, but Quaternion Engineering has received all required approval to operate with the Piccolo II.

4.4 Test Project Management

This section will outline all personnel who will participate in the tests. At a minimum, the following people are required to be present during phase 3 testing: Flight Test Director, Primary Ground Station Operator/ Test Pilot/Vehicle Technician, Secondary Ground Station Operator/Pilot Assistant, Primary Pilot, Backup Pilot, and Range Safety Officer. Efforts will be made to have at least 2 additional people on site during flight testing to serve as observers or ground crew. For phases 1 and 2, only the Flight Test Director and the Primary Ground Station Operator/ Test Pilot/ Vehicle Technician are required to be present.

Table 9- Flight Test Personnel

Name	Title	Responsibilities
Dr. Ned Lindsley	AFRL Program Manager	Oversee the administration of the program, including the TRB and SRB. Point of Contact (POC) at AFRL.
Jeff Garnand-Royo	Flight Test Director	Plan, coordinate and oversee all tests. Awareness of test area, equipment and procedure. Exercise Go/No Go authority as well as direct pilot during testing (including termination of flight if necessary). Communicates all information to pilot.
Jenner Richards	Primary Ground Station Operator/ Test Pilot/Vehicle Technician	Primary Ground Station Operator - Operate the ground station. Monitor and oversee data collection and storage. Provide real-time aircraft state and health information to the test director. Additionally, operate the RPV via the tethered transmitter in the event that the aircraft travels outside of visual range.

		Vehicle Technician – Oversee and direct all on-site test article set-up, maintenance, and tear down.
Kelly Williams	Pilot	Perform flight maneuvers listed on the test cards under direct direction from the test director. The pilot will control the RPV through the primary transmitter.
Jon Harwood	Backup Pilot	The Backup Pilot will be in charge of the backup transmitter. The Backup Pilot will take control of the aircraft if he is directly directed to do so by the primary pilot in the event of a primary link failure or if the pilot becomes incapacitated. The Backup Pilot will also provide assistance to the pilot as required (trim assistance, range assessment, visual orientation, etc.).
Gord Cooney	Range Safety Officer (RSO)	Intimately aware of the flying site as well as all safety requirements imposed by the flying site. Provides safety briefing at the beginning of each Phase 3 testing day. Authority to call an immediate stop to testing (abort flight) in the event that an unsafe situation arises.
Wanjohi Mugo	Secondary GSO/Pilot Assistant	Secondary GSO- Will monitor KPP's and avionics system health/link to ground station. Pilot Assistant- Provide airspeeds and other performance parameters (bank angle, altitude, etc…) to pilot when requested. This role takes precedence.
TBD (Will be provided by VT, Quaternion Engineering or UVic)	Observers/Ground Crew	Observe test operations, help with RPV operations as required and provide assistance as required by other personnel.
Dr. Robert Canfield	Virginia Tech Technical Advisor	Advisor to Jeff Garnand-Royo, provide technical guidance and expertise throughout the program.
Dr. Afsal Suleman	University of Victoria Technical Advisor	Advisor to Jenner Richards, provide technical guidance and expertise throughout the program.
Dr. Craig Woolsey	Virginia Tech Technical Advisor	Advisor to Jeff Garnand-Royo, provide technical guidance and expertise throughout the program.

4.4.1 Qualifications of Pilots

Kelly Williams is a Mechanical Engineer and has been flying R/C aircraft since 1989, including flying turbine powered R/C jets since 1998. He serves at the Committee Chair on the R/C Jet Committee of The Model Aeronautics Association of Canada. Prior to flying the ATRPV, Kelly will have logged several hours flying the Mini-SensorCraft airframe in preparation for his role. Additionally, he will train on the 6DoF simulator. Furthermore, he was the Primary Pilot for the Flight Demonstration Program and was the first to fly the GSRPV.

Jon Harwood has 15 years' experience as a R/C pilot and holds his private pilot's license. He has served as the primary test pilot during the majority of Quaternion Engineering's Mini -SensorCraft flight tests. He holds his CCUVS UAS Operator Certificate. Jon will also continue training on the 6DoF simulator and with the Mini-SensorCraft. Furthermore, Jon served as the backup pilot of the GSRPV for the Flight Demonstration Program

Jenner Richards is a doctoral candidate at the University of Victoria and is tasked with aeroelastic tuning of the next phase JWSC RPV as well as overseeing the design and construction of the test platform itself. Jenner Richards is responsible for the design and fabrication of the previous Geometrically Scaled JWSC RPV including the Mini-SensorCraft. He has served as back up pilot to previous Mini-SensorCraft flights and was the primary ground station operator/ tethered pilot for the Flight Demonstration Program.

A jet aircraft, purchased to serve as a trainer platform for Jon Harwood and to allow for the practicing of flight test maneuvers in Foremost has been purchased by Quaternion. Kelly Williams will use this aircraft to give Jon further experience flying turbine powered aircraft. Additionally, this will give the Flight Test Support Team members the opportunity to further familiarize themselves with the operation and flight characteristics of a turbine powered aircraft.

4.4.2 Other Qualifications

Jeff Garnand-Royo, Jenner Richards, Gord Kooney, Wanjohi Mugo, and Jon Harwood have all taken and passed the Transport Canada Radio Operator Certificate Exam. The Transport Canada Radio Operator Certificate gives each the authority to monitor airfield air traffic. Jenner Richards and Jon Harwood have both taken and pass the CCUVS UAS Operators course. The CCUVS UAS Operator Certificate recognizes each as an official CCUVS UAS Operator.

4.4.3 Operations NOTAM

Prior to flight operations, the JWSC Flight Crew will have been given the authority to post a Transport Canada NOTAM, a notice to all pilots, alerting them to JWSC flight operations in the area of the Foremost Airstrip. Additionally, flight test personnel will monitor NOTAMs in order to identify potential conflicts.

5 Test Procedures

On each test day, the specific testing procedure will consist of the following steps:

Pre-Operations :

1. Test Day Overview Briefing
    a. Full Day Mission Briefing
    b. Safety Briefing
2. AFRL SUAS Test Ops ORM Assessment
3. Pre-Operations Checklist
    a. Full Airframe Checklist
    b. Ground Station Checklist

Flight Operations:

1. **Pre-Flight:**
    a. Pre-Flight Mission Briefing
    b. Pre-Flight Log
    c. Pre-Flight checklists:
        1. Pre-Flight Airframe
        2. JetCat P200-SX turbines
        3. Piccolo II
        4. Ground Station
        5. Instrumentation
    d. Comply with SFOC Requirements
    e. Go/No-go Decision
2. ***In-Flight (Test Execution)***
3. **Post-Flight:**
    a. Post-Flight Log
    b. Post-Flight Checklists
        1. Post Flight-Airframe Checklist
        2. Post flight Data Checklist
    c. Post-Flight Briefing

Post-Operations:

1. Post Operations Airframe Checklist
2. Post Operations Briefing

5.1 Pre-Operations

The pre-operations segment encompasses the overview for the entire test day and is completed once at the beginning of each test day. Pre-Operations include the test day overview briefing which contains a full day mission briefing and a safety briefing specific for the current test day. This is followed by the test director completing the AFRL SUAS Test Ops ORM Assessment; Appendix B. Having

completed administrative duties, a full airframe and ground station inspection are completed. These inspections are meant to be the most stringent of the checklists to verify full operational readiness of both critical flight test articles before flight test operations begin.

5.1.1 Test Briefing

The test briefing will be conducted by the Test Director and will consist of an overview of all tests planned for the current test day. All personnel present for the days testing will be required to attend. The briefing will serve to allow everyone on site to unify their understanding of the goals for that particular day. The test briefing may also consist of:

1. A review of results of the previous days test, if any
2. Proposed test schedule for the given operational day
3. Weather report
4. Complete the AFRL SUAS ORM form and brief participants on ORM level (AFRL SUAS ORM Form shown in Appendix A)
5. Security issues

5.1.2 Safety Briefing

The safety briefing will be conducted by the Range Safety Officer and will include the following:

1. Test boundaries for the day (this may change day to day by sharing airspace on base or other factors)
2. Safety concerns for any of the planned tests
3. Review of THA's

5.1.3 Pre-Operations Checklist

The pre-operations Checklist will be completed once each current test day before the beginning of any flight operations. There are separate pre-operation checklists for:

1. Airframe
2. Ground Station

The pre-operations airframe checklist will investigate all mechanical aspects of the flight vehicle including verifying all internal avionics connections. The pre-operations ground station checklist is meant to verify ground station power and operation before flight operations begin.

Each flight critical personnel will be responsible for portions of the Pre-Flight checklists.

5.2 Flight Operations

The flight operations segment will include pre-flight, in-flight, and post-flight operations and is meant to be repeated for as many tests indicated in the full day mission briefing completed in pre-operations.

5.2.1 Pre-Flight

The pre-flight portion of the flight operations segment is the flight line preparation of a planned individual test point outlined in the full day mission briefing. The pre-flight procedure will be conducted at the onset of any new flight of the ATRPV within a given test day. All items outlined in the subsequent sections must be completed to move on to actual in-flight operations and test point execution.

5.2.1.1 Pre-Flight Mission Briefing

The pre-flight mission briefing will be conducted by the test director prior to each test. The Pre-flight mission briefing will consist of:

1. Brief description of the test item configuration (if any changes have been made since any previous tests)
2. Overview of the test objective(s) and procedure
3. Review of Test Cards (Test Card Template shown in Appendix B)
4. Weather report (visibility, wind direction and strength, precipitation forecast)

5.2.1.2 Pre-Flight Log

The flight log is an operational document meant to be filled out by the test director for an individual flight. The document contains sections for both pre-flight and post-flight. The pre-flight sections include logistics of the current test including a summary of the aircraft configuration for the current test. Most important in the pre-flight section is the inclusion of a checklist completion verification. Outlined in the subsequent section are the pre-flight checklists. Each checklist is the responsibility of one or more flight critical personnel. Once completed and signed by the responsible personnel, the test director must indicate on the flight log the checklist has been performed without complication. This provides the test director with necessary knowledge to perform the Go/No-go decision before in-flight operations begin.

5.2.1.3 Pre-Flight Checklist

Pre-Flight Checklists will be completed prior the start of each test. There are separate pre-flight checklists for:

1. Airframe
2. JetCat P200-SX Turbines
3. Piccolo II
4. Ground Station
5. Instrumentation

Each flight critical personnel will be responsible for portions of the Pre-Flight checklists.

5.2.1.4 Comply with SFOC Requirements

Prior to flight, all SFOC requirements must be met. The following list represents the previous SFOC requirements for the GSRPV:

1. Notify Nac Canada, Edminton FIC at 866-514-4102 prior to each flight.

2. Monitor the Foremost UNICOM VHF frequency on 123.2 commencing 15 minutes prior to and during all flights.
3. Make an Advisory call to "All Traffic in the Foremost Area" prior to all flights warning aircraft of location, altitude and duration of proposed flight.
4. Cell phone or radio contact will be available with the nearest Air Traffic Control Agency (Medicine Hat Municipal Airport - MHMA)
5. Aerodrome operator must be notified of all intended UAS operation and have no objections.

5.2.1.5 Go/No-go Decision

The Go/No-go decision will be made by the Test Director. The Range Safety Officer has the authorization to terminate testing at any time should a safety concern arise. The following are the required conditions:

1. Weather
   a. Daylight VFR conditions
   b. No current precipitation with favorable forecast
   c. No lightning within a 10 mile radius
   d. Visibility: >3 miles
   e. Ceiling: >1700 feet (AGL)
   f. Wind: Calm, gusting to no more than 10 kts
   g. Sustained Maximum Crosswind: 4 kts
2. AFRL SUAS Test Ops ORM Assessment must be complete.
3. All pre-flight checklists must be complete with no concerns

5.2.2 In-Flight (Test Execution)

All flight operations will be conducted based on the provided information within the flight test cards for the particular test. An example of a flight test card is shown in Appendix B. All communications will be ceased except for the communication between the test director, primary pilot, tethered pilot, RSO, and GSO.

5.2.3 Post-Flight

The post-flight procedure is conducted following the completion of each flight. Each post-flight operation is meant to close the loop of the current test and prepare the vehicle for any follow on tests left within an operational day. If another test is to be performed, following the post-flight procedure will be the preflight procedure for the following test. If the current-test was the final test of the day, post-flight procedures would be followed by post-operations

5.2.3.1 Post-Flight Log

The flight log is an operational document meant to be filled out by the test director for an individual flight. The document contains sections for both pre-flight and post-flight. The post-flight section includes a summary of the in-flight test including post-flight comments from the acting pilots and subsequent flight critical personnel.

5.2.3.2 Post-Flight Checklists

Post-Flight checklists will be completed after the completion of the recently completed in flight test execution. There are separate post-flight checklists for:

1. Airframe
2. Piccolo II
3. Instrumentation
4. Data

Each flight critical personnel will be responsible for portions of the Post-Flight checklists.

5.2.3.3 Post-Flight Briefing

The post-flight briefing will be conducted by the flight test director and will consist of (but is not limited to):

1. System Status
2. System Performance
3. Overall Review of the Test
4. Action Items
5. Preliminary Results from completed flight.

5.3 Post-Operations

Post-Operations will be conducted once the operational day has ended. This could be a completion of outlined tests within an operational day, or outside influences preventing further flights within an operational day.

5.3.1.1 Post-Operations Airframe Checklist

This is the final airframe checklist to be performed in an operational day. Once this checklist has been completed, the ATRPV will be stored until the next operational day.

5.3.1.2 Post-Operations Briefing

The Post-Operations briefing will be conducted by the Flight Test Director and will consist of (but is not limited to):

1. System Status
2. System Performance
3. Overall Review of the Test
4. Lessons Learned
5. Action Items
6. Preliminary Results from full test day.
7. Brief Overview of Tests for the Next Day

5.4 Test Procedure Summary

The outlined test procedure is meant to facilitate an efficient and safe flight test operation. The operational day test procedure is summarized in Fig. 45.

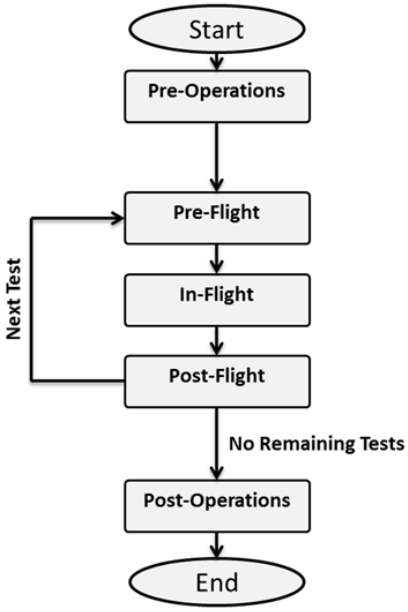

Figure 45- Operational day flowchart

Fig. 46 below presents an organizational structure indicating the documents needed on hand for each subsequent operation within an operational day. It is important to note these only cover the documents outlined in this test procedure section and a few extra operational documents required by personnel throughout an operational day. There are administrative documents that are not covered in Fig. 46 .

Figure 46- Document organizational structure

6 Risk Minimization and Safety Considerations

All testing, both ground testing and flight testing, will be conducted in accordance with this approved test plan. If any changes are necessary, the test team will contact the Safety Review Board for approval prior to completing the test. If, at any point during the test, a conflict between technical and safety issues should arise, safety concerns will always take precedence.

The following sections will outline safety considerations and risk minimizing procedures for several key risks during flight operations.

6.1 Required Test Conditions

All ground tests will be conducted indoors when possible. All outdoor tests, both ground tests and flight tests, during which the Aeroelastically Tuned RPV is in motion, will take place in daylight, with VFR conditions. The following weather conditions must exist at all times for testing to continue:

1. No current precipitation with favorable forecast
2. No lightning within a 10 mile radius
3. Visibility: >3 miles
4. Ceiling: >1700 feet (AGL)
5. Wind: Calm, gusting to no more than 10 kts
6. Sustained Maximum Crosswind: 4 kts

The weather will be evaluated at the beginning of each test to satisfy the Go/No-Go determination, and the test director will monitor the weather throughout the test. The test director will confirm his assessment of the weather with the primary pilot prior to all flights. If at any time the primary pilot, test director or range safety officer raises any concerns about current conditions, testing will be immediately suspended until all 3 parties agree it is safe to continue. If these conditions are exceeded during a flight test, the pilot will be asked to land the RPV as safely and quickly as possible.

6.1.1 Personnel Locations During Testing

During all flight tests, all personnel will be positioned behind the primary pilot (behind a horizontal line parallel to the runway, at the pilot's distance from the runway) to ensure that the primary pilot has an unobstructed view of the runway and all personnel are accounted for. A rope barrier will be used to mark this line during all flight operations. During taxi, takeoff and landing, all personnel will be required to remain around the ground station. Once the RPV has reached a safe altitude, spotters may move to other locations in the field, as required, but they will return to the ground station for landing. The desired location or each person involved in the testing will be communicated prior to beginning testing. The final positions of all personnel will be decided once the test group reaches the flight facility in Foremost.

6.1.1.1 Safe Zone

A pre-defined safe zone will be established at the flying site to serve as a gathering point in the event that the aircraft is in danger of impacting on or near personnel. This safe zone will be placed at

least 50 feet behind the Ground station, and this will serve as a protective barrier. The safe zone will be away from batteries and fuel, and will be kept unobstructed during all flight operations.

6.2 Hazardous Materials

The ATRPV is powered by twin JetCat P200-SX turbines, and as such, the RPV will carry an onboard fuel supply consisting of 1-K Kerosene and turbine oil. In order to minimize the risk, all operation of the JetCat turbines will follow the JetCat Safety Protocol (see Appendix B for more information) and fuel will be stored in approved containers. Additionally, a fire extinguisher will be located at the ground station at all times. Finally, all flight crew members will be given hearing protection for use when operating the JetCat P200SX turbine engines.

The ATRPV will also have electrical power provided by lithium polymer (LiPo) batteries. Only LiPo approved chargers will be used, and all batteries will never be charged at a rate greater than 1C. LiPo batteries will also be stored carefully, away from fuel and other combustibles.

6.3 Risk Minimization to Technical Objectives

The overall technical objective of the Aeroelastic Response Program as defined by the primary goal is to experimentally demonstrate and measure the nonlinear aeroelastic aft wing response of the JWSC configuration utilizing the ATRPV. Achieving the primary goal thus requires robust measurements and data logging of the nonlinear geometric response. Therefore, the primary risks to achieving the overall program goal and technical objectives are failure in these two aspects.

6.3.1 Loss of Downlink Telemetry

The Piccolo II provides the GSO with real time data including GPS position, GPS altitude, barometric altitude, attitude, airspeed information and so on. Additional modifications however will provide real time monitoring of fuel burn, critical point strain (strain gage data), angle of attack and side slip information. The data is sent via telemetry packets at a user specified rate during flight and is automatically saved by the ground station to the computer. A loss of downlink signal from the autopilot to the ground station thus represents a loss of telemetry and will present a loss in data for that period of time. It is important to note this does not represent a loss in communication between the Piccolo II and the pilot, and thus does not present a hazardous situation. To combat this potential loss in data due to loss of downlink telemetry, the strain gage system will have onboard storage capability. However, because of the inability to monitor the KPP, maneuvers will not be performed until downlink telemetry has been restored.

6.3.2 Instrumentation Failure

The ATRPV has been equipped with two methods for measuring the nonlinear aft wing response during flight. This redundancy in instrumentation provides the advantage of obtaining the necessary measurements should one instrumentation system fail during flight.

6.4 Failure Protocol

All testing of the ATRPV performed prior to phase 3 is aimed at not only achieving technical objectives but also minimizing the potential for failures. Should there be a failure during flight operations of the vehicle, the flight test director will guide all flight critical personnel in an appropriate manner to respond to the failure. To respond to a failure, a logical stepwise response decision tree has been implemented to all flight operations. This hierarchal decision process is presented below in Fig. 47.

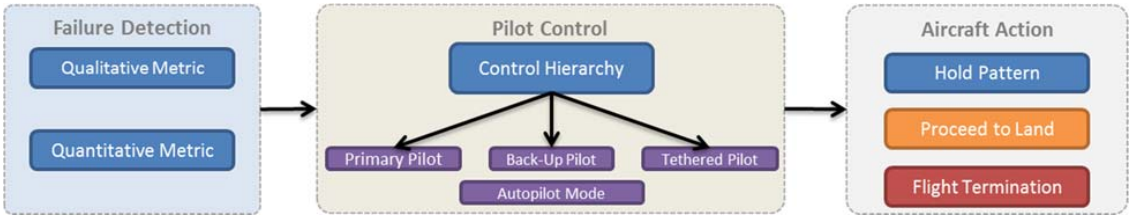

Figure 47- Three step failure protocol

6.4.1 Failure Detection

The first step in the failure protocol is the detection of a failure during flight. A failure can be detected based on a breach of an established qualitative metric, or a breach of an established quantitative metric. The qualitative metrics are based on the pilot input and primary GSO input. The pilot in control will indicate a failure should there be an undesirable change in control characteristics for the vehicle. The primary GSO will utilize the gimbal camera for structural health monitoring and upon video indication of undesirable deflection or a growing oscillation will indicate a failure. The primary and secondary GSO will continually monitor all telemetered aircraft parameters to the ground station. Should the vehicle venture outside an established target or the ground station indicates a failure of a monitored system, the failure will be relayed to the flight test director.

6.4.2 Pilot Control

The first act following the detection of a failure is establishing which pilot will be in control of the ATRPV. This decision will be made based on the control hierarchy and the perceived failure.

6.4.2.1 Control Hierarchy

The control hierarchy is as follows:

Piccolo II Primary Controller→ RC Rx Backup Control → Piccolo II Tethered Controller → Failsafe

To safely hand over control between the three pilots without introducing the potential for additional failures, a protocol has been developed. When the primary pilot hands over control to the back up pilot, the primary pilot must be in manual mode and vice versa. Should the tether pilot take control from the primary pilot, the primary pilot must be in Auto mode. If the Tethered pilot hands control back to the primary it will be in manual mode. All possible permutations of control switch are shown below in the control hierarchy flowchart; Fig. 48.

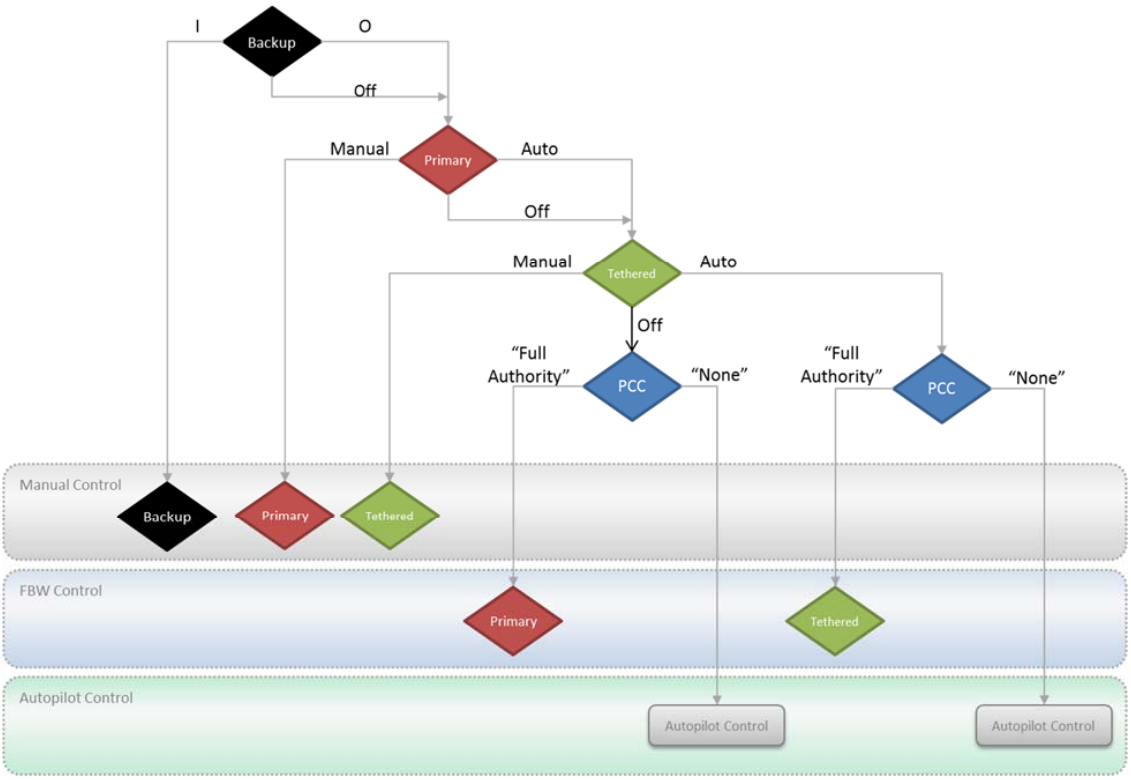

Figure 48-Control hierarchy

The horizontal blocks indicate the three potential modes of control; manual, FBW, or full autopilot. The Piccolo Command Center (PCC) is integrated into the ground station and provides the capability of switching between FBW mode and full autopilot mode for the primary and tethered transmitters.

6.4.2.2 Link Loss

Link loss is a communication failure occurring between a transmitter and the RPV. For a link loss, the Piccolo II will flash a warning on the ground station and the GSO will relay this information to the TD and primary pilot. In the event of primary controller link loss a warning is given on the ground station display. Should this happen during the flight of the ATRPV, the backup pilot will immediately take control. The Piccolo II does not allow for automatic switch of control to the backup transmitter, so the backup pilot will need to manually take control via a toggle switch on the backup transmitter. In the event that that the aircraft is within visual range but neither the primary nor the backup pilot can comfortably fly the aircraft, the primary ground station operator will take control of the RPV using the Piccolo II Tethered Controller. The primary ground station operator will return the aircraft to a location where the primary pilot can assess the attitude of the aircraft and take control. In the event that the RPV leaves visual range, the last effort to control the aircraft will be using the Piccolo II tethered

controller. Using the emergency navigation camera as well as the Piccolo II telemetry (which includes an artificial horizon), the Ground Station Operator will steer the aircraft back into visual range at which point the primary pilot will take control. Flying the aircraft using the emergency navigation camera is the last option, and should this prove unsuccessful, the failsafe protocol will be executed.

In the event of total communication loss with the RPV (primary and RC backup controls all fail), a failsafe procedure will automatically be executed. For more information about the failsafe procedure, see section6.4.3.1.2. This automatic failsafe procedure will be tested *at full range* at the Foremost Airfield prior to commencing flight operations.

6.4.3 RPV Action

There are three primary actions for the aircraft to take once the appropriate pilot has taken control of the RPV. The action will be decided on based upon the perceived failure. The first is to hold a figure 8 pattern north of the runway near the lost com way point in an attempt to work at correcting the failure. The aircraft must be fully controllable for this to occur. Should fixing the failure in air not be possible, the aircraft will safely proceed to land. Should the aircraft be in a situation where neither of the previous actions are possible, the flight termination system will be utilized.

6.4.3.1 Flight Termination System

The flight termination system (FTS) consists of a failsafe procedure that will be executed manually (commanded kill) in the event that the RPV is uncontrollable or if it travels outside of visual range and the backup navigation systems fail. The failsafe procedure will be executed automatically in the event of a total loss in link (loss in link with the backup transmitter), or in the event that the RPV travels outside of approved airspace.

6.4.3.1.1 Flight Termination Criteria

The following list consists of situations in which the failsafe procedure would be executed:

1. Unresponsive flight controls
2. Total loss of link
3. ATRPV travels outside of the approved airspace boundary
4. Complete visual contact is lost and the backup navigation systems (GPS, emergency navigation camera, artificial horizon) fail

6.4.3.1.2 Failsafe Procedure

The failsafe condition is executed during full loss of link, and corresponds to a controlled crash: full up elevator, full right rudder, full right aileron, turbines shutdown. The failsafe condition is designed to minimize residual damage and results in the aircraft experiencing a tip stall on the right wing and entering a tight, downward spiral until impact.

There is no documentation of the total time delay before failsafe is initiated; however, there is a manufacturer specified time delay of less than 4 ms for the JR-12x to regain control in SmartSafe mode. SmartSafe mode is a failsafe mode in which, if signal is regained, the failsafe condition will be removed

and manual control is resumed. If the JR-12x is able to regain control in 4 ms, then it is a reasonable assumption that it is also able to detect a loss of signal in 4 ms.

6.4.3.1.3 Commanded Kill

In the event that the RPV is uncontrollable or travels outside of visual range and the backup navigation systems fail a manual kill command will be executed. A manual kill corresponds to a commanded executed failsafe condition. The manual kill can be executed via both the backup controller and the ground station.

6.4.3.1.4 Automatic Failsafe Procedure

The following control schematic incorporates a change from previous GSRPV operations. This switch incorporates a number of changes, all which increase safety, reduce risk and promote the successful flight of the ATRPV

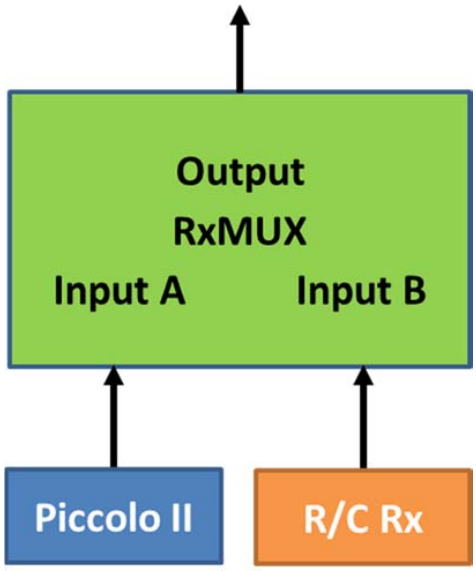

Figure 49- RxMUX Control Schematic

In this setup, the backup receiver will be attached to Input B and the Piccolo II will be attached to Input A of the RxMUx. The RxMUX is designed such that in the event that Input B is lost, the RxMUX will default to Input A; however, the reverse process is not permitted. In the event of a total loss of link (the RPV is unresponsive to input from either the primary or backup transmitter) the aircraft will enter an autonomous loiter around a pre-set waypoint in a safe area north of the flying site, within the "Safety Template" of the approved airspace (section 4.2.2). This autonomous loiter will allow the team to troubleshoot the problem while the aircraft loiters, rather than force the aircraft to automatically failsafe (in whatever location the loss of link occurred). Additionally, if the transmitters experience range issues (and/or a total loss of link is encountered), the aircraft will enter the autonomous loiter until the

problem can be fixed or the aircraft runs out of fuel and a controlled descent (in the loiter pattern) is completed.

In extreme cases, if neither the primary or backup pilot can successfully control the aircraft due to inadequate control margins and/or an onboard failure, the ground station operator can manually aerodynamically terminate the aircraft. In the event that the aircraft is under manual control and reaches the geo-fence, the ground station operator will manually aerodynamically terminate the aircraft. If the aircraft approaches the geo-fence but manual failsafe is unresponsive due to a loss of link, the aircraft will enter autonomous mode and either return to the pre-set loiter waypoint or automatically aerodynamically terminate at the geo-fence.

In all cases, the aircraft will either be under manual control (in which case manual failsafe can be executed at any time) or under emergency autonomous control, in which case aerodynamic termination will occur automatically if the aircraft attempts to leave the airspace and passes the geo-fence.

6.5 General Safety Mitigating Considerations

This section will elaborate on several topics relating to general safety.

6.5.1 Loss of Link

The use of the Acroname RxMUX allows for the incorporation of an independent backup control system. For more information about this control system, see Section 2.8.

6.5.1.1 RF Masking/ Shielding

The use of carbon fiber composite materials and the unique shape of the JWSC creates a situation where RF masking and/or shielding is a concern. To combat these issues, remote receivers are placed with the antennas outside of the fuselage to avoid masking. Additionally, the placement of these receivers allows communication to be maintained with the RPV in any attitude. All servo extension wires will be braided to avoid EMI issues. Note that all onboard systems will be rigorously tested for interference/masking/shielding issues during phase 2 tests (EMI/RF Tests).

The Piccolo II ground station contains a 900MHz spectrum analyzer. Through the user interface on the ground station, the Ground Station Operator can generate a spectrum analysis table that provides an indication of other RF users and potential sources of interference across the 900MHz band. The spectrum analyzer will be used survey the spectrum before all flight operations and during range/EMI testing.

6.5.1.2 Automatic Turbine Shutdown

In the event of total loss of signal, the JetCat ECU will automatically take the turbines to idle, or shut them down if necessary. The default parameters in the JetCat ECU take the turbines to idle after 0.1 seconds of total signal loss. If the signal loss persists for 3 seconds, the turbines are shut down.

6.5.2 Airspace

All flights will take place at the Foremost Airstrip in Foremost, AB. All flights will take place in the approved airspace. For more details about the airspace, see section 4.2.2.

6.5.2.1 Midair Collision

In the event of a midair collision (bird strike, FOD ingestion in flight), the pilot will land the aircraft as quickly and safely as possible. Spotters will be used to help locate possible collision risks, and inform the test director if necessary.

6.5.2.2 Geo-Fence Failsafe Protocol

The geo-fence programmed into the Piccolo II Autopilot is defined as the Kill Zone shown in red on the airspace requirements figure (Fig. 42) in section 4.1.2. The aircraft upon entering the Kill Zone and reaching the geo-fence will failsafe via aerodynamic termination. The failsafe enacted depends on the current mode control of the RPV (Manual, FBW, or Autopilot) as it reaches the geo-fence. The failsafe enacted are summarized for the different flight modes (Table 10).

Table 10- Failsafe protocol for geo fence in various control modes

Situation	Protocol
Aircraft encounters Geo-Fence in manual mode	Manual Failsafe executed by the ground station operator
Aircraft encounters Geo-Fence in FBW mode	Manual Failsafe executed by the ground station operator
Aircraft Encounters Geo-Fence in Autopilot	Automatic Failsafe executed

6.5.3 Unresponsive Flight Controls

In the event that flight controls are unresponsive, the backup controller will be activated and the backup pilot will take control of the aircraft. If the backup controller is unable to control the aircraft due to a total loss in uplink, the failsafe procedure will automatically execute.

6.5.4 Loss of Vehicle Position Data

A loss of vehicle position information (GPS) while the vehicle is flying within visual contact represents a loss of downlink telemetry, and not a hazardous situation. At all times during the flight, the pilot and backup pilot will keep visual reference on the aircraft. The ground station operators will monitor the telemetry feeds from the aircraft and the spotters will assist in visual referencing of the aircraft.

If the ATRPV inadvertently travels outside of visual contact, but remains within the allotted airspace, the primary ground station operator will take control of the aircraft using the live feed from the emergency navigation camera to navigate the aircraft back into visual contact. The camera feed will be placed next to the artificial horizon (from the Piccolo II) on the ground station to assist with maintaining constant altitude while flying using the emergency navigation camera. In the event that the emergency navigation camera fails, the artificial horizon and GPS information available in real time on the Piccolo II ground station display can be used to navigate the aircraft. In the event that the emergency navigation camera feed fails and either the GPS or artificial horizon fails, the failsafe procedure will be executed.

6.5.5 Malfunction/Failure Ground Operations

A malfunction or failure of the aircraft or related systems during ground operations could be caused by mishandling of the aircraft by ground crew, equipment failure or by not following all pre-flight

checklists and procedures. The effects of a malfunction or failure during ground operations could include damage to or loss of the vehicle as well as property damage, personal injury or death.

In order to minimize the risk of a malfunction or failure during ground operations, all personnel who will be in contact with the aircraft at any time during the test procedures will be trained by either the Test Director or Primary Ground Station Operator before arriving at the test site. This training will include an overview of all systems on board of the aircraft as well as general safety guidelines. Additionally, the ATRPV will be disassembled, packed and transported in protective containers to the test site to avoid damage during travel. Finally, the Test Director will ensure that all checklists and procedures are completed as required and the Range Safety Officer and Test Director will be present at all Phase 3 tests to observe pre-flight preparations.

In the event that a malfunction or failure occurs, the primary pilot will shut down the JetCat P200-SX turbines immediately. Once the turbines are shut down, a single member of the ground grew will approach the aircraft from the nose of the aircraft, with a fire extinguisher in hand, and shut down power. JetCat specifies that the recommended minimum safe distances are 15 ft in front of the turbine, 25 ft on either side and 15 ft behind the turbine. These distances will be enforced at all times during turbine operation.

Remaining personnel are free to approach the aircraft only after Test Director and Range Safety Officer confirm that the aircraft is powered down and call “all clear.” Flight testing will resume only after the Test Director, Primary Ground Station Operator/Vehicle Technician and Pilot approve any/all repairs.

6.5.6 Malfunction/ Failure During Takeoff

A malfunction/ failure during takeoff could be caused by a loss of control during, taxi, takeoff roll, or climb out, a total Loss of link with the aircraft, pilot error during takeoff or FOD ingestion. The effects of a malfunction or failure during ground operations could include damage to or loss of the vehicle as well as property damage, personal injury or death.

In order to minimize the risk of a malfunction or failure during takeoff, both the primary and backup pilot have trained on several reduced complexity flight models in preparation for their roles in this project. Additionally, the Test Director will ensure that all checklists and procedures are complete as described in this flight test plan and the runway will be examined for FOD prior to each flight. The backup controller will be tested prior to each flight for reliable link with the aircraft as well as the ability to take control of the aircraft at any time and the backup pilot will have the backup transmitter in his hands at all times during test operations, ready to take control if a loss of primary link situation arises. Finally, the primary pilot will be ready at all times to re-direct the aircraft away from people or property.

In the event that a malfunction or failure occurs, the pilot will perform evasive maneuvers if required to avoid personnel and property damage and landing the aircraft as quickly as safely possible and shut down the JetCat P200-SX turbines immediately. Once the turbines are shut down, a single member of the ground crew will approach the aircraft from the nose of the aircraft and shut down power. Remaining personnel are free to approach the aircraft only after Test Director and Range Safety

Officer confirm that the aircraft is powered down and call "all clear." Any available personnel will perform first aid if needed and inform proper facilities personnel as necessary.

6.5.7 JetCat P200-SX Turbine Malfunction During Flight

A failure of one or both turbines during flight could be caused by FOD ingestion, fuel pump failure, ECU battery failure, fuel tubing coming loose or turbine mechanical failure. The effects of such a failure may include a forced dead stick landing, damage to the turbines, loss of the vehicle, property damage, personal injury or death.

In order to minimize the risk of turbine failure during flight, FOD screens will be checked during preflight and the runway will be cleared of any noticeable FOD before each flight. A fuel filter will be used on all fuel containers. All batteries, including flight packs, transmitter batteries ground station backup batteries will be fully charged according to manufacturer specifications, and voltage checked before each flight and zip ties will be used to secure all fuel tubing connections. The manufacturer's specified 25 hour maintenance interval will be strictly adhered to, and the total turbine run time will be checked prior to each flight. Finally, the pilot and backup pilot will have trained on a simulator for degraded modes of flight, including both single and double turbine failure.

In the event that a single turbine malfunctions or shuts down, the primary pilot will attempt to land the aircraft as quickly as safely possible under the power of the remaining turbine. In the event that single engine operations results in an uncontrollable yawing moment or undesired handling characteristics, the second turbine will be shut down and a power off landing will be attempted. In the event that both turbines fail, a power off landing will be attempted as quickly as safely possible. dIf failure occurs during ground operations, all personnel will wait until turbines have completely stopped spinning to approach aircraft. If failure occurs during flight, the pilot will call "DEADSTICK" and begin an emergency approach. All personnel will clear the landing surface and keep eyes on the aircraft at all times. After landing/impact, a single member of the ground crew will approach aircraft carefully *with a fire extinguisher in hand.* In the event of a fire, the Test Director will contact the local fire department.

6.5.8 Fire

A fire could be caused by faulty/malfunctioning electronics, improper charging of batteries or a fuel spill. The effects of a fire could include damage to or loss of the vehicle, property damage or personal injury or death.

In order to minimize the risk of a fire, all batteries charged according to manufacturer specifications. Electrical connections will be checked for frayed wires and possible short circuits before flight. Fuel will be stored in approved containers only, away from the flight line, test equipment, test personnel and the flight test article. The Test Director will ensure that all checklists and procedures are complete as described in this flight test plan and a fire extinguisher will be present at the test site at all times.

In the event that a fire occurs, the local fire department will be contacted immediately. If the fire is small enough, a single member of the ground crew will carefully approach the aircraft and attempt to put out the fire with the fire extinguisher. If in doubt, wait and let the fire patrol take care of

the fire. Additionally, the following lists will be followed, depending on the location and/or cause of the fire.

1. If the fire is inside of the aircraft:
    a. The primary pilot will immediately shut down both turbines.
    b. A single member of the ground crew will carefully approach the aircraft use the fire extinguisher to put out the fire.
    c. After the fire is extinguished, the ground crew member will power down the RPV, if it is safe to do so.
    d. All remaining personnel will wait 15 minutes after the flames are extinguished to approach the aircraft.
2. In the event that a LiPo battery begins to show signs of swelling during charging:
    a. The person charging the battery will immediately disconnect battery from charger.
    b. Wait for swelling to stop increasing
    c. DO NOT attempt to start charging the battery again
    d. Place the battery in a location away from the ground station away from any combustible material.
    e. Dispose of LiPo battery according to manufacturer's specifications as soon as safely possible.

6.5.9 Structural Damage

Structural damage could be caused by loss of control and resulting dive causes pilot to fly outside of safe flight speed range, failure of one or more structural components during flight, a hard impact on landing, a mid-air collision or mishandling of vehicle. The most important structural component to monitor during flight is the aft wing. The effects of structural damage could include loss of the vehicle, property damage or personal injury or death.

In order to minimize the risk to structure, the primary and backup pilots will have extensive simulator training before flying the ATRPV, including training for degraded modes of flight, including structural failure. To prevent a mid-air collision, spotters will actively search the airspace for collision hazards, and inform the pilot if necessary. In order to prevent mishandling of the vehicle, all personnel who will be in contact with the aircraft at any time during the test procedures will be trained by either the flight test director or primary ground station operator/vehicle technician before arriving at the test site and the vehicle will be disassembled and transported in protective containers. During flight, the pilot will be prepared for inadvertent flight maneuvers due to loss of link, stuck control surfaces, or other degraded modes of flight and the backup pilot will be prepared to take control in the event that the primary pilot loses control. Finally, the aircraft structure will be checked for wear and tear before each flight in pre-flight operations.

Driving the aft wing to produce the target geometric nonlinearity could lead to a potential snap through response and buckling of the aft wing. In order to monitor the aft wing during flight to avoid this potential hazard, the primary GSO will monitor the structure via the gimbal camera and the secondary GSO will monitor the telemetered strain data making sure to indicate once a strain threshold

has been reached at which point the pilot will discontinue the maneuver in the safest method possible without introducing additional loading to the vehicle.

In the event that structural damage occurs during shipping or ground operations, the appropriate repairs will be made and checked before testing is resumed. If damage occurs in flight, the pilot will perform an emergency landing (if possible) as quickly as possible to minimize collateral damage. In the event that the structural damage renders the aircraft uncontrollable, all personnel will clear the landing surface and keep eyes on the aircraft at all times.

6.5.10 Malfunction/ Failure during Landing

A malfunction or failure during landing could be caused by a loss of control during approach or landing, heavy crosswind or adverse weather conditions, landing gear failure, pilot error during approach or landing or a total loss of link. The effects of such a failure include damage to or loss of the vehicle, property damage and personal injury or death.

In order to minimize the risk of such a malfunction or failure, the flight test director will ensure that all checklists and procedures are complete as described in this flight test plan. Both pilots will have had extensive training on both reduced complexity flight models. Additionally, the primary pilot will be ready at all times to re-direct the aircraft away from people or property and the Backup Pilot will have the backup transmitter in his hands at all times during test operations, ready to take control if a loss of primary link situation arises. The backup controller will be tested prior to each flight for reliable link with the aircraft as well as the ability to take control of the aircraft at any time.

In the event that a malfunction or failure occurs during landing, the primary pilot will shut down the turbines as quickly as possible. If airborne, the pilot will perform evasive maneuvers if required to avoid personnel and property damage. If possible, a "go around" maneuver will be performed to avoid a hard landing and give the pilot more time to assess the situation and the pilot will land aircraft as soon as safely possible. After landing, a single member of the ground crew will carefully approach and power down the aircraft. Remaining personnel are free to approach the aircraft only after flight test director and RSO confirm that the aircraft is powered down and call "all clear." Flight testing will resume only after the TD, primary GSO/vehicle technician and primary pilot approve any/all repairs.

6.6 Test Hazard Analysis

A detailed test hazard analysis will be completed in the following drafts of the document.

6.7 Mishaps

For the purposes of this test, a mishap will be defined as:

> ***Mishap:*** An event that results in damage to the aircraft (outside of normal wear and tear from operations), injury to personnel, damage to private property and/or damage to airfield property at the flight location in Foremost, Alberta.

In the event of a mishap, the Test Director will contact the AFRL Flight Test and Evaluation Office as well as the AFRL Flight Safety point of contact as soon as possible (within 8 hours) to inform them of the event. The decision to continue, postpone or cancel testing will be made in collaboration with the

flight test director, pilots, ground station operator, range safety officer, and AFRL Safety Review Board. Immediately after the RPV is recovered and damage is assessed, AFRL Form 29 – AFRL Test Safety Mishap Form will be completed. The unfilled form is located in Appendix C. Efforts will be made to be as detailed and descriptive as possible about the cause and effects (both short and long term) of the mishap, as well as its implications on future testing.

6.7.1 Emergency Personnel

Emergency Personnel, including the fire department, will be local to the Foremost, AB and available by phone during all flight operations.

Flight Test Plan References

[1]Blair, M., Canfield, R. A., and Roberts Jr., W., "Joined-Wing Aeroelastic Design with Geometric Nonlinearity," Journal of Aircraft, Vol.42, No.4, 2005, pp. 832-848.

[2]Bond, V., "Flexible Twist for Pitch Control in a High Altitude Long Endurance Aircraft with Nonlinear Response," Ph.D. Dissertation Prospectus, Department of the Air Force, Air Force Institute of Technology, Wright-Patterson AFB, Dayton, OH, 2007.

[3] The Boeing Company. "Selected Results from Test of Model on Sting", Presentation Excerpts, NASA Langley, Hampton VA, slides 2-5.

[4] Lucia, David J., "The SensorCraft Configurations: A Non-Linear AeroServoElastic Challenge for Aviation," AIAA Paper 2005-1943, 2005.

[5]Roberts, R. W., Jr., Canfield, R. A., and Blair, M., "Sensor-Craft Structural Optimization and Analytical Certification," AIAA Paper 2003-1458, April 2003.

[6]Richards, J., Suleman, A., Aarons, T. and Canfield, R.A., "Multidisciplinary Design for Flight Test of a Scaled Joined Wing SensorCraft," AIAA Paper 2010-9351, Sep. 2010.

[7]Richards, J., Aarons, T., Suleman, A., Canfield, R.A., Woolsey, C., Lindsley, N. and Blair, M., "Design for Flight Test of a Scaled Joined Wing SensorCraft," AIAA Paper 2011-2011, Apr. 2011.

[8]CAD work completed by Jenner Richards of Quaternion Engineering/ University of Victoria

[9]Richards, J., Garnand-Royo, J., Ricciardi, A., Suleman, A., Can_eld, R. A., and Woolsey, C., \Design and Evaluation of Aeroelastically Tuned Joined-Wing Sensor- Craft Flight Test Article," 54th AIAA/ASME/ASCE/AHS/ASC Structures, Structural Dynamics and Materials Conference, April, Boston, Massachusetts, 2013, pp. 1-18.

[10]Aarons, T. D., *Development and Implementation of a Flight Test Program for a Geo-metrically Scaled Joined Wing SensorCraft Remotely Piloted Vehicle* , Master's thesis, Virginia Polytechnic Institute and State University, 2011.

[11]http://www.jetcatusa.com/p200.html

[12]Richards, J., Aarons, T., Suleman, A., Can_eld, R. A., and Woolsey, C., \Airworthiness Evaluation of a Scaled Joined-Wing Aircraft 1," 53rd AIAA/ASME/ASCE/AHS/ASC Structures, Structural Dynamics and Materials Conference, April, Honolulu,Hawaii, 2012, pp. 1-37.

[13]"PS081 Single Chip Solution for Strain Gauges," ACAM mess electronic, 2010, DP_PS081_en VO.7.

[14]PhotoModeler[C] Manual

[15]http://gopro.com/hd-hero3-camera

Appendix A. JetCat P200-SX Operation Protocol

The following is taken directly from the *JetCat Instruction Manual, V6.0J2 ECU*. The full document is available online at the JetCat USA website: http://www.jetcatusa.com/PDFFiles/Instruction%20manual%20V6.0J2.pdf.

Safety Precautions

If other persons or animals are present while operating the *JetCat ENGINE*, **ALWAYS ENFORCE THE PROPER MINIMUM SAFE DISTANCES FROM** THE TURBINE! The recommended minimum safe distances are:

In front of the turbine = 15 feet
On the side of the turbine = 25 feet
Behind the turbine = 15 feet

In case of a mishap, fire extinguishers should be on hand at all times. *JETCAT USA* recommends the CO/2 variety. Powdered extinguishers will contaminate the precision components, upsetting the integrity of the turbine.

To the avoid hearing damage, always use hearing protection when you are near a running turbine engine!

When the turbine is running, never place your hands closer than six inches into the area of the intake. **An extreme suction** - which can grasp a hand, fingers or other objects in a flash - prevails in this area. Be aware of this source of danger, always!

Prevent foreign materials from entering the intake or exhaust when working with the turbine. Before operation, make sure there are no lose parts or debris near the turbine. Objects being sucked in can cause severe damage.

Always exercise caution around the hot parts of the turbine, to avoid burns. The outer case at the turbine stage and nozzle reaches 450-500° (Celsius), while the exhaust gas may exceed 720 °C.

Assure that the fuel is mixed with approximately 5% synthetic oil. Use only synthetic turbine oils available at local airport fuel suppliers or from *JETCAT USA*. Synthetic turbine oils are dangerous and should only be handled per the manufactures MDS sheets

Never run the turbine in a closed room, or an area near any kind of flammable matter. Do not fly turbine-powered aircraft near flammable materials, nor in forested tracts or areas experiencing drought or dryness. Obey all forest fire regulations and warnings by refraining from operating the *JetCat ENGINE* in restricted fire zones. Never operate model turbine jet aircraft in or around residential or heavily populated areas.

Installation of unauthorized parts from another manufacturing source may also result in engine failure. Do not introduce engine or electronic components other than those delivered by *JETCAT USA*, unless you are willing to risk destroying your turbine! *JETCAT USA's* parts are designed and engineered specifically for the *JetCat P80/ P120/P160*. Accept no substitutes, unless you are prepared to sacrifice your aircraft.

Appendix B. AFRL SUAS ORM Assessment Form

Date: _____ Program: _____ Vehicle: _____ Flight # ____

	GREEN	YELLOW	RED
HUMAN		Place "X" in appropriate box	
Vehicle Operator			
Qualified *	Fully Qualified	In-Training	No Training at All
Currency (this vehicle) *	< 30 Days	30-60 Days	> 60 Days
Sleep (Crew Rest)	≥ 8 Hours	6 – 8 Hours	≤ 6 Hours
Ground Control Station (GCS) Operator			
Qualified	Fully Qualified	In-Training	No Training at All
Currency (this GCS/vehicle)	< 30 Days	30-60 Days	> 60 Days
Sleep (Crew Rest)	≥ 8 Hours	6 – 8 Hours	≤ 6 Hours
Payload Operator			
Qualified	Fully Qualified	In-Training	No Training at All
Currency (this payload/vehicle)	< 30 Days	30-60 Days	> 60 Days
Sleep (Crew Rest)	≥ 8 Hours	6 – 8 Hours	≤ 6 Hours
Launch Crew			
Qualified	Fully Qualified	In-Training	No Training at All
Currency (this launch system/vehicle)	< 30 Days	30-60 Days	> 60 Days
Sleep (Crew Rest)	≥ 8 Hours	6 – 8 Hours	≤ 6 Hours
Observers			
Qualified (if flying in the National Airspace	Fully Qualified	In-Training	No Training at All
Sleep (Crew Rest)	≥ 8 Hours	6 – 8 Hours	≤ 6 Hours
Crew/Personal Concerns	None	Minor	Major
MISSION/OPS		Place "X" in appropriate box	
Test Location Familiarity	> 3 Previous Tests at this Location	1 - 3 Previous Tests at this Location	First Time at this Location
Test Location Weather	All Criteria Acceptable	1-2 Criteria Within 30% of Limits	1-2 Criteria Within 10% of Limits or > 2 Criteria Within 30% of Limits
Mission Duration	< 30 minutes	30-120 minutes	> 120 minutes
Takeoff Times	Between Sunrise & Sunset	All Other Times	At Night
Landing Times	Between Sunrise & Sunset	All Other Times	At Night
Bird Activity (check US Avian Hazard Advisory System at www.usahas.com, verify on-site, prior to start of testing)	Low	Moderate	Severe
Duration of Duty Day	< 8 Hours	8 - 12 Hours	> 12 Hours
Mission Complexity	Low/Normal	Demanding	Extremely Demanding
Safety Risk	Low	Medium	High
Check AFRL Flight Crew Information Folder (Flight Crew Information Folder)	0 Notices pertaining to systems under test or all relevant issues have been satisfactorily addressed		Relevant notices exist and not yet complied with
VEHICLE/GCS/LAUNCH SYSTEM/RECOVERY SYSTEM		Place "X" in appropriate box	
Config Changes (hardware/software)	None	Minor or first flight after down time > 30 days	Major modifications or Functional Check Flight or down time > 90 days
Maintenance Write-ups	0 Write-ups outstanding	≤ 3 Minor Write-ups outstanding – no impact on meeting test objectives and/or compromising safety	≥ 1 Major Write-up(s) outstanding impacting meeting test objectives and/or compromising safety or > 3 Minor Write-ups outstanding
Service Bulletins/Safety Supplements **	0 New Bulletins / Supplements outstanding; all existing complied with and reviewed/approved by SRB and TAA		Bulletin/Supplement exists, applicable to system under test, and not yet complied with

TOTAL ORM LEVEL		GREEN (< 3 Total Yellows/Reds, with no more than 1 Red)		YELLOW (≥ Total 3 Yellows/Reds, with no more than 1 Red)		RED (2 or More Reds)

AFRL Form 33A DRAFT 4 Aug 10
Prescribing Directive AFRLI 61-103, Volume 1

*** Review FAA Interim Operational Approval Guidance 08-01, dated 13 Mar 08, Section 9.0 Personnel Qualifications, for specific requirements.**

**** Mandatory for all commercial products used in test (vehicle, ground control station, launch system, and recovery system). If using an in-house system designed and developed by another organization, check with that organization for any cautions and warnings. Assessment only needs to be completed prior to first flight of each week's testing.**

Test Director: Discuss How ORM Which Shows Up as Yellow or Red Was Addressed/Mitigated/Who Was Notified (use continuation page as needed)

This is a preliminary form filled out in anticipation of the first flight of the Geometrically Scaled RPV. The pilots will have both flown at the test site prior to the first flight of the RPV, and the Virginia Tech/Quaternion Engineering crew will have performed ground operations at the test site (as part of this test plan) before the aircraft goes wheels up. The only yellow ORM level comes from the fact that this is the first flight of a new aircraft. The pilots will have both flown reduced scale models of this aircraft prior to flying the full 1/9th scale RPV.

Mission Completed (y/n): _____

If Not, Why:

Initials _____

GREEN ORM: If any specific area is Red, look at ways to lower risk in that area. Test Director or Test Safety Officer discretion to continue test.

YELLOW ORM: Try to mitigate to Green ORM. Work with Test Director, Vehicle Operator, and Test Safety Officer to lower ORM risk. If unable to lower risk, AFRL Branch Chief must be notified and approve test start.

RED ORM: Try to mitigate to Green or Yellow ORM. Work with Test Director, Vehicle Operator, and Test Safety Officer to lower ORM risk. If unable to lower risk, AFRL Division Chief must be notified and approve test start.

INSTRUCTIONS:

1. Complete this assessment prior to each flight or like series of consecutive sorties.
2. Maintain completed forms in test log book.
3. If Total ORM level is Yellow or Red, notify AFRL/SEF and AFRL/RBCT that approval to continue with testing was sought/garnered by the appropriate level of authority. Notification should be made within 4 hours of the start of the test. Preferred method of notification is by e-mailing the completed form to Afrl.se.workflow@wpafb.af.mil and AFRLDL.flighttestandevaluation@wpafb.af.mil
4. Provide copy of completed forms to AFRL/SEF and AFRL/RBCT upon the completion of the test program.

AFRL Form 33A DRAFT Aug 10
Prescribing Directive AFRLI 61-103, Volume 1

Appendix C. AFRL Form 29- AFRL Test Safety Mishap Worksheet

AFRL Test Safety Mishap Worksheet

Complete General Information and Mishap Notification Contacts in advance.
Mishap to be reported within 8 hours of occurrence.

General Information

		AFRL Costs	Non-AFRL Costs
Program Title:	Vehicle:		
Program Manager/Symbol/Phone: Dr. Ned Lindsley	Non-Vehicle		
	Total System		

Mishap Notification Contacts/Record

Name/Office	Phone/Cell	Email	Date/Time Notified
AFRL Det Safety:			
Branch Chief:			
Division Chief:			
SRB Chair:			
AFRL Flight Safety:			
Host Safety Office:			

For use only in the case of a Class A, B, or C mishap.

TD Executive Officer: _____

Tech Director: _____

Mishap Information: Class A, B, or C? (See instructions on Page 2) ☐ Yes ☐ No

Location of Mishap: _____ Date of Mishap: _____

Brief Narrative: _____ Time of Mishap: _____

Personnel

Injuries? ☐ Yes ☐ No If Yes: ☐ Military ☐ Gov't ☐ Civilian ☐ Contractor ☐ Non Gov't

How many people were injured? _____ Hospitalization Required? _____

Extent of Injuries (be as specific as possible):

Name of responding emergency organization: _____

Point of contact at organization (name & number):

Name of clinic or hospital where injured was taken: _____

Property

Property Damage? ☐ Yes ☐ No If Yes: ☐ Gov't ☐ Contractor ☐ Non Gov't

Approx dollar cost: _____

Extent of Damage:

Additional Notes: _____

FOR OFFICAL USE ONLY (FOUO) When Form is Completed

AFRL Form 29, Previous Editions Obsolete
Prescribing Directive: AFRLI 61-103, Volume 1

As a reminder, in case a mishap occurs the test team should follow the initial responses listed below:

- Ensure everyone is safe and contact emergency services, if needed.
- Minimize fire damage to wreckage, if applicable.
- Do not disturb the accident scene – preserve all wreckage and surrounding areas in their original state.
- Only move or change things at the scene in the interest of safety. Photograph the site before and after anything is disturbed. Take lots of pictures so an investigator can easily retrace the situation before it was changed.
- Gather pertinent personal information from everyone at the scene (name, duty, title, office symbol, contact information).
- Gather witness statements as soon as possible to ensure clarity and freshness of memory. Write down exactly what was personally witnessed.
- Follow the contact procedures on the front of the AFRL Form 29. Report mishap to identified contacts as soon as possible but no later than 8 hours after occurrence.
- **For Class A, B, or C mishaps, notify the Tech Directorate's Executive Officer or Tech Director to initiate OPREP-3 reporting procedures IAW AFI10-206 AFMCSUP 1.** (See below for additional information on OPREP reporting.)
- Wait for guidance from range safety, a trained safety investigator, or HQ safety personnel before removing, cleaning, or disturbing a crash site.

If in doubt, wait and ask AFRL Safety. Remember that all safety investigations are non-retribution in nature and are conducted for mishap prevention purposes only.

OPREP-3 Reporting Matrix

Event/Incident	Submit Report When (Description)	Type Report
Aircraft Mishap	Any AF aircraft mishap involving civilian causalities or damage to civilian property	PINNACLE
Aircraft Mishap Class A	A. aircraft destroyed, B. damage of $2,000,000 or more, C. mishap resulting in an AF fatality	BEELINE
Aircraft Mishap Class B	A. damage of $500,000 but less than $2,000,000, B. aircraft mishap resulting in a permanent partial disability, C. aircraft mishap resulting in inpatient hospitalization of three or more personnel	BEELINE
Aircraft Mishap Class C	Damage of $50,000 or more but less than $500,000 not reportable under BEELINE criteria	HOMELINE
Civil Aircraft Mishap	Any civil aircraft mishap that occurs on AF property or under the control of/in airspace controlled by an AF air traffic control facility	HOMELINE

For Determining Vehicle and Non-vehicle Costs:

For "Vehicle" cost consider providing quantity and cost of each vehicle, chase aircraft, or unmanned aerial vehicle.

For "Non-vehicle" cost consider infrastructure, ground control station, trailers, ground equipment, etc.

Note 1: Vehicle and Non-vehicle costs shall be mutually exclusive.
Note 2: Non-AFRL and AFRL costs shall be mutually exclusive.

AFRL FORM 29, Prescribing Directive: AFRLI 61-103, Volume 1 PREVIOUS EDITIONS OBSOLETE